ION EXCHANGE OF LEAD AND CADMIUM WITH THE SODIUM AND AMMONIUM FORMS OF SOME NATURAL ZEOLITES

BY

Maria Loizidou

A thesis submitted for the
Degree of Doctor of Philosophy of
The City University, London.

The Department of Chemistry.

June 1982.

TABLE OF CONTENTS

LIST OF TABLES

LIST OF FIGURES

ACKNOWLEDGMENTS

My sincere thanks go to Dr. R.P. Townsend for his continuous advice and encouragement throughout this project.

My appreciation goes to [redacted] for his help with the computing and useful discussion.

I would also like to express my gratitude to [redacted] for his patience with the diagrams and tables of results.

Finally my thanks are due to [redacted] for typing this thesis.

LIST OF PRINCIPAL SYMBOLS

A_s , A_c	Equivalent fraction of ion A^{Z_A+} in solution and crystal respectively.
$A_c max$	Maximum level of exchange.
A_c^N	Normalised equivalent fraction of ion A^{Z_A+} in the crystal.
$a_{A(c)}$, $a_{B(c)}$	Activity of ion A^{Z_A+}, B^{Z_B+} in crystal.
$a_{A(s)}$, $a_{B(s)}$	Activity of ion A^{Z_A+}, B^{Z_B+} in solution.
CLI	Clinoptilolite
c	Crystal phase.
e	Charge on the electron (1.602×10^{-19} c).
f	Zeolite phase activity coefficient (binary systems)
f_N	Normalisation factor.
FER	Ferrierite.
G	Gibbs free Energy.
ΔG^{Θ}	Standard free energy per equivalent of exchange.
H	Enthalpy of a system.
ΔH^{Θ}	The standard enthalpy change.
I	Ionic Strength.
K_a	Thermodynamic equilibrium constant.
K_C	Kielland quotient.
K_m	Mass action quotient.
M_A	Molality of ion A^{Z_A+} in crystal (equation 2.3).
MOR	Mordenite
m	Solution Molarity ($mol.dm^{-3}$).
N	Normality ($equiv.dm^{-3}$).
Na-CLI	Sodium clinoptilolite
R	Gas constant (8.314 JK^{-1} mol^{-1})

S	Entropy of the system.
T	Absolute temperature.
T_N	Total solution normality (equiv.dm^{-3}).
V	Vapour phase.
Z	Charge on ion.
α	Separation factor (or practical selectivity).
α^{UN}	Unormalised separation factor.
α^{N}	Normalised separation factor.
γ_A , γ_B	Individual ion activity coefficients in solution for ions $_A{}^{Z_A^+}$, $_B{}^{Z_B^+}$.
$\gamma_{\pm}$	Mean molal stoichiometric activity coefficients.
Γ	Ratio of solution phase activity coefficients raised to their appropriate powers.
Δ	Zeolite phase water activity term.
ϵ_0 ϵ_r	Permittivity of free space and relative permittiv.
Λ_{ij}	An excess interaction energy term arising when ion i interacts with ion j.
μ	Chemical potential.
Φ	Zeolite activity coefficient for ternary systems.

ABSTRACT

The necessity to find efficient and economic methods of treating waste water which contains heavy metals has led to this work. The properties of several natural zeolites, specifically clinoptilolite, mordenite and ferrierite have been examined with a view to their use in the removal of lead and cadmium from both fresh water and for saline environments.

Binary equilibrium studies were performed using either sodium forms of the minerals (which were then exchanged with lead cadmium or ammonium) or the ammonium zeolites which were similarly exchanged with either lead or cadmium. In the case of experiments involving cadmium, two different co-ions were used, the nitrate and the chloride. Most binary exchanges were carried out at a total external solution concentration of 0.1 equiv.dm^{-3} and at 25^{o}C, but some exchanges involving lead in the sodium zeolites were performed at higher concentrations (0.5 equiv.dm^{-3}). The thermodynamic parameters were calculated where possible, but some of the exchanges turned out to be ternary in nature. The overall affinities indicated that lead was preferred over cadmium in the presence of all the sodium zeolites while the ammonium forms of the minerals were less selective for both lead and cadmium.

In addition some ternary equilibrium studies were carried out for the systems Pb/Cd/Na and Pb/Cd/NH_4. Clinoptilolite has been found to effectively remove lead and cadmium in the

presence of sodium or ammonium, while for mordenite the ammonium ion inhibits the exchange of the heavy metals. Ferrierite shows no selectivity for either lead or cadmium and can only be used to a limited degree.

CHAPTER ONE INTRODUCTION

1.1. GENERAL INTRODUCTION

1.2. ZEOLITE FRAMEWORKS AND STRUCTURES

1.2.1. Classification of Zeolite Structures

1.3. GENESIS OF NATURAL ZEOLITES

1.4. CLINOPTILOLITE

1.4.1. Structure

1.4.2. Ion Exchange Studies

1.5. MORDENITE

1.5.1. Structure

1.5.2. Ion Exchange Studies

1.6. FERRIERITE

1.6.1. Structure

1.6.2. Ion Exchange Studies

CHAPTER ONE INTRODUCTION

1.1. General Introduction

The term zeolite was introduced by Cronstedt in 1756[1-3] from the Greek ζέειν (to boil) and λίθος (stone), for minerals which expel water when heated and hence seem to "boil". Although natural zeolites were known for a long time[4], it is only in the last thirty years that their properties have been examined systematically.

Before the advent of the organic exchange resins, "permutites" were used commercially as water softeners. Permutites were crystallographically amorphous aluminosilicates. However, these inorganic exchangers were completely abandoned later in favour of the organic resins, which are still used for most commercial ion exchange processes for two reasons. First, the open structure of the resins means that very rapid exchange of ions may be effected, and second, the resins are far more resistant to acid attack than are the inorganic exchangers.

The high and increasing cost of resins results in there being limits to their use, especially for pollution control. Their place has been taken by either synthetic or natural zeolites. During the 1950's[5,6] zeolites of high chemical purity and crystalline structure were synthesised. Of these, zeolite A (which has no known analogue in nature), zeolites X,Y (which are isotypic with the mineral faujasite) and synthetic mordenite[7] are readily available commercially, and employed in industrial processes. A recent development[8] has been the synthesis of a new series of zeolites characterised by a high silica: alumina ratio and also hydrophobic properties[9]. These materials

(normally called the ZSM series) represent a significant departure from earlier zeolites in their properties so that it has been proposed that they be named "2nd generation zeolites"[7]. Pure silica analogues of them may be synthesised such as "silicalite"[10] and because their structural framework is characterised by a very high number of 5-rings, Meier has proposed the name "Pentasil" for the series. However, Vaughan and Breck[11] both express reservations on this nomenclature.

Manufactured zeolites have the advantage over natural zeolites of being fairly uniform in character, but they can be considerably more expensive, and it is desirable to find uses for the extensive deposits of the natural minerals. Thus detailed examination of the properties of the natural zeolites are of interest.

Natural zeolites are very common and can be found as fine crystals of hydrothermal genesis in geodes and in fissures of volcanic rocks, or as microcrystalline masses of sedimentary origin. The first report of zeolites in sedimentary deposits was made in 1891[4] and concerned phillipsite in deep-sea sediments.

More than thirty distinct species of zeolites occur in nature, and of these, about twenty occur in sedimentary deposits. However, only eight zeolites commonly comprise the major part of sedimentary rocks. These are analcine, chabazite, clinoptilolite/heulandite, erionite, ferrierite, laumontite, mordenite and phillipsite. Analcine and clinoptilolite are the most abundant of these zeolites.

Natural zeolites are of considerable interest today in several

seemingly unrelated areas of technology, and as such are the subject of numerous geological, mineralogical, chemical and agricultural research projects. The utilization of natural zeolites is a rapidly expanding area. In recent years zeolite minerals have found especial application in the field of pollution control and they are fast becoming important components in the design and construction of such facilities. Both ion exchange and adsorption properties of zeolites can be utilized in this context. However, most applications that have been developed involving natural zeolites are based on the ability of certain zeolites to exchange cations selectively. Some examples are given below.

Zeolites can remove selectively radioactive ions from waste effluents by ion exchange. Also they can be used to store these isotopes due to their high thermal stability and their resistance to the high energy radiation. In 1959 L.L. Ames[12,13] demonstrated the specificity of clinoptilolite for the removal of radioactive caesium137 and strontium 90 out of low-level waste streams from nuclear installations. The ions can be extracted with high efficiency from the effluent and then either stored indefinitely in the zeolite, or removed by elution for subsequent purification and recovery. Using clinoptilolite in particular, solutions containing the radioactive cations were passed through columns packed with the zeolite until breakthrough occurred. The "saturated" columns can then be removed from the system, sealed, and buried as solid waste. The general implications to the environment of this method of disposal have been discussed more recently[14] and indeed millions of gallons[15]

of low-level caesium 137 wastes have been processed this way using zeolite ion exchangers. A similar process has been developed to recover this species from high-level effluents using a chabazite-rich material[16,17]. In another process[18,19], steel drums filled with granular clinoptilolite also were used as ion exchange columns for the retention of Sr90 and Cs137 (half-lives 25 and 33 years respectively). Once the capacity of the drum was reached, they were removed, buried and replaced with new drums containing fresh clinoptilolite. The subject of disposal of radioactive metal ions using zeolites was reviewed in 1980 by Breck[20].

Another application of natural zeolites concerns the control of river pollution. Ames[21] and Mercer[22] have showed that clinoptilolite is also highly selective for ammonium ions, and they suggested that it could be useful for the extraction of ammoniacal nitrogen from sewage and agricultural effluents. The presence of NH_4^+ is not only toxic to fish and other forms of aquatic life, but it also contributes to the rapid growth of algae, leading in turn to eutrophic conditions in lakes and rivers.

Due to this severe problem, local and national environmental protection agencies have limited the amount of nitrogen that is permissible in municipal and industrial waste effluents to only one part per million[15]. Zeolites, and especially clinoptilolite, are now being used as anti-pollutants, employing several designs. Some schemes suggest that powdered zeolite be added to the effluent andthen filtered or sedimented out[23], while

others employ ion exchange columns filled with crushed clinoptilolite . Recent articles include studies by Semmens et al[24,25] on the mathematical modelling of columns of clinoptilolite for NH_4^+ removal.

One zeolite-ammonium removal process[26] involved release of ammonia to the atmosphere (air stripping) during the regeneration steps. This created other problems which have been overcome by several methods. One method involves contacting the exhaust gas with dilute sulphuric acid[27] to produce ammonium sulphate, a useful fertilizer in itself. Liberti et al[28,29] have also made an interesting combination of selective phosphate exchange on a weak anion resin exchanger, and selective NH_4^+ exchange on clinoptilolite. In this process a fertilizer is produced ($Mg\ NH_4PO_4 6H_2O$) from the concentrated regenerant stream. Semmens[30] carried out studies on biological regeneration. In this process the ammonium-saturated clinoptilolite is regenerated with sodium nitrate brine. As the ions are liberated they are oxidised by the nitrifying bacteria. The overall process yields sodium clinoptilolite, sodium nitrate, water and carbon dioxide. The nitrate-rich waste is valuable since the oxygen content of the nitrate is available and can be used for the oxidation of organic matter. The main disadvantage of this method is that the process relies on the sensitive nitrifying bacteria to oxidize the ammonium content of the regenerant.

Another interesting use of zeolites for pollution control is their addition as builders in detergents[31-33]. Polyphosphate salts (which are used as water softeners) are highly polluting

in excess, since the presence of the phosphate ions causes eutrophic conditions in fresh water lakes. Substitution of polyphosphates with zeolites can prevent or minimise the phosphate pollution. The zeolites used for this particular application are, however, mainly synthetic (Na-A and Na-X), but lately research has taken place on the natural zeolites[34], and it has been shown that natural zeolites with high selectivity and capacity for Ca^{+2} ion can be considered as partial replacements for phosphate in detergents.

Recently, the necessity of controlling heavy metal content of waste water has become more apparent. Studies on zeolites for this particular purpose have been so far very limited, and have mainly concerned the use of the synthetic materials. Chelischev et al[35] were the first to study the exchange of heavy metals on clinoptilolite, and reversible isotherms were reported for Na-Pb, Na-Ag, Na-Cd, Na-Cu, Na-Zn equilibria. Filizova et al[36] have extended these studies to include mercury and thallium. Equilibrium studies have also been undertaken by Semmens[37] using natural clinoptilolite and the selectivities for Ba^{+2}, Cd^{+2}, Cu^{+2}, Pb^{+2}, Zn^{+2} were determined. Gal and co-workers[38] and also Dubinin et al[39] examined the ion exchange of cadmium with Na-A. More recently Sherry[40] undertook a detailed study of the ion exchange of cadmium and lead using the synthetic zeolite Na-A, because of the likely presence of traces of these metals as pollutants when using A in detergent[41].

Zeolites, mainly of natural origin, find an extensive application in the field of agriculture, where they are used in

fertilizers, herbicides, pesticides and animal nutrition[42]. Zeolites exchanged with ammonium and potassium ions can serve as fertilizers and nutrient is released gradually. Additionally, they may function as soil conditioners improving its physical properties. Farmers in Japan[43,44] have used natural zeolites for years to control moisture content; the addition of clinoptilolite powder improved strikingly the growth and yield of crops. It is possible that these effects are due to the adsorption and retention of ammonium nitrogen and potassium, good retention of water and prevention of root decay.

The high ion-exchange and adsorption capacities of natural zeolites make them effective carriers of herbicides and pesticides. Clinoptilolite was found to be an excellent carrier of benzylphosphorothiate used to control stem blasting in rice[45]. Since 1965[42] experiments have been in progress in Japan on the use of clinoptilolite and mordenite as dietary supplements; up to 10% zeolite has been added to the diets of pigs, chickens and ruminants. Significant increases in gain of body weight per unit of feed were achieved. Also roosters raised on a diet that contained clinoptilolite showed an increased weight gain[46].

In the present work, the selectivities of the sodium and ammonium forms of the natural zeolites clinoptilolite, mordenite and ferrierite have been examined under various conditions. First, the selectivities of the zeolites in the presence of just sodium and ammonium ions in aqueous solutions were studied and this was followed by similar examinations in the presence of lead and cadmium, present either as binary or ternary

systems. In the literature[21-30], much of the data reported are concerned with the selectivity for ammonia using sodium forms of the zeolites. However, few really detailed studies have been published on any of the systems described above[35,37,47]

1.2. Zeolite Frameworks and Structures

The three dimensional frameworks of zeolites are constructed of tetrahedra of oxygen ions, each of which has a silicon or substituting ion (normally aluminium) at its centre.[48-50] Since each oxygen ion is shared by two adjacent tetrahedra, structures made exclusively of silicon and oxygen are neutral. However, normally zeolites do include ions (usually aluminium) which isomorphously replace the tetravalent silicon. On occasion, ferric ions may also occur in the structure. The aluminiums give the framework a net negative charge which must be balanced by additional cations that are occluded in the interstices in the zeolite lattice. Cations commonly found in the interstices of natural zeolites are sodium, potassium, calcium, and to a lesser extent the other alkali and alkaline earth cations. Electroneutrality requires the equivalents of alkali and alkaline earth cations present to be equal to the moles of trivalent cations in the framework.

Zeolites may be presented[51] generally by the empirical formula

$$M_{2/n} \cdot Al_2O_3 \cdot xSiO_2 \cdot yH_2O$$

In this oxide formula n is the cation valence and x is generally equal to or greater than 2. Until recently, this was

thought to arise from the impossibility of two aluminiums being directly linked through an oxygen within the zeolite framework (the so-called "Loewenstein rule"[52]. Recently[53] evidence has been put forward on the basis of chemical shift measurements using 29Si "magic angle spinning" NMR suggesting that for A at least Loewenstein's rule is broken. This matter is still controversial[54] and under discussion.

1.2.1. Classification of Zeolite Structures

Zeolites have been classified[55] into seven groups. This classification is based on the common features of the aluminosilicate framework structure. The characteristic of each group is a common subunit, which refers to the (Al, Si)O_4 tetrahedra arrangement. Meier[56] named these subunits Secondary Building Units (S.B.U.) and these are shown in Figure 1.1. The primary units are the SiO_4, AlO_4 tetrahedra. In some cases the zeolite framework can be considered in terms of polyhedral cages which are combinations of some of the secondary building units. The polyhedra are designated by the letters α, β, γ, etc. The α-cage is the largest unit and refers to the truncated cuboctahedron. Figure 1.2 shows the various polyhedra structures.

1.3. Genesis of Natural Zeolites

Most zeolites in sedimentary deposits were formed after burial by the enclosing sediments. Reaction of aluminosilicate materials in the sediment with the pore water leads to zeolite

FIG. 1.1 Secondary Building Units (SBU)

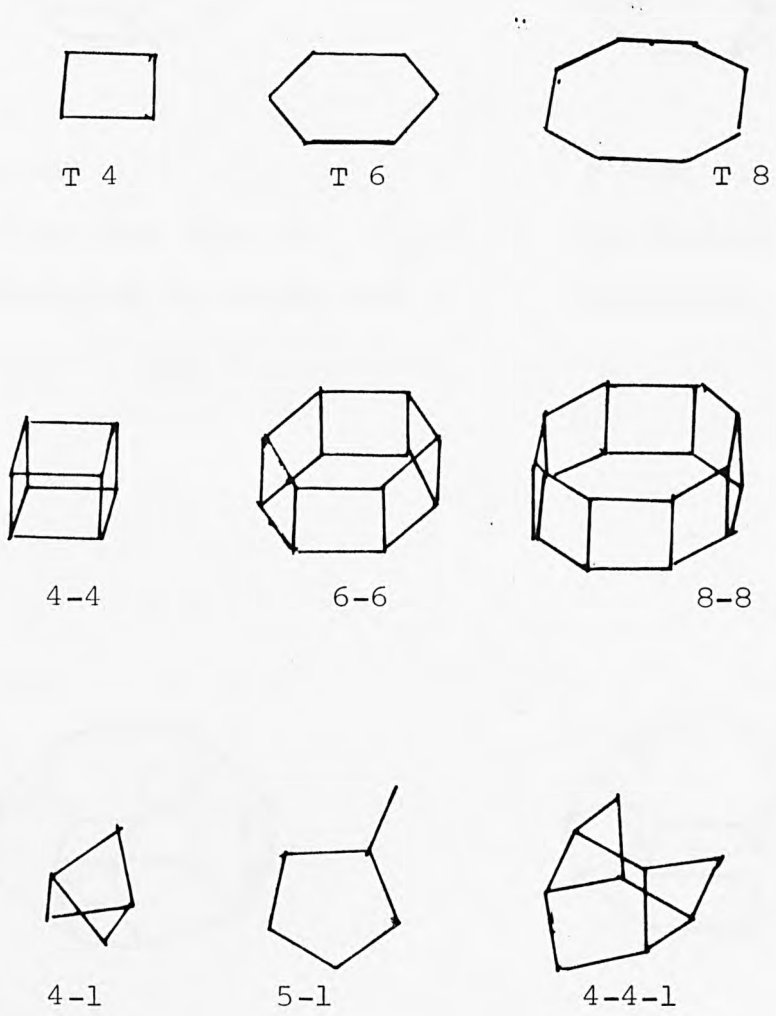

FIG.1.2 : Polyhedra

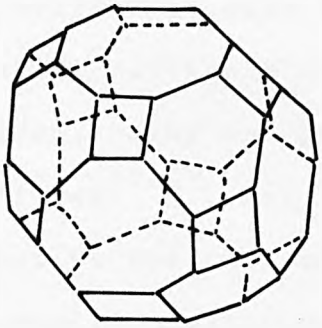

α cage

(26-hedron type I)

Truncated cuboctahedron

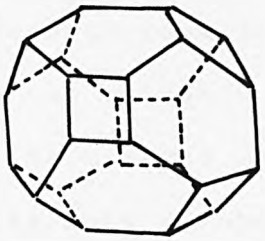

β cage

(14-hedron type I)

Truncated octahedron

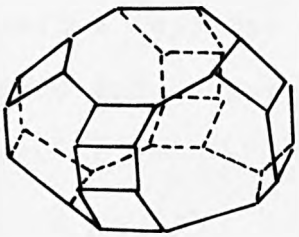

γ cage

(18-hedron)

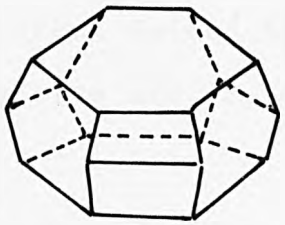

ϵ cage

(11-hedron)

formation. Silicic volcanic glass is the aluminosilicate material that most commonly serves as a precursor for the zeolite, although materials such as clay minerals, feldspars, feldspathoids and gels also have reacted locally to form zeolites[57-59]. At low temperature the volcanic glass is more reactive for the formation of zeolite mineral than are other crystalline materials, because it is more soluble and has a higher free energy. Formation of most of the common zeolites in sedimentary deposits is favoured by a relatively high chemical activity ratio of alkali ion to hydrogen ion, and a high chemical activity of silica in the pore water. The presence of hydroxyl ion influences the concentration or silica activity because it catalyses the crystallization of silica to quartz consequently diminishing the availability of silica[59].

1.4. Clinoptilolite

Clinoptilolite occurs naturally mainly as sedimentary deposits. Extensive deposits occur in the Western United States, New Zealand and Hungary. Volcanic deposits are found in Wyoming, U.S.A.

1.4.1. Structure of Clinoptilolite.

The structure of clinoptilolite was uncertain until recently. In 1975 Alberti[60] confirmed that clinoptilolite is isostructural with heulandite, but there is an extra ion site at the origin of the unit cell, which contributes significantly towards the thermal stability of clinoptilolite. The structure of

FIG.1.3 Clinoptilolite Structure.

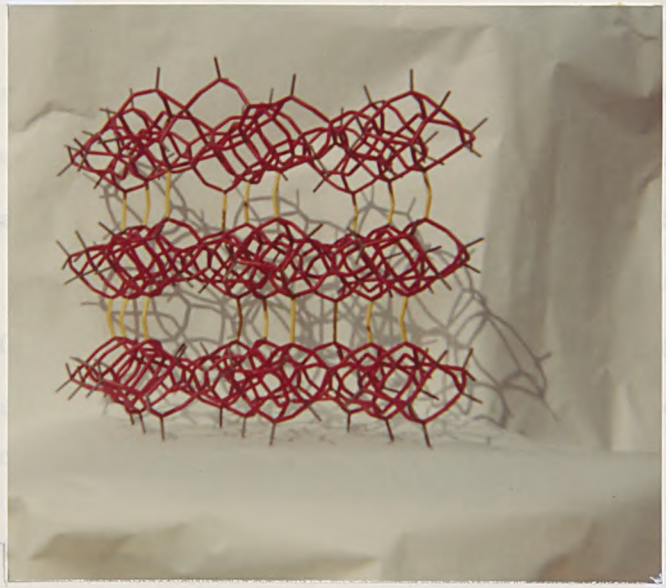

Figure 1.3a Two sets of channels parallel to the c-axis.

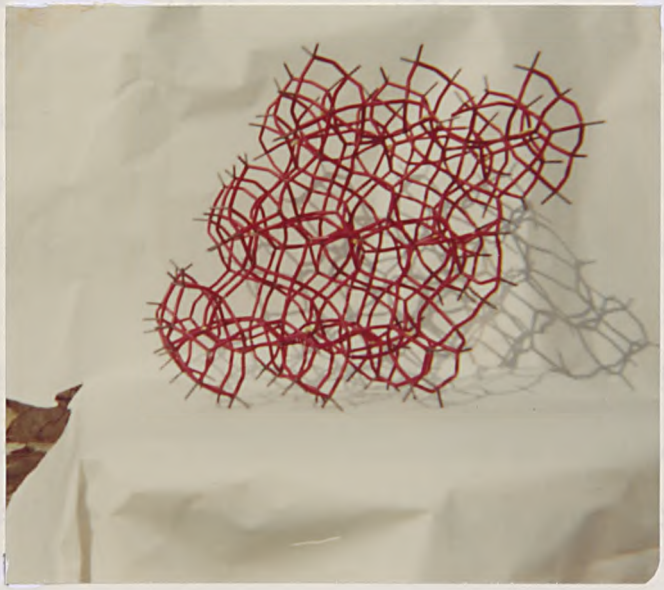

Figure 1.3b Clinoptilolite structure in the b-direction,no channels exist.

heulandite was determined by Merkle and Slaughter[61] in 1968. The Si:Al ratio may vary from a low of about 2.7 for heulandite to a high of about 5.3 for clinoptilolite. Calcium, sodium and potassium are the major cationic constituents with high calcium generally prevailing in the lower Si/Al ratio heulandite and high potassium in the higher Si:Al ratio clinoptilolite. The low silica calcium heulandites tend to degrade between 500-550°C[62,63], but potassium-exchanged heulandites and various potassium and hydrogen clinoptilolites are stable up to 800°C[62,64,65].

The structure of clinoptilolite is shown in Figure 1.3. The secondary building unit (S.B.U.) is the complex 4-4-1 proposed by Meier[56]. Each tetrahedron belongs to both a 4- and a 5-ring[66-67] of silicons and aluminiums and the units $(Si, Al)_{10}O_{20}$ are arranged in layers. Each layer is cross-linked to other layers by Si-O-Si, Si-O-Al bonds. Between these layers are open 10-ring and 8-ring channels parallel to the c-axis with free dimensions 4.4 x 7.2Å, 4.1 x 4.7Å and parallel to the a-axis is one set of channels with apertures 4 x 5.5Å.

1.4.2. Ion Exchange Studies in Clinoptilolite.

The ion exchange properties of clinoptilolite have been investigated more intensively than those of any other natural zeolite.

Ames[12] showed that both Cs_{137} and Sr_{90} can be selectively removed from radioactive waste water even in the presence of

high concentrations of competing cations and Honstead et al[68] (1960) showed that rare-earth cations and Co_{60} can also be isolated by ion exchange using clinoptilolite. As described earlier, Ames[21] (1967) and Mercer et al[22] (1969) also demonstrated the superior properties of clinoptilolite for the removal of ammonia and ammonium ions from municipal sewage treatment.

Howery and Thomas[69] (1965) reported a selectivity sequence of $C_s > NH_4 >> Na$ and more recently Chelishchev et al[35,70] (1974) reported a sequence of $Cs > Rb > K > Na > Sn > Li$ and $Pb > Ag > Cd \sim Zn \sim Cu > Na$ (1975). Selectivity reversals were observed for lead at 80% exchange and also for cadmium, copper and zinc at 20% exchange. Filizova[36] studied the exchange of caesium, thallium, mercury and silver, and the break-down of the clinoptilolite structure was observed. Their work differs from Chelishchev's results in some respects. Semmens[37], studied the exchange of sodium clinoptilolite with various heavy metals, the sequence obtained in this case was $Pb \sim Ba >> Cu, Zn, Cd$. All exchanges were reversible. Also Semmens[71] carried studies on the removal of lead, silver and cadmium by clinoptilolite in the presence of competing concentrations of calcium, magnesium and sodium. The observed selectivity sequence was $Pb > Ag > Cd$ and the competing cations strongly influenced removal. Townsend[72] examined the exchange of ammonium clinoptilolite with aminated copper and zinc and selectivity sequences for the exchanges over a range of compositions were obtained. Recently Dyer et al[73] carried studies on

natural clinoptilolite examining the mobilities of various ions.

Apart from the selectivity of clinoptilolite for inorganic ions, the selectivity of the zeolite for a series of organic cations has also been studied, using initially the sodium form. Various alkyl-ammonium cations revealed both ion-sieve[74] and volume-steric[75] exclusion effects[76].

1.5. Mordenite

Mordenite is found extensively in Nova Scotia, and is in fact named after a village in that locality. The occurrence is volcanic in origin[77]. Also sedimentary deposits are reported in the U.S.S.R., California and Nevada.

Apart from the natural occurrence, mordenite is synthesised on a large scale by the Norton Company and more recently by Laporte, but its properties differ from the natural material. In particular it can sorb larger molecules than the mineral.

Mordenite has a nearly constant Si:Al ratio of 5:1, giving the typical oxide formula as

$$Na_2O.Al_2O_3.10SiO_2.6H_2O$$

1.5.1. Structure of Mordenite.

The crystal structure of mordenite was determined by Meier[78] in 1961, who examined a sample of ptilolite. Ptilolite, flokite and ashtcnite are considered to have the same structure as mordenite[79]; the building unit is regarded to be $(Si,Al)_8O_{16}$[80].

The main features are large continuous elliptical channels which are parallel to the c-direction and have free dimensions $\sim$ 6.7 x 7.0Å Figure 1.4a. They are lined on both sides by side-pockets having entrances of $\sim$ 3.9Å free diameter which are directed along the b-direction Figure 1.4b. The pockets belonging to adjacent channels are displaced by $\frac{1}{2}$c with respect to each other. A pocket in one channel is linked to each of two pockets belonging to an adjacent channel by shared, distorted, 8-ring windows of free dimension $\sim$ 2.8Å. A sodium ion located in each of these 8-rings accounts for half the exchangeable cations in the zeolite [81].

Mordenite is characterised by the "small port" and "large port"[82] forms. The former sorb a negligible amount of benzene or cyclohexane, while the latter sorb 6.7 wt% of these molecules. One possible explanation for this is that the small port mordenite contains extraneous amorphous matter within the structure so that the ion exchange and sorption properties are affected[83,84]. Natural mordenites are mainly "small port", while the synthetic varieties may be either small or large port depending on the conditions during their synthesis[80].

1.5.2. Ion Exchange in Mordenite.

The rates of self-exchange of the ions potassium, rubidium and caesium were measured by Rao and Rees[85], using natural sodium mordenite from Nova Scotia.

Synthetic mordenite in its sodium form was used by Wolf[86] to study potassium, rubidium and caesium self-exchange kinetics.

FIG.1.4: Structure of mordenite.

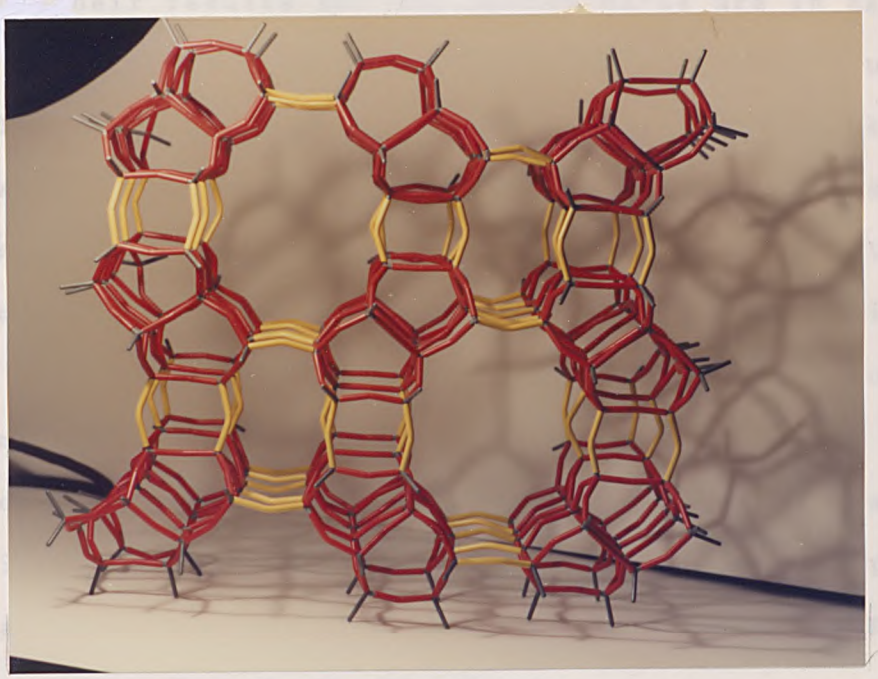

Figure 1.4a: Mordenite viewed in the c-direction.

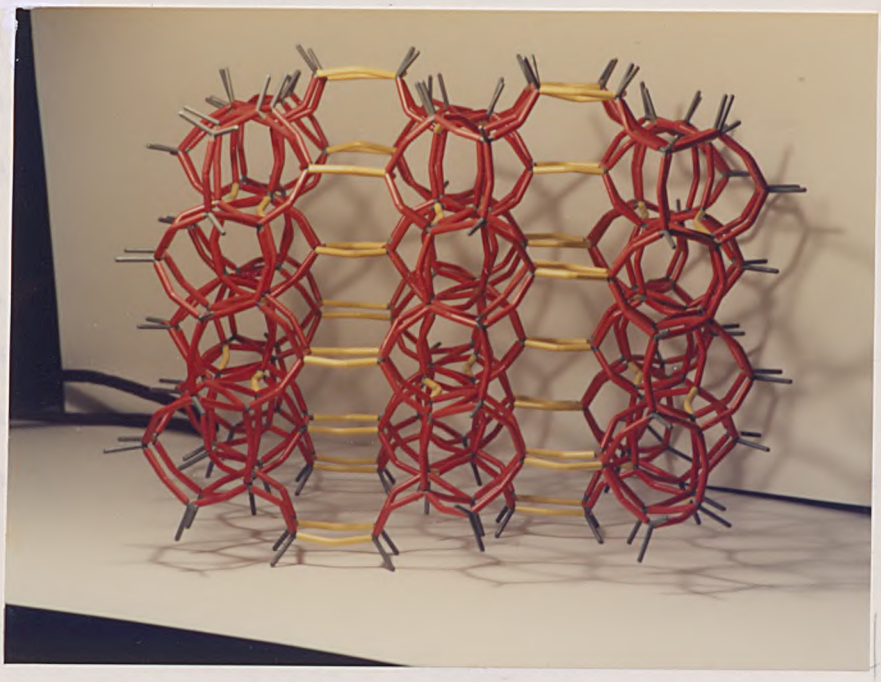

Figure 1.4b: Mordenite viewed in the b-direction.

Grivkova et al[87] presented isotherms for the ion exchange of the systems Na-Cs, NH_4-Cs, K-Cs, Rb-Cs using synthetic mordenite. In fact their results for the system Na-Cs are in agreement with those of Wolf[86] and Rao[85]. Barrer and Klinowski[81] undertook detailed studies of the exchange of alkali and alkaline earth metals in both sodium and ammonium mordenite. Barrer and Townsend[88-90] studied the exchange of transition metals in sodium and ammonium mordenite and gave the selectivity sequence $NH_4^+ > Na^+ > Mn^{+2} > Cu^{+2} > Co^{+2} \sim Zn^{+2} > Ni^{+2}$. In contrast, the amminated complexes of Cu^{+2}, Zn^{+2} and Co^{+2} were found to be preferred much more strongly than were the corresponding aquo ions[91]. Hagiwara et al[92] carried studies on (processed) natural mordenite for the ion pairs $Na^+ - NH_4^+$, Na-K, $K-NH_4$. Their results for the $Na-NH_4$ system are in agreement with earlier work[81]. Fletcher and Townsend[93] examined in detail the exchange of aqueous silver ions and the aminated species of silver, platinum and palladium using synthetic sodium mordenite. Also Susuki et al[94] obtained isotherms for the exchange of alkaline earth metal ions, hydrogen and ammonium ions using synthetic sodium mordenite. Very recently Golden et al[95], tested predicitions made by Barrer and Klinowski[81] and Barrer and Townsend[89] regarding ion exchange in mordenite. These predictions employed the triangle rule[89] and the recent tests[95] show good agreement between theory and experiment.

1.6. Ferrierite

Few studies were carried out on ferrierite after its discovery by Graham in 1918 until new locations were described in the late 1960's in Italy, California, Nevada, Japan and Austria.

The silica to alumina ratios are generally in the ranges 3.2 to 6.2 and the zeolite exhibits a tendency to be selective for potassium and magnesium. In the large deposit at Lovelock Nevada, where beds of ferrierite are associated with thick layers of pure montmorillonite and amorphous ash, high magnesium contents tend to characterise the montmorillonite whilst high potassium levels are found in the ferrierite.[96]

1.6.1. Structure of Ferrierite.

The structure of ferrierite has been determined by Vaughan[97] and Kerr[98] and consists of parallel 8-ring and 10-ring channels in the a–b plane, interconnected by 8-ring windows in the a–c plane, Figure 1.5. The dimensions of the 10-ring channels are 5.4 x 4.2Å and of the 8-ring windows 4.7 x 3.4Å. In the hydrated zeolite the cavities contain hydrated Mg^{+2} as shown. The Mg^{+2} ions are held tightly within the hydrated zeolite and are difficult to exchange.

1.6.2. Ion Exchange Studies in Ferrierite.

There are few literature reports on systematic studies on ion exchange in ferrierite. Since analyses of the natural material show high levels of potassium and magnesium in the mineral, a

preference for these ions is inferred. Barrer and Marshall[99,100], synthesised ferrierite and they found that it showed some preference for strontium. Synthesis by Vaughan[101] indicated a preference for lithium. Experiments by Hawkins[102] confirmed the earlier reference of Barrer and Marshall[99,100] that ferrierite preferred strontium over calcium. Following this, quite recently, Dyer et al[103] carried out studies on natural ferrierite from Lovelock, Nevada, examining the selectivities for ammonium ions, alkali and alkaline earth metals.

Figure 1.5 : Structure of ferrierite.
c-direction.

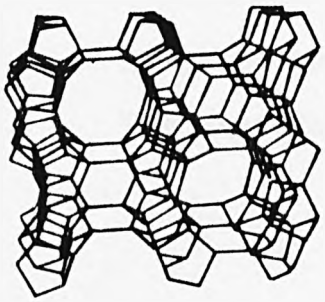

CHAPTER TWO THEORY

2.1. THE ION EXCHANGE ISOTHERM

2.1.1. Types of Binary Ion Exchange Isotherms

2.1.2. Partial Ion Exchange

2.2. THERMODYNAMICS OF ION EXCHANGE

2.2.1. Solution Phase Activity Corrections

2.2.2. Zeolite Phase Activity Coefficients

2.2.2.1. Prediction of Activity Coefficients

2.3. THERMODYNAMIC PROCEDURE FOR PARTIAL EXCHANGE

2.4. THE WATER ACTIVITY TERM IN THE EXCHANGER PHASE

2.5. THE IMPORTANCE OF THE THERMODYNAMIC APPROACH

2.5.1. Solution Concentration Changes

2.5.2. Temperature and Pressure Changes

2.1. The Ion Exchange Isotherm

The ion exchange process generally can be presented by the following equation[104] for the binary case.

$$z_A\ B_c^{z_B+} + z_B\ A_s^{z_A+} \rightleftharpoons z_A\ B_s^{z_B+} + z_B\ A_c^{z_A+} \quad ....2.1.$$

where z_A, z_B are the valencies of the exchange cations A and B and the subscripts (c) and (s) refer to the exchanger and solution phases respectively. The ion A which is the initial ion in the solution is called the counter ion.

The equilibrium properties of an ion exchange system are depicted by an isotherm. This is an equilibrium plot of the exchanging ion concentration in solution against the corresponding equilibrium concentration of the same ion in the zeolite at constant temperature and solution concentration (g equiv.dm^{-3}).

The equilibrium concentrations were frequently expressed as equivalent fractions A_s, A_c for the solution and exchanger phases respectively. For a binary exchange[105] the equivalent fractions are defined by

$$A_s = \frac{z_A\ m_A}{z_A m_A + z_B m_B} \quad ...2.2.$$

$$A_c = \frac{z_A\ M_A}{z_A M_A + z_B M_B} \quad ...2.3.$$

where m_A, m_B are the concentrations of ions A^{z_A+}, B^{z_B+} in

solution ($mol.dm^{-3}$) and M_A, M_B are the concentrations ($mol.kg^{-1}$) of the ions in the exchanger phase (normally by convention not the dry exchanger, but that which has taken up a known quantity of water by equilibration at constant temperature under a known and constant water vapour pressure).

To obtain an isotherm experimentally, different concentrations of the counter ion A are equilibrated with known quantities of exchanger but always keeping the total normality T_N of the solution constant. This is achieved by concomitantly altering the concentration of ion B in solution.

T_N must be kept constant because the selectivity of the zeolite for the counter ion A can be not only a function of A_c but also of total normality. So different total normalities will correspond to different isotherms and for a given A_c, A_s can take any value from 0 to 1 according to the magnitude of T_N. The concentrations ($mol.dm^{-3}$) of the ions A^{z_A+} and B^{z_B+} for a binary exchange can be determined from the expressions

$$m_A = \frac{A_s T_N}{z_A} \qquad \ldots 2.4.$$

$$T_N = z_A m_A + z_B m_B$$

$$m_B = \frac{(1 - A_s) T_N}{z_B} = \frac{B_s T_N}{z_B} \qquad \ldots 2.5.$$

since $B_s = 1 - A_s$ and $B_c = 1 - A_c$

The preference of an exchanger for one of two ions may be defined by the so-called separation factor α' where

$$\alpha' = \frac{A_c B_s}{B_c A_s} \qquad \ldots 2.6.$$

α' can be determined for any value of A_c from an isotherm from the ratio of Area I to Area II as shown in Figure 2.1. The conditions are then

$\alpha' > 1$	exchanger selective for A^{z_A+}
$\alpha' = 1$	exchanger shows no preference
$\alpha' < 1$	exchanger selective for B^{z_B+}

Since thermodynamic quantities describing ion exchange in zeolites usually are expressed in terms of molar concentrations ($mol.dm^{-3}$) in solutions separation factors can also be expressed the same way.

The appropriate molar separation quotient α is given by the expression

$$\alpha = \frac{A_c m_B}{B_c m_A} \qquad \ldots 2.7.$$

The two separation quotients α, α' are therefore related through

$$\alpha = (z_A/z_B)\alpha' \qquad \ldots 2.8.$$

The above is obtained by substituting equation 2.4. and 2.5., into 2.7.

If the exchange takes place between ions with the same valency so that $z_A = z_B$, then the two separation quotients are equal. Often ion exchange is between ions of different valencies (i.e. $z_A \neq z_B$) and then the requirements for the incoming

counter ion to be prefered are

$$\alpha = \frac{z_A}{z_B} \frac{\text{Area I}}{\text{Area II}} \qquad \ldots 2.9.$$

$\alpha > z_A/z_B$ exchanger selective for A^{z_A+}

$\alpha = z_A/z_B$ exchanger shows no preference

$\alpha < z_A/z_B$ exchanger is selective for B^{z_B+}

For any ion exchange reaction an expression can be obtained for the mass action quotient K_m.

Considering equation 2.1.

$$K_m = \frac{A_c^{z_B} \, m_B^{z_A}}{B_c^{z_A} \, m_A^{z_B}} \qquad \ldots 2.10$$

The separation quotient α can be related[106] to the mass action quotient K_m.

Rearranging equation 2.10

$$K_m^{1/z_A} = \frac{m_B}{B_c} \cdot \left(\frac{A_c}{m_A}\right)^{z_B/z_A}$$

$$K_m^{1/z_A} = \frac{A_c m_B}{B_c m_A} \cdot \left(\frac{A_c}{m_A}\right)^{-\frac{z_B - z_A}{z_A}}$$

$$\alpha = \frac{A_c m_B}{B_c m_A}$$

$$K_m^{1/z_A} = \alpha \left(\frac{A_c}{m_A}\right)^{\frac{z_B - z_A}{z_A}}$$

$$\alpha = K_m^{1/z_A} \cdot \left(\frac{A_c}{m_A}\right)^{\frac{z_A - z_B}{z_A}} \qquad \ldots 2.11$$

Equation 2.11 can be used to find the relation between α and K_m for any ion-exchange system.

In cases where the two ions have the same valencies (i.e. $z_A = z_B$) then $\alpha = K_m^{1/z_A}$ and thus for the simplest case $\alpha = K_m$ when $z_A = z_B = 1$, uni-univalent exchange.

2.1.1. Types of Binary Ion Exchange Isotherms

Considering zeolite ion exchange only, the various types of the ion exchange isotherms are shown in Figure 2.2. and can be arranged in three groups[107].

The first group consists of a set of simple isotherm shapes (Figure 2.2.a,b.c). 'a' shows preference for the ingoing ion as for example in the case of Na/NH_4 in mordenite[81]. 'b' shows no preference; a typical example is the Na/Sr exchange in phillipsite[108]. 'c' shows preference for the ion already present in the zeolite, as in the case of the Na/Li exchange in sodalite hydrate[109].

Group two comprises isotherms of sigmoidal shape as shown in Figure 2.2.d. The exchange of barium and ammonium ions in synthetic mordenite[81] gives this shape of isotherm.

A third group includes isotherms showing a hysteresis loop (Figure 2.2.e) as in the Li-Ag or Na-Ag exchanges in basic cancrinite[109]. Isotherms of this type are characteristic of an exchange system in which recrystallisation of the zeolite or felspathoid phase occurs during exchange.

2.1.2. Partial Ion Exchange

So far the isotherms shown exhibit 100% exchange of the initial ion for the incoming counter-ion. In Figure 2.3 isotherms are shown which arise from partial exchange, so that $A_c max < 1$. The partial exchange might arise from either the so-called ion-sieve[74] or volume-steric[75] effects. In the case of ion-sieving, the ingoing ions are larger than the channel apertures and therefore are excluded, the zeolite in effect acting as a "sieve". Thus for example, the ions $(CH_3)_4N^+$, $(C_2H_5)N^+$ are totally excluded from zeolite A[110-1]. The volume-steric effect arises when bulky ions exchange into channels. In the absence of an ion-sieve effect the incoming bulky ions already in the zeolite may have occupied all the available space and thus the crystal cannot accommodate more ions even though its exchange capacity limit has not been reached. Barrer, Papadopoulos and Rees[76] examined the exchange of sodium clinoptilolite with $(CH_3)_3NH^+$, $n\text{-}C_4H_9NH_3^+$ and $iso\text{-}C_3H_7NH_3^+$ and found that the exchange levels were 46,40,and 27% respectively of the full sodium replacement. Also Townsend[112] observed volume-steric effects for the exchange of nickel complexed with triethanolamine in ammonium mordenite.

Ion-sieve and volume-steric effects are not the only explanation for partial exchange however. Barrer and Klinowski[113] predicted the conditions under which partial exchange may arise using a statistical thermodynamic treatment of the ion exchange equilibrium. They showed that if A is the entering ion and B is the ion in the crystal, then exchange can only be incomplete

when $z_A < z_B$ and $\frac{N}{N_o} < \frac{1}{z_A}$. Where z_A, z_B are the charges of ions A and B, N is the number of available sites for the cations and N_o the total charge of the exchanger.

2.2. Thermodynamics of Ion Exchange

During an ion exchange reaction involving two or more ions, apart from the exchange of ions between the solution and the exchanger, some other changes may occur as well. These are sorption of solvent (usually water), salt imbibition, resistance to swelling during the solvent uptake giving rise to osmotic pressure, and finally weak and/or non-electrolyte sorption.

For the rigorous thermodynamic treatment of the ion exchange process a model must be considered which includes the influence of all the above factors.

For an exchange involving two ions (i.e. binary case) the phenomenological model of Gaines and Thomas[114] for exchange in clay minerals is quite adequate. Two cases were investigated. In the first case, the model consisted of an exchanger which was capable only of exchanging cations and adsorbing solvent from solution, but in which no imbibition of salt took place. In their second case, the exchanger was considered to be capable of all three functions. Regarding zeolites in particular, from experimental work[115] it has been shown that salt imbibition from solution occurs in exchangers at high salt comcentrations (> 0.5 mol.dm^{-3}). Also for zeolites, swelling during

the solvent uptake is negligible due to the rigid alumino-silicate structure[116]; thus osmotic pressures in zeolites can be very high (> 1000 atm).

For the work under consideration in this thesis, the first model of Gaines and Thomas may be used provided the solution concentrations are low ($\leq$ 0.5 mol.dm^{-3}). The model considers that the system consists of three phases, viz. vapour, solution and exchanger. The exchanger comprises the wet solid. This is so because the exchanger imbibes water and the degree of imbibition can be different for different ion-exchanged forms. Ignoring the water content of the solid means that a separate hydration term will contribute to the standard free energy of exchange. This complication can be avoided by considering the wet solid.

For a binary exchange, the exchange reaction can be written as (Section 2.1.)

$$z_B\, A^{z_A+}_{(s)} + z_A\, B^{z_B+}_{(c)} \leftrightharpoons z_B A^{z_A+}_{(c)} + z_A B^{z_B+}_{(s)} \qquad \ldots 2.11$$

The thermodynamic equilibrium constant is then

$$K_a = \frac{a_{A(c)}^{z_B}\; a_{B(s)}^{z_A}}{a_{A(s)}^{z_B}\; a_{B(c)}^{z_A}} \qquad \ldots 2.12$$

where $a_{A(c)}$ is the activity of ion A in the crystal phase and $a_{A(s)}$ the activity of the same ion in the solution phase.

The thermodynamic equilibrium constant, K_a, can be expressed either as the molal equilibrium constant or the rational equilibrium constant depending on the reference states chosen. The molal equilibrium constant K_a is given as

$$K_a = \frac{m_{A(c)}^{z_B} \cdot m_{B(s)}^{z_A} \cdot \gamma_{A(c)}^{z_B} \cdot \gamma_{B(s)}^{z_A}}{m_{A(s)}^{z_B} \cdot m_{B(c)}^{z_A} \cdot \gamma_{A(s)}^{z_B} \cdot \gamma_{B(c)}^{z_A}} \qquad \ldots 2.13$$

where $m_{A(s)}$, $m_{A(c)}$ are the concentration ($mol.Kg^{-1}$) of ion A in solution and the crystal respectively, $\gamma_{A(s)}$, $\gamma_{A(c)}$ are the solution and exchanger molal activity coefficients of ion A^{z_A+}. In this case the standard states for the exchanger phase and the solution phase are the hypothetical ideal molal solutions for each phase in terms of Henry's law. So in the standard states the molal equilibrium constant K_a is close to unity [117].

The <u>rational</u> thermodynamic equilibrium constant is expressed as

$$K_a = \frac{A_c^{z_B} \, f_A^{z_B} \, m_B^{z_A} \, \gamma_{B(s)}^{z_A}}{m_A^{z_B} \, \gamma_{A(s)}^{z_B} \, B_c^{z_A} \, f_B^{z_A}} \qquad \ldots 2.14$$

where A_c, B_c are the equivalent fractions of ions A and B in the exchanger, m_A, m_B are the concentrations ($mol.kg^{-1}$) of the same ions in solution, f_A, f_B are the <u>rational</u> activity coefficients in the exchanger for the corresponding ions and $\gamma_{A(s)}$, $\gamma_{B(s)}$ are molal activity coefficients of A and B in the solution phase.

For the rational equilibrium constant, the standard states chosen are different for the solution and exchanger phases. The standard states for the ions in the solution phase are defined in terms of the hypothetical ideal molal solutions of their salts, obeying Henry's law. Thus considering ion A^{z_A+}, $m_A = a_{A(s)} = \gamma_A = 1$ in the standard state, where m_A is the concentration ($mol.kg^{-1}$), $a_{A(s)}$ is the activity of ion A in solution and γ_A is the "individual ion activity coefficient" in solution (which, of course, cannot be evaluated - see however section 2.2.1). For the exchanger phase the standard states are chosen in terms of Raoult's law, and this requires the exchanger being in the respective homoionic forms. Since for equilibrium it must be true that the chemical potentials of the water (μ_w) be the same in all phases, then

$$\mu_{w(v)} = \mu_{w(s)} = \mu_{w(c)} \qquad ...2.15$$

where (v) refers to the vapour phase. This implies that in the standard state, when it must be true that

$\mu_{w(s)} = \mu^{\theta}_{w(s)}$, $\mu_{w(v)} = \mu^{\theta}_{w(v)}$ and $\mu_{w(c)} = \mu^{\theta}_{w(c)}$, then the water activity must be unity in all phases. For the exchanger phase this occurs when the zeolite has imbibed its equilibrium quantity of water after immersing the homoionic exchanger in an infinitely dilute solution of the same ion. Thus, the standard state of the exchanger phase is the homoionic form of the exchanger immersed in an infinitely dilute solution of the same ion. For the ion A^{z_A+} in the exchanger

in the standard state, $A_c = a_{A(c)} = f_A = 1$, where $a_{A(c)}$ is the activity of the ion in the crystal or exchanger phase and f_A is the activity coefficient of ion A^{z_A+} in association with its equivalent of the exchanger framework.

For the rest of the thermodynamic treatment described in this thesis, the rational equilibrium constant and rational activity coefficients will be employed.

The equilibrium constant K_a, as given by 2.14, can be related to the mass action quotient K_m as follows

$$K_m = \frac{A_c^{z_B} \cdot m_B^{z_A}}{B_c^{z_A} \cdot m_A^{z_B}} \qquad \ldots 2.15$$

$$K_a = K_m \frac{f_A^{z_B} \gamma_B^{z_A}}{f_B^{z_A} \gamma_A^{z_B}} \qquad \ldots 2.16$$

Also a third quotient K_c is used for the thermodynamic treatment. This is the so-called Kielland[118] quotient which is also termed the corrected selectivity coefficient because it includes the solution activity correction (section 2.2.1.).

The relation between the quotients is

$$K_c = K_m \Gamma \qquad \ldots 2.17$$

$$\Gamma = \frac{\gamma_B^{z_A}}{\gamma_A^{z_B}} \qquad \ldots 2.18$$

$$K_a = K_c \frac{f_A^{z_B}}{f_B^{z_A}} \qquad \ldots 2.19$$

The equilibrium constant K_a can be calculated as follows. Firstly the solution activity correction must be calculated in order to give K_c (equ.2.17), and then secondly, the evaluation of the rational activity coefficients of the ions in the exchanger, $f_A^{z_B}$, $f_B^{z_A}$ is undertaken in order to finally obtain K_a. The standard free energy per equivalent of exchange is then calculated from

$$\Delta G^{\circ} = \frac{-RT}{z_A z_B} \ln K_a \qquad \ldots 2.20$$

ΔG° is the free energy change per equivalent associated with the reaction described by equation 2.1 when the reactants proceed completely to products, all of the reactants and products being in their respective standard states.

For the ternary ion exchange[119] the standard states are the same as in the binary case stated above but there are now three reference states for each phase because of the presence of three ions A^{z_A+}, B^{z_B+}, C^{z_C+}. In contrast to the ion exchange involving two ions, three equations can be written to describe the ternary exchange reaction.

$$2z_B z_C A^{z_A+}_{(s)} + z_A z_C B^{z_B+}_{(c)} + z_A z_B C^{z_C+}_{(c)} \rightleftharpoons 2z_B z_C A^{z_A+}_{(c)} + z_A z_C B^{z_B+}_{(s)} + z_A z_B C^{z_C+}_{(s)} \qquad \ldots 2.21$$

$$z_B z_C A_{(c)}^{z_A+} + 2z_A z_C B_{(s)}^{z_B+} + z_A z_B C_{(c)}^{z_C+}$$

$$\rightleftharpoons z_B z_C A_{(s)}^{z_A+} + 2z_A z_C B_{(c)}^{z_B+} + z_A z_B C_{(s)}^{z_C+} \quad \ldots 2.22$$

$$z_B z_C A_{(c)}^{z_A+} + z_A z_C B_{(c)}^{z_B+} + 2z_A z_B C_{(s)}^{z_C+}$$

$$\rightleftharpoons z_B z_C A_{(s)}^{z_A+} + z_A z_C B_{(s)}^{z_B+} + 2z_A z_B C_{(c)}^{z_C+} \quad \ldots 2.23$$

Let Ka1, Ka2, Ka3 be the thermodynamic equilibrium constants corresponding to the reaction depicted in equations 2.21, 2.22,2.23 respectively.

Then

$$Ka1 = \frac{a_{B(s)}^{z_A z_C} \; a_{C(s)}^{z_A z_B} \; a_{A(c)}^{2z_B z_C}}{a_{B(c)}^{z_A z_C} \; a_{C(c)}^{z_A z_B} \; a_{A(s)}^{2z_B z_C}} = K_{m1} \Gamma_1 \Phi_1 \quad \ldots 2.24$$

where K_{m1} is the mass action quotient

$$K_{m1} = \frac{m_B^{z_A z_C} \; m_C^{z_A z_B} \; A_C^{2z_B z_C}}{B_C^{z_A z_C} \; C_C^{z_A z_B} \; m_A^{2z_B z_C}} \quad \ldots 2.25$$

Γ_1 is the ratio of solution-phase individual ion activity coefficients:

$$\Gamma_1 = \frac{\gamma_B^{z_A z_C} \; \gamma_C^{z_A z_B}}{\gamma_A^{2z_B z_C}} \quad \ldots 2.26$$

and Φ_1 is the ratio of activity coefficients for the ions

in the exchanger phase

$$\Phi_1 = \frac{\Phi_A^{2z_B z_C}}{\Phi_B^{z_A z_C}\ \Phi_C^{z_A z_B}} \qquad \ldots 2.27$$

Similarly

$$Ka2 = \frac{a_{A(s)}^{z_B z_C}\ a_{C(s)}^{z_A z_B}\ a_{B(c)}^{2z_A z_C}}{a_{A(c)}^{z_B z_C}\ a_{C(c)}^{z_A z_B}\ a_{B(s)}^{2z_A z_C}} \quad Km_2 \Gamma_2 \Phi_2 \qquad \ldots 2.28$$

$$Ka3 = \frac{a_{A(s)}^{z_B z_C}\ a_{B(s)}^{z_A z_C}\ a_{C(c)}^{2z_A z_B}}{a_{A(c)}^{z_B z_C}\ a_{B(c)}^{z_A z_C}\ a_{C(s)}^{2z_A z_B}} = Km_3 \Gamma_3 \Phi_3 \qquad \ldots 2.29$$

For the reaction 2.21, the free energy per equivalent of exchange is given by

$$\Delta G_1^{\circ} = -\left(\frac{RT}{z_A z_B z_C}\right) \ln K_{a1} \qquad \ldots 2.30$$

2.2.1. Solution Phase Activity Corrections

Values of the "single ion activity coefficients" cannot be obtained experimentally since ions in solution are accompanied by an equivalent number of ions of opposite charge in order that electrical neutrality be maintained. Mean molal activity coefficients for various salts are given in the literature[120],

but often the values do not extend over the appropriate range of ionic strength required. This problem can be overcome by appropriate extrapolation or interpolation using modified Debye-Hückel relationship[121] (Section 4.4.3.1.).

Although individual γ values cannot be determined, values of the ratio Γ can be obtained through algebraic manipulation of the experimentally measured[120] mean molal activity coefficients $(\gamma_{\pm})_{AX}$ and $(\gamma_{\pm})_{BX}$, where the subscripts AX, BX refer to salts with a common anion X.

The relations between $(\gamma_{\pm})_{AX}$ and $(\gamma_{\pm})_{BX}$ and the activity coefficients of the individual ions γ_A, γ_B are obtained from the definitions of the mean molal activity coefficients:

$$(\gamma_{\pm})_{AX} = (\gamma_A^{z_X} . \gamma_X^{z_A})^{\frac{1}{z_A + z_X}} \quad \ldots\ldots 2.31$$

$$(\gamma_{\pm})_{BX} = (\gamma_B^{z_X} . \gamma_X^{z_B})^{\frac{1}{z_B + z_X}} \quad \ldots\ldots 2.32$$

Thus

$$\ln(\gamma_{\pm})_{AX} = \frac{1}{z_A + z_X}\left[z_X \ln\gamma_A + z_A \ln\gamma_X\right] \quad \ldots\ldots 2.33$$

$$\ln(\gamma_{\pm})_{BX} = \frac{1}{z_B + z_X}\left[z_X \ln\gamma_B + z_B \ln\gamma_X\right] \quad \ldots\ldots 2.34$$

and multiplying 2.33 throughout by $\frac{z_B(z_A + z_X)}{z_X}$ and

2.34 by $\frac{z_A(z_B + z_X)}{z_X}$ gives

$$\frac{z_B(z_A + z_X)}{z_X} \ln(\gamma_{\pm})_{AX} = z_B \ln\gamma_A + \left(\frac{z_A z_B}{z_X}\right)\ln\gamma_X \quad \ldots\ldots 2.35$$

and

$$\left[\frac{z_A(z_B + z_X)}{z_X}\right] \ln(\gamma_{\pm})_{BX} = z_A \ln\gamma_B + \left(\frac{z_A z_B}{z_X}\right)\ln\gamma_X \quad \ldots\ldots 2.36$$

Subtracting 2.35 from 2.36 gives

$$\ln \Gamma = \ln\left[\frac{\gamma_B^{z_A}}{\gamma_A^{z_B}}\right] = \frac{1}{z_X}\left\{z_A(z_B + z_X)\ln(\gamma_{\pm})_{BX} - z_B(z_A + z_X)\ln(\gamma_{\pm})_{AX}\right\} \quad \ldots\ldots 2.37$$

However, the equation 2.37 expresses Γ in terms of the mean molal ionic activity coefficients of the pure salts AX, BX. What is in fact required is an expression which gives Γ in terms of the mean molal activity coefficients of the salts AX, BX in mixed solutions, which are the actual experimental conditions. These coefficients in a mixed binary

solution are denoted as $(\gamma_{\pm})^{(BX)}_{(AX)}$ (activity coefficient of AX in the presence of BX) and $(\gamma_{\pm})^{AX}_{BX}$ (activity coefficient of BX in the presence of AX). For the binary case Glueckauf[122] extended Guggenheim's[123] original theory to derive expressions for these quantities in terms of the pure salt mean molal activity coefficients. The resulting equations are

$$\log(\gamma_{\pm})^{(BX)}_{(AX)} = \log(\gamma_{\pm})_{AX} - \frac{m_B}{4I}\left[K_1 \log(\gamma_{\pm})_{AX} - K_2 \log(\gamma_{\pm})_{BX} - \frac{K_3}{1+I^{\frac{1}{2}}}\right] \quad \ldots\ldots 2.38$$

and

$$\log(\gamma_{\pm})^{(AX)}_{(BX)} = \log(\gamma_{\pm})_{BX} - \frac{m_A}{4I}\left[K_4 \log(\gamma_{\pm})_{BX} - K_5 \log(\gamma_{\pm})_{AX} - \frac{K_6}{1+I^{\frac{1}{2}}}\right] \quad \ldots\ldots 2.39$$

where $K_1, K_2, K_3, K_4, K_5, K_6$ are constants[105] and I is the ionic strength of the solution

$$I = \frac{1}{2} \sum_i m_i z_i^2 \quad \ldots\ldots 2.40$$

$$K_1 = z_B(2z_B - z_A + z_X)$$
$$K_2 = z_A(z_B + z_X)^2 (z_A + z_X)^{-1}$$
$$K_3 = \tfrac{1}{2} z_A z_B z_X (z_A - z_B)^2 (z_A + z_X)^{-1}$$
$$K_4 = z_A (2z_A - z_B + z_X)$$
$$K_5 = z_B (z_A + z_X)^2 (z_B + z_X)^{-1}$$
$$K_6 = \tfrac{1}{2} z_A z_B z_X (z_B - z_A)^2 (z_B + z_X)^{-1}$$

The ratio Γ in mixed solutions is given by analogy with equation 2.37 as

$$\ln\Gamma = \frac{1}{z_X}\left\{z_A(z_B + z_X)\ln(\gamma_{\pm})_{BX}^{AX} - z_B(z_A + z_X)\ln(\gamma_{\pm})_{(AX)}^{(BX)}\right\} \quad \ldots\ 2.41$$

The first step is thus to calculate $(\gamma_{\pm})_{AX}^{(BX)}$ and $(\gamma_{\pm})_{BX}^{(AX)}$ in terms of $(\gamma_{\pm})_{AX}$ and $(\gamma_{\pm})_{BX}$ over the range of I values covered by the isotherm solutions then Γ as a function of composition can be obtained from 2.41.

For exchanges involving three salts Fletcher and Townsend[124] derived various equations for the ratios and then extended Glueckauf's treatment to yield a generalized equation for $\gamma_{\pm}$ values in mixed solutions. The simplest case they considered involved three salts having a common anion X, the salts being AX, BX, CX. The mean stoichiometric activity coefficients and their corresponding single ion activity coefficients are related by[125]

$$\ln\gamma_{\pm AX} = \frac{1}{z_A + z_X}(z_X\ln\gamma_A + z_A\ln\gamma_X) \quad \ldots\ 2.42$$

$$\ln\gamma_{\pm BX} = \frac{1}{z_B + z_X}(z_X\ln\gamma_B + z_B\ln\gamma_X) \quad \ldots\ 2.43$$

$$\ln\gamma_{\pm CX} = \frac{1}{z_C + z_X}(z_X\ln\gamma_C + z_C\ln\gamma_X) \quad \ldots\ 2.44$$

Multiplying equation 2.42 by $z_B z_C z_X^{-1}(z_A + z_X)$, equation 2.43 by $z_A z_C z_X^{-1}(z_B + z_X)$ and equation 2.44 by $z_A z_B z_X^{-1}(z_C + z_X)$, followed by elimination of terms involving

γ_X, yielded expressions for the Γ ratios in terms of salt activity coefficients:

$$\ln(\Gamma_3/\Gamma_1) = \frac{3}{z_X} \ln(\xi_{AX}/\xi_{CX}) \quad \ldots. 2.45$$

$$\ln(\Gamma_3/\Gamma_2) = \frac{3}{z_X} \ln(\xi_{BX}/\xi_{CX}) \quad \ldots. 2.46$$

where

$$\xi_{AX} = \gamma_{\pm AX}^{z_B z_C (z_A + z_X)}$$

$$\xi_{BX} = \gamma_{\pm BX}^{z_A z_C (z_B + z_X)} \quad \ldots. 2.47$$

$$\xi_{CX} = \gamma_{\pm CX}^{z_A z_B (z_C + z_X)}$$

The generalised equations (for this case) for the Γ ratios in mixed solutions are

$$\ln(\Gamma_3/\Gamma_1) = \frac{3}{z_X} \ln(\xi_{AX}/\xi_{CX}) - \frac{1.727}{z_X I}\Big(\tau_1 \log \xi_{AX} + \tau_2 \log \xi_{CX} + \tau_3 (1 + I^{-\frac{1}{2}})^{-1} + [z_B z_C (z_A + z_X)\tau_1 + z_A z_B (z_C + z_X)\tau_2] \log Q\Big)$$

$\ldots. 2.48$

where

$$\tau_1 = z_A m_A (z_A + z_X) - z_B m_B (z_A - 2z_B - z_X) - z_C m_C (z_A - 2z_C - z_X)$$

$$\tau_2 = z_A m_A (z_C - 2z_A - z_X) + z_B m_B (z_C - 2z_B - z_X) - z_C m_C (z_C + z_X)$$

$$\tau_3 = z_A z_B z_C z_X (z_C - z_A)\left[(z_A m_A - z_C m_C)(z_C - z_A) + z_B m_B (z_A + z_C - 2z_B)\right]$$

and

$$\ln(\Gamma_3/\Gamma_2) = \frac{3}{z_X}\ln(\xi_{BX}/\xi_{CX}) - \frac{1.727}{z_X I}(\tau_4 \log \xi_{BX} + \tau_5 \log \xi_{CX} + \tau_6 (1 + I^{-\frac{1}{2}})^{-1} + z_A z_C (z_B + z_X)\tau_4 + z_A z_B (z_C + z_X)\tau_5 \log Q)$$

where

$$\tau_4 = z_B m_B (z_B + z_X) - z_A m_A (z_B - 2z_A - z_X) - z_C m_C (z_B - 2z_C - z_X)$$

$$\tau_5 = z_B m_B (z_C - 2z_B - z_X) + z_A m_A (z_C - 2z_A - z_X) - z_C m_C (z_C + z_X)$$

$$\tau_6 = z_A z_B z_C z_X (z_C - z_B)[(z_B m_B - z_C m_C)(z_C - z_B) + z_A m_A (z_B + z_C - 2z_A)]$$

.... 2.49

2.2.2. Zeolite Phase Activity Coefficient

To determine the solid phase activity coefficient for the binary case Gaines and Thomas[114] model is appropriate.

The system is considered to consist of three phases **vapour (v)** solution(s) and exchanger(c). At equilibrium the water chemical potential is the same for all three phases

$$\mu_w(v) = \mu_w(s) = \mu_w(c) = \mu_w(c)^{\theta} + RT \ln a_W(c) \quad .... 2.50$$

at a given temperature and pressure.

$a_{w(c)}$ is the activity of water in the exchanger and $\mu_{w(c)}$ is the water chemical potential in the exchanger.

Also for ions A and B

$$\mu_A(s) = \mu_A(c) = \mu_A(c)^{\theta} + RT \ln a_A(c) = \mu_{A(c)}^{\theta} + RT \ln A_c f_A$$

.... 2.51

$$\mu_B(s) = \mu_B(c) = \mu_B^{\theta}(c) + RT\ln a_B(c) = \mu_B^{\theta}(c) + RT\ln B_c f_B$$

.... 2.52

For a system at equilibrium

$$SdT - VdP + \Sigma_i n_i \, d\mu_i = 0 \qquad \text{.... 2.53}$$

and at constant temperature and pressure the Gibbs-Duhem equation is obtained.

$$\Sigma_i n_i \, d\mu_i = 0 \qquad \text{.... 2.54}$$

where n_i is the number of moles of the ith component of a particular phase. Expression 2.53 can be applied to exchanger phase but under the following conditions. The summation must include the minimum number of separate components in the exchanger that serve to define the system as a whole, but salt imbibition is ignored. This implies that the total number of exchange sites per mole of exchanger is invariant, (a variable exchange capacity, which could arise in the case of salt imbibition requires the inclusion of this factor as an independent variable component).

Combining equations 2.50, 2.51, 2.52, 2.54

$$n_w RTd\ln a_w(c) + n_A RTd\ln A_c f_A + n_B RTd\ln B_c f_B = 0 \qquad \text{.... 2.55}$$

The terms in RT cancel, and multiplying through by

$$\frac{z_A z_B}{z_A n_A + z_B n_B}$$

puts the equation in terms of equivalent fractions of ions in the zeolite.

$$\frac{n_W z_A z_B}{z_A n_A + z_B n_B} \, d \ln a_W(c) + \frac{n_A z_A}{z_A n_A + z_B n_B} \, z_B d\ln A_c f_A +$$

$$+ \frac{n_B z_B}{z_A n_A + z_B n_B} \, z_A d\ln B_c f_B = 0 \qquad \ldots\ 2.56$$

since $A_c + B_c = 1$

$$n_W z_A z_B d\ln a_W(c) + z_B A_c d\ln A_c f_A + z_A B_c d\ln B_c f_B = 0 \qquad \ldots\ 2.57$$

Separating the logarithmic terms and simplifying

$$n_W z_A z_B d\ln a_W(c) + z_B dA_c + z_A dB_c + A_c d\ln f_A^{z_B} + B_c d\ln f_B^{z_A} = 0 \qquad \ldots\ 2.58$$

Expressions for $f_A^{z_B}$, $f_B^{z_A}$ are obtained using equation 2.19

$$K_a = K_c \, f_A^{z_B} / f_B^{z_A} \qquad \ldots\ 2.19$$

Taking the logarithms of the above equation

$$\ln K_a = \ln K_c + \ln f_A^{z_B} - \ln f_B^{z_A} \qquad \ldots\ 2.59$$

and

$$d\ln K_c + d\ln f_A^{z_B} - d\ln f_B^{z_A} = 0 \qquad \ldots\ 2.60$$

Combining 2.58 and 2.60, explicit expressions for f_A and f_B can be derived by elimination of either f_A or f_B to give

$$d\ln f_A^{z_B} = (z_B - z_A) dB_c - B_c d\ln K_c - n_w z_A z_B d\ln a_W(c) \qquad \ldots\ 2.61$$

$$d\ln f_B^{z_A} = -(z_B - z_A)dA_c + A_c d\ln K_c - n_w z_A z_B d\ln a_w(c)$$

.... 2.62

Gaines and Thomas evaluated these expressions by integrating between the standard states and the experimental value of A_c. For the case of f_A, the integration is between $f_A^{z_B} = A_c = 1$ and $f_A^{z_B}$ at A_c. In the case of a zeolite it can generally be assumed that the water activity term is negligible[106]. If the water activity term is ignored then $f_A^{z_B} = 1$ at $A_c = 1$ even when the concentration of ions in the solution phase is not zero[126].

The integration of the equation 2.61 then becomes

$$\int_{f_A=A_c=1}^{f_A(A_c)} d\ln f_A^{z_B} = (z_B - z_A)\int_1^{A_c} dB_c - \int_{K_c(A_c=1)}^{K_c(A_c)} (1 - A_c)d\ln K_c$$

.... 2.63

Integrating 2.62:

$$\int_{f_B(B_c=1)}^{f_B(B_c)} d\ln f_B^{z_A} = -(z_A - z_B)\int_{B_c=1}^{B_c} dA_c + \int_{K_c(B_c=1)A_c=0}^{A_c} A_c d\ln K_c \quad .... 2.64$$

Equation 2.63 gives

$$\ln f_A^{z_B} = (z_B - z_A)B_c - \int_{K_c(A_c=1)}^{K_c(A_c)} (1 - A_c)d\ln K_c$$

.... 2.65

Transformation of the integrals gives

$$\ln f_A^{z_B} = (z_B - z_A)B_c - \ln K_c^{(A_c)} + A_c \ln K_c^{(A_c)} + \int_{A_c}^{1} \ln K_c \, dA_c \qquad \ldots.2.66$$

where $\ln K_c^{(A_c)}$ is the value of $\ln K_c$ at A_c.

Similarly

$$\ln f_B^{z_A} = -(z_B - z_A)A_c + A_c \ln K_c^{(A_c)} - \int_{0}^{A_c} \ln K_c \, dA_c \qquad \ldots. \; 2.67$$

The substitution of 2.66, 2.67 into 2.19 gives

$$\ln K_a = (z_B - z_A) + \int_{0}^{1} \ln K_c \, dA_c \qquad \ldots. \; 2.68$$

Using equation 2.68 the thermodynamic equilibrium constant K_a can be obtained by graphical or analytical integration of a plot of $\ln K_c$ against A_c using data derived from the experimental isotherm.

For the case of ternary ion exchange Fletcher and Townsend[126] derived expressions for the evaluation of activity coefficients following the Gaines and Thomas[114] approach for the binary case. The activity coefficients ϕ_A, ϕ_B, ϕ_C can be determined directly using data from the ternary exchange equilibrium isotherm.

Elprince and Babcock[127] followed a different approach for ternary ion exchange in clays. Instead of calculating

phenomenological activity coefficients from a ternary equilibrium isotherm, they used binary data to predict activity coefficients for ternary ion exchange using a model similar to Guggenheim's[123] original approach for the solution phase.

2.2.2.1. Prediction of Activity Coefficients

Elprince and Babcock[127] started with an expression for the excess Gibbs energy g^E (J mole^{-1}) in terms of the mole fractions of all components.

$$\frac{\partial}{\partial n_i}\left[n_T\, g^E\right]_{nj,T,P} = RT \ln f_i \qquad \ldots. 2.69$$

$$g^E = RT \sum_{i=1}^{m} N_i \ln f_i \qquad \ldots. 2.70$$

where

n_T is the total number of moles of ions present, n_i, n_j are the moles of the ions i,j, f_i is the rational activity coefficient of ion i in the solid phase and N_i its equivalent fraction.

They then used Wilson's equation[128] to express the excess free energy of non ideal mixtures

$$\frac{g^E}{RT} = -\sum_{i=1}^{m} N_i \ln\left[\sum_{j=1}^{m} \Lambda_{ij} N_j\right] \qquad \ldots. 2.71$$

where

$$\Lambda_{ij} = (\nu_j/\nu_i)\exp\left[-(\lambda_{ij} - \lambda_{ii})/RT\right] \qquad \ldots. 2.72$$

ν_j, ν_i are the molar volumes of the pure components

and $(\lambda_{ij} - \lambda_{ii})$ is related to the difference in interaction energy between unlike (ij) and like (ii) ion pairs. Λ_{ij} is thus an excess interaction term arising when ion i interacts with ion j, rather than with another ion i.

Substituting equation 2.71 into 2.69 the activity coefficient f_i can be expressed in a generalised form as follows:

$$\ln f_i = 1 - \left\{ \ln\left[\sum_{j=1}^{m} N_j \Lambda_{ij} \right] \right\} - \sum_{k=1}^{m} \frac{N_K \Lambda_{ki}}{\sum_{j=1}^{m} N_j \Lambda_{kj}} \qquad \ldots\ldots 2.73$$

From 2.73 it is clear that only binary coefficients are involved. Also the interaction energy between like ion pairs (Λ_{ii}, Λ_{jj} etc) is taken as being equal to unity.

For the binary case involving ions A and B equation 2.73 reduces to

$$\ln f_A = -\ln(N_A + \Lambda_{AB} N_B) + N_B \left[\frac{\Lambda_{AB}}{N_A + \Lambda_{AB} N_B} - \frac{\Lambda_{BA}}{\Lambda_{BA} N_A + N_B} \right] \qquad \ldots\ldots 2.74$$

$$\ln f_B = -\ln(N_B + \Lambda_{BA} N_A) + N_A \left[-\frac{\Lambda_{AB}}{N_A + \Lambda_{AB} N_B} + \frac{\Lambda_{BA}}{\Lambda_{BA} N_A + N_B} \right] \qquad \ldots\ldots 2.75$$

where f_A, f_B are activity coefficients obtained experimentally from the exchange isotherm.

The aim is then to estimate Λ_{AB}, Λ_{BA} from the equations 2.74

2.75 by solving them using an iterative scheme.

For the prediction of ternary activity coefficient data three binary exchange isotherms must be used. The three binary isotherms yield values of $f_{A(B)}$, $f_{A(C)}$, $f_{B(A)}$, $f_{B(C)}$, $f_{C(A)}$ and $f_{C(B)}$. Then for the ternary exchange involving the three ions A,B,C the activity coefficients ϕ_A, ϕ_B, ϕ_C are obtained from 2.73 to give

$$\begin{aligned} \ln\phi_A = 1 &- \left[\ln\left\{N_A + N_B\Lambda_{AB} + N_C\Lambda_{AC}\right\}\right] \\ &- \left\{N_A/(N_A + N_B\Lambda_{AB} + N_C\Lambda_{AC}) \right. \\ &+ N_B\Lambda_{BA}/(N_A\Lambda_{BA} + N_B + N_C\Lambda_{BC}) \\ &\left. + N_C\Lambda_{CA}/(N_A\Lambda_{CA} + N_B\Lambda_{CB} + N_C)\right\} \quad \ldots\ 2.76 \end{aligned}$$

$$\begin{aligned} \ln\phi_B = 1 &- \left[\ln\left\{N_A\Lambda_{BA} + N_B + N_C\Lambda_{BC}\right\}\right] \\ &- \left\{N_A\Lambda_{AB}/(N_A + N_B\Lambda_{AB} + N_C\Lambda_{AC}) \right. \\ &+ N_B/(N_A\Lambda_{BA} + N_B + N_C\Lambda_{BC}) \\ &\left. + N_C\Lambda_{CB}/(N_A\Lambda_{BA} + N_B\Lambda_{CB} + N_C)\right\} \quad \ldots\ 2.77 \end{aligned}$$

$$\begin{aligned} \ln\phi_C = 1 &- \left[\ln\left\{N_A\Lambda_{CA} + N_B\Lambda_{CB} + N_C\right\}\right] \\ &- \left\{N_A\Lambda_{AC}/(N_A + N_B\Lambda_{AB} + N_C\Lambda_{AC}) \right. \\ &+ N_C\Lambda_{BC}/(N_A\Lambda_{BA} + N_B + N_C\Lambda_{BC}) \\ &\left. + N_C/(N_A\Lambda_{CA} + N_B\Lambda_{CB} + N_C)\right\} \quad \ldots\ 2.78 \end{aligned}$$

Using equations 2.76, 2.77, 2.78 the activity coefficients ϕ_A, ϕ_B, ϕ_C for the ternary exchange can then be evaluated

since all the interaction energies (Λ_{AB}, Λ_{AC}, etc) have been obtained from the binary data.

2.3. Thermodynamic Procedure for Partial Exchange

As stated in Section 2.1.2 the maximum level of exchange in many ion exchange systems is less than one, so partial exchange takes place.

For cases of partial ion exchange Sherry[129-130] Barrer, Rees and Samzuzzoha[131] "normalised" their isotherm by expressing the exchange in terms of the exchangeable cations only. If the maximum level of exchange is $A_{c(max)}$ for the counter ion A^{z+}_A, then the normalised equivalent fraction of ion A in the zeolite is A^N_c.

A^N_c and A_c are related by the normalising factor f_N, where

$$A^N_c = f_N A_c \qquad \ldots\ 2.79$$

$$f_N = \frac{1}{A_{c(max)}} \qquad \ldots\ 2.80$$

Then

$$B^N_c = 1 - A^N_c \qquad \ldots\ 2.81$$

The ions in the zeolite that do not exchange with the counter ion are regarded as part of the zeolite lattice.

For the thermodynamic treatment the standard states remain the same (section 2.2.) but the total exchange capacity now corresponds to the maximum level of exchange achieved by A^{z+}_A, rather than that achieved by B^{z+}_B. The Gaines and Thomas[114] expression for K_a for the binary case becomes

$$\ln K_a = (z_B - z_A) + \int_0^1 \ln K_c^N \, dA_c^N \qquad \ldots. \; 2.82$$

where K_c^N is the normalized Kielland quotient. For ternary exchange no simple procedure is possible, studies are under way at present to solve this problem.

The normalisation approach was criticized by Vansant and Uytterhoeven[132] for two reasons. Firstly they stated that the normalization procedure was based on the assumption that the unexchanged fraction of the ion has no influence on the exchange equilibria. Secondly they considered that the normalization procedure made no allowance for $A_{c(max)}$ being a function of temperature. On this basis they proposed a new procedure for the determination of K_a which involves an **extra** integration from $A_{c(max)}$ to $A_c = 1$.

Since not all the sites into which $B^{z\dagger}_A$ can exchange are accessible to $A^{Z\dagger}_A$ it follows that the standard state for the A zeolite is physically unattainable and the <u>standard state</u> is consequently the homoionic zeolite in terms of the exchanger capacity with respect to the original ion $B^{z\dagger}_B$

This hypothetical standard state is problematical in that the properties cannot be inferred by extrapolation from a situation in which the system is behaving ideally. Barrer, Klinowski and Sherry[133] then justified their original normalization procedure in terms of formulation in which ΔG^θ was factorised into site sets. Their arguments are summarized elsewhere[134].

2.4. The Water Activity Term in the Exchanger Phase

In the Gaines and Thomas[114] treatment of ion exchange, the water activity term is taken into consideration. For exchanges involving two ions most workers have ignored the water terms when calculating activity coefficients and standard free energy values. If this assumption is not valid the error in calculating ΔG^{θ} can be substantial.

This possible error is introduced by ignoring the fact that the standard states for the exchanger phase are each homoionic solid in equilibrium with an infinitely dilute solution of the relevant ion[114]. In fact the actual exchange experiments are performed at a total solution normality T_N. Under these conditions the activity of the water in each of the homoionic A and B zeolites when contacted respectively with solution A^{z+}_A and B^{z+}_B of normality T_N will not necessarily be unity. Also, from the Gibbs-Duhem equation, it follows that the activity coefficients f_A in the A zeolite and f_B in the B zeolite will deviate from unity[126] even though the zeolite is still in its homoionic form

The expression for K_a in the binary case is

$$\ln K_a = (z_B - z_A) + \int_0^1 \ln K_c \, dA_c + \Delta \qquad \ldots. 2.90$$

where[108]

$$\Delta = -z_A z_B \left[\int_1^{a_w(a)} n_w^A \, d\ln a_w + \int_{a_W(a)}^{a_W(b)} n_w^{AB} d\ln a_W - \int_1^{a_w(b)} n_w^B d\ln a_W \right]$$

$$\ldots. 2.91$$

Applying the mean value theorem[106] the equation 2.91 is transformed to

$$\Delta = -z_A z_B \left[\bar{n}^{A}_{w} \ln a_w(a) + \bar{n}^{AB}_{w} \ln \frac{a_w(b)}{a_w(a)} - \bar{n}^{B}_{w} \ln a_w(b) \right] \quad \ldots\ldots 2.92$$

where $\bar{n}^{A}_{w}$, $\bar{n}^{B}_{w}$ are the mean water contents of the homoionic A and B forms of the zeolite in transition from the infinitely dilute solutions to T_N and the water activities are $a_w(a)$, $a_w(b)$ respectively. $\bar{n}^{AB}_{w}$ is the mean water content of the exchanger in passing from homoionic A to homoionic B zeolite. When the exchange is carried out in dilute solution $\ln \frac{a_w(b)}{a_w(a)} \rightarrow 0$ since Raoult's law applies and equation 2.92 reduces to

$$\Delta = -z_A z_B \left[\bar{n}^{A}_{w} - \bar{n}^{B}_{w} \right] \ln a_W \quad \ldots\ldots 2.93$$

Barrer and Klinowski[106] calculated values of Δ using equations 2.91 to 2.93, for exchanges in zeolite A as well as in organic resins. The Δ values obtained were very small. Though the values of the first and third integral of the equation 2.91 could be larger, in fact their contribution was always small due to their opposite sign. The second term involving n^{AB}_{w}, was generally found to be at least an order of magnitude lower than the other two terms and therefore insignificant.

So for determination of the thermodynamic equilibrium constant K_a the Δ term is ignored up to solution normalities of around unity.

Fletcher and Townsend[126] examined the effect of the water activity term on ternary exchange data. They obtained values of the activity coefficient ϕ_{Na}, ϕ_K, ϕ_{Li}, ϕ_{Ca} at $Na_c = K_c = Li_c = Ca_c = 1$ at different total solution normalities. The error introduced by ignoring the change in water activity which occurs in moving from the standard states to a normality of 0.1 equiv.dm^{-3} is found to be <1%, which is within the experimental uncertainty. At much higher concentrations the error was significant. For concentrations up to 0.5 equiv.dm^{-3} however, the general condition was that the contribution of the water terms to the ternary equilibrium constant K_{ai} could be ignored.

2.5. The Importance of the Thermodynamic Approach

So far in this discussion the aim has been to calculate the thermodynamic equilibrium constant K_a, which refers to a particular free energy ΔG^θ for a given reference state (eg latm p 298K). K_a is constant irrespective of the solution strength at which it is determined. The importance of the thermodynamic approach is that in principle the value of K_a so obtained can be used to predict the behaviour of a particular system for a range of conditions, without having to carry out further experiments. The changes can be in the external solution total normality T_N, the temperature, and also the pressure of the system.

2.5.1. Solution Concentration Changes

In a significant contribution towards the development of reliable prediction of ion exchange equilibria, Barrer and Klinowski[106] showed that while the solid phase ion activity coefficients f_A, f_B do change with external solution concentration, their ratio remains nearly constant.

This implies that an isotherm shape can be predicted at a certain total normality provided an experimental isotherm exists over the complete composition range for one particular value of the total solution normality.

Considering Gaines' and Thomas' treatment[114] once more, and taking into consideration the water activity terms, the expressions for the activity coefficients of ions A and B in the exchanger phase are as follows, for the binary case

$$\ln f_A^{z_B} = (z_B - z_A)B_c - \ln K_c^{(A_c)} + A_c \ln K_c^{(A_c)} + \int_{A_c}^{1} \ln K_c \, dA_c - z_A z_B \left[\int_{1}^{a_w(a)} n_w^A \, d\ln a_w + \int_{a_w(a)}^{a_w(A_c)} n_w^{AB} d\ln a_w \right] \quad \ldots. 2.94$$

$$\ln f_B^{z_A} = -(z_B - z_A)A_c + A_c \ln K_c^{(A_c)} - \int_{0}^{A_c} \ln K_c \, dA_c + z_A z_B \left[\int_{a_W(A_c)}^{a_W(b)} n_w^{AB} \, d\ln a_w - \int_{1}^{a_w(b)} n_w^B \, d\ln a_w \right] \quad \ldots. 2.95$$

The value of the square brackets of the expressions (2.94

2.95) were evaluated[106] and they were found to be quite significant in themselves for the estimation of the activity coefficients f_A, f_B. Therefore as the external solution concentration is changed and the activity of the water in the exchanger changes, the $f_A^{z_B}$, $f_B^{z_A}$ values change concomitantly. Thus a given value of A_c can correspond to different values of f_A, f_B, depending on the external solution concentration. Combining expressions 2.94, 2.95 gives

$$\ln\left[\frac{f_A^{z_B}}{f_B^{z_A}}\right] = (z_B - z_A) - \ln K_c^{A_c} + \int_0^1 \ln K_c \, dA_c + \Delta \qquad \ldots. \; 2.96$$

and using equation 2.90

$$\ln\left[\frac{f_A^{z_B}}{f_B^{z_A}}\right] = \ln K_a - \ln K_c^{(A_c)} + \Delta \qquad \ldots. \; 2.97$$

Since $K_c^{(A_c)}$ is the value of the Kielland quotient at a particular A_c value, the only factors that can influence the <u>ratios</u> of the activity coefficients are the value of Δ and the level of salt imbibition. The water activity term Δ is small[106] and the salt imbibition at low concentrations is negligible[115]. Thus Barrer and Klinowski[106] concluded that $\frac{f_A^{z_B}}{f_B^{z_A}}$ must be near-independent of external solution if the total solution normalities are low. Transformation of equations 2.10 and 2.16 results (for a given value of A_c) in the expression

$$\left(\frac{m_B^{z_A}}{m_A^{z_B}}\right)\Gamma = \left[\frac{K_a f_B^{z_A}}{f_A^{z_B}}\right] \frac{(1 - A_c)^{z_A}}{A_c^{z_B}} = \text{constant}$$

.... 2.98

Thus, provided activity coefficnet data for the two salts are available for the range of total electrolyte concentrations which are of interest, values of $(m_B^{z_A}\,\Gamma)/m_A^{z_B}$ can be computed[119] for different ratios of the two ions $A^{z_A^+}$ and $B^{z_B^+}$ at each total tolution concentration. Since for binary exchange it is also true that

$$z_A m_A + z_B m_B = T_N \qquad \text{.... 2.99}$$

m_A values for the solution can be predicted for any value of A_c over a range of total solution concentrations.[119]

2.5.2. Temperature and Pressure Changes

In this section it is indicated how the thermodynamic parameters K_a, ΔG^θ obtained at a particular temperature and pressure can be used to predict the behaviour of the system when the temperature or pressure changes[135]

From the definition of free energy

$$G = H - TS \qquad \text{.... 2.100}$$

the so-called master equation

$$dG = \bar{V}dP - SdT \qquad \text{.... 2.101}$$

may be derived, combining the 1st and 2nd Laws of Thermodynamics. Also, at constant temperature, for a reaction

$$\Delta G^{\theta} = \Delta H^{\theta} - T\Delta S^{\theta} \quad \ldots\ 2.102$$

Under standard conditions the master equation 2.101 becomes

$$d\Delta G^{\theta} = \Delta V^{\theta} dP - \Delta S^{\theta} dT \quad \ldots\ 2.103$$

where ΔH^{θ} is the standard enthalpy change for the reaction (2.1), ΔV^{θ} is the standard volume change of the system (ion exchanger plus solution and vapour).

At constant temperature 2.103 becomes

$$\left(\frac{\partial \Delta G^{\theta}}{\partial P}\right)_T = \Delta V^{\theta} \quad \ldots\ 2.104$$

but

$$\Delta G^{\theta} = -RT\ln K_a \quad \ldots\ 2.105$$

Substituting 2.105 into 2.104

$$\left(\frac{\partial \ln K_a}{\partial P}\right)_T = -\frac{\Delta V^{\theta}}{RT} \quad \ldots\ 2.106$$

which describes the relationship between the equilibrium constant and pressure, and is, of course, a quantitative description of the Chatelier's principle.

At constant pressure, equation 2.103 becomes

$$\left(\frac{\partial \Delta G^{\theta}}{\partial T}\right)_P = -\Delta S^{\theta} \quad \ldots\ 2.107$$

Combining 2.107 and 2.102 gives the Gibbs-Helmholtz equation.

$$\Delta G^{\theta} = \Delta H^{\theta} + T\left(\frac{\partial \Delta G^{\theta}}{\partial T}\right)_P \quad \ldots\ldots 2.108$$

Substituting for ΔG^{θ}

$$-RT\ln K_a = \Delta H^{\theta} + T\left(\frac{\partial}{\partial T}(-RT\ln K_a)\right)_P$$

$$\left(\frac{\partial \ln K_a}{\partial T}\right)_P = \frac{\Delta H^{\theta}}{RT^2} \quad \ldots\ldots 2.109$$

This equation describes the variation of the equilibrium with temperature.

Appropriate integration of either equation 2.106 or equation 2.109 enables in principle the evaluation of K_a at any temperature or pressure.

In practice, ΔV^{θ} is very small for ion exchange involving zeolites so that it is not expected that the ion exchange will be markedly affected by pressure changes. The use of equation 2.109 may be problematical, since the ion site set populations may change with temperature, meaning that the standard states are not comparable; this is a problem which merits further investigation.

2.5.3. Prediction of Thermodynamic Parameters Using The Triangle Rule.

The triangle rule has been used extensively[136] to predict thermodynamic reaction parameters for reactions which may be

inter-related through appropriate summations and subtractions of the reaction equations. Thus, considering for example the binary exchange systems M_1/Na-MOR and M_2/Na-MOR for which the equilibrium constants K_a and standard free energies ΔG^{θ} have been obtained experimentally (section 4.4.3.2.), then using the triangle rule, the thermodynamic parameters for the systems M_1/M_2-MOR, or M_2/M_1-MOR should be predictable. The argument is described below.

Let M_1 and M_2 be divalent metal ions.
Then the reactions

$$M^{+2}_{1(s)} + 2Na^{+}_{(c)} \rightleftharpoons M^{+2}_{1(c)} + 2Na^{+}_{(s)} \quad .... \ 2.110$$

$$M^{+2}_{2(s)} + 2Na^{+}_{(c)} \rightleftharpoons M^{+2}_{2(c)} + 2Na^{+}_{(s)} \quad .... \ 2.111$$

$$M^{+2}_{2(s)} + M^{+2}_{1(s)} \rightleftharpoons M^{+2}_{2(c)} + M^{+}_{1(s)} \quad .... \ 2.112$$

Let K_{a1}, K_{a2}, K_{a3} be the equilibrium constants for the reactions 2.110, 2.111, 2.112 respectively, and ΔG^{θ}_1, ΔG^{θ}_2, ΔG^{θ}_3 the corresponding free energies

Since

$$K_{a1} = \frac{a_{M1(c)} \cdot a^2_{Na(s)}}{a_{M1(s)} \cdot a^2_{Na(c)}} \quad .... \ 2.113$$

$$K_{a2} = \frac{a_{M2(c)} \cdot a^2_{Na(s)}}{a_{M2(s)} \cdot a^2_{Na(c)}} \quad .... \ 2.114$$

$$Ka_3 = \frac{a_{M2(c)} \cdot a_{M1(s)}}{a_{M2(s)} \cdot a_{M1(c)}} \quad \ldots\ldots 2.115$$

then K_{a3} can be expressed in terms of K_{a1}, K_{a2} and

$$K_{a3} = K_{a2}/K_{a1} \quad \ldots\ldots 2.116$$

Now consider the reactions

$$M^{+2}_{1(s)} + 2Na^{+}_{(c)} \rightleftharpoons M^{+2}_{1(c)} + 2Na^{+}_{(s)} \quad \ldots\ldots 2.117$$

$$M^{+2}_{1(s)} + 2NH^{+}_{4(c)} \rightleftharpoons M^{+2}_{1(c)} + 2NH^{+}_{4(s)} \quad \ldots\ldots 2.118$$

$$NH^{+}_{4(s)} + Na^{+}_{(c)} \rightleftharpoons NH^{+}_{4(c)} + Na^{+}_{(s)} \quad \ldots\ldots 2.119$$

where K_{a4}, K_{a5}, K_{a6} are the equilibrium constants for the reaction 2.117, 2.118, 2.119 respectively. K_{a6} can be predicted when K_{a4}, K_{a5} are known since

$$K_{a6} = \left(\frac{K_{a4}}{K_{a5}}\right)^{\frac{1}{2}} \quad \ldots\ldots 2.120$$

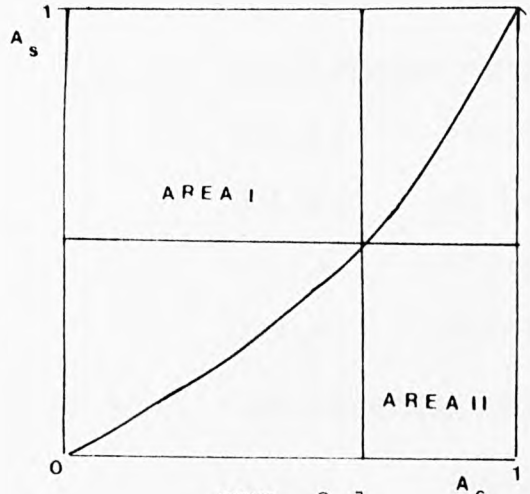

FIG. 2.1

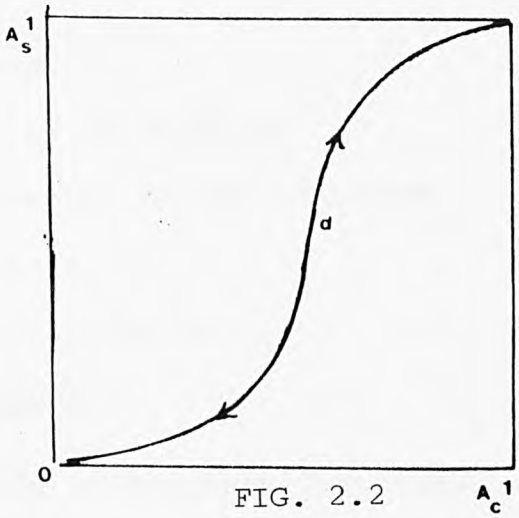

FIG. 2.2

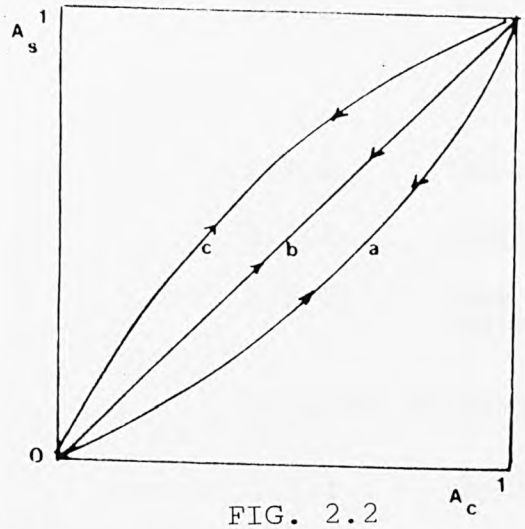

FIG. 2.2

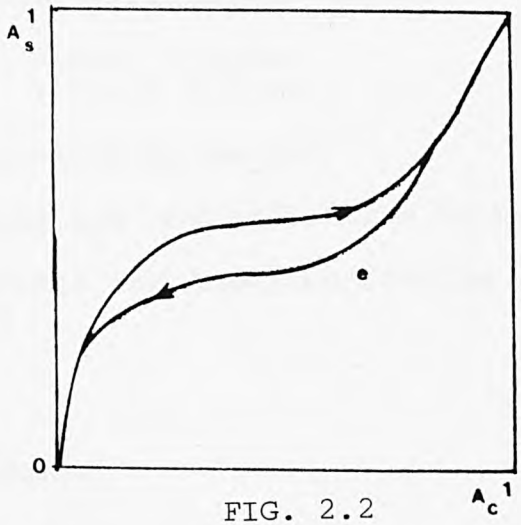

FIG. 2.2

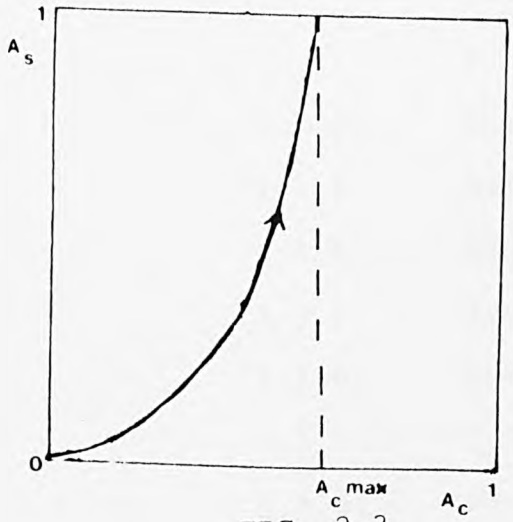

FIG. 2.3

CHAPTER THREE EXPERIMENTAL

3.1. PRELIMINARY PROCEDURES

3.1.1. Purification of Zeolites

3.1.2. pH Measurements of the Solutions

3.1.3. Kinetic Tests

3.1.4. Reversibility Tests

3.2. ION EXCHANGE EXPERIMENTS

3.2.1. Preparation of Isotherm Solutions

3.2.2. Ion Exchange Experiments

3.2.2.1. Binary Systems
3.2.2.2. Ternary Systems

3.2.3. Sodium/Ammonium Exchanges

3.2.4. Sodium/Lead and Sodium/Cadmium Exchanges

3.2.5. Ammonium/Lead and Ammonium/Cadmium Exchanges

3.3. ZEOLITE ANALYSES

3.3.1. Silica Content

3.3.1.1. Fusion Method

3.3.1.2. Hydrofluoric Acid Method

3.3.2. Water

3.3.3. Ammonia and Ammonium Ion Content

3.3.4. Aluminium

3.3.5. Iron

3.3.6. Sodium, Potassium

3.3.7. Calcium

3.3.8. Magnesium

3.3.9. Lead and Cadmium

3.4. ANALYTICAL PROCEDURES FOR SOLUTION PHASE

3.4.1. Lead by EDTA

3.4.2. Cadmium by EDTA

3.4.3. Lead and Cadmium by Atomic Absorption

3.4.4. Calcium by Atomic Absorption

3.4.5. Sodium and Potassium by Flame Photometry

3.4.6. Ammonia by the Kjeldhal Method

3.5. X-RAY ANALYSES

3.6. THERMOGRAVIMETRIC ANALYSES

CHAPTER THREE EXPERIMENTAL

3.1. Preliminary Procedure

The three zeolites used were from the sedimentary deposits of Nevada, as supplied by W.R. Grace. As a consequence the zeolites had to be purified and converted to the homoionic forms before any ion exchange studies were carried out.

For the equilibrium studies the divalent metal salts used were $Pb(NO_3)_2$, $Cd(NO_3)_2\ H_2O$ and $CdCl_2\ H_2O$, all supplied by B.D.H. and of "AnalaR" grade. Also "AnalaR" $NaNO_3$, NH_4NO_3, NaCl and NH_4Cl salts were used.

X-ray diffraction studies were performed before and after any exchange to check for any structural changes that may have occurred. Thermogravimetric and differential thermal analyses were also undertaken for the sodium and ammonium forms of the zeolites.

As far as the isotherm solutions are concerned, pH values for all metal solutions were taken, and they were left for a few weeks to check for any precipitation. To study the equilibrium thermodynamics of a system, initial kinetic tests were performed to establish conditions for equilibrium, and reversibility tests must be undertaken.[105]

3.1.1. Purification of Zeolites.

Since the zeolites under study are of natural origin, they contain many impurities. The purification was carried out as follows. The first step was sedimentation so that light

particles could be removed by flotation. Ferrierite contained a lot of impurities which were removed in this way. After drying, the zeolites were ground gently and passed through a 100 mesh sieve. Then about 20g of each zeolite were equilibrated with300cm^3 sodium chloride solution (1 mol dm^{-3}) for the sodium form of zeolite and with ammonium chloride (1 mol dm^{-3}) for the ammonium form. The solutions were changed daily for at least eight days. Afterwards the zeolites were centrifuged, washed thoroughly and dried at 80^{o}C. From the analyses that were carried out on the zeolites it was found that they still contained other ions so the exchange was repeated at 70^{o}C. After drying and leaving the zeolites to equilibrate over saturated ammonium chloride solution[105] for a couple of weeks, the analyses showed that the exchanges were achieved. Hundred-gram samples for each zeolite were made by this method.

3.1.2. pH Measurements of the Solutions.

After preparation of sets of isotherm solutions, before equilibrations with zeolites, their pH values were recorded and were in the region 3.8→ 5.0. The solutions were left for a few weeks to check whether precipitates would form. None of the solutions showed signs of precipitation. After equilibrating solutions with the zeolites, the pH values were recorded again after centrifugation.

3.1.3. Kinetic Tests.

Before any ion exchange experiments were carried out for the

construction of isotherms, kinetic tests were performed for all zeolites. These tests indicate how long it will take for a system to equilibrate.

Solutions of 0.05 mol dm^{-3} of the metal salts under examination were made. Then 150 cm^3 were added to 0.3g of zeolite and the mixture was constantly agitated at 25°C. Samples were withdrawn and centrifuged at certain intervals. Analyses were performed on the ions released from the zeolite as well as on the counter ions in solution. From these results the uptake of metal ion by each zeolite as a function of time could be calculated. The graphs obtained are shown in Figures 3.1, 3.2. Most of the ion exchange took place during the first two hours for both lead and cadmium ions, and also for both forms of the zeolite.

The highest metal uptake occurred when lead was equilibrated with ammonium clinoptilolite, but during the exchange, sodium still present in the zeolite (even after exhaustive ammonium exchanges) was also removed.

3.1.4. Reversibility Tests.

Thermodynamics can only be applied to systems which have been proved to be reversible over the whole isotherm composition range. For this reason the ion exchange of these particular systems (i.e. lead and cadmium exchanges with the sodium and ammonium forms of clinoptilolite, mordenite and ferrierite) must be checked for reversibility. The method employed was as

follows.

0.3g of the zeolite were equilibrated with 50 cm^3 of a known solution concentration of the appropriate ion. After equilibration the forward point of the isotherm was obtained (A_s,A_c) which was the starting point for the reverse process. The suspension was centrifuged, then 25 cm^3 of the equilibrated solution were removed and replaced by 25 cm^3 of a solution of the same total normality, but with a very low lead or cadmium concentration. The system was then left to equilibrate again and re-analysed for the new values (A_{sr}, A_{cr}), which were the reverse points. For a reversible system, A_{sr}, A_{cr} should fall on the curve representing the forward isotherm. The points usually chosen for reversibility are those with the highest values of A_s, A_c and the aim was to shift those points to values that were as low as possible during the reverse process. This ensured that the isotherm was reversible over the whole range of compositions.

3.2. Ion Exchange Experiments

Ion exchange experiments were undertaken for both binary and ternary systems. Tables 3.1 - 3.3 list all the sets of isotherms that were examined. Preparation of the isotherm solutions as well as the procedures involved in the exchange experiments are described in the following section.

3.2.1. Preparation of Isotherm Solutions

All metal salts were readily soluble in water. Normal solutions (1g equiv dm^{-3} - hereafter designated by the symbol 'N') were made up for each pure salt, then a total of 25 cm^3 aliquots were taken containing known proportions of the heavy metal and the corresponding sodium or ammonium salts, but always at the same total normality (1N). These were then diluted to 250 cm^3 to give solution concentrations of 0.1N. In the case where 0.5N was required for the isotherm solutions 100 cm^3 of 1N solution were first taken and then diluted to 200 cm^3.

3.2.2. Ion Exchange Experiments.

3.2.2.1. Binary systems.

The ion exchange experiments were carried out at 25°C. The total normality for some exchanges was 0.1 g equiv. dm^{-3} and for others 0.5 g equv.dm^{-3} (Table 3.1,3.2)

Weighed amounts of the appropriate homoionic zeolite (usually 0.3g) were equilibrated with 50 cm^3 of the appropriate isotherm solution in plastic bottles. The bottles (immersed in a water bath at 25°C) were shaken continuously until equilibrium was obtained. From the kinetic tests it was decided to leave the systems to equilibrate for at least a week before any analyses were performed. The solutions and zeolites were then separated by centrifuging at 4000 rpm for 10 minutes. The initial solutions, as well as the corresponding solutions after exchange, were analysed by the methods outlined in section 3.4.1 to 3.4.6 and the values of A_c (equivalent fraction of

Table 3.1 Binary Exchange Equilibria at Total Concentration 0.1 equiv.dm^{-3}

Pb/$Na(NO_3)$-CLI	Pb/$NH_4(NO_3)$-CLI
Cd/$Na(NO_3)$-CLI	Cd/$NH_4(NO_3)$-CLI
NH_4/$Na(NO_3)$-CLI	
Pb/$Na(NO_3)$-MOR	Pb/$NH_4(NO_3)$-MOR
Cd/$Na(NO_3)$-MOR	Cd/$NH_4(NO_3)$-MOR
Cd/Na(Cl)-MOR	Cd/NH_4(Cl)-MOR
NH_4/$Na(NO_3)$-MOR	
Pb/$Na(NO_3)$-FER	Pb/$NH_4(NO_3)$-FER
Cd/$Na(NO_3)$-FER	Cd/$NH_4(NO_3)$-FER
Cd/Na(Cl)-FER	Cd/NH_4(Cl)-FER
NH_4/$Na(NO_3)$-FER	

Table 3.2 Binary Exchange Equilibria at Total Concentration 0.5 equiv.dm^{-3}.

Pb/$Na(NO_3)$-CLI
Pb/$Na(NO_3)$-MOR
Pb/$Na(NO_3)$-FER

ion A in the zeolite), A_s (equivalent fraction of ion A in the solution) were calculated from these data. Data points in the regions $A_s \rightarrow 0$ and $A_s \rightarrow 1$ were obtained by varying the solution to zeolite ratio as shown in Table 3.4.

Each analytical determination was repeated at least twice and where necessary isotherm points themselves were duplicated.

Apart from the isotherm solution analyses, direct analyses were also performed on the zeolites. Balances were carried out on the ingoing ion and the outgoing ions. Certain equilibria were found to be of a ternary nature (section 4.2.6). In some of the equilibria, calcium was released which most probably was due to gradual dissolution of the calcite impurity within the zeolite[76] (section 4.2).

For any binary exchange it is essential to obtain the maximum level of exchange $A_c(max)$ (section 4.4.1.). This was achieved by exhaustively equilibrating the zeolite (usually 0.3g) with 50 cm^3 of 0.1N solution of the appropriate ion. The contents after a day were centrifuged and the zeolite was equilibrated again with fresh solution. This procedure was repeated several times until the exchange was completed (i.e. the exchange level became constant). The zeolite was washed and dried. Direct analyses on the zeolite gave $A_c(max)$.

3.2.2.2. Ternary systems

Again the ion exchange experiments were carried out at 25°C and at a total concentration 0.1 g equiv.dm^{-3}. 0.3g of the appropriate zeolite were weighed into a plastic bottle and

Table 3.3. Ternary exchange equilibria at total concentration 0.1 equiv.dm^{-3}.

Pb/Cd/Na(NO_3)-CLI	Pb/Cd/NH_4(NO_3)-CLI
Pb/Cd/Na(NO_3)-MOR	Pb/Cd/NH_4(NO_3)-MOR
Pb/Cd/Na(NO_3)-FER	Pb/Cd/NH_4(NO_3)-FER
Pb/Na/NH_4(NO_3)-CLI	Cd/Na/NH_4(NO_3)-CLI
Pb/Na/NH_4(NO_3)-MOR	Cd/Na/NH_4(NO_3)-MOR

Table 3.4. Ion Exchange Isotherm at 0.1 equiv.dm^{-3}.

Counter Ion concentration equiv.dm^{-3}.	Zeolite weight g.	Solution volume cm^3.
0.10	0.1	75
0.10	0.2	75
0.095	0.2	75
0.09	0.2	50
0.09	0.3	50
0.08	0.3	50
0.07	0.3	50
0.06	0.3	50
0.05	0.3	50
0.04	0.3	50
0.03	0.3	50
0.02	0.3	50
0.01	0.3	50
0.01	0.5	25
0.005	0.5	25
0.005	0.7	25

equilibrated with 50cm^3 of the isotherm solution. For the systems involving Cd-Pb-NH_4 and Cd-Pb-Na, the analyses were quite complicated, since both cadmium and lead complexed with EDTA[137]. Polarography[138] did not give satisfactory results either. The isotherm solutions before exchange were therefore analysed for lead and cadmium by atomic absorption spectrophotometry . The solutions after exchange were analysed for lead, cadmium and calcium by atomic absorption, and for sodium and potassium by flame photometry. Direct analyses on the zeolites were performed as well.

For the systems involving the ions Pb-Na-NH_4 and Cd-Na-NH_4, no direct analyses on the zeolites were carried out. Instead titrimetric analyses were employed for lead and cadmium in solution before and after the exchanges were effected.

3.2.3. Sodium/Ammonium Exchanges

For exchanges involving these ions, 0.3g aliquots of the sodium clinoptilolite, mordenite and ferrierite samples were equilibrated with 50 cm^3 aliquots of the sodium/ammonium isotherm solutions. Then analyses for ammonia determination were carried out on the zeolite using the Kjeldhal method[139] (section 3.3.3.) as well as on the initial solutions, and on the solutions after exchange (section 3.4.6). Tests for potassium and calcium content were also carried out on the solution afterwards to check for stoichiometry of exchange. (section 3.4.4., 3.4.5.)

3.2.4. Sodium/Lead and Sodium/Cadmium Exchanges

0.3g aliquots of the sodium zeolites (clinoptilolite, mordenite and ferrierite) were equilibrated with 50 cm^3 of the sodium/lead or sodium/cadmium isotherm solutions in plastic bottles. The bottles were shaken constantly and kept at a constant temperature of 25°C(section 3.2.2.1). After the equilibration was over various analyses were performed. For the sodium/lead systems the lead content of the isotherm solution before and after the exchange was obtained by EDTA (section 3.4.1). Also direct analyses were performed on the zeolites (section 3.3.9). Calcium content was obtained by atomic absorption (section 3.4.4.). For the sodium/cadmium systems a similar procedure was followed as for the sodium/lead exchange.

3.2.5. Ammonium/Lead and Ammonium/Cadmium Exchanges

For these systems the three ammonium zeolites were equilibrated with the appropriate solutions as in section 3.2.1. Analyses for ammonia, (section 3.4.6.) were carried out on the isotherm solution before and after the equilibration. Lead and cadmium were obtained by EDTA (3.4.1, 3.4.2) and direct zeolite analyses were done (sec.3.3.9).Analyses were also performed for calcium, sodium and potassium (section 3.4.4, 3.4.5).

3.3. Zeolite Analyses

3.3.1. Silica Content

The silica content of a zeolite can be determined by the so-called "wet methods", using either the fusion method or the hydrofluoric acid method.[140]

3.3.1.1. Fusion method

A sample of the zeolite (usually 0.2g) was weighed accurately into a platinum crucible and five times the zeolite weight of fusion mixture was added. The two components were mixed using a glass rod. (The fusion mixture is prepared by mixing sodium carbonate and potassium carbonate in a molar ratio 1:1). The crucible was partially covered and heated, slowly at first, to 1000°C using Meker burners. The crucible was left on the burner at that temperature for about half an hour. It was then allowed to cool below red-heat, and immersed in a porcelain dish containing water. The dish was covered with a clock glass and about 30 cm^3 of concentrated hydrochloric acid were added carefully. When efferverscence ceased, the dish was warmed on a steam bath and 1cm^3 H_2SO_4 was added. The crucible was removed from the dish after washing it carefully. The dish was left on the steam bath and the evaporation was carried to complete dryness. Then about 30 cm^3 of 1:1 hydrochloric acid were added, followed by a few drops of sulphuric acid, and the suspension was re-evaporated to absolute dryness again. Finally, 50cm^3 of 5% hydrochloric

acid were added and the mixture was digested further for about 10 minutes on the steam bath, then filtered hot through a no.42 Whatman ashless filter paper. The precipitate was washed thoroughly, first with hot dilute hydrochloric acid, then water, and finally the wet filter paper was ignited slowly to 1000°C in a preweighed platinum crucible to constant weight. This gave the direct weight of the SiO_2 content of the zeolite The filtrate was made up to 250ml and put aside for aluminium and iron analyses.

3.3.1.2. Hydrofluoric acid method

A known weight of the zeolite (usually 0.2g) was placed in a platinum crucible and heated to a constant weight at 1000°C on a Meker burner. The loss of weight was noted and the residue was treated twice with hydrofluoric acid. Each time a few drops of sulphuric acid were added followed by ~20ml of 40% hydrofluoric acid and the contents of the crucible were heated to dryness on a hot plate. Then the residue was ignited to constant weight, and the difference between the two ignited weights gave the silica content of the zeolite.

3.3.2. Water in zeolites

To obtain the equilibrium water content accurately the zeolites had to be left in a desiccator to equilibrate over a saturated solution of sodium chloride or ammonium chloride for at least two weeks.[105]

Then a known quantity of sodium or ammonium zeolite was heated

to constant weight as for the silica determination described earlier (section 3.3.1.1). For sodium zeolites the weight loss gave the moisture content directly, but for the ammonium zeolites the total weight loss included ammonia, and this quantity had to be subtracted after analyses of ammonium using the Kjeldahl[139] method.

The probable mechanism for the thermal decomposition of the ammonium zeolites is as follows[141].

The zeolite can be expressed as

$$(NH_4)_n \quad (Al\ O_2)_n \quad (SiO_2)_m . \quad xH_2O$$

On heating, the zeolite loses its intracrystalline water. Further heating to a higher temperature causes ammonia to be evolved leaving the hydrogen zeolite:

$$H_n \ (AlO_2)_n \quad (SiO_2)_m$$

At higher temperatures still, this hydrogen is then lost together with oxygen by means of a dehydroxylation reaction , and this leaves Al_2O_3, SiO_2.

3.3.3. Ammonia and Ammonium Ion

The ammonia determination by the Kjeldahl method gives very accurate results. The apparatus was set up and a known quantity of the zeolite was added followed by boiling stones to assist boiling. Then about 50 cm^3 of 20% sodium hydroxide were added as well as 100cm^3 of distilled water, and the whole

flask content was heated for about one hour to ensure that all ammonia was expelled from the zeolite. The liberated ammonia and condensate were trapped into a flask containing a known volume of standard hydrochloric acid (0.1N). At the end of the distillation the flask containing ammonia was removed first before switching off the heating mantle to avoid suck-back. The ammonia content was determined by back-titration using a standard sodium tetraborate solution (borax) with methyl red as indicator.

3.3.4. Aluminium

The filtrate obtained from the fusion method (3.3.1.1) was used to determine the aluminium content of the zeolites. A known aliquot of the filtrate (usually 50cm^3) was pipetted into a 600cm^3 beaker and neutralized with 1:1 ammonia solution. Then 4cm^3 of 1:1HCl were added and the solution was made to 200cm^3, warmed and sufficient 5% 8-hydroxyquinoline[142] solution was added (this quantity was dependent on the aluminium content of the sample, and had to be found by trial and error). The solution was warmed to 50^{o}C and 40cm^3 of 40% ammonium acetate solution was added slowly with stirring. The resulting suspension was heated to 70^{o}C on a steam bath and kept at this temperature (not higher) for 10 minutes only. A precipitate could be observed which usually had a green colouration due to the presence of iron impurity. After cooling, the suspension was filtered through a preweighed P4 sintered crucible, washed with hot water, then dried between

140°C and 150°C for two hours, cooled in a desiccator and finally weighed. Separate analyses for iron had to be made (3.3.5) since both aluminium and iron are obtained together as the oxinates $Al(C_9H_6ON)_3$, $Fe(C_9H_6ON)_3$ using this method.

3.3.5. Iron

Standards and samples of the fusion filtrate (3.3.1.1) were transferred into 50cm^3 volumetric flasks. To each flask was added 5cm^3 of 10% hydroxylammonium chloride solution, 5cm^3 of 1N sodium acetate and 4cm^3 of a 0.25%w/v 1:10 phenanthroline solution. All solutions were then made up to 50cm^3 with distilled water and analysed colorimetrically against a reagent blank using an EEL absorptiometer (604 filter). In the presence of iron, phenanthroline gives a brown-red colour. Beer's law is obeyed in the range of up to 6ppm.

3.3.6 Sodium

For sodium determinations, the hydrofluoric acid method was used to dissolve the zeolite (3.3.1.2), but with the exception that the final contents of the crucible were not heated to constant weight. Instead the platinum crucible containing the alumina and sodium residue was placed in a 250cm^3 beaker with about 100cm^3 1:1 Hcl and digested for an hour. The resulting solution was made up to 250cm^3. Sodium was determined using a flame photometer, The working range was up to 20ppm.

3.3.7 Calcium

The presence of sodium caused excessive interference so that the flame photometer could not be used to measure the calcium content of the zeolite. Atomic absorption can be used but interference from aluminium must be taken into account.

The best method with which to measure calcium accurately was found to be gravimetric precipitation of calcium tungstate at a pH just above 7[143].

50cm^3 of fusion filtrate (3.3.1.1) were treated with 1:1 ammonia solution until the pH was in the region of ~ 8. The suspension was left on the steam bath for an hour and then filtered. The precipitate was washed thoroughly and all washings were added to the filtrate. By this procedure aluminium was removed as aluminium hydroxide. The filtrate was then evaporated to near-dryness and 1cm^3 of concentrated nitric acid was added. The next step was to remove ammonium salts which hamper precipitation of calcium tungstate. This was done by heating the contents for an hour on a hot plate to sublime the ammonium nitrate. Using hydrochloric acid (1:1) the residue was then dissolved and the volume made to 100cm^3 with distilled water. The pH was adjusted to ~ 8 with 5% sodium hydroxide solution and 2cm^3 of sodium tungstate solution (19g of $Na_2WO_4 2H_2O$ per 100cm^3 of distilled water) were added. A precipitate was formed slowly which was digested for 30 minutes at 80°C. After washing with warm water and drying at 10°C the precipitate was weighed as $CaWO_4$.

3.3.8 Magnesium

Natural zeolites might contain magnesium so tests were carried out to check for its presence. In fact, and as expected[144], ferrierite was found to contain significant amounts of magnesium. The filtrate obtained from the hydrofluoric treatments of the zeolite (3.3.6) was used. Atomic absorption gave satisfactory results. The working linear range was up to 0.5ppm so the solution had to be quite dilute. Using 0.3g ferrierite and a total filtrate of $50cm^3$ the dilution required was as much as 1:50.

3.3.9 Lead and Cadmium

To obtain the lead and cadmium contents, the zeolites had to be dissolved. This was done by digesting the zeolites in nitric acid over a steam bath for a week. Hydrochloric acid and aqua regia (which attacks the zeolites more easily) could not be used because of the precipitation of lead as the insoluble lead chloride. The suspension was filtered and made up to $250cm^3$. Then after suitable dilutions, lead and cadmium were measured using atomic absorption . The conditions required are given in Table 3.5.

3.4. Analytical Procedures for the Solution Phase.

For the analyses of isotherm solutions various techniques were employed. They were mainly analysed by titrimetric methods when the concentrations of ions were high, but for low concentrations atomic absorption spectrophotometry or flame photo-

metry were used.

If the atomic absorption method is applied for high concentrations, the dilution factor is so high that any error introduced can alter the final results significantly.

3.4.1. Lead by EDTA

Lead is easily determined[137] by EDTA using xylenol orange as indicator. The end-point is very sharp.

10ml of the lead solution were pipetted into a 250ml volumetric flask, then diluted with about 50ml with distilled water. Three drops of xylenol orange were added, followed by a few drops of very dilute nitric acid. This latter addition gave the solution a yellow colour. After this stage, powdered "hexamine" (hexamethylenetetramine) was added until the colour was intensely red. This step ensures that the solution has the correct pH (~6) for the subsequent titration. The flask contents were finally titrated with standard EDTA (0.05M) until the colour changed from red to yellow.

3.4.2. Cadmium by EDTA

The method used to determine lead (3.4.1) was employed for cadmium also. In cases involving ternary exchange, where lead and cadmium were present together, different procedures were followed in order to obtain lead and cadmium concentrations separately (3.2.2.2). The EDTA titration for cadmium does not give as sharp an end-point as with lead, so the addition of

EDTA was made slowly with much shaking as the end-point was approached.

3.4.3. Lead and Cadmium by Atomic Absorption Spectrophotometry

Both lead and cadmium can be measured easily by atomic absorption. The working conditions are given in Table 3.5.

3.4.4. Calcium by Atomic Absorption Spectrophotometry

Calcium can be obtained by atomic absorption spectrophotometry quite accurately. Table 3.5 gives the working conditions. When analysing the isotherm solution after exchange, the reading for calcium is precise since no other ions interfere. Usually this method was employed to check whether calcium was released during the exchange of a sodium or ammonium zeolite.

3.4.5. Sodium and Potassium by Flame Photometry

As for calcium (3.4.4.) it was necessary to check whether sodium and potassium were exchanged along with ammonia when an ammonium zeolite was used for the exchange. Since sodium and potassium were present in traces, flame photometry gave very reliable results.

3.4.6. Ammonia by Kjeldhal

The ammonia content of an isotherm solution before and after the exchange was obtained by the Kjeldahl method[139]. Usually aliquots of 5ml of the ammonia solution were used together with

Table 3.5. Atomic Absorption Spectrophotometry - Working conditions.

Element	Wave-length nm.	Flame	Linear region µg/ml	Response µg/ml	Response Abs.units
Pb	283.3	Air-Acetyl.	0 -20	2.0	0.180
Cd	228.8	Air-Acetyl.	0 -2.0	2.0	0.35
Ca	422.7	Air-Acetyl.	0 -7.0	4.0	0.22
Mg	285.2	Air-Acetyl. or nitrous ox. Acetylene	0 -0.5	0.3	0.19

10ml of 0.1N standard hydrochloric acid to trap the ammonia evolved during distillation. The detailed description is given in section 3.3.3.

3.5. X-Ray Analyses

X-ray analyses were performed for all zeolites before and after the exchange using a Guinier camera and employing CuK_a radiation. This was essential to check for any structural change. No apparent loss of crystallinity of the zeolites was observed after the exchanges with lead and cadmium.

3.6. Thermogravimetric Analyses

Thermogravimetric Analyses were carried out for the sodium and ammonium zeolites in air and nitrogen atmospheres using a Mettler thermoanalyser. The temperature of 900°C was reached and the heating rate was 5°/min. The results obtained are shown in table 3.6.

Table 3.6

Thermal decomposition of Na-MOR, NH_4-MOR, Na-CLI, NH_4-CLI in air.

	Na-MOR	NH_4-MOR	Na-CLI	NH_4-CLI
Initial weight (mg)	51.95	55.02	48.35	51.
Total weight lost(%)	8.64	8.25	12.87	14.28
First wt. loss				
Weight lost (%)	1.16	0.59	1.46	1.20
Temperature range (^{0}C)	RT-34	RT-30	RT-40	RT-30
Second wt. loss				
Weight lost (%)	4.79	4.54	9.67	8.21
Temperature range (^{0}C)	34-188	30-219	40-404	30-313
Max. rate of volatil. (%.min^{-1})	3.58	3.93	2.49	2.75
Temp. of max.rate (^{0}C)	90	86	106	77
Third wt. loss				
Weight lost (%)	1.96	0.21	0.22	3.48
Temperature range (^{0}C)	188-453	219-281	404-592	313-582
Max. rate of volatil. (%.min^{-1})	4.13	9.74	-	3.04
Temp. of max.rate (^{0}C)	232	251	475	462
Fourth wt. loss				
Weight lost (%)	0.73	2.26	1.52	1.30
Temperature range (^{0}C)	453-688	281-594	592-716	582-822
Max. rate of volatil. (%.min^{-1})	7.63	2.49	9.46	5.18
Temp. of max.rate (^{0}C)	624	444	674	704
Fifth wt. loss				
Weight lost (%)		0.67		
Temperature range (^{0}C)		594-839		
Max.rate of volatil.		2.73		
Temp. of max.rate (^{0}C)		746		

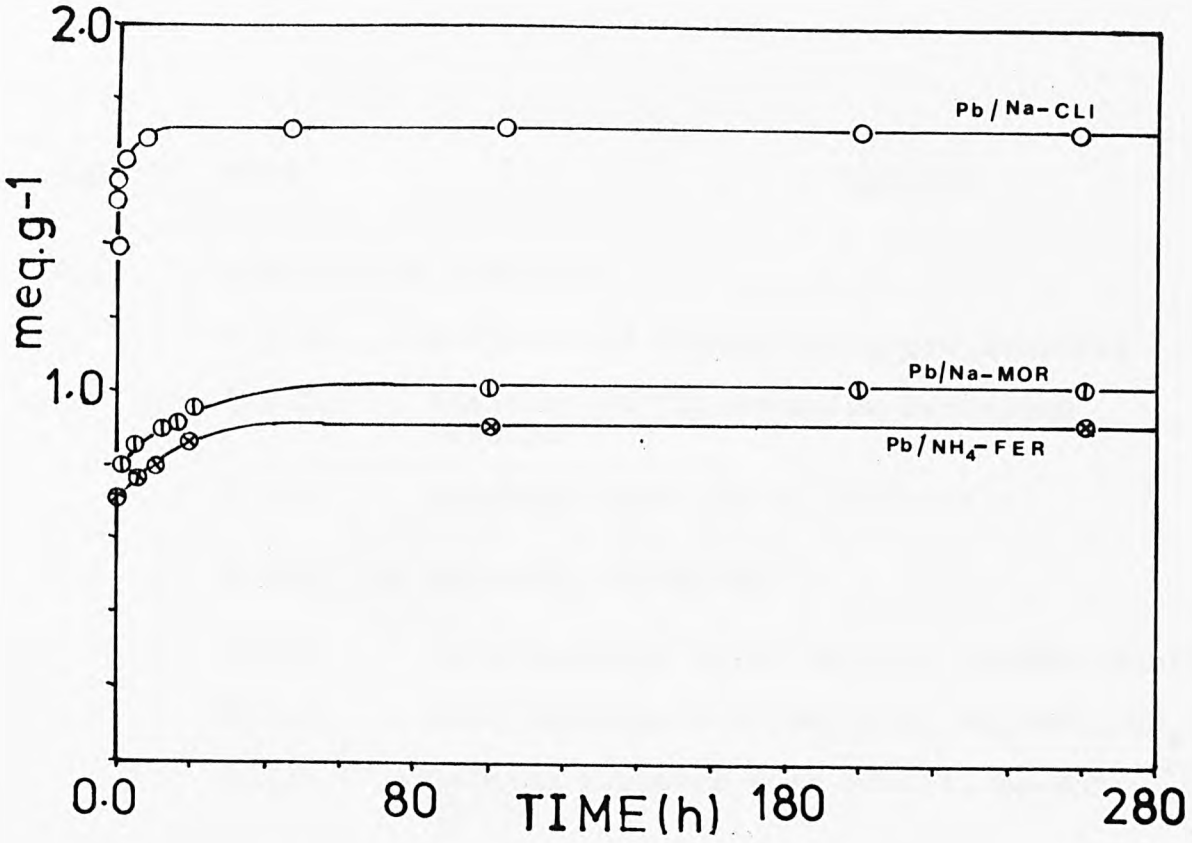

FIGURE 3.1

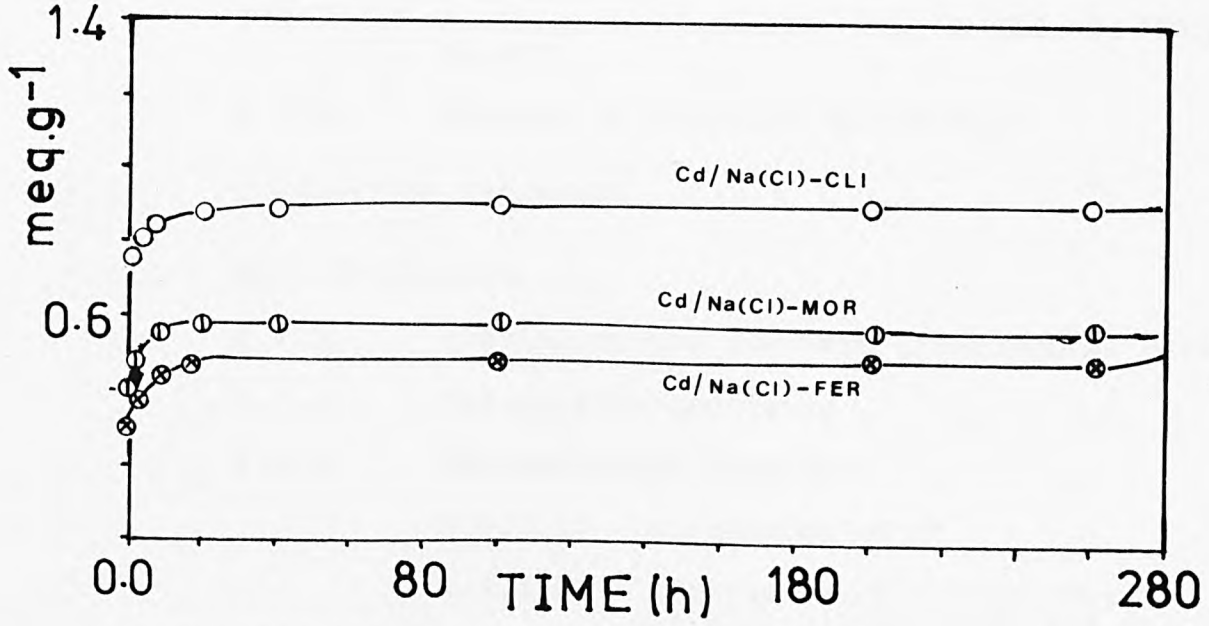

Kinetic Plots: Pb,Cd /CLI,MOR,FER

FIGURE 3.2

CHAPTER FOUR RESULTS

CHAPTER FOUR RESULTS

4.1. Analyses of Zeolites

The conversion of zeolites to the homoionic forms required the use of elevated temperatures. At room temperature (25°C) the final exchange level achieved was quite low even though the equilibration was carried out for eight days and the solutions were changed daily. For ammonium clinoptilolite the final exchange level achieved at 25°C was 1.8%$(NH_4)_2O$ whereas at 70°C this was about 5%. Mordenite and ferrierite also yielded low ammonia contents on analysis after exchange when the exchange was carried out at 25°C. It was therefore decided that all the conversions to homoionic forms (either sodium or ammonium) should be carried out at 70°C.[145]

4.1.1. Analysis of the Sodium-Exchanged Zeolite.

The chemical analysis of the sodium clinoptilolite (Na-CLI) sodium mordenite (Na-MOR), sodium ferrierite (Na-FER) are given in tables (4.1-4.3). The analytical data are also expressed below as oxide formulae. Even after exhaustive exchange, the sodium did not replace all the other apparently exchangeable ions, so that potassium and calcium ions were detected as well. Extra calcium impurity (deduced from other evidence to be calcite) are not included in the formulae below.

Sodium Clinoptilolite

$0.87Na_2O \cdot 0.038K_2O \cdot 0.095CaO \cdot Al_2O_3 \cdot 9.4SiO_2 \cdot 9.15H_2O$

Sodium Mordenite

$0.515Na_2O.0.39K_2O.0.109CaO.Al_2O_3.11.07SiO_2.4.0H_2O$

Sodium Ferrierite

$0.48Na_2O.0.341K_2O.0.217MgO.Al_2O_3.12.76SiO_2.7.28H_2O$

4.1.2. Analysis of the Ammonium-Exchanged Zeolites.

The chemical analyses of the ammonium clinoptilolite(NH_4-CLI) ammonium mordenite (NH_4-MOR), ammonium ferrierite (NH_4-FER) are given in tables 4.4.-4.6). From these analyses the suggested oxide formulae are given below. Excess calcium (probably present as calcite) and iron oxide are considered as impurities and not included in the formulae below.

Ammonium Clinoptilolite

$0.160Na_2O.0.0145K_2O.0.874(NH_4)_2O.Al_2O_3.9.36SiO_2.9H_2O$

Ammonium Mordenite

$0.112Na_2O.0.358K_2O.0.56(NH_4)_2O.Al_2O_3.11.25SiO_2.3.66H_2O$

Ammonium Ferrierite

$0.058Na_2O.0.268K_2O.0.569(NH_4)_2O.Al_2O_3.12.94SiO_2.6.67H_2O$

Tables 4.4.-4.6 show that the ammonium ion did not exchange with all the apparently available exchangeable ions in the zeolites. In all three ammonium forms, sodium and potassium are present.

Table 4.1 Analyses of Sodium Clinoptilolite

Component	% w/w	mequiv.g^{-1}	mol/100g	mol/Al_2O_3
SiO_2	61.750		1.0280	9.397
Al_2O_3	11.160	2.188	0.1094	1.000
H_2O	18.010		1.0006	9.146
Na_2O	5.890	1.900	0.0950	0.868
K_2O	0.392	0.083	0.0042	0.038
CaO	1.950	0.2047	0.0104	0.095
Fe_2O_3	0.936		0.0059	
% Total	100.09			

Table 4.2 Analyses of Sodium Mordenite

Component	% w/w	mequiv.g^{-1}	mol/100g	mol/Al_2O_3
SiO_2	70.25		1.1696	11.066
Al_2O_3	10.78	2.114	0.1057	1.000
H_2O	7.60		0.4222	3.995
Na_2O	3.37	1.087	0.0544	0.5143
K_2O	3.88	0.824	0.0412	0.390
CaO	2.30	0.230	0.0115	0.109
Fe_2O_3	1.40		0.0080	
% Total	99.58			

Table 4.3 Analyses of Sodium Ferrierite

Component	% w/w	mequiv.g^{-1}	mol/100g	mol/Al_2O_3
SiO_2	68.75		1.1447	12.757
Al_2O_3	9.15	1.795	0.0897	1.000
H_2O	11.75		0.653	7.275
Na_2O	2.678	0.864	0.0432	0.481
K_2O	2.88	0.611	0.0306	0.341
CaO	2.65		0.0473	
Fe_2O_3	1.24		0.0078	
MgO	0.604	0.299	0.0149	0.167
% Total	99.704			

Table 4.4 Analyses of Ammonium Clinoptilolite

Component	% w/w	mequiv.g^{-1}	mol/100g	mol/Al_2O_3
SiO_2	61.99		1.032	9.358
Al_2O_3	11.25	2.206	0.1103	1.000
H_2O	17.86		0.9922	8.996
Na_2O	1.096	0.354	0.0177	0.1602
K_2O	0.15	0.032	0.0016	0.0145
CaO	1.48		0.0264	
Fe_2O_3	0.95	0.119	0.0059	
$(NH_4)_2O$	5.01	1.927	0.0963	0.8736
% Total	99.47			

Table 4.5 Analyses of Ammonium Mordenite

Component	% w/w	mequiv.g^{-1}	mol/100g	mol/Al_2O_3
SiO_2	71.85		1.1963	11.245
Al_2O_3	10.85	2.130	0.1064	1.000
H_2O	7.00		0.3880	3.656
Na_2O	0.74	0.238	0.0194	0.112
K_2O	3.60	0.764	0.0382	0.359
CaO	0.75		0.0134	0.126
$(NH_4)_2O$	3.10	1.192	0.0596	0.560
Fe_2O_3	1.44		0.0091	
% Total	99.30			

Table 4.6 Analyses of Ammonium Ferrierite

Component	% w/w	mequiv.g^{-1}	mol/100g	mol/Al_2O_3
SiO_2	70.85		1.1797	12.940
Al_2O_3	9.298	1.823	0.0912	1.000
H_2O	10.940		0.6077	6.670
Na_2O	0.330	0.1064	0.0053	0.058
K_2O	2.300	0.4880	0.0244	0.268
CaO	1.460		0.0261	0.286
Fe_2O_3	1.300		0.0082	0.089
$(NH_4)_2O$	2.697	1.0373	0.0519	0.569
MgO	0.502	0.2490	0.0125	0.137
% Total	99.680			

4.1.3. Exchange Capacity of Zeolites.

For synthetic zeolites the exchange capacity can be safely based on aluminium content under normal conditions. However for this work natural zeolites were used and it was therefore quite difficult to decide what was the true exchange capacity of impurities which are likely to be present. Thus some of the aluminium present may not contribute to the ion exchange capacity. Considering sodium clinoptilolite and ammonium clinoptilolite, the following observations were made.

For the sodium form, if the exchange capacity is based on the sodium content of the zeolite, its value comes to be 1.896 meq g^{-1}. This is in close agreement with the exchange capacity of 1.83 meq g^{-1} which was obtained by Barrer, Papadopoulos and Rees[76]. The above workers used clinoptilolite from the same location and the exchange capacity was based on the sodium content. From the chemical analyses of sodium clinoptilolite undertaken in this work, it was found that other ions remain, such as potassium and calcium, that could in principle be exchangeable cations. If the aluminium content is used to assess the total exchange capacity the value of this function is found to be 2.188 meq g^{-1}. Balancing sodium, potassium and calcium it is found that some of the calcium could be present as an exchangeable ion and some probably as calcite impurity[76,146].

An examination of the ammonium clinoptilolite analysis suggests that the above observations are justified. The exchange capacity of NH_4-CLI based on the aluminium content is 2.206 meq g^{-1}.

This figure balances well with sodium, potassium and ammonium present in the zeolite (2.211 meq g^{-1}) The remaining calcium present is likely to be remaining calcite impurity, any exchangeable calcium having been replaced by ammonium ions. In the case of sodium clinoptilolite the sodium ions do not appear to exchange readily with calcium. These observations are in line with known selectivity sequences of sodium, ammonium, calcium[81]. With these observations in mind it was therefore decided to regard the aluminium content as the basis for the exchange capacity.

For practical reasons also (as in the case of the use of zeolites for pollution purposes) it is convenient to base the exchange capacity on their aluminium content. Note also that for ammonium clinoptilolite from the same location (Hector, California) an exchange capacity of 2.14 meq g^{-1} was given by Townsend[146].

Similar behaviour was observed with the other zeolites and therefore their exchange capacities were regarded as being equal to their aluminium content.

For sodium mordenite this results in an exchange capacity of 2.114 meq g^{-1}. The level of sodium exchange was only 1.087 meq g^{-1} whereas that of potassium was 0.824 meq g^{-1}. It is clear that only half of the exchange sites were occupied by sodium and also that the zeolite had a little calcium present as an exchangeable ion (<10%, 0.203 meq g^{-1})

As was observed with ammonium clinoptilolite, so with the

Table 4.7 Exchange Capacities

Zeolite	Capacity mequiv.g^{-1}
Na-CLI	2.188
Na-MOR	2.114
Na-FER	1.795
NH_4-CLI	2.206
NH_4-MOR	2.130
NH_4-FER	1.823

ammonium mordenite the calcium remaining must be an impurity since the exchange capacities of ammonia, sodium and potassium balanced the aluminium one.

In the case of ferrierite, the magnesium present must be considered as an exchangeable ion[144], although it does not exchange easily due to its position (section 1.6). For ferrierite exhaustively exchanged with sodium the exchange capacity on the basis of the aluminium content is 1.795 meq g^{-1}, and this is balanced well by the sodium (0.864 meq g^{-1}) potassium (o.611 meq g^{-1}) and magnesium (0.299 meq g^{-1}) contents together. Although the calcium content is quite high (2.65%w/w) the sodium ferrierite appears to have little exchangeable calcium present, in contrast to the cases of sodium clinoptilolite and sodium mordenite, which do include part of the calcium content as an exchangeable ion. Finally, considering the ammonium ferrierite, an exchange capacity of 1.823 meq g^{-1} was deduced on the basis of aluminium content. The ion exchange capacities for the sodium and ammonium forms of all three zeolites are given in Table 4.7.

4.2. The Ion Exchange Isotherms

The ion exchange equilibria are presented by isotherms, which are plots of the equivalent fraction of the counter ion in solution (A_s) against the equivalent fraction of the same ion in the zeolite(A_c). The point A_c when $A_s = 1$ gives the maximum level of exchange (A_{cmax})

The isotherms obtained are shown in the figures 4.1 to 4.24.

Also the figures 4,25 - 4.40 give the Kielland plots (Section 2.2.1) and the variations with composition of activity coefficients f_A, f_B for the zeolite phase (Section 2.2.2.) are given in figures (4.25-4.40).

4.2.1. Lead Exchange with NaCLI, Na-MOR, Na-FER.

Fig.(4.1.-4.3) give the isotherms for the exchange of lead with the sodium form of clinoptilolite, mordenite and ferrierite. The common feature for the three isotherms is the fact that the exchange does not proceed to 100%. The highest exchange is observed for the Pb/Na-CLI system where the maximal exchange level is 79.5%. For mordenite and ferrierite the $A_{c\ max}$ levels were 0.49 and 0.506 respectively. Examining the Pb/Na-CLI system first, the following observations were made.

When the solution phase was analysed, not only sodium, but also potassium and calcium were detected. The quantity of potassium (in equivalent fractions) varied from zero for low A_c values to 0.023 at $A_{c\ max}$(0.795), which indicates that 2.3% of the lead ions exchanged at the point of maximum exchange level were due to potassium released, and the rest (77.2%) were due to the exchanged sodium ions. The calcium released was quite high, but this quantity must be due to calcite impurity released from the zeolite, and not exchangeable ions. This must be so because direct analyses of the zeolite gave a lead content exactly equal to the sodium and potassium released (and found by analysis) in the solution.

For the analyses of isotherm solutions after exchange, the

EDTA titrimetric method was employed.[137] Also direct analyses on the zeolites were carried out (section 3.3.9). The isotherm solution after exchange was checked for calcium (section 3.4.4), and found that significant quantities were present (2.8 → 2.5 mg per 0.3g Na-CLI).

The Pb/Na-MOR exchange reaction was examined in the same manner as was the Pb/Na-CLI. The solution after exchange was analysed for calcium and potassium. No potassium was detected and the calcium released was very low (0.12 mg of calcium per 0.3g Na-MOR). Balances in the sodium exchanged for lead indicate that the calcium again arose from dissolution of calcite impurity and therefore was not an exchangeable ion. The isotherm was proved to be reversible over the whole range. The maximum level of exchange obtained was only 50% of the theoretical exchange capacity. (Section 4.1.3).

The Pb/Na-FER exchange was definitely ternary in nature. During the exchange, potassium was released. The quantity released changed from 0 to 6.2% of the exchanged ions as the lead loading in the zeolite was increased. When Na-FER was exhaustively exchanged to get $A_{c\ max}$, much higher quantities of potassium were released (9%). So at $A_{c\ max}$ (0.506) 9% of the exchange capacity was due to potassium and 41.6% due to sodium. The potassium left in the zeolite expressed in equivalent fraction is shown in Fig. 4.3. This represents the quantity of potassium that did not exchange with lead.

Though calcium was detected in the solution (0.52 - 0.49 mg per 0.3 g Na-FER), this was again likely to be due to some dissolution of an impurity since potassium plus sodium again balanced closely the lead content of the zeolite. Due to the ternary nature of this system thermodynamic treatments developed for binary ion exchange could not be applied.

The three ion exchanges mentioned above were carried out at a total solution concentration of 0.1 equiv.dm^{-3}. For the same systems, exchanges were performed at higher concentrations (0.5 equiv.dm^{-3}) and the isotherms are given in Figures (4.22-4.24). For comparison purposes, the isotherms obtained at lower concentration (0.1 equiv.dm^{-3}) are shown as well.

The general observation is that the higher the concentration the less selective is the zeolite, which is to be expected from the concentration-valency effect[117] which predicts an increasing selectivity for the divalent ion as the total normality of the solution phase decreases.[81,106]

4.2.2. Lead Exchange with NH_4-CLI, NH_4-MOR, NH_4-FER.

Ion exchange isotherms for the Pb/NH_4-CLI, Pb/NH_4-MOR, Pb/NH_4-FER systems are shown in Figure (4.4.-4.6).

The Pb/NH_4-CLI system shows that 100% exchange was achieved for lead. The lead ion exchanges with NH_4^+ as well as Na^+ already present in the zeolite and which could not be removed by exhaustive exchange with ammonium ion(Section 4.1). At $A_{c\ max}$=1, 16.2% of the exchange capacity was due to the sodium ions removed from the zeolite by lead. Also as the

exchange level for lead was increased from 0 to $A_{c\ max}$, analyses showed that the sodium and ammonium replaced as a function of Pb_c were not in constant ratio. At low Pb_c values the lead principally exchanged with ammonium ions, and at higher Pb_c values, the sodium replaced increased. So it is important to emphasise that the exchange is essentially ternary in nature. The exchange was proved to be irreversible, Figure 4.4., so thermodynamic treatments could not be applied. Also during the exchange, calcium impurity was detected, but this quantity was much lower than that released during the Pb/Na-CLI exchange. This follows because the ammonium clinoptilolite contained less calcium impurity anyway due to the removal of calcium carbonate by the ammonium nitrate solution (1M NH_4NO_3) during the conversion of the clinoptilolite to the homoionic form NH_4-CLI (Section 3.1.1.).

The Pb/NH_4-MOR exchange is a binary one with $A_{c\ max}$=0.517. No sodium, potassium or calcium were detected in any case in the solution after attainment of ion exchange equilibrium, so thermodynamic treatment of these data was possible. Although the reversible points were slightly out of the isotherm shape, it was considered that the system was reversible. The discrepancies are likely to be due to experimental error.

The Pb/NH_4-FER system was also binary, even though the NH_4-FER zeolite contained high quantities of sodium and potassium ions (Table 4.6).

The exchange that took place was only between lead and ammonium ions. Calcium detected was present only in the minutest

trace (0.04 mg/0.3g). The maximum level of exchange of 48.6% was lower than the Pb/Na-FER exchange (50.6%), Section 4.2.1. Direct comparison of the systems Pb/Na-FER, and Pb/NH_4-FER shows that the potassium present in the two forms of ferrierite exhibited some preference for the zeolite phase in the presence of Pb^{+2} and NH_4^+ ions, while in the presence of Pb^{+2} and Na^+ ions, it showed more preference for the solution phase. Also in the case of the Pb/Na-FER system, the calcium released was about ten times higher than that found in the isotherm solutions for the Pb/NH_4-FER exchange.

4.2.3. Cadmium Exchange with Na-CLI, Na-MOR, Na-FER.

For the cadmium exchanges, two salts were used, viz $Cd(NO_3)_2$ and $CdCl_2$. Figures (4.7.-4.9), represent the exchange equilibria observed with the three sodium zeolites when cadmium nitrate salt was used, while Figures (4.13-4.15) are the corresponding results for the cadmium chloride case. The isotherm shapes for the two cadmium salts and the same zeolite are quite different but the maximum level of exchange is the same. The cadmium ion generally shows greater preference for the solution phase when the co-ion in solution is chloride.

Considering first the $Cd/Na(NO_3)$ exchange in clinoptilolite, the $A_{c\ max}$ value obtained was 0.656 and the isotherm has no inflection point. In contrast, for the Cd/Na(Cl)-CLI system an inflection point is seen at high cadmium concentrations (i.e. as $A_s \rightarrow 1$). Both isotherms are reversible and binary,

since only sodium was released during the exchange. The calcium detected in the isotherm solutions was always negligible.

Figures 4.8., 4.14, give the isotherms for the systems Cd/Na(NO_3)-MOR and Cd/Na(Cl)-MOR respectively. Both give the same value for the maximum level of exchange ($A_{c\ max}$= 0.334). It is again observed that cadmium shows a greater preference for the solution phase when the co-ion is chloride. During the exchange the only ions that were released from the sodium mordenite were the sodium ions. No potassium was detected and again calcium was only found in traces. The reversibility tests carried out confirmed that the isotherms were fully reversible and hence thermodynamic parameters could be determined for these systems.

The isotherms presented by the Figures4.9, 4.15. are those obtained for the Cd/Na(NO_3)—FER and Cd/Na(Cl)—FER systems respectively. The maximum level of exchange was $A_{c\ max}$= 0.339 for both salts. This exchange level is almost identical to that seen with Na-MOR but much lower than that seen with Na-CLI,($A_{c\ max}$= 0.656). The isotherm solutions after the exchanges contained no potassium, and again only traces of calcium. The tests carried out showed that the isotherms were fully reversible. A common feature for the three zeolites exchanged with the two cadmium salts is that the systems were without any doubt binary and also that calcium carbonate dissolution occurred only to a limited extent. This is in marked contrast to what was observed in the case of the lead

exchanges with the same zeolites (Section 4.2.1.).

4.2.4. Cadmium Exchange with NH_4-CLI, NH_4-MOR, NH_4-FER.

The isotherms for cadmium exchanged with ammonium clinoptilolite in the presence of either nitrate or chloride co-ions are given in Figures 4.10, 4.16. Both isotherms show an inflection at high cadmium concentrations but with the $Cd/NH_4(Cl)$-CLI system is more distinct. Both exchanges give a value for $A_{c\ max}$ of 0.81 and were ternary in nature since sodium was found in solution along with ammonium. At high equilibrium cadmium concentrations in solution, (i.e. as $A_s \rightarrow 1$), the sodium released in solution from exchange with cadmium was quite high, finally reaching at $A_{c\ max}$ a value of 17% of the total exchange capacity of the zeolite. The rest (64%) was due to exchange of ammonium ions. At low Cd_c values the cadmium mainly exchanged with ammonium ions, but as Cd_c increased the ratio of sodium to ammonium replaced increased. Both scdium left in the zeolite and lead taken up are shown in Figure 4.10. In addition, traces of potassium were detected. The calcium present in solution after exchange was also found to be quite high, and when the zeolite was exhaustively exchanged with cadmium solution, still more calcium impurity came out. Along the isotherm, the calcium content of the isotherm solution varied from 0 → 0.4 mg per 0.3g, the lower values (obviously) being found at lower cadmium loadings in the zeolite.

The exchanges for the $Cd/NH_4(NO_3)$-MOR and $Cd/NH_4(Cl)$-MOR systems

are given in Figures 4.11 and 4.17. $A_{c\ max}$ was 0.327 irrespective of which co-ion was present in solution, and reversibility was proved. Again, this pair of isotherms suggests that cadmium shows a greater preference for the solution phase when chloride is the co-ion. For the $Cd/NH_4(Cl)$-MOR isotherm (Figure 4.17) an inflection point was observed at values of Cd_s close to unity. Both exchanges were binary and reversible so again thermodynamic data could be calculated.

The lowest exchange levels were observed between ammonium ferrierite and cadmium. Figures 4.12,4.18 represent $Cd/NH_4(NO_3)$-FER and $Cd/NH_4(Cl)$-FER exchanges respectively. The maximum level of exchange obtained was 28% irrespective of the cadmium salt used. The $Cd/NH_4(Cl)$-FER system shows a distinct inflection point at high Cd_s values (Cd_s = 0.8→1.0). Both isotherms were fully reversible and no potassium, sodium or calcium were detected in the isotherm solutions after the exchanges had reached equilibrium, so the systems were binary, and thermodynamic treatments were possible. Comparing the Cd/Na-FER and Cd/NH_4-FER systems it is apparent that the zeolite shows preference for the ammonium ion over the sodium ion, since the exchange in NH_4-FER is lower than that of Na-FER for the same counter ion (i.e. cadmium).

4.2.5. Exchange of Ammonium with Na-CLI, Na-MOR, Na-FER.

The sodium/ammonium isotherms, employing as the initial material the sodium clinoptilolite, mordenite and ferrierite (analysis data in tables 4.1 - 4.3) are given in Figures 4.19-

4.21. For the NH_4/Na-CLI system the maximum level of exchange obtained was 76.5%. In order to estimate $A_{c\ max}$, direct measurements on the zeolite were undertaken to obtain the ammonium ion content. Also the washings were kept and analysed in order to check for the stoichiometry of exchange. The equivalent fractions of sodium and potassium in the zeolite that have been exchanged were respectively 0.755 and 0.01. These two figures exactly balance the ammonium content found in the zeolite after exchange. The calcium found in the isotherm solutions was quite high, but again this cannot be exchangeable ion but must be due to the dissolution of impurities from the zeolite. The calcium quantity eluted varied from 2.5→3.38 mg per 0.3g of Na-CLI, the lower values corresponding to low $(NH_4)_s$ values. At $(NH_4)_{c\ max}$ the calcium content in solution was found to be 4.61 mg for the same zeolite quantity (i.e. 0.3g).

The NH_4/Na-MOR exchange proceeded only to 50.1% of the measured exchange capacity (table 4.2). For the determination of $(NH_4)_{c\ max}$, direct measurements were carried out on the zeolite to get its ammonium content (Section 3.3.3.). Also the washings, after the exhaustive exchange of Na-MOR with ammonia solution, were analysed. Exchange only took place between the sodium and ammonium ions. No potassium was found and the calcium present in the solution was again impurity. The quantity varied from 1.45→1.69 mg(per 0.3g zeolite) as $(NH_4)_s$ increased. The exchange was found to be reversible and the shape of the isotherm was highly rectangular.

Examining the NH_4/Na-FER exchange, it can be seen that the shape of the isotherm is highly rectangular, and similar to the NH_4/Na-MOR system. The maximum level of exchange was 49.9%, which is again very close to that found with mordenite (50.1%). From the solution analyses it was confirmed that the exchange was ternary in nature, since potassium along with sodium was found in solution. At $(NH_4)_{c\ max}$ (which equalled $0.499(NH_4)_c$) the sodium released from the zeolite accounted to an equivalent of $Na_c = 0.389$. Similarly, the amount of potassium released was in proportion to the total exchange capacity, equivalent to 0.11. The sum of these two agreed excellently with the measured $(NH_4)_{c\ max}$.

In addition, at low $(NH_4)_c$ values the ammonium ions principally exchanged with sodium ions but as $(NH_4)_c$ increased, potassium was released in the solution as well. The high calcium content of the isotherm solution was again due to calcium impurity (2.057→2.703 mg per 0.3g zeolite).

4.2.6. Summary of Analysis and Results

For an easier comparison of the systems discussed in section 4.2., a summary of the analysis and results obtained are given in Table 4.8.

4.3. Ternary Ion Exchange.

So far the systems discussed (section 4.2) were intended to be binary studies, even though in some cases, incidental exchange by a third ion species rendered them ternary in nature.

Table 4.8 Binary Isotherm Results.

System	Exchanging Species	Reversib.	$A_c$max
Pb/Na-CLI	Pb,Na,K	Reversible	0.795
Pb/Na-MOR	Pb,Na	Reversible	0.490
Pb/Na-FER	Pb,Na,K	Irreversible	0.506
Pb/NH_4-CLI	Pb,Na,NH_4	Irreversible	1.000
Pb/NH_4-MOR	Pb,NH_4	Reversible	0.517
Pb/NH_4-FER	Pb,NH_4	Reversible	0.486
Cd/Na(NO_3)-CLI	Cd,Na	Reversible	0.656
Cd/Na(NO_3)-MOR	Cd,Na	Reversible	0.334
Cd/Na(NO_3)-FER	Cd,Na	Reversible	0.339
Cd/NH_4(NO_3)-CLI	Cd,NH_4,Na	Irreversible	0.810
Cd/NH_4(NO_3)-MOR	Cd,NH_4	Reversible	0.327
Cd/NH_4(NO_3)-FER	Cd,NH_4	Reversible	0.280
Cd/Na(Cl)-CLI	Cd,Na	Reversible	0.656
Cd/Na(Cl)-MOR	Cd,Na	Reversible	0.334
Cd/Na(Cl)-FER	Cd,Na	Reversible	0.339
Cd/NH_4(Cl)-CLI	Cd,NH_4,Na	Irreversible	0.810
Cd/NH_4(Cl)-MOR	Cd,NH_4	Reversible	0.327
Cd/NH_4(Cl)-FER	Cd,NH_4	Reversible	0.280
NH_4/Na-CLI	Na,NH_4	Reversible	0.765
NH_4/Na-MOR	Na,NH_4	Reversible	0.501
NH_4/Na-FER	Na,NH_4,K	Irreversible	0.490

Some studies were carried out in addition which were intended to be ternary in nature. Complete ternary isotherms were not constructed however, since for these, points would be required to cover the whole surface of the triangular composition diagram[126]. The systems examined are given in table 3.3.. Two sets of ternary exchanges were performed. The first set involved lead and cadmium present together in the solutions exchanging with either the sodium or the ammonium forms of the three zeolites. The other sets involved lead plus sodium or cadmium plus sodium in solution, exchanging with either NH_4-CLI or NH_4-MOR.

The equivalent fractions of each ion in solution and zeolite phases (i.e. A_s, A_c) were evaluated and these values can be used to estimate the separation factor (practical selectivity) for a ternary exchange system. The results are given in Appendix II (derived data) and discussed in detail in chapter five.

4.4. Derived Results.

In order to obtain values of the separation factor which is a "practical" function, describing the selectivity of the zeolite for an ion under the prescribed conditions and defined by the equation 2.6, 2.7, the experimental isotherm data points had to be best-fitted. In addition to best-fitting data, the thermodynamic parameters (section 2.2.) can only be evaluated when the isotherms are normalised. The procedures involved are described in the following section.

4.4.1. Fitting of the Isotherm Experimental Data.

The isotherm points obtained experimentally were smoothed by a best-fitting procedure using polynomial equation.

The polynomial equation is of the form

$$y = A_0 + A_1 x + A_2 x^2 + A_3 x^3 \quad A_n x^n$$

where y represents the A_c values of the isotherm

x represents the A_s values of the isotherm

For each isotherm various equations of different orders were fitted by altering n from 2→5 and the best fit was considered to be the one which combined a smooth fit with a low value of the fitting factor R.

$$R = \sqrt{\frac{\sum(yobs - ycalc)^2}{N - M - 1}}$$

where N = number of experimental points

M = order of polynomial

R is the sum of the residuals between the observed values of y and the predicted values of y using the polynomial equation.

Usually, when high order polynomial equations were fitted to the experimental data points, low values for the R factor were observed , but the isotherm plotted was of a "wavy" shape. Such a shape is not a smooth fit and definitely not consistent with that expected from experimental data. The most difficult isotherm to treat using the polynomial approach were the highly rectangular ones. The problem is exemplified in Figure 4.41.

The best fit obtained is shown as the line joining the experimental points and it is clearly seen that it is a very bad fit for low $A_s(x)$ values. This was partially overcome by using a polynomial for high values of $A_s(x)$ where it fits well, while for the low x values the experimental data points were used. This procedure had to be followed for all the experimental isotherms of rectangular shape. If the polynomial equation chosen by the computer on the basis of R value data was acceptable as the best fit, then the corrected $A_c(y)$ values were used for the thermodynamic treatment. The $A_{c\ max}$ value was the calculated value of y at x=1 (i.e. $A_s=1$). Since the value of $A_{c\ max}$ is used for the normalisation of the isotherm (sections 2.3, 4.5.2) it was essential to "force" the best fitting polynomial through the experimental data of the $A_{c\ max}$ point for reasons which are explained in section (4.5.2) This was achieved by statistically weighting the point $A_s=1$, $A_{c\ max}$, so that the $A_{c\ max}$ value predicted by the polynomial coincided with the experimental one. For most of the isotherms statistical weighting of the point $A_{c\ max}$ was required. Figure 4.4.2 represents an isotherm with no statistical weighting of $A_{c\ max}$ while Fig. 4.4.3 represents the same isotherm with $A_{c\ max}$ weighted by a factor of five.

4.4.2. Selectivity Quotients

Figures (4.44-4.47) show values of the separation factor α (unnormalized values α^{UN}), for the various ion exchange systems. These values in fact indicate the preference of a certain ion for the solution or zeolite phase (section 5.5).

Figures (4.48-4.51) show corresponding separation factors α^N obtained after the isotherms had been normalized.

4.4.3. Thermodynamic Treatment

For the thermodynamic treatment for two different ionic species to be valid, the ion exchange process must be reversible, (section 2.2.), and also binary. As mentioned in section 4.2, some of the systems were found to be intrinsically ternary in nature. In these cases, no thermodynamic parameters were calculated. Table 4.8 lists the above systems.

Using a computer programme, the solution phase Γ values were calculated first and then the zeolite activity coefficients. Details of the procedures are given below.

4.4.3.1. Calculation of Γ.

Values of the activity coefficient ratio Γ were obtained using Glueckauf's[122] method (section 2.2.1). Before Γ could be calculated, the mean molal activity coefficients $\gamma_{\pm}$ of the pure salts used had to be determined. This was so because in the literature[120] the values of $\gamma_{\pm}$ given do not cover the range of the ionic strengths used in the experiments. In order to obtain the values of $\gamma_{\pm}$ over the complete range of the experimental ionic strength (I), a modified Debye Huckel[121] expression was used of the form.

$$\log(\gamma_{\pm}) = \frac{-A/z_A z_B/\sqrt{I}}{1 + Ba\sqrt{I}} + bI \qquad \ldots\ldots 4.1.$$

where A and B were functions of the absolute temperature and

permittivity of the medium.

$$A = \frac{1}{2.303}\sqrt{\left(\frac{125N}{4\pi^2}\right)}\left(\frac{e^2}{k\epsilon_r\epsilon_o T}\right)^{3/2}$$

$$B = \left(\frac{Ne^2}{5k\epsilon_r\epsilon_o T}\right)^{\frac{1}{2}} \quad cm^{-1}\ dm^{3/2}\ mol^{-\frac{1}{2}}$$

where ϵ_r, ϵ_o are the relative permittivity and the permittivity of free space respectively.

At the temperature T of 298K using water as a solvent, A and B take the values

$$A = 0.5115\ mol^{-\frac{1}{2}}\ dm^{3/2}$$

$$B = 3.291 \times 10^{-9} cm^{-1} mol^{3/2}\ dm^{3/2}\ K^{\frac{1}{2}}$$

The parameters a,b are dependent on the properties of both the electrolyte (salt) and the solvent (water) and are nearly constant[147] over a wide range of ionic strengths. The constant a[123] is considered to be the "radius of the ionic atmosphere" surrounding the particular ion, and b is introduced to compensate for interactions arising at higher concentrations[121].

To obtain $\gamma_\pm$ a and b must be calculated and this is done by taking the $\gamma_\pm$ values of the particular salt at two values of ionic strength and substituting into expression 4.1. Two equations result having a and b as unknowns. Solving the equations simultaneously yields values for both a and b, but since the expressions are quite complicated a computer programme was used. Two values of a were produced by this

procedure, one being negative and the other positive. Due to the physical significance of the parameter a[121], the positive value was taken, then b was obtained. The values of the parameters 'a' and 'b' so calculated are shown in table 4.9. For all the salts used it was possible to calculate the above parameters except in the case of cadmium chloride where complex roots were obtained, the physical significance of which is questionable. Obviously for the cadmium chloride salt, the Debye-Hückel model is not an adequate description. To overcome this problem therefore, instead of using the modified Debye-Hückel[121] expression (eq. 4.1) a polynomial was fitted for a set of $\gamma_{\pm}$ values of $CdCl_2$[148] over a range of ionic strength.

It must be noted that the activity coefficients $\gamma_{\pm}$ so calculated from the Deby-Hückel equation were those of the pure salts, so corrections were then required for the actual experimental conditions (i.e. the activity coefficients of the mixed salts). For this purpose Gluekauf's[122] expressions were used and the values of the activity coefficients of the mixed solutions so obtained were substituted into equation 2.41, to finally estimate Γ (the ratio of the single ion activity coefficients raised to the powers of the appropriate ion valences).

The Γ values obtained were substituted into equation 2.17 and the corresponding Kielland coefficients K_c were next calculated (section 2.2.1).

Table 4.9. Debye Hückel parameters a,b.

Salt	I	Γ	a x 10^{-9}	b x 10^{-1}
NaCl	0.1	0.778	0.4029	0.4937
	0.2	0.735		
$NaNO_3$	0.1	0.762	0.4403	-0.7118
	0.2	0.703		
NH_4Cl	0.1	0.770	0.4370	-0.2357
	0.2	0.718		
NH_4NO_3	0.1	0.740	0.1618	0.7670
	0.2	0.677		
$Pb(NO_3)_2$	0.3	0.405	0.2683	-0.4954
	0.6	0.316		
$Cd(NO_3)_2$	0.3	0.516	0.4825	0.4111
	0.6	0.467		

4.4.3.2. Calculation of Zeolite Phase Activity Coefficients and the Thermodynamic Parameters K_a, ΔG^{θ}.

The zeolite phase activity coefficients f_A, f_B were calculated using equations 2.66, 2.67.

Firstly the integral of the Kielland quotient K_c with respect to A_c had to be evaluated. For this a polynomial equation was used to express $\ln K_c$ in terms of the corresponding A_c values.

$$\ln K_c = A_0 + A_1 A_c + A_2 A_c^2 + A_3 A_c^3 \ldots A_n A_c^2$$

The best fitting polynomial procedure followed was the same as that used for fitting isotherm data (section 4.4.1). Figures 4.25-4.40 give the Kielland plots, as well as the activity coefficients for the A_c range from 0→1. The equilibrium constants, and the free energies of the various exchange systems, were then calculated from the equations 2.19, 2.20) , and the results obtained are shown in tables 4.10-12.

4.5. Errors

Errors arise mainly from two sources. Firstly the experimental inaccuracies, and secondly the errors introduced due to the mathematical procedures adopted in order to evaluate the required parameters (section 4.4.1).

4.5.1. Experimental Inaccuracies.

The experimental methods used were mainly titrimetric and

Table 4.10 ΔG^{Θ} /kJ(g.equiv.)$^{-1}$, K_a values obtained at 0.1 equiv.dm^{-3}

Counter Ion	Pb		Cd*		Cd**	
Zeolite	ΔG^{Θ}	K_a	ΔG^{Θ}	K_a	ΔG^{Θ}	K_a
Na-CLI	-3.81	21.87	2.26	0.160	2.755	0.107
Na-MOR	-4.63	42.52	1.07	0.419	1.108	0.408
Na-FER	-	-	2.05	0.190	1.676	0.257
NH_4-CLI	-	-	-	-	-	-
NH_4-MOR	3.28	0.070	1.23	0.370	2.880	0.097
NH_4-FER	1.42	0.317	2.98	0.089	3.660	0.052

* Cadmium nitrate , ** Cadmium chloride

Table 4.11 ΔG^{Θ}/kJ(g.equiv.)$^{-1}$ values for Na $\rightleftharpoons$ NH_4 exchange equilibria at 0.1 equiv.dm^{-3}

Zeolite	ΔG^{Θ}	K_a
Na-CLI	-4.033	5.12
Na-MOR	-4.590	6.43
Na-FER	-	-

Table 4.12 ΔG^{Θ}, K_a values for Pb $\rightleftharpoons$ Na equilibria at 0.5 equiv.dm^{-3}

Zeolite	ΔG^{Θ}	K_a
Na-CLI	-3.969	24.90
Na-MOR	-3.507	17.13
Na-FER	-	-

gravimetric ones. Atomic absorption and flame photometric techniques were also employed, but not to a great extent. For the zeolite analyses (section 3.3.) gravimetric techniques were used to determine silica and aluminium. These methods are difficult, and require much practice before reproducible results are the norm. The analyses were repeated many times until the results obtained were in a reasonable agreement. For silica the difference should not be greater than 0.25% and for the aluminium $\not>$0.05%. Since aluminium is used for the calculation of the zeolite exchange capacity (section 4.1.3), its accurate determination is essential.

The flame photometer gave very good results for sodium and potassium and reproducibility was almost perfect when the same samples were examined at different times. Tha main problem was atomic absorption, since great fluctuations in the absorbance reading can occur. Errors could be as high as 20% and were minimized by using standards for every two or three measurements taken. Atomic absorption spectrophotometry was only used to get the low A_s values (i.e. the equivalent fraction of the metal ion in solution) because the difference between initial and final solution phase concentrations cannot be measured as accurately using titrimetric methods in these cases. Table 4.13 indicates the errors that can arise when atomic absorption is employed as an analytical technique. For analysis of the solution phase at higher A_s and hence A_c values (i.e. the equivalent fractions of the metal ion in the solution and zeolite phases

Table 4.13. Errors introduced when absorbance varies. Consider Pb measurements at low A_s values.

ABSORBANCE (Initial Solution)	ABSORBANCE (Solution after) (exchange)	% Error
0.140 ± 0.002	0.069 ± 0.002	± 5.6
0.140 ± 0.005	0.069 ± 0.005	± 14.08
0.110 ± 0.002	0.040 ± 0.002	± 5.7
0.110 ± 0.005	0.040 ± 0.005	± 14.2

Table 4.14. Effect on A_c value for the system Pb/NH_4-MOR when EDTA readings vary in the range $\pm$ 0.02ml.

EDTA (Initial-final Solution)	A_c
0.49 ± 0.02	0.416 ± 0.016
0.43 ± 0.02	0.361 ± 0.021
0.34 ± 0.02	0.290 ± 0.015
0.30 ± 0.02	0.255 ± 0.017
0.24 ± 0.02	0.204 ± 0.017
0.12 ± 0.02	0.102 ± 0.017

respectively) titrimetric methods were used. The repeated burette reading for a particular ion concentration should be in agreement to ±0.02ml. Higher differences were not acceptable. Tables 4.14 indicate the errors which can arise from this source, using as a criterion agreement between readings of ± 0.02ml.

4.5.2. Normalization and Its Effects

The normalization procedure alters all the A_c values obtained by dividing the best fit value by $A_{c\ max}$ before the calculation of thermodynamic parameters is initiated. So $A_{c\ max}$ has to be accurately determined experimentally and the isotherm best-fitting procedure must be suitably weighted in favour of $A_{c\ max}$ (section 4.4.1). To indicate how critical are the points in the region $A_c \rightarrow A_{c\ max}$, various parameters were calculated for different $A_{c\ max}$ values within the range ±0.02 of the experimentally estimated $A_{c\ max}$ value. Table 4.15 indicates the K_a and ΔG^θ values so obtained when $A_{c\ max}$ was varied in this manner for the systems Cd/Na-CLI, Cd/Na-MOR and Pb/NH_4-MOR. Also Figure 4.52 -4.57 show the variations in the Kielland plots and zeolite activity coefficients that arise from this procedure.

Considering the systems examined, it is obvious that for a given A_c value $\ln K_c$ changes markedly as $A_{c\ max}$ is varied. These changes are very large in the region of $A_c \rightarrow A_{c\ max}$ and less significant in the region $0 < A_c < 0.6$. This difference in behaviour between the two regions arises from the fact

that B_c tends to zero when $A_c \rightarrow A_{c\ max}$,

Considering the expressions 2.10, 2.17 respectively

$$K_m = \frac{A_c^{z_B} \, m_B^{z_A}}{B_c^{z_A} \, m_A^{z_B}}$$

$$K_c = K_m \, \Gamma$$

it is apparent that a slight change in A_c for the region $A_c \rightarrow A_{c\ max}$ can result in a 100% change in B_c value and hence great variations in K_m which in turn will alter K_c significantly. It must be noted that the Γ term does not change with A_c variations. For the region $0<A_c<0.5$ the same change in A_c value will alter B_c, but the percentage change will be much lower and hence will have a lesser effect on K_m. Consequently K_c in this case does not change significantly.

From the equation (2.66,2.67) it is seen that the zeolite activity coefficients f_A, f_B are functions of Kielland quotients so that any changes in K_c will affect them. As $A_{c\ max}$ changes, f_A shows less variations in the region $A_c \rightarrow A_{c\ max}$ while f_B exhibits the greatest variations.

Finally the effect of reducing $A_{c\ max}$ is seen to result in an increase in K_c, giving higher values for the equilibrium constant K_a since

Table 4.15 Values of ΔG^{θ} and K_a obtained by varying $A_c max$

Exchange system	$A_c max$	ΔG^{θ} kJ(g.equiv)$^{-1}$	K_a
Cd/Na-CLI	0.635	2.015	0.196
	0.640	2.072	0.187
	0.645	2.130	0.178
	0.650	2.188	0.170
	0.656*	2.246	0.162
	0.660	2.305	0.155
	0.675	2.484	0.134
	0.680	2.544	0.127
Cd/Na-MOR	0.334*	1.074	0.419
	0.340	1.125	0.402
	0.345	1.224	0.371
	0.350	1.350	0.337
	0.355	1.480	0.302
	0.360	1.620	0.268
Pb/NH_4MOR	0.490	3.014	0.087
	0.500	3.173	0.077
	0.505	3.201	0.075
	0.510	3.227	0.072
	0.513*	3.276	0.070

* $A_c max$ obtained by best-fitting polynomial of isotherm data

$$K_a = (z_B - z_A) + \int_0^1 \ln K_c \, dA_c$$

This will result in more negative values for the standard free energy (Table 4.15).

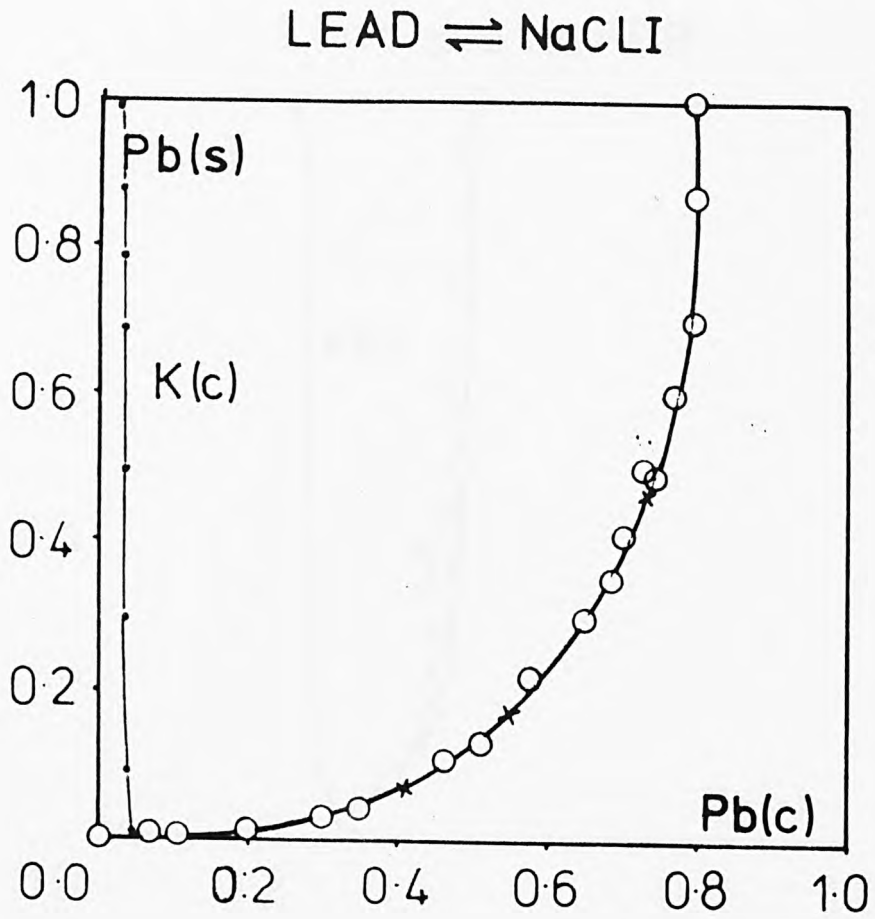

A_c max = 0·795

FIG.4.1

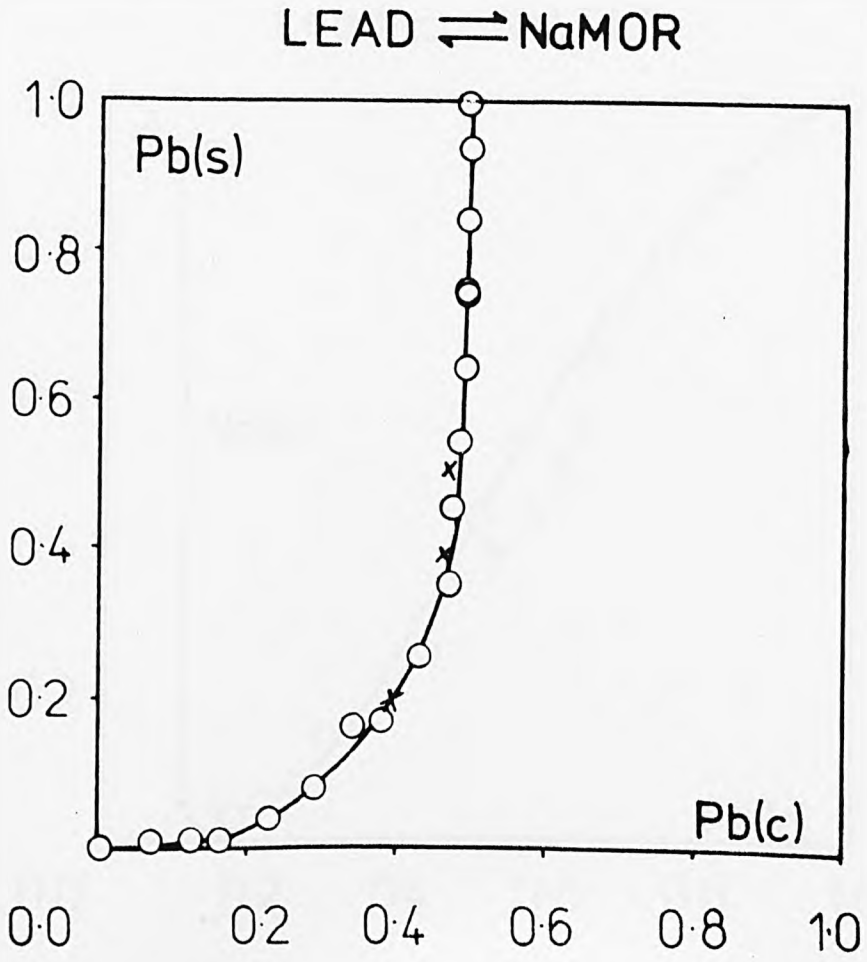

A_c max = 0·490

FIG.4.2

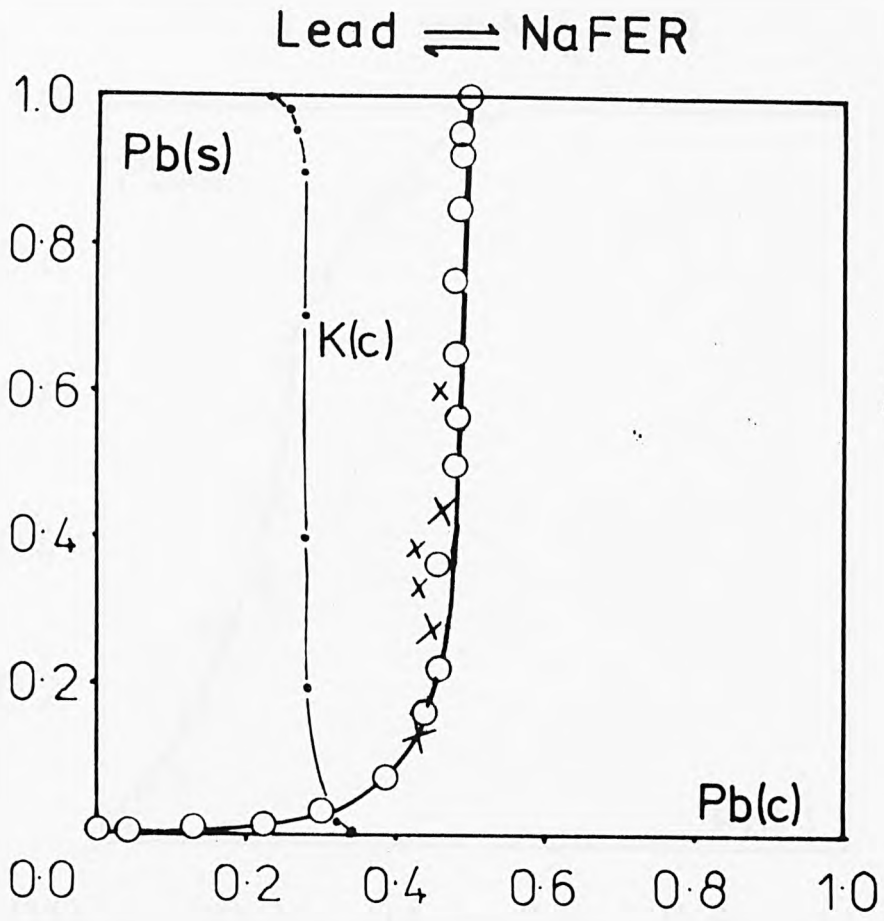

$A_c max = 0{\cdot}506$

FIG.4.3

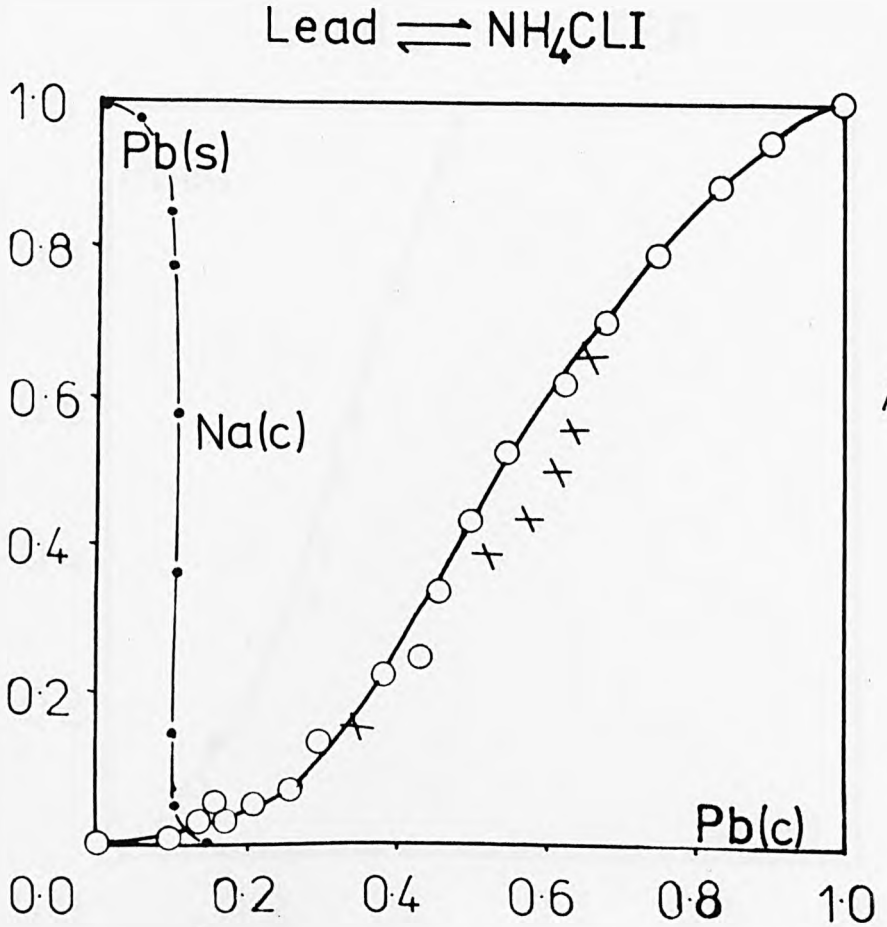

$A_c max = 1{\cdot}0$

FIG.4.4

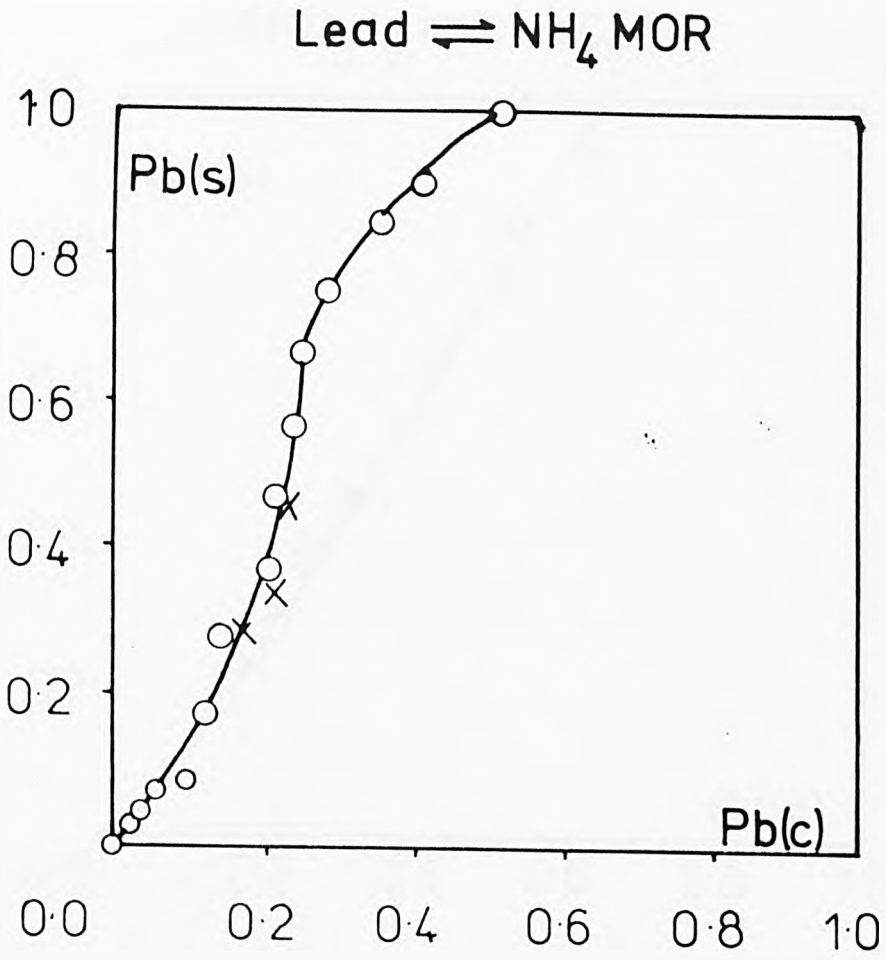

A_c max=0·517

FIG.4.5

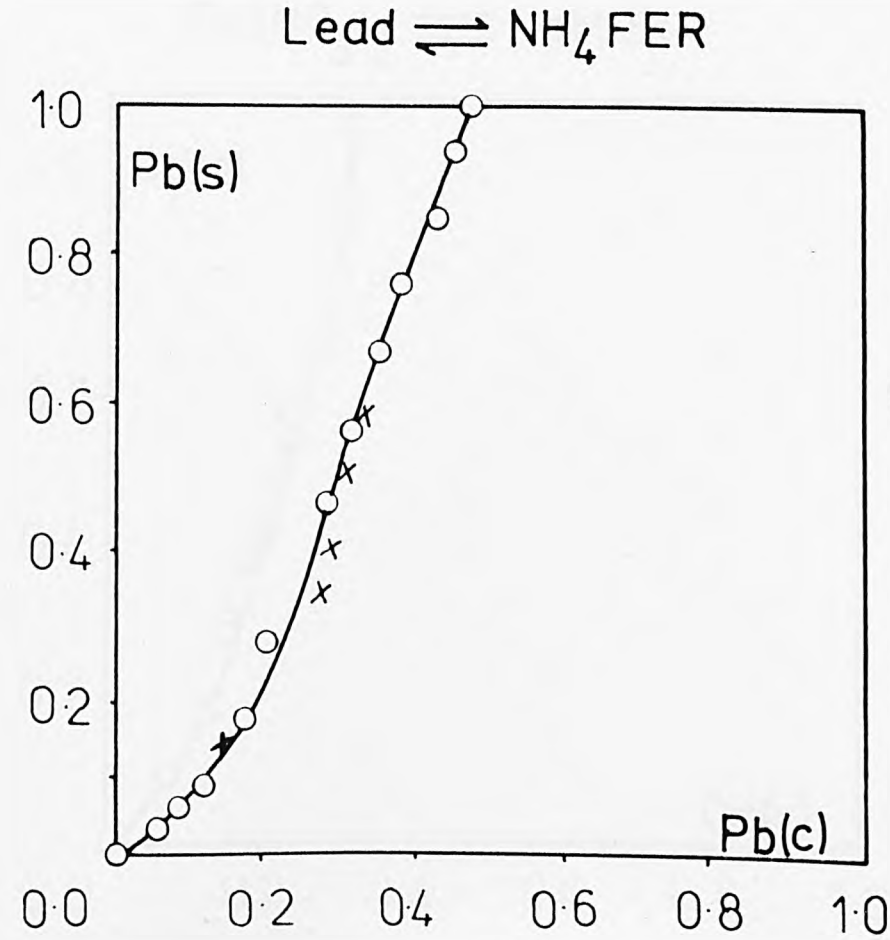

A_c max=0·486

FIG.4.6

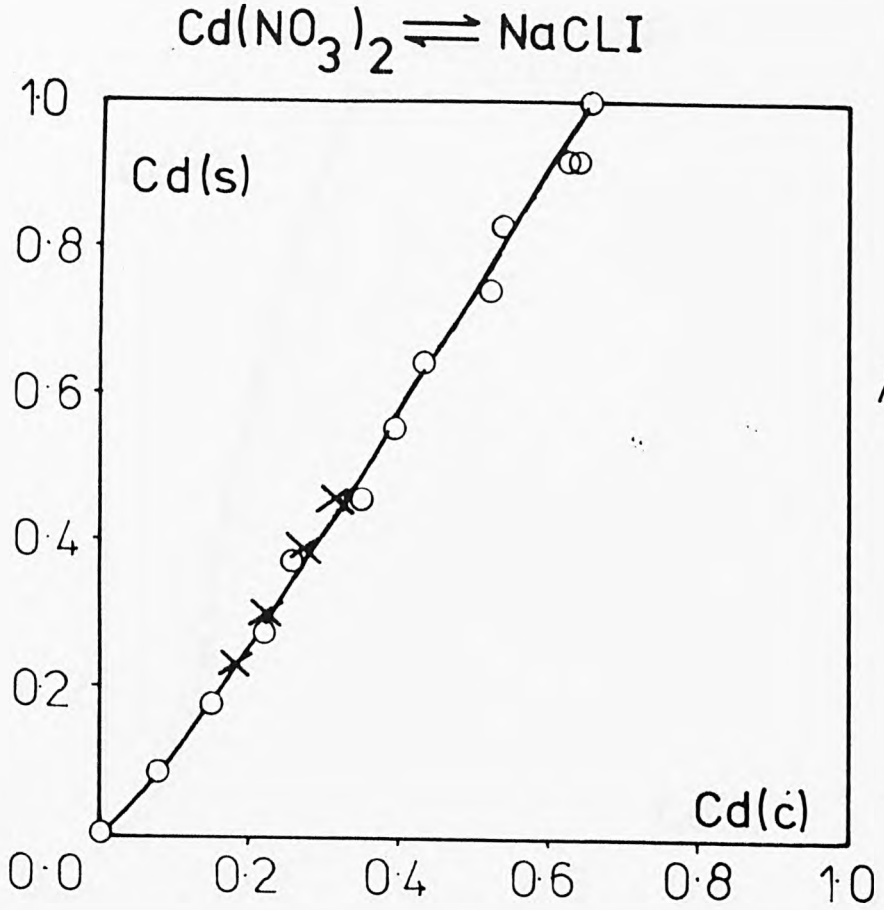

A_c max= 0·656

FIG.4.7

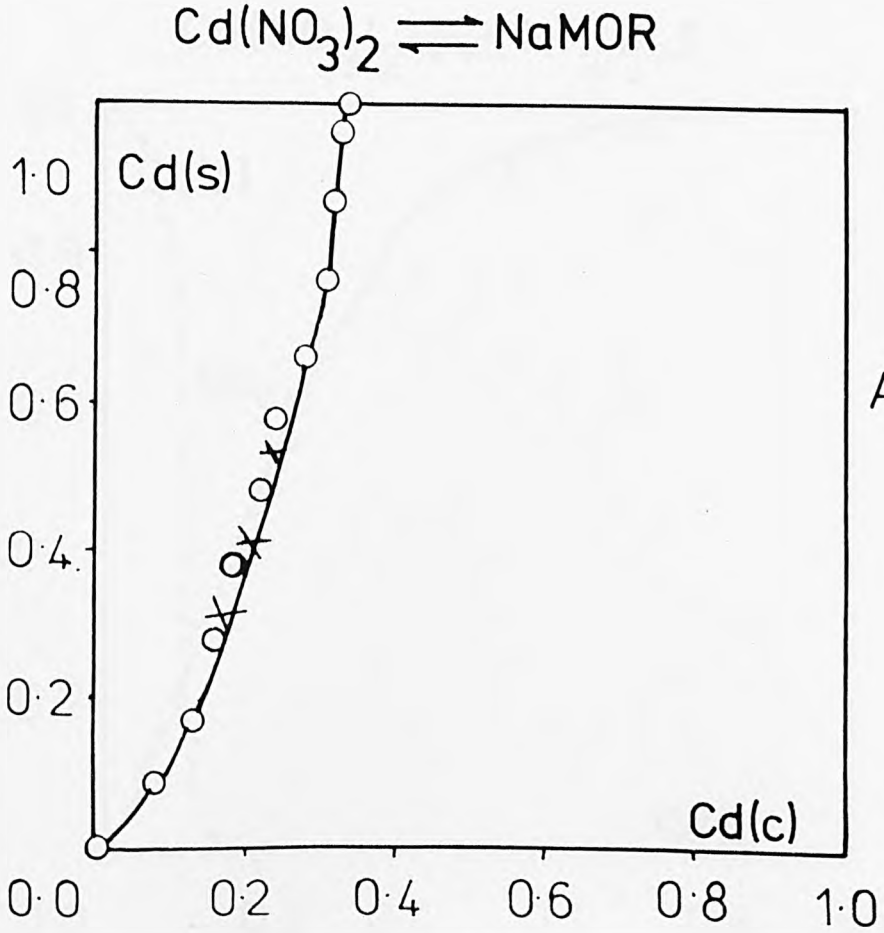

A_c max= 0·334

FIG.4.8

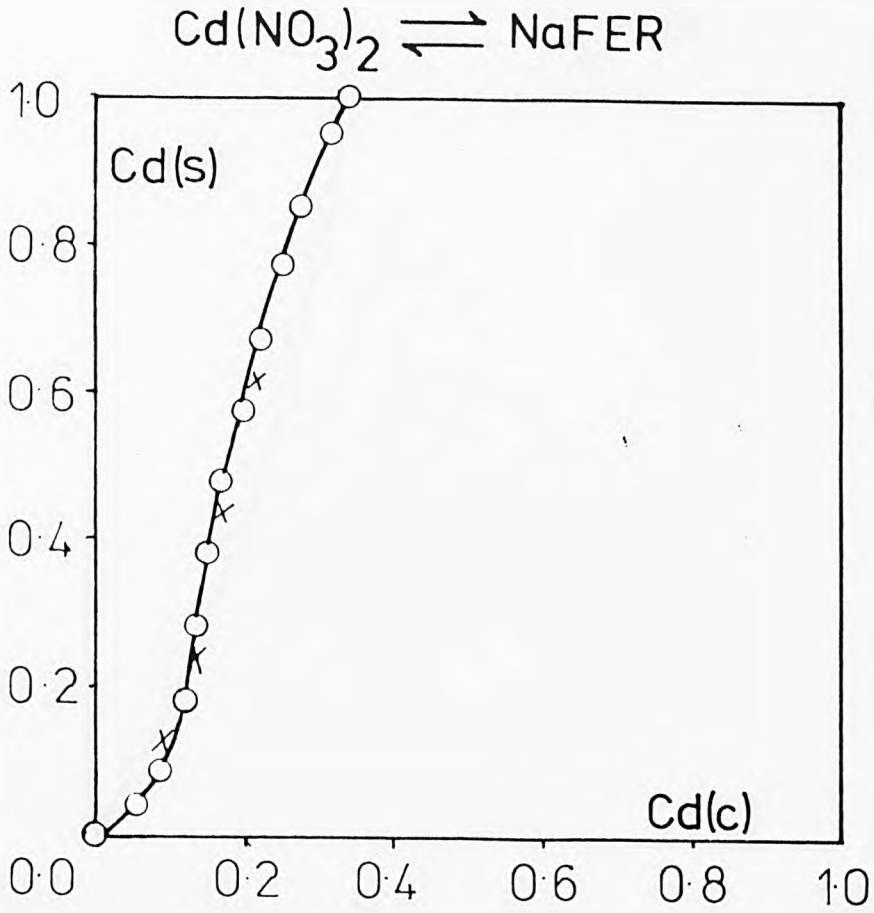

$A_c max = 0.339$

FIG.4.9

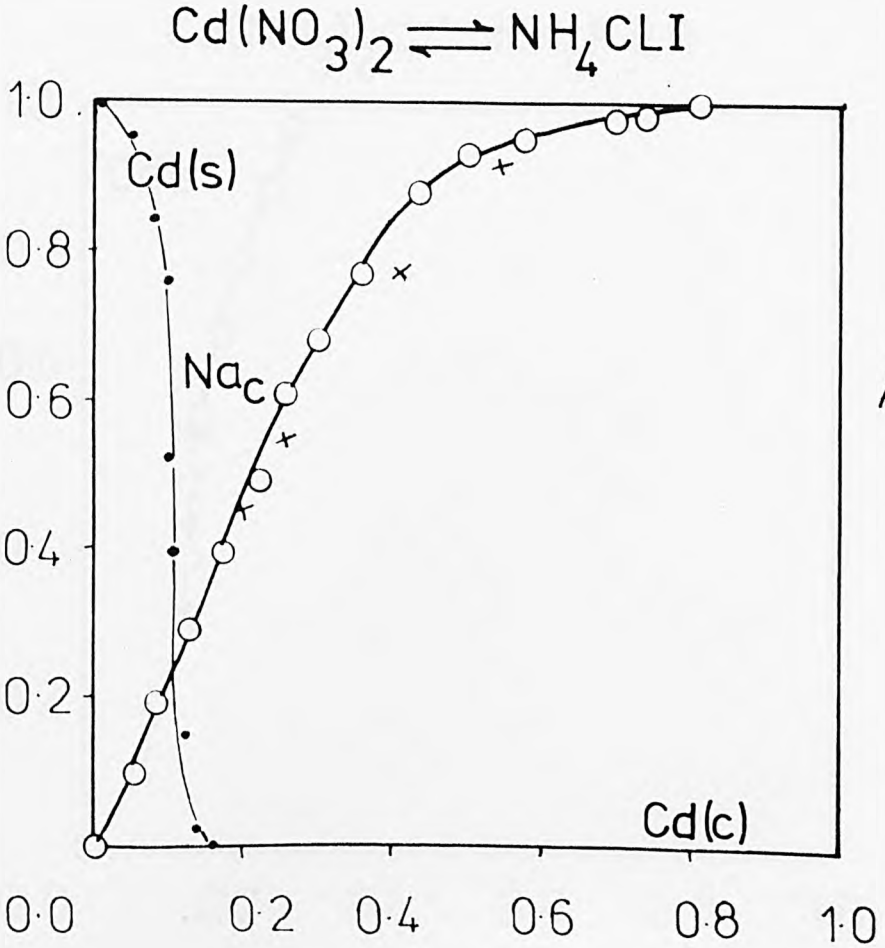

$A_c max = 0.810$

FIG.4.10

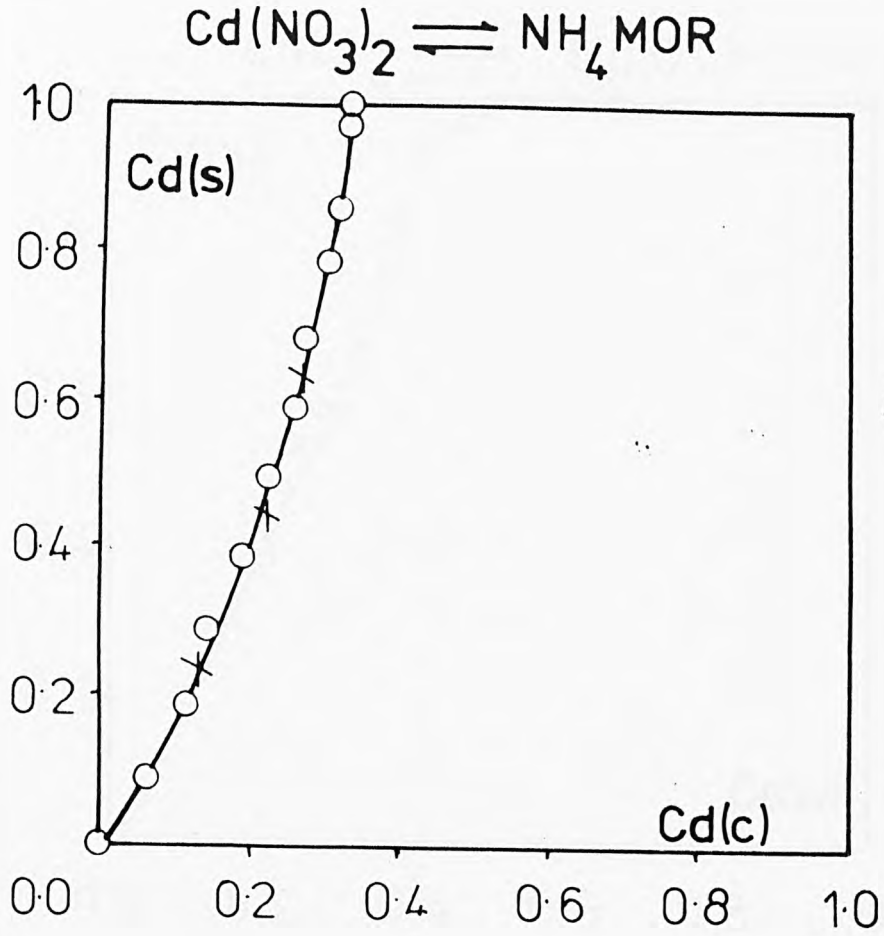

A_c max=0·327

FIG.4.11

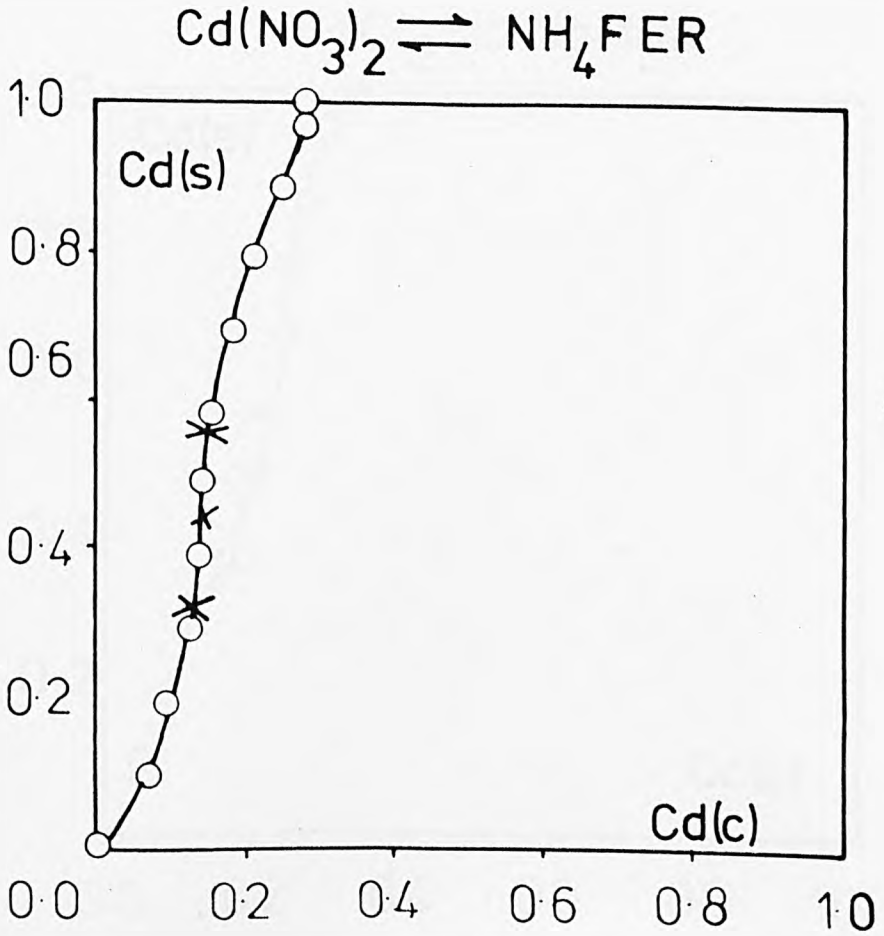

A_c max=0·280

FIG.4.12

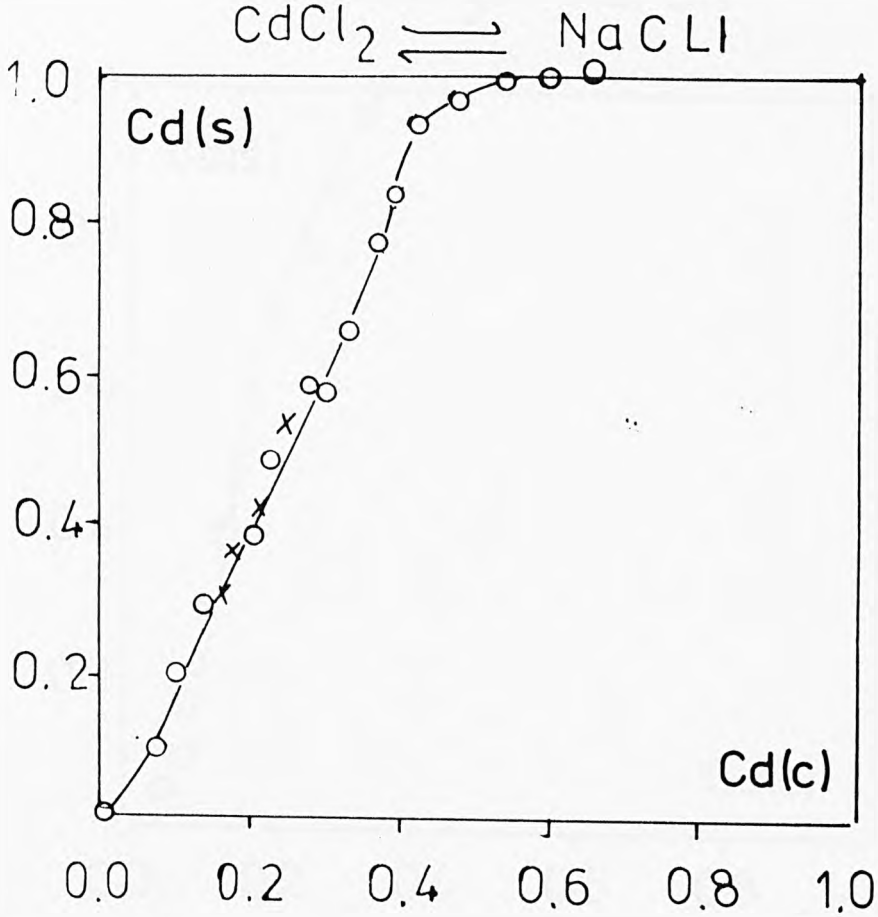

A_c max = 0.656

FIG.4.13

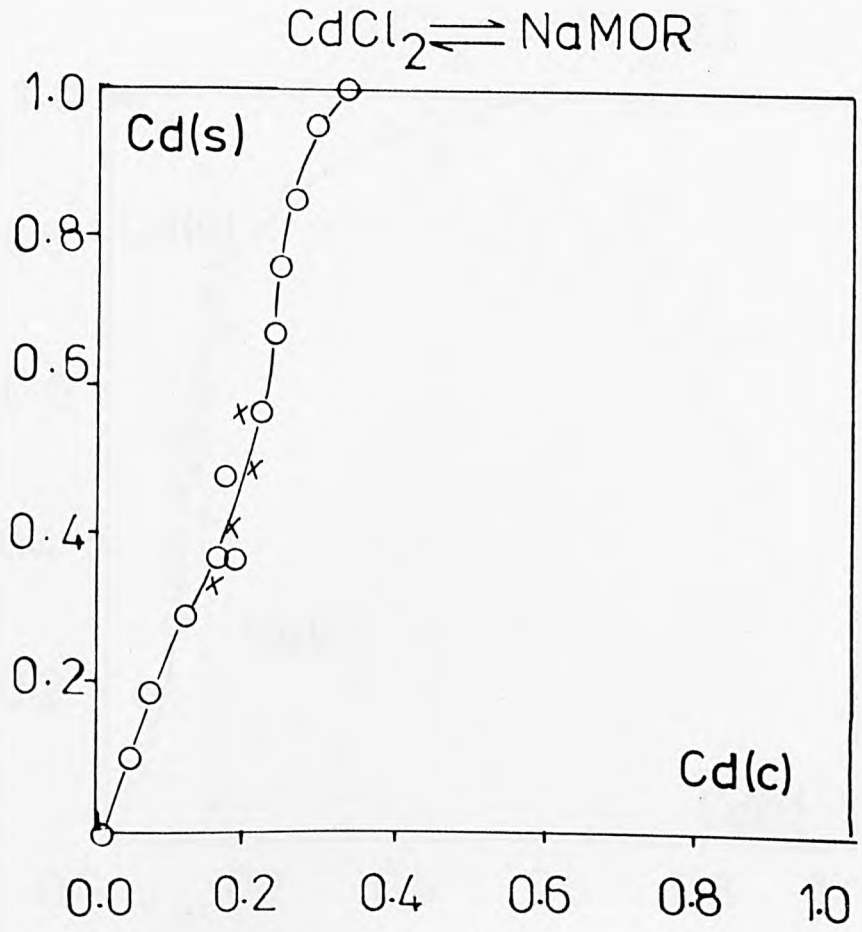

A_c max = 0.334

FIG.4.14

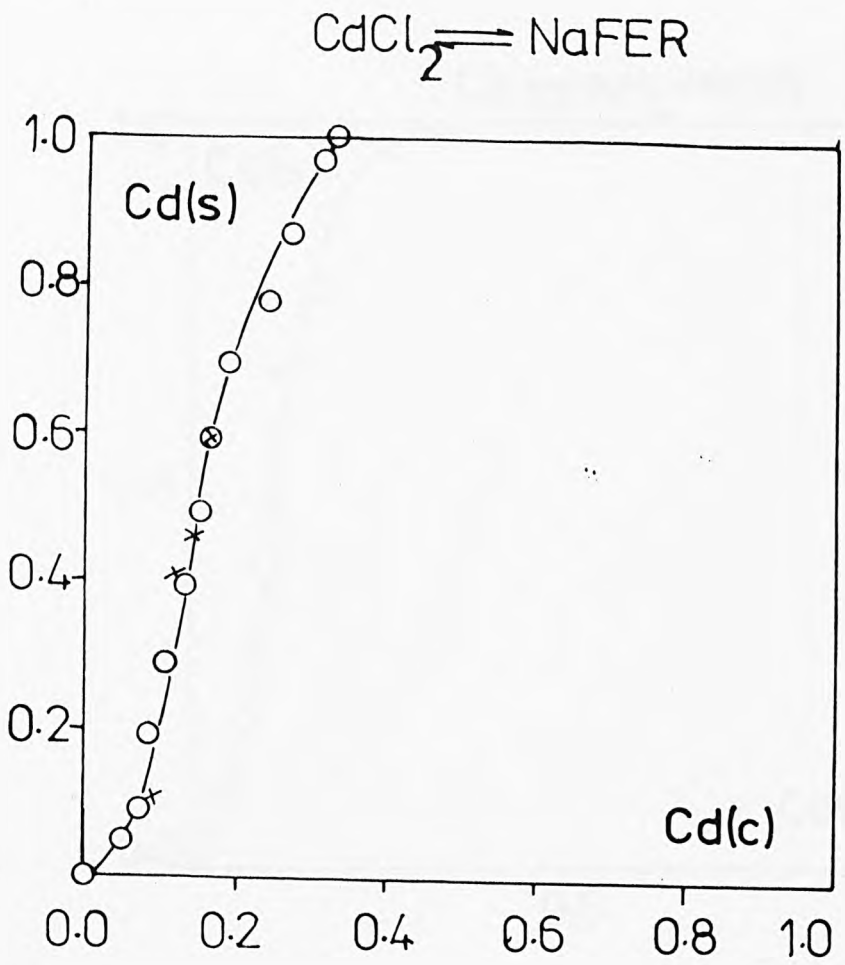

$A_c max = 0.339$

FIG.4.15

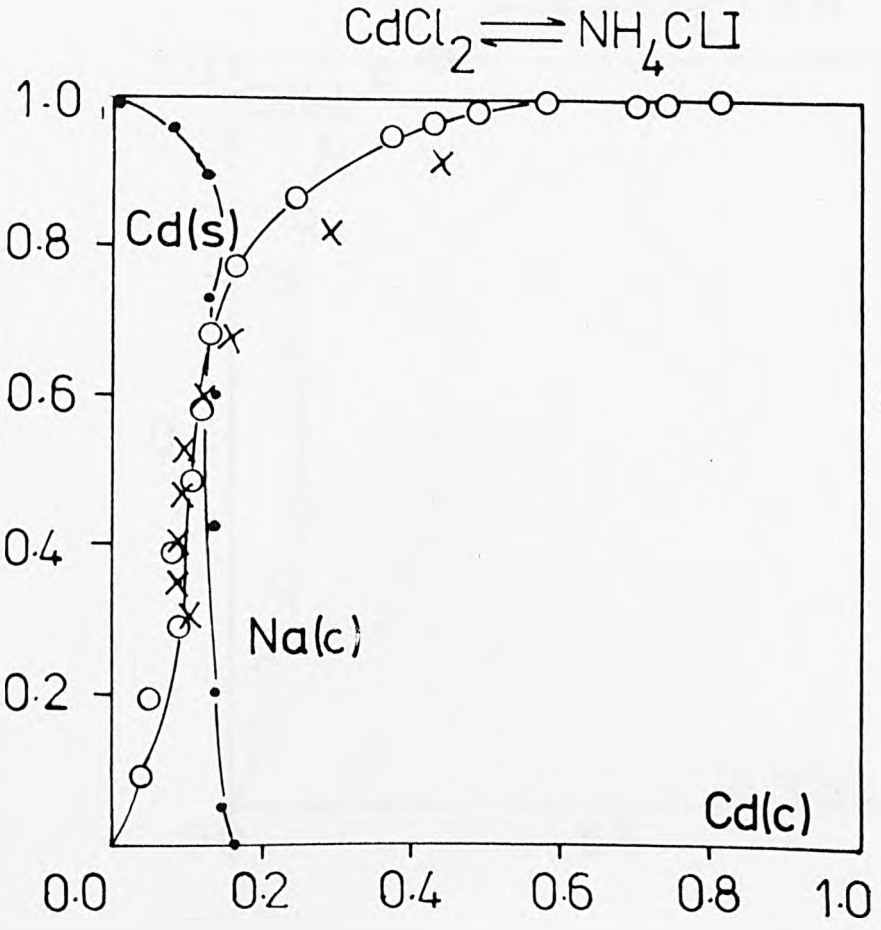

$A_c max = 0.81$

FIG.4.16

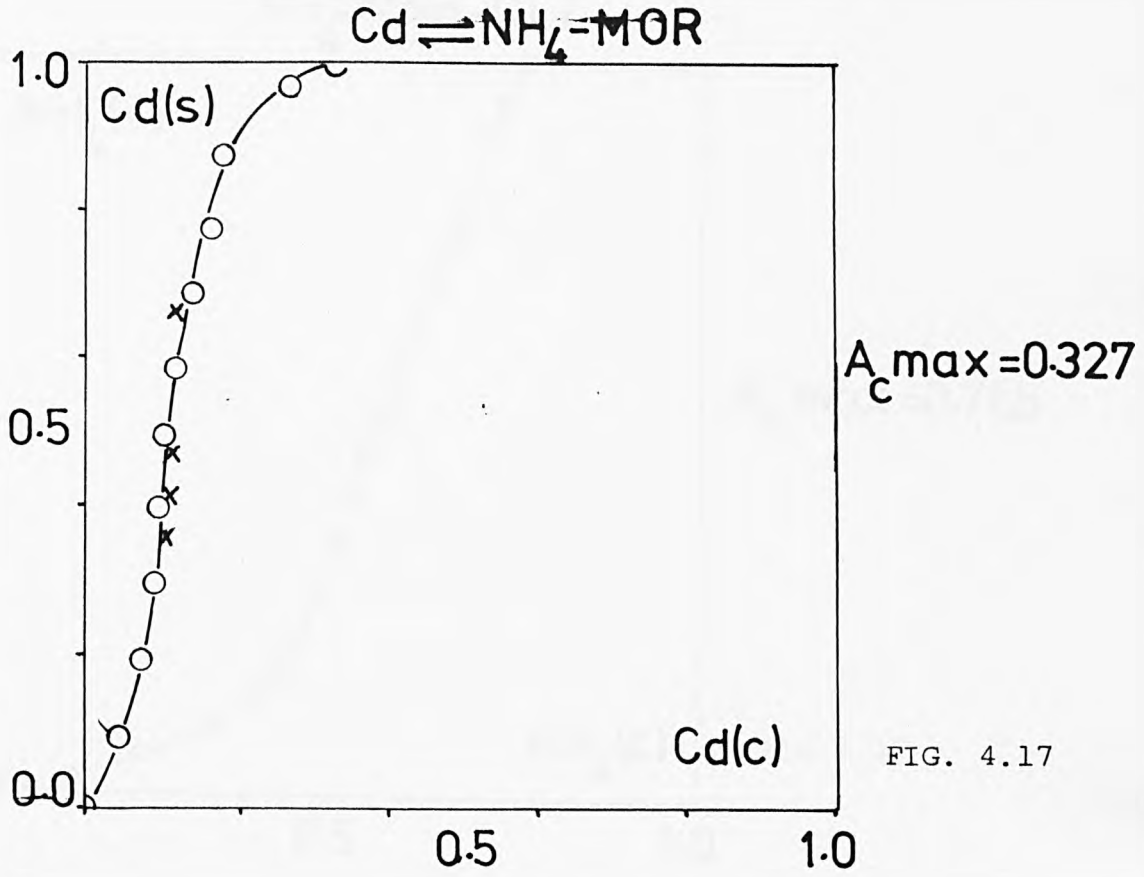

FIG. 4.17

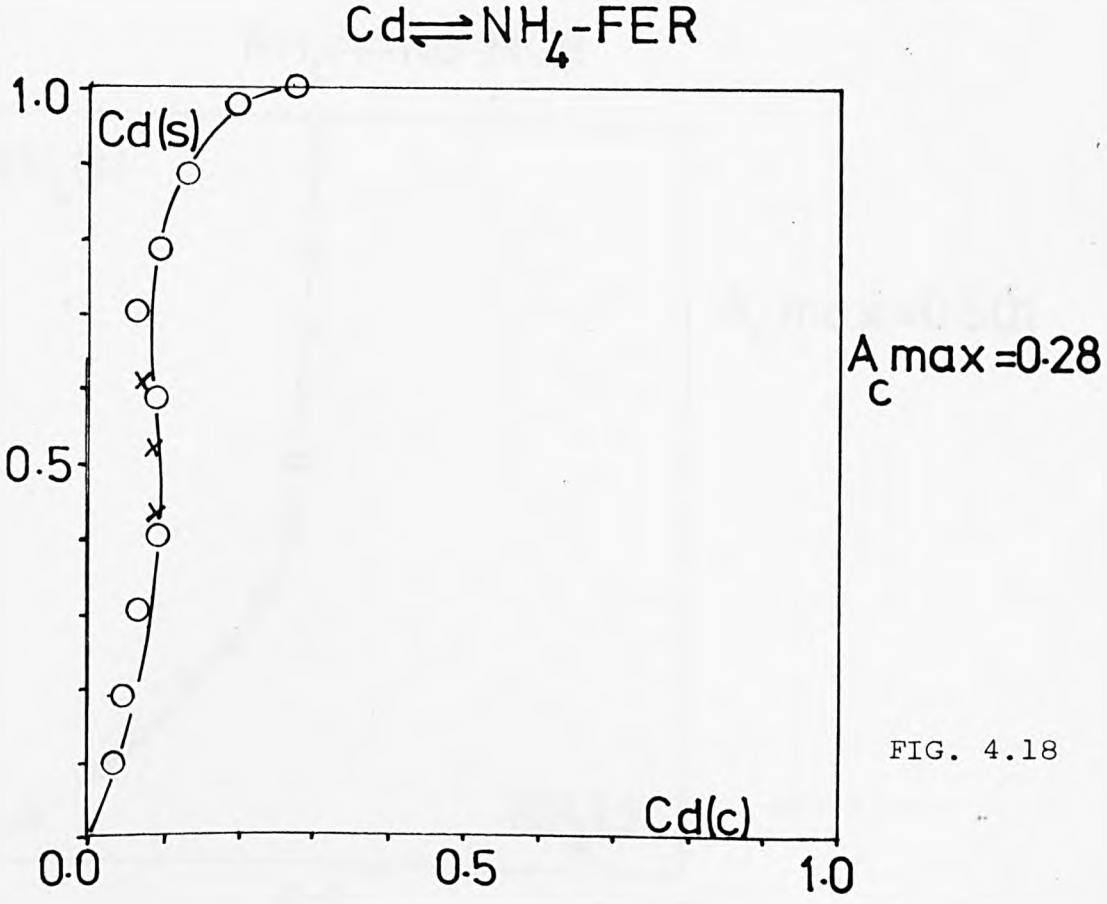

FIG. 4.18

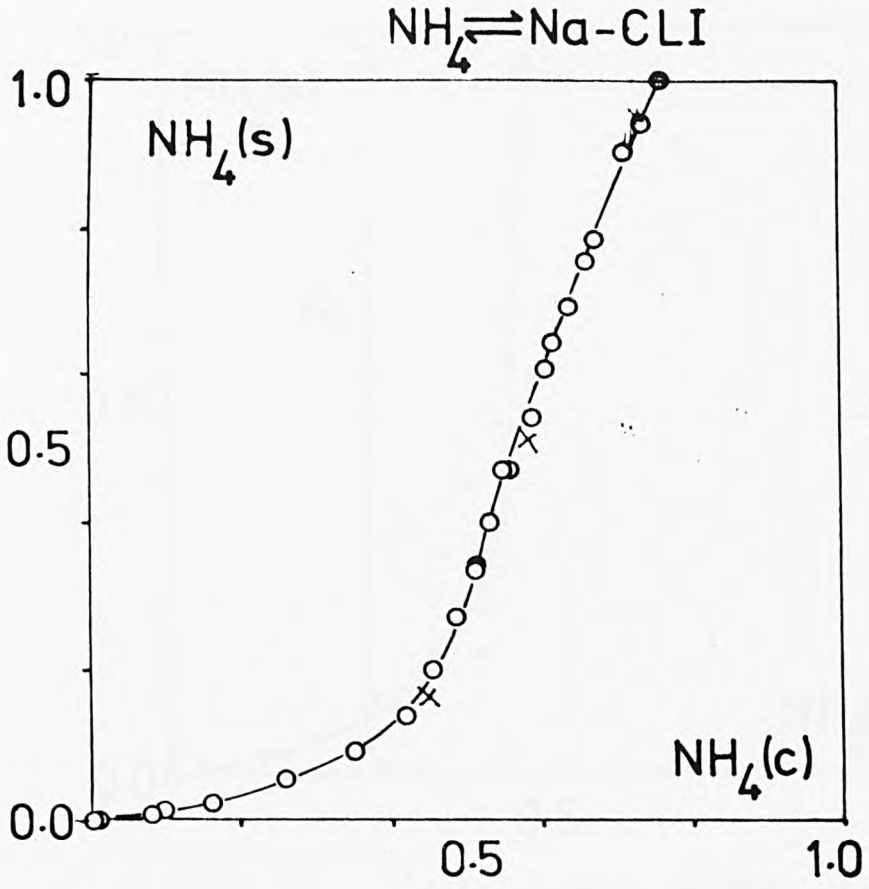

A_c max = 0·765

FIG.4.19

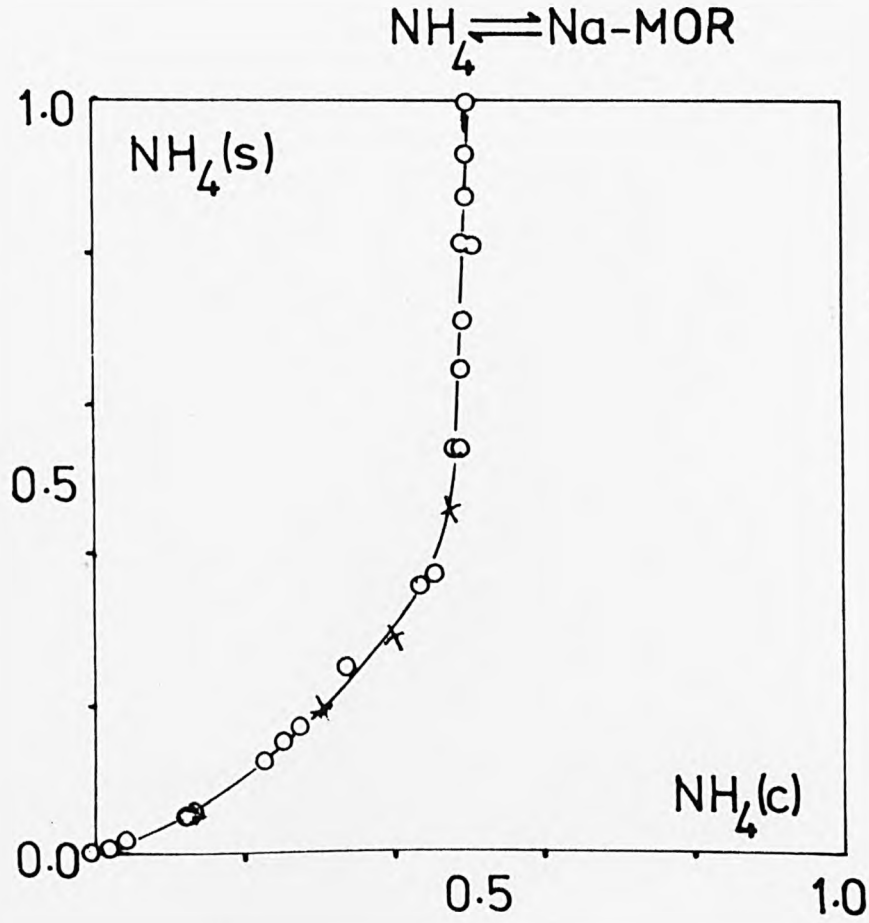

A_c max = 0·501

FIG.4.20

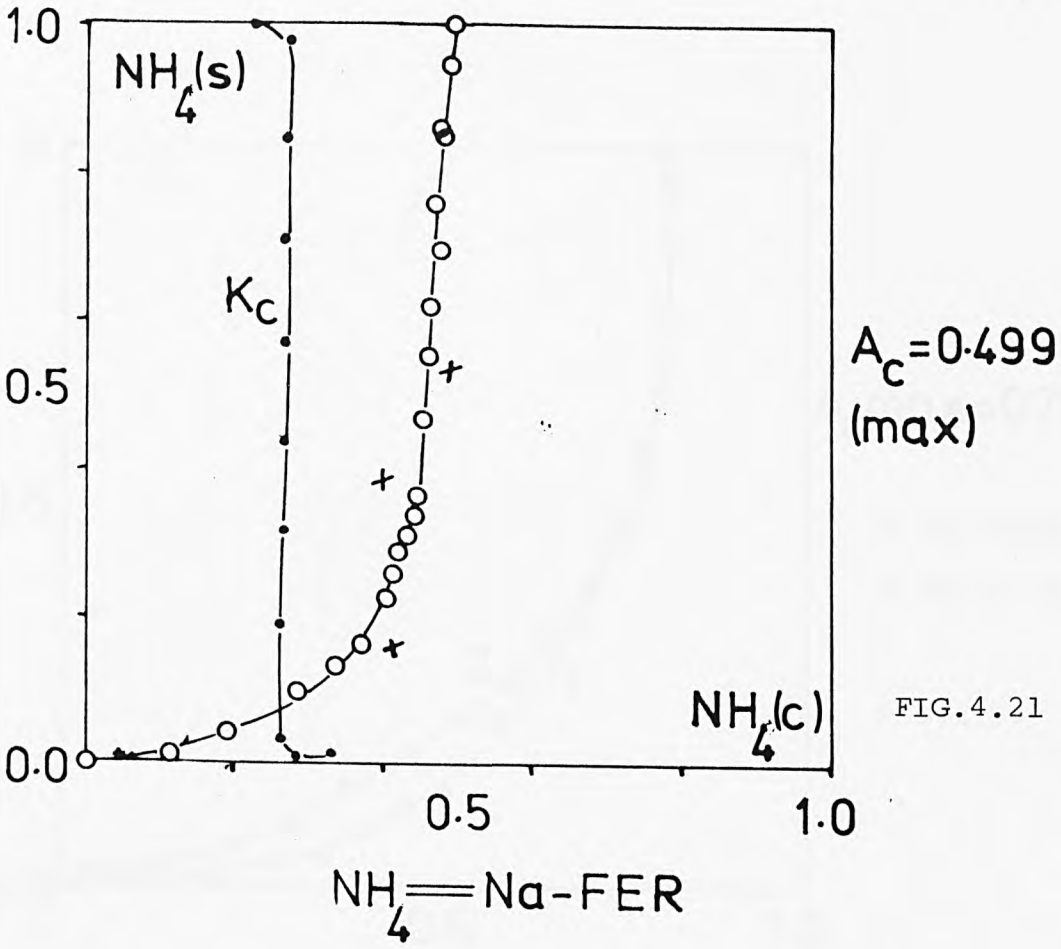

FIG.4.21

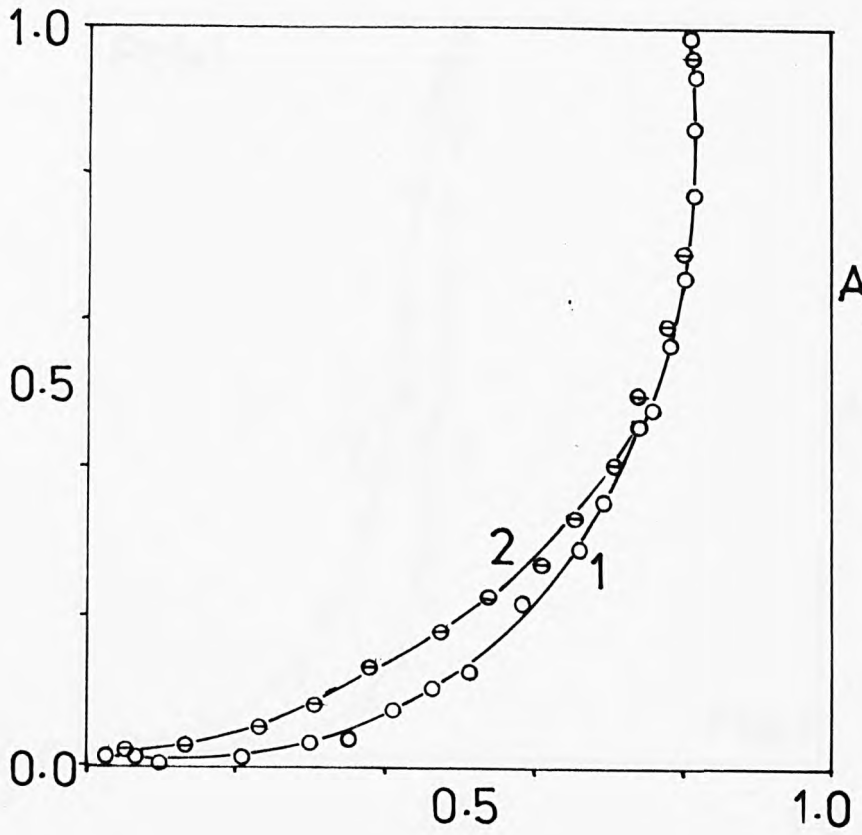

$A_c max = 0.795$

1. Pb/Na-CLI 0.1N
2. Pb/Na-CLI 0.5N

FIG.4.22

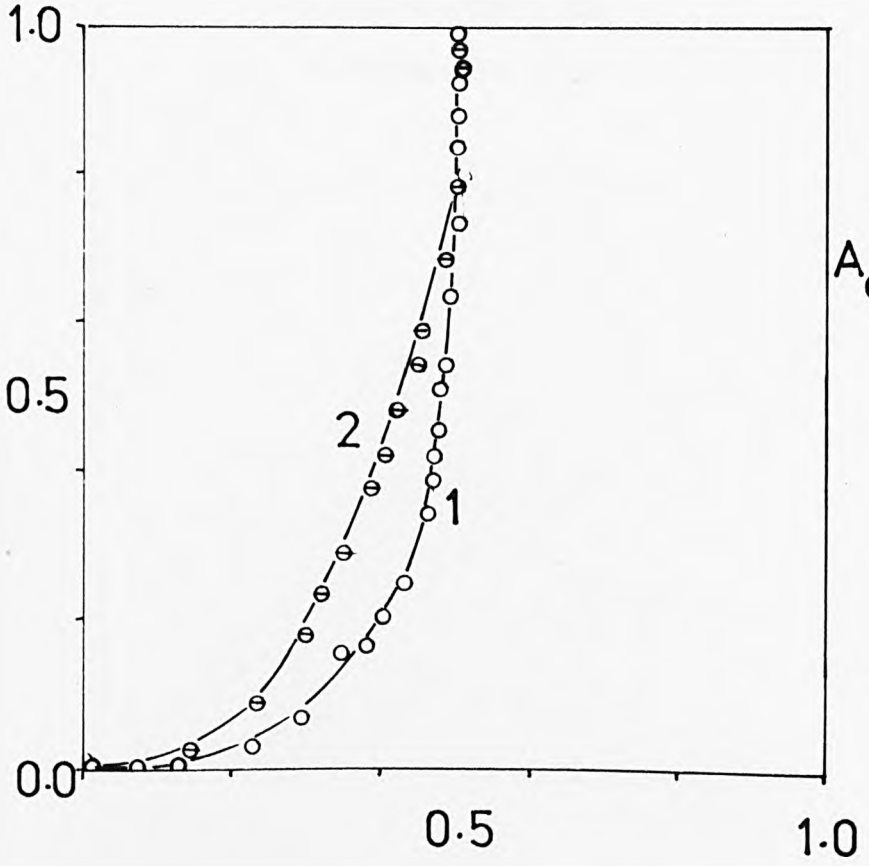

$A_c max = 0.49$

1. Pb/Na-MOR 0.1N
2. Pb/Na-MOR 0.5N

FIG.4.23

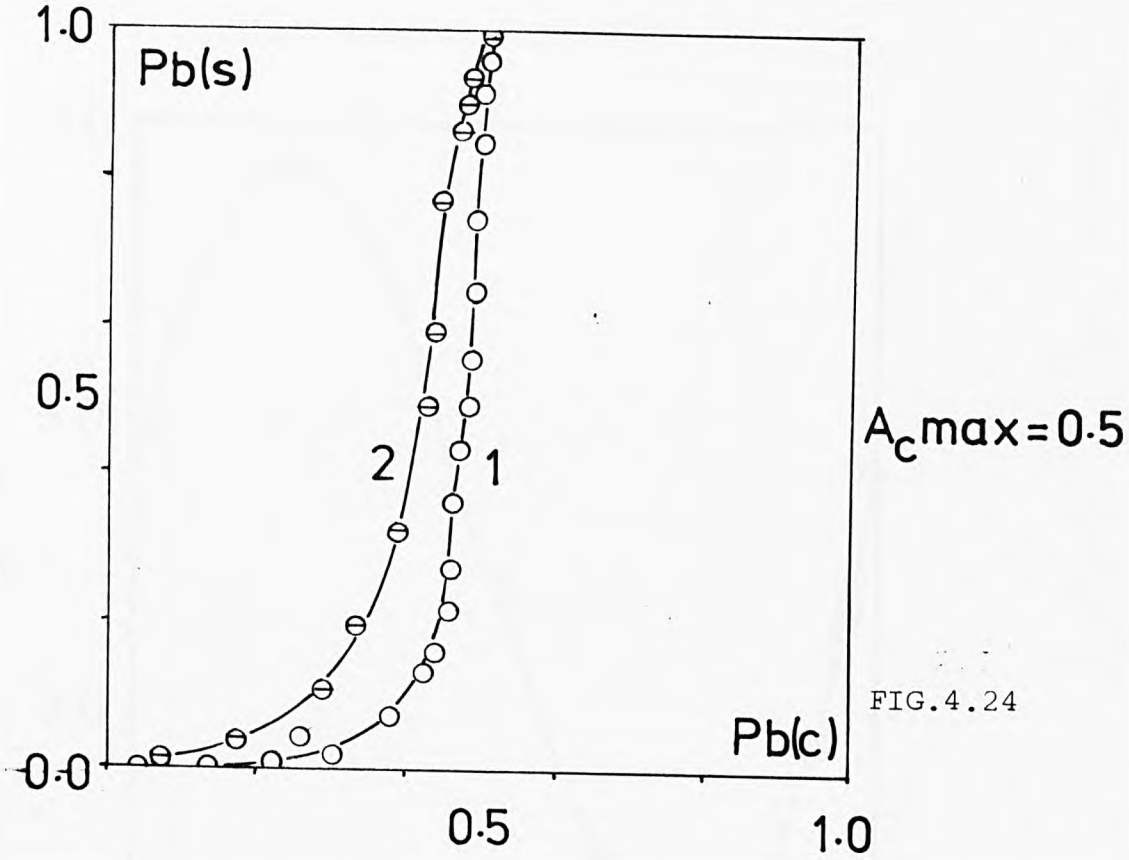

FIG.4.24

1. Pb/Na-FER 0.1N

2. Pb/Na-FER 0.5N

Kielland plot and zeolite activity coefficients for Pb/Na-CLI.

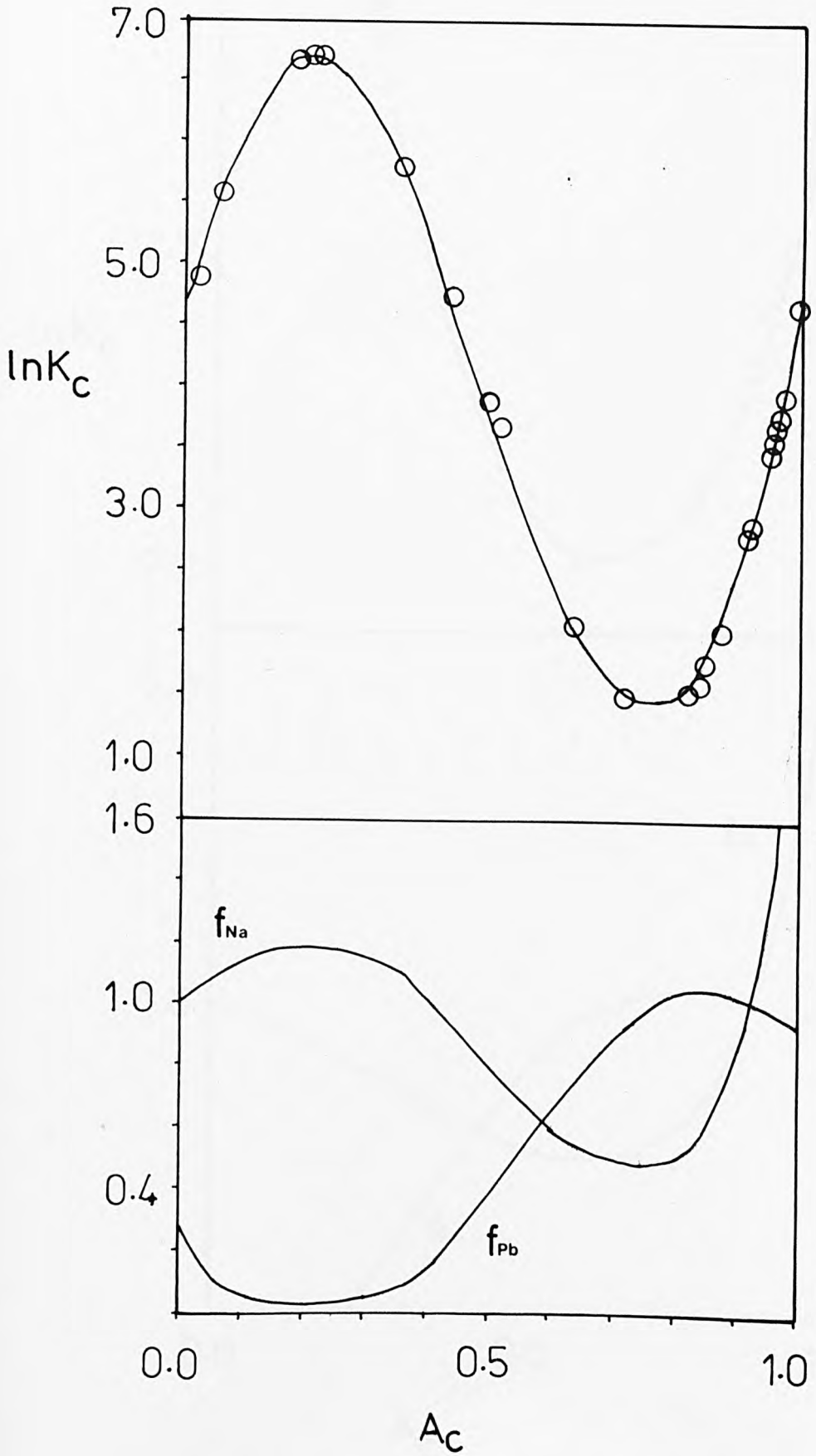

FIG. 4.25

Kielland plot and zeolite activity coefficients for Pb/Na-MOR.

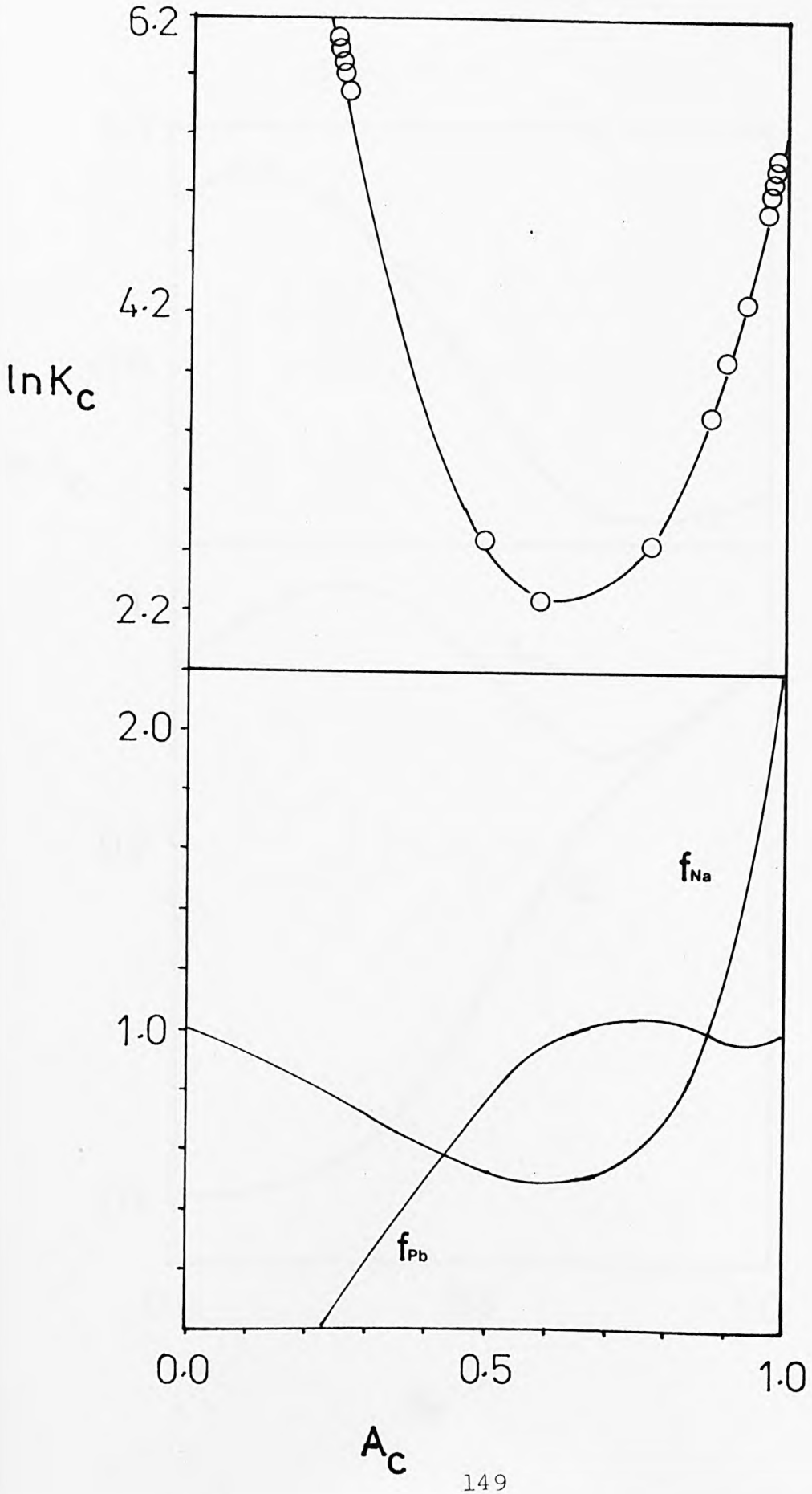

FIG. 4.26

Kielland plot and zeolite activity coefficients for Pb/NH_4-MOR.

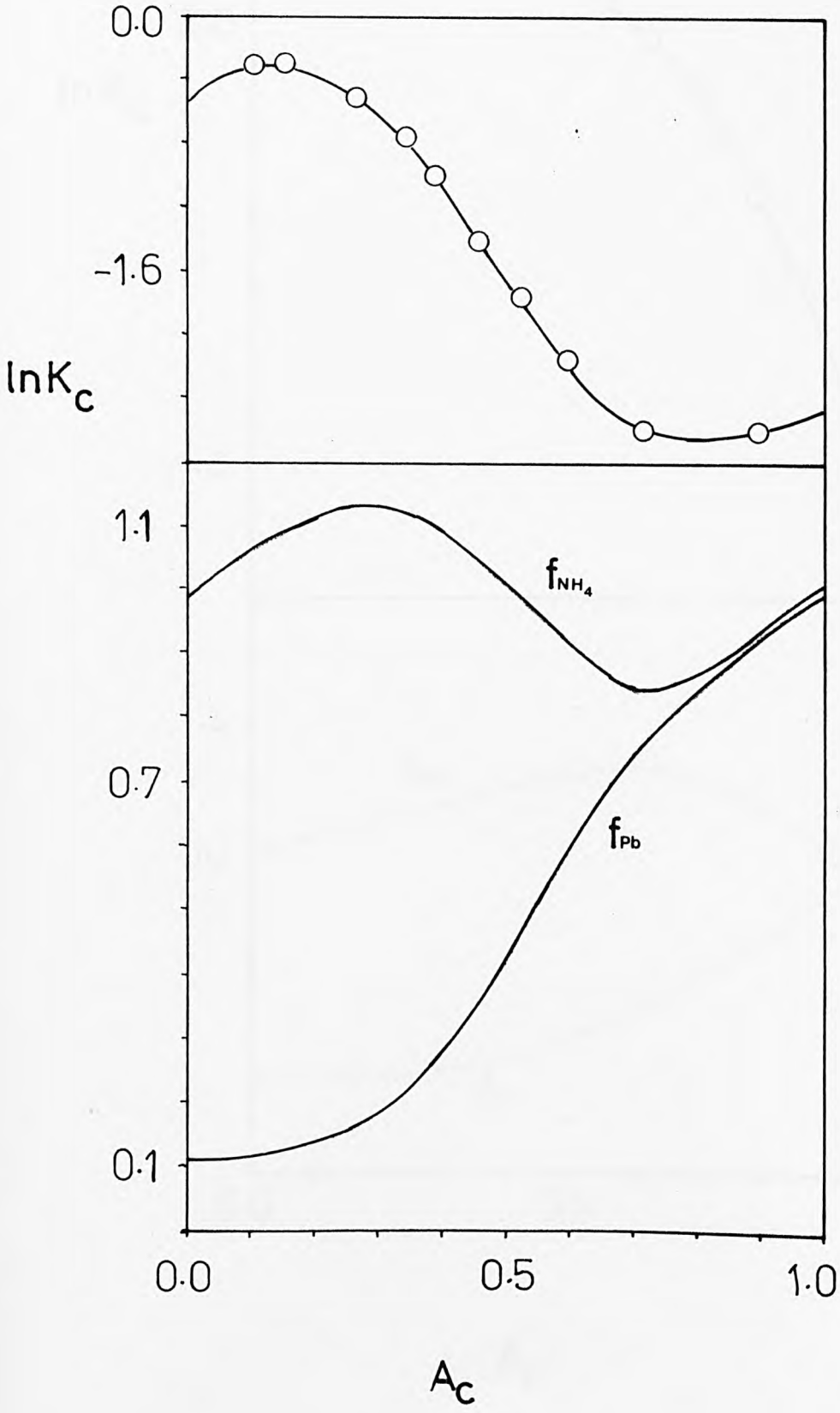

FIG. 4.27

Kielland plot and zeolite activity coefficients for Pb/NH_4-FER.

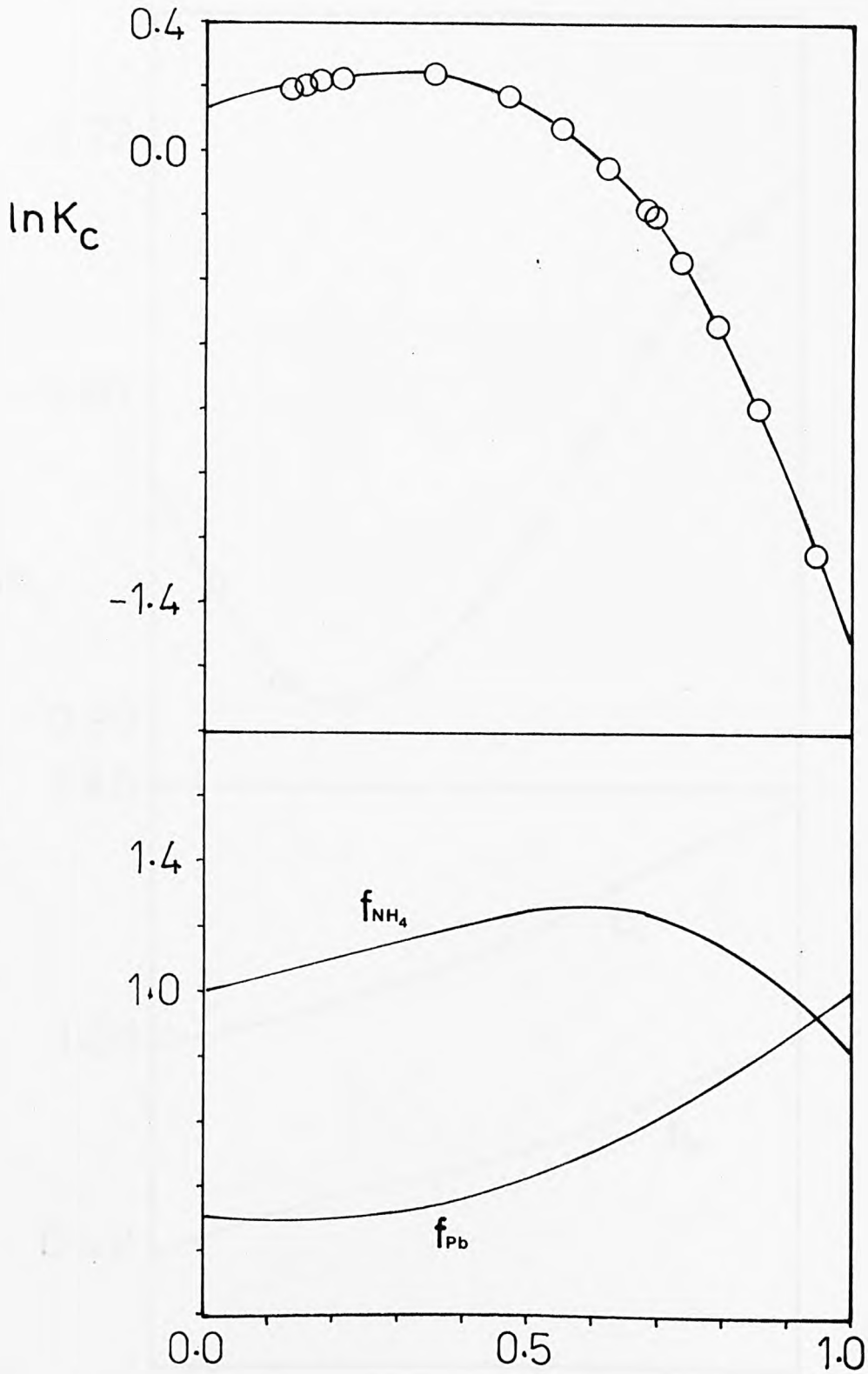

FIG. 4.28

Kielland plot and zeolite activity coefficients for $Cd/Na(NO_3)$-CLI.

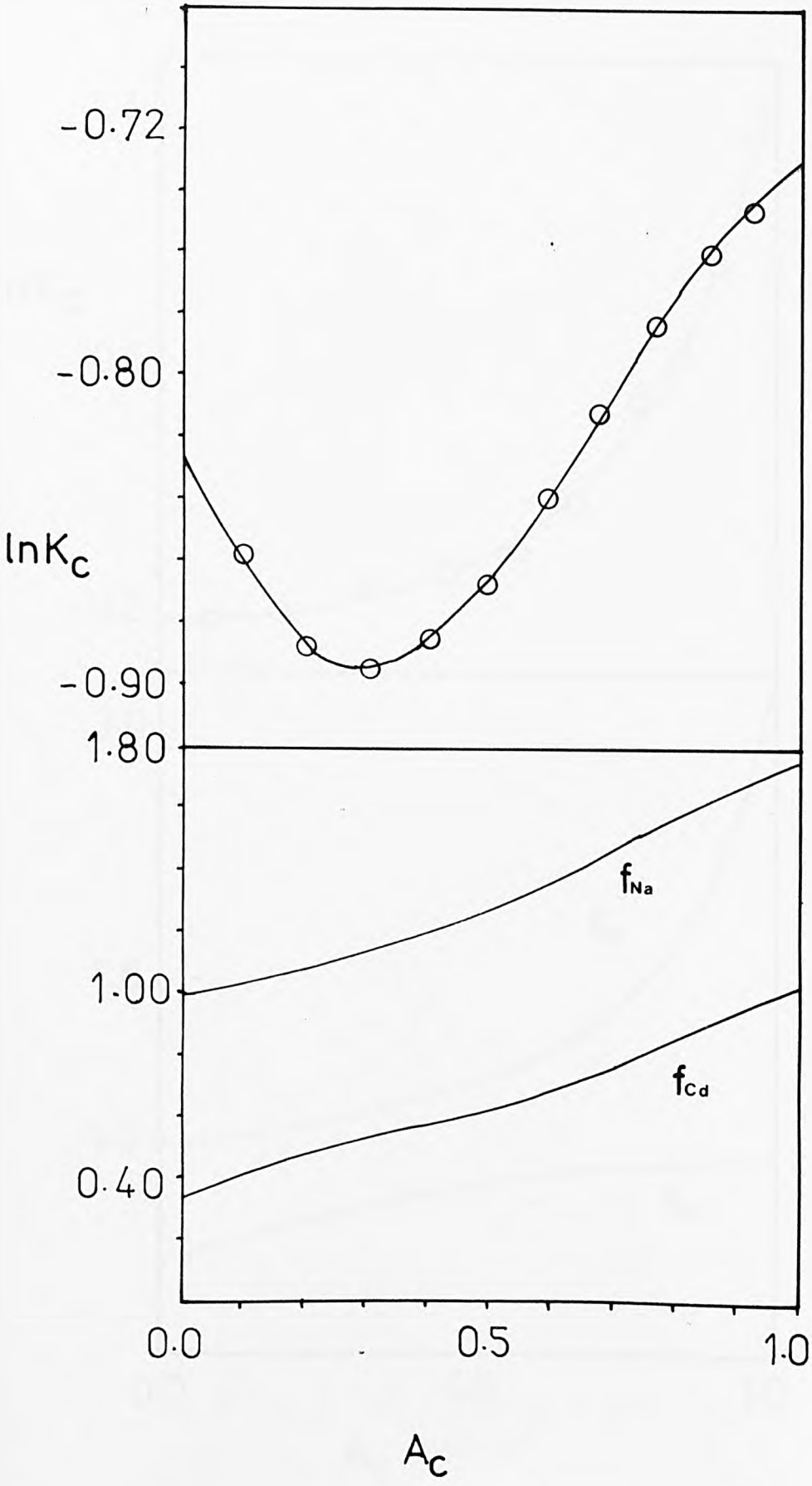

FIG. 4.29

Kielland plot and zeolite activity coefficients for $Cd/Na(NO_3)$-MOR.

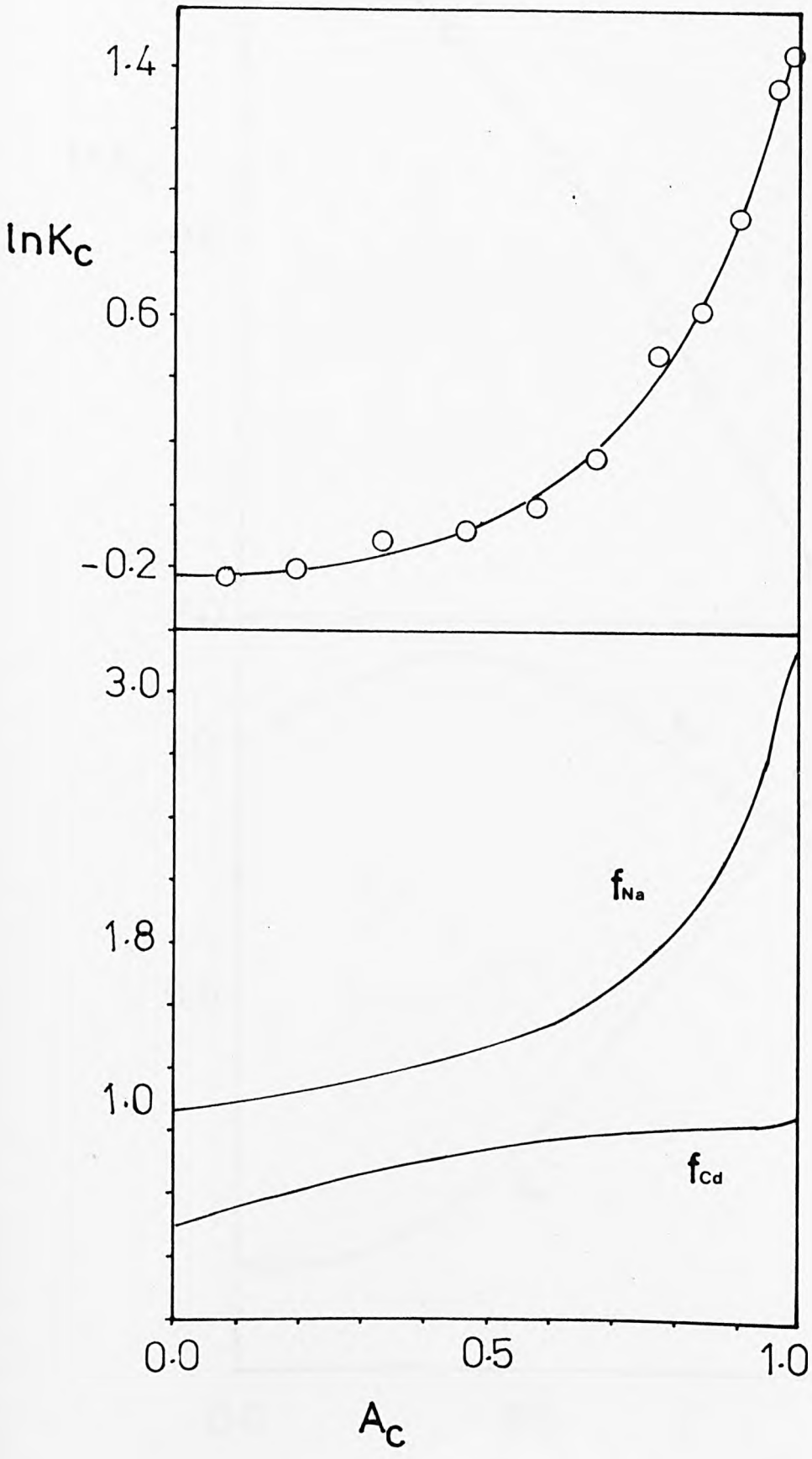

FIG. 4.30

Kielland plot and zeolite activity coefficients for Cd/Na(NO_3)-FER

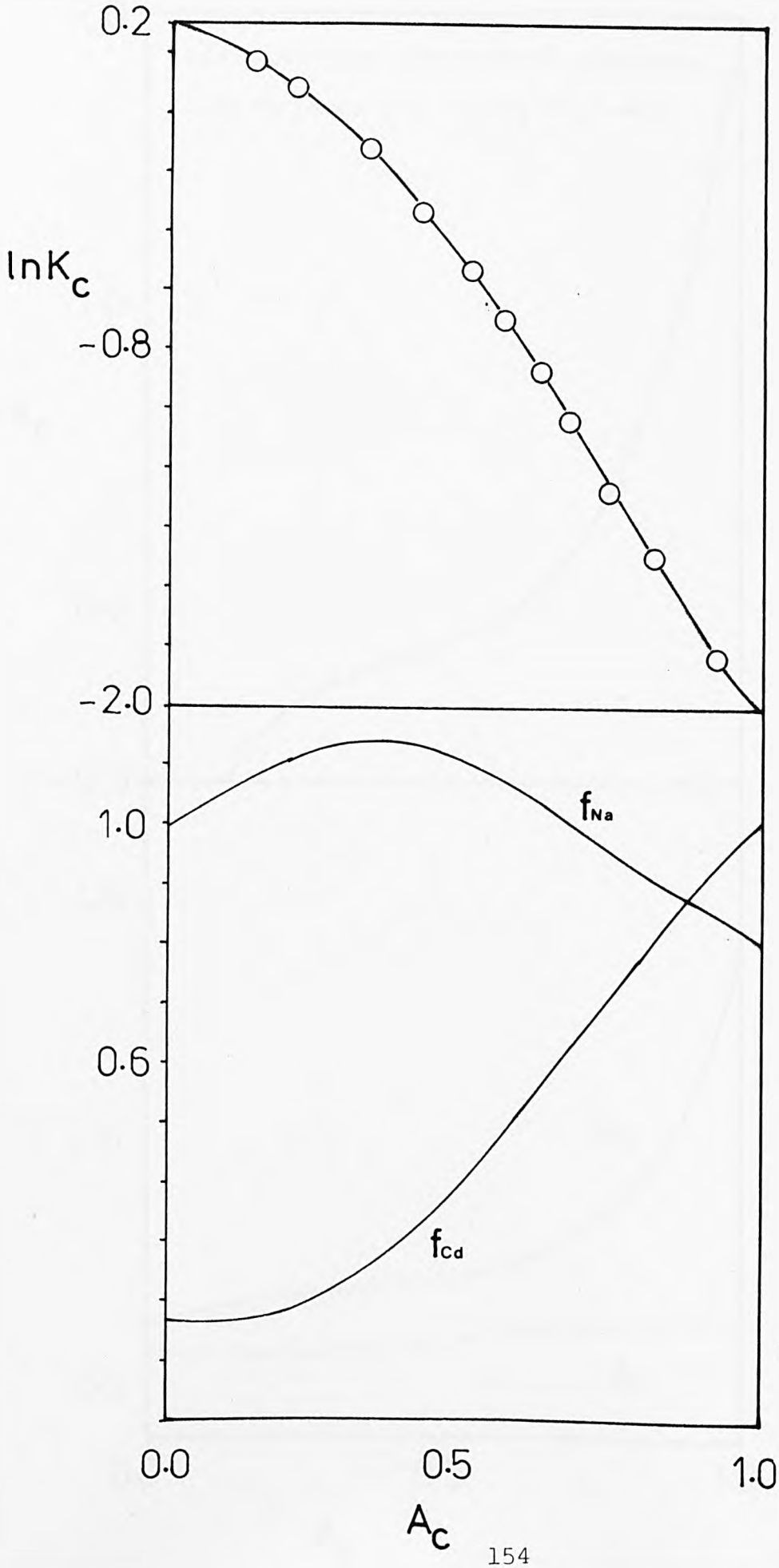

FIG. 4.31

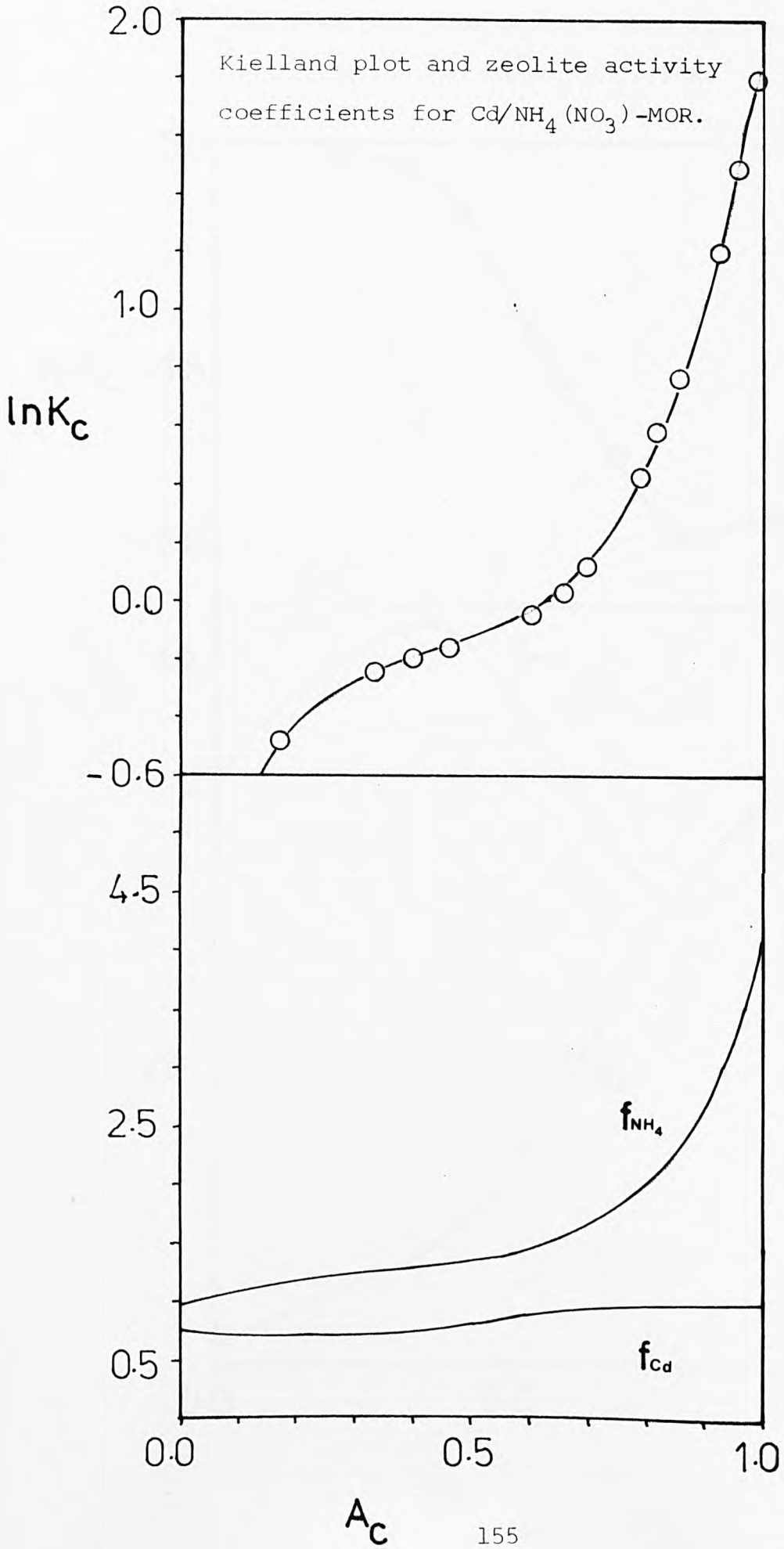
Kielland plot and zeolite activity coefficients for Cd/NH4(NO3)-MOR.
2·0
1·0
0·0
-0·6
lnKc
4·5
2·5
0·5
fNH4
fCd
0·0
0·5
1·0
Ac

FIG. 4.32

Kielland plot and zeolite activity coefficients for $Cd/NH_4(NO_3)$-FER.

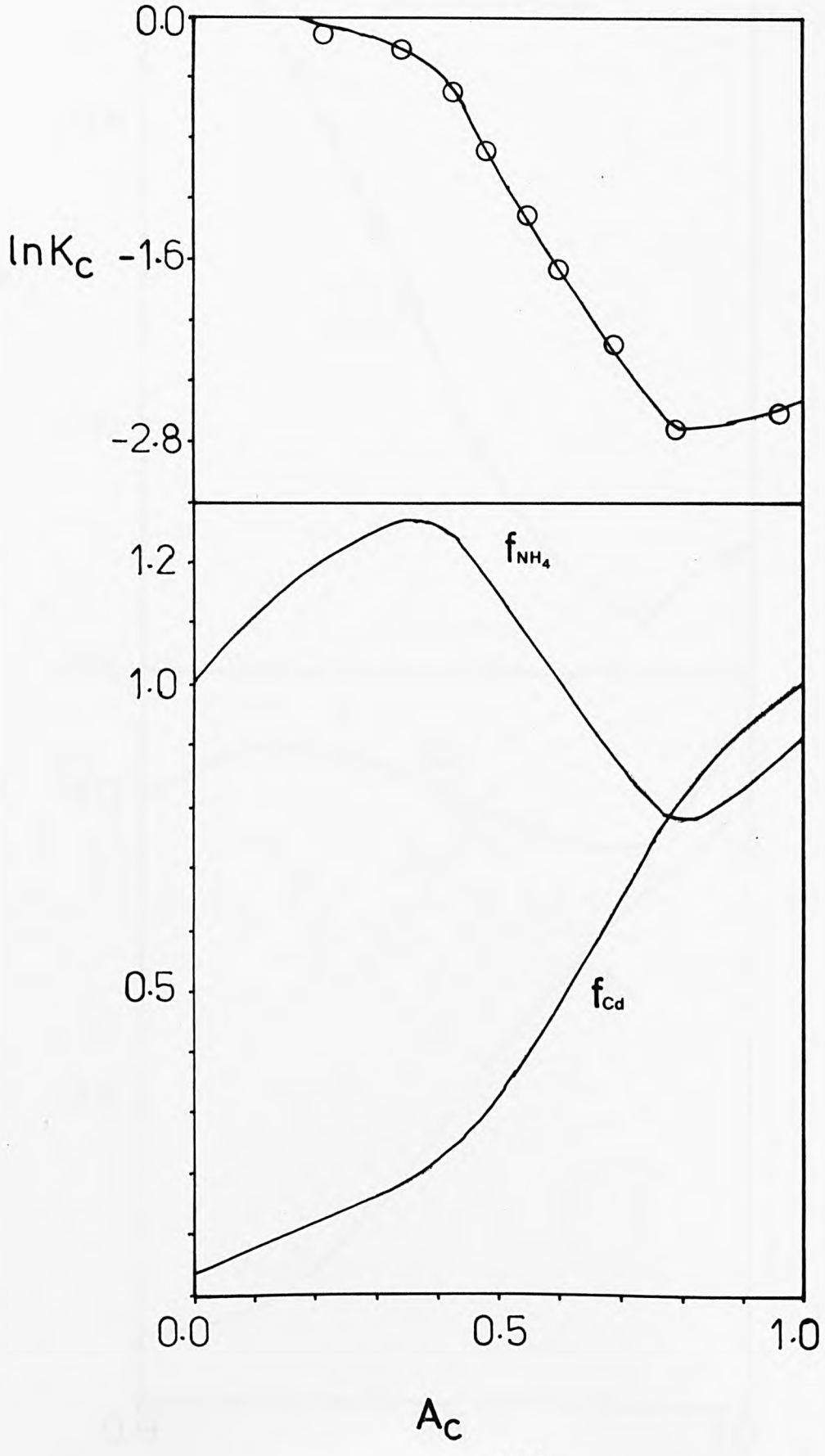

FIG. 4.33

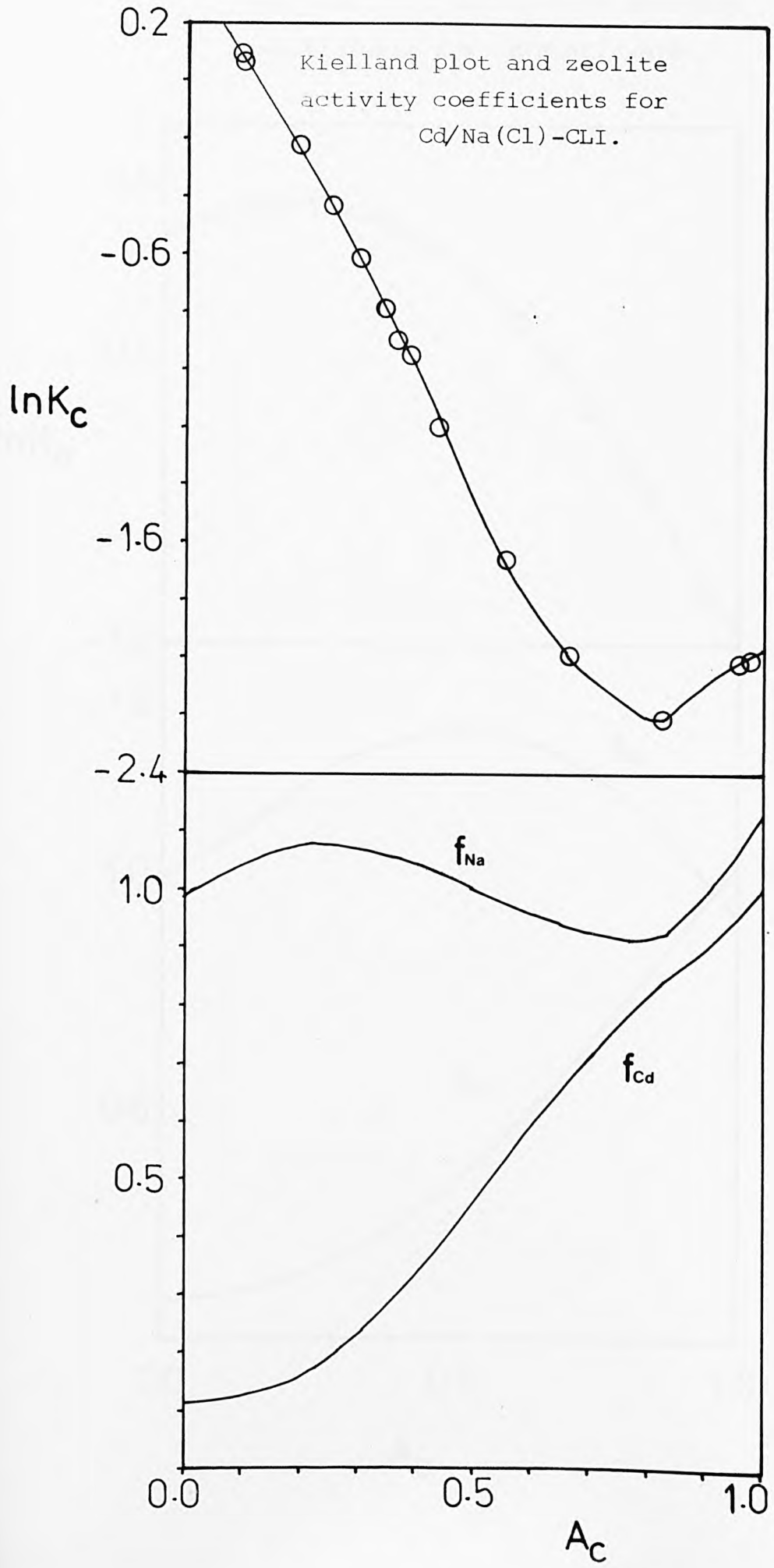
Kielland plot and zeolite
activity coefficients for
Cd/Na(Cl)-CLI.
0.2
-0.6
-1.6
-2.4
lnK_c
f_Na
f_Cd
1.0
0.5
0.0
0.5
1.0
A_c

FIG. 4.34

Kielland plot and zeolite activity coefficients for Cd/Na(Cl)-MOR.

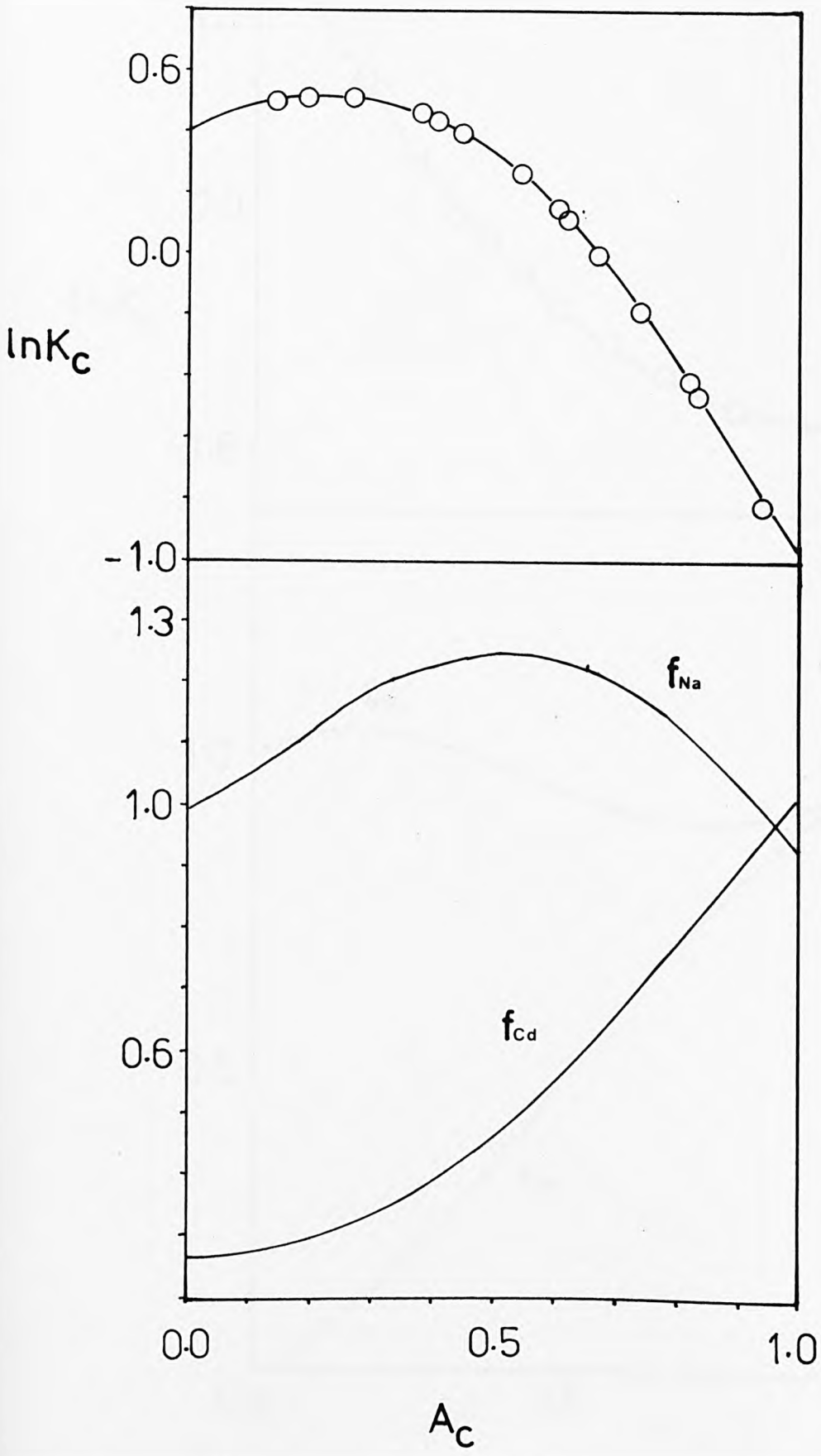

FIG. 4.35

Kielland plot and zeolite activity coefficients for Cd/Na(Cl)-FER.

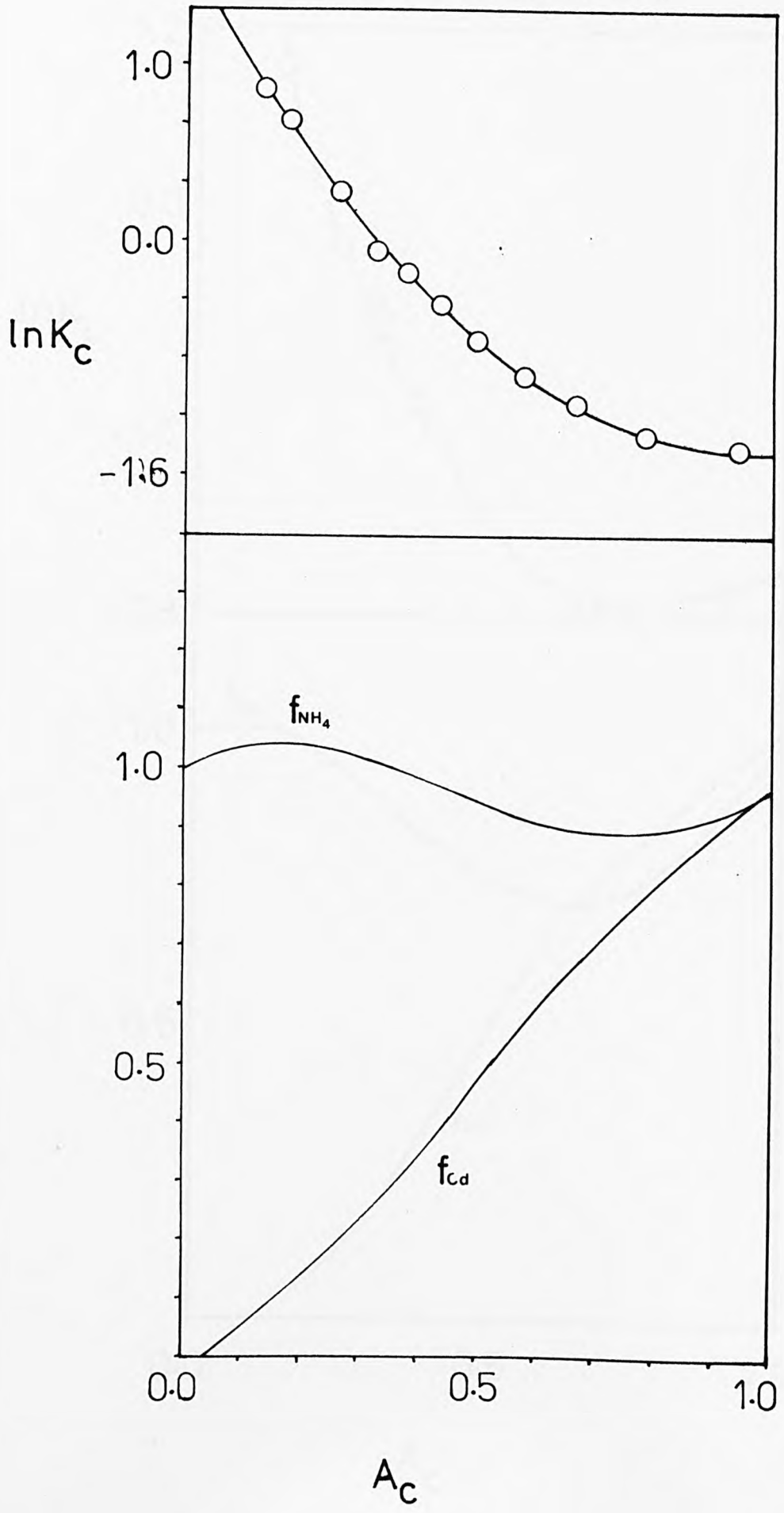

FIG. 4.36

Kielland plot and zeolite activity coefficients for Cd/NH_4(Cl)-MOR.

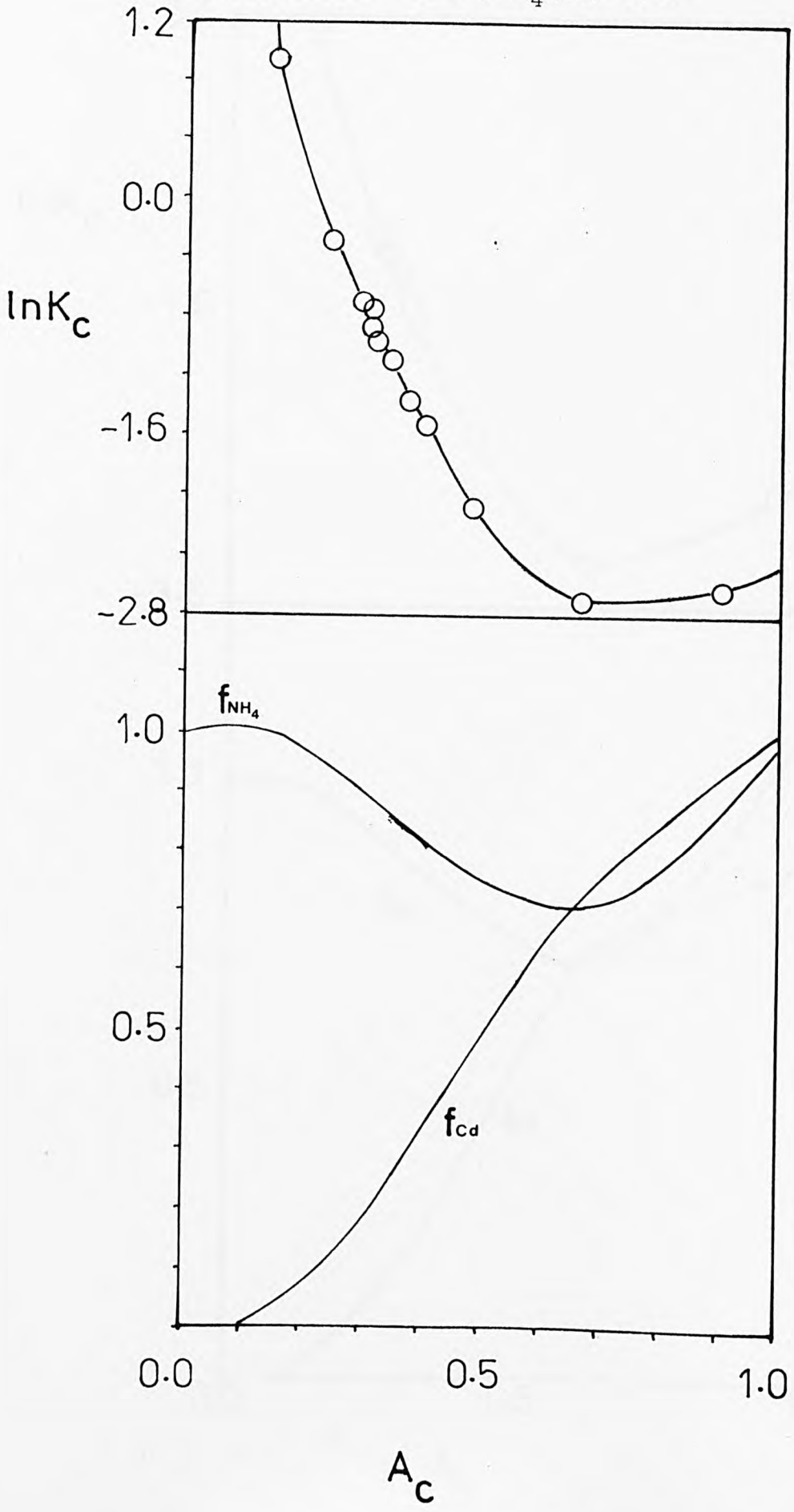

FIG. 4.37

Kielland plot and zeolite activity coefficients for $Cd/NH_4(Cl)$-FER.

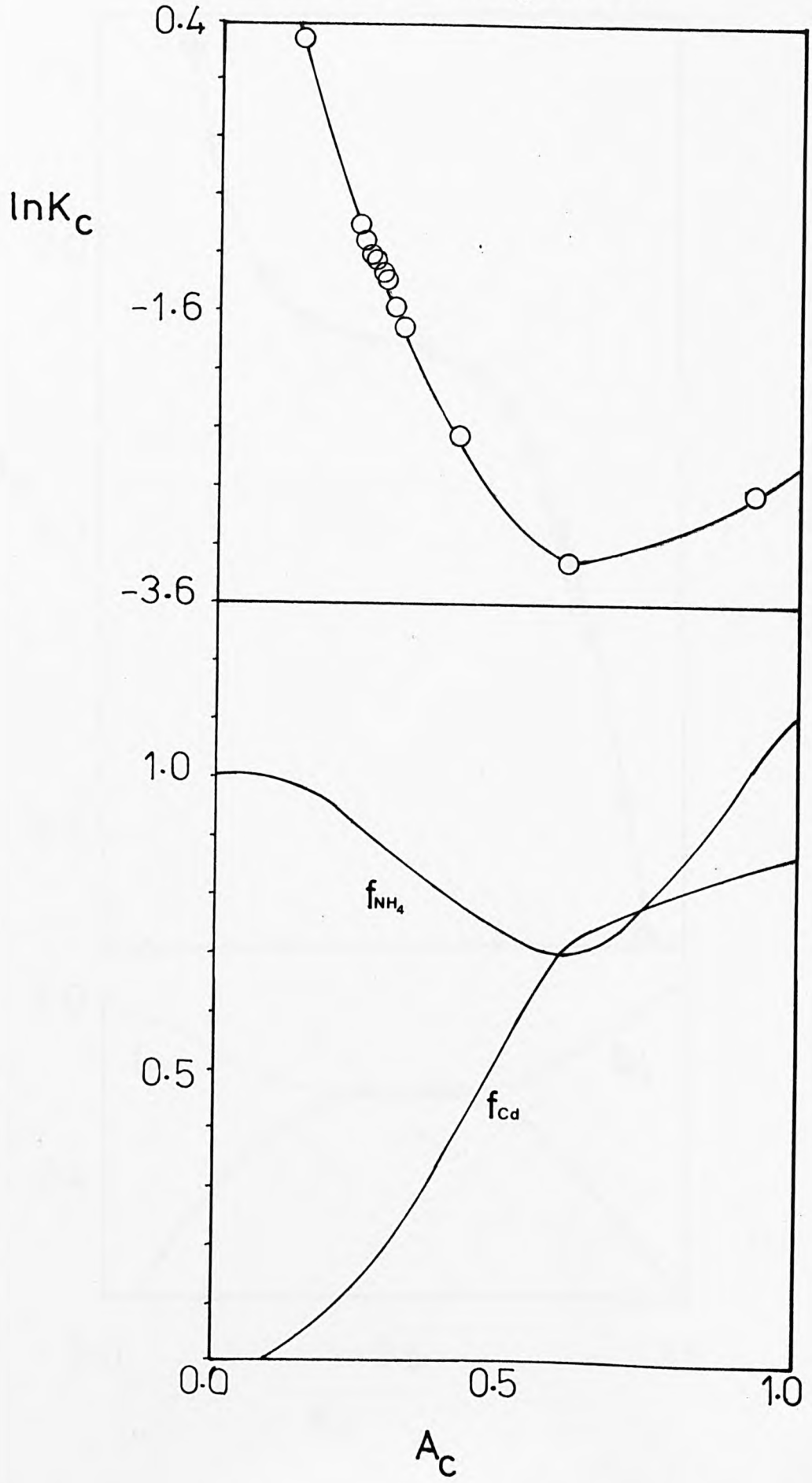

FIG. 4.38

Kielland plot and zeolite activity coefficients for NH_4/Na-CLI.

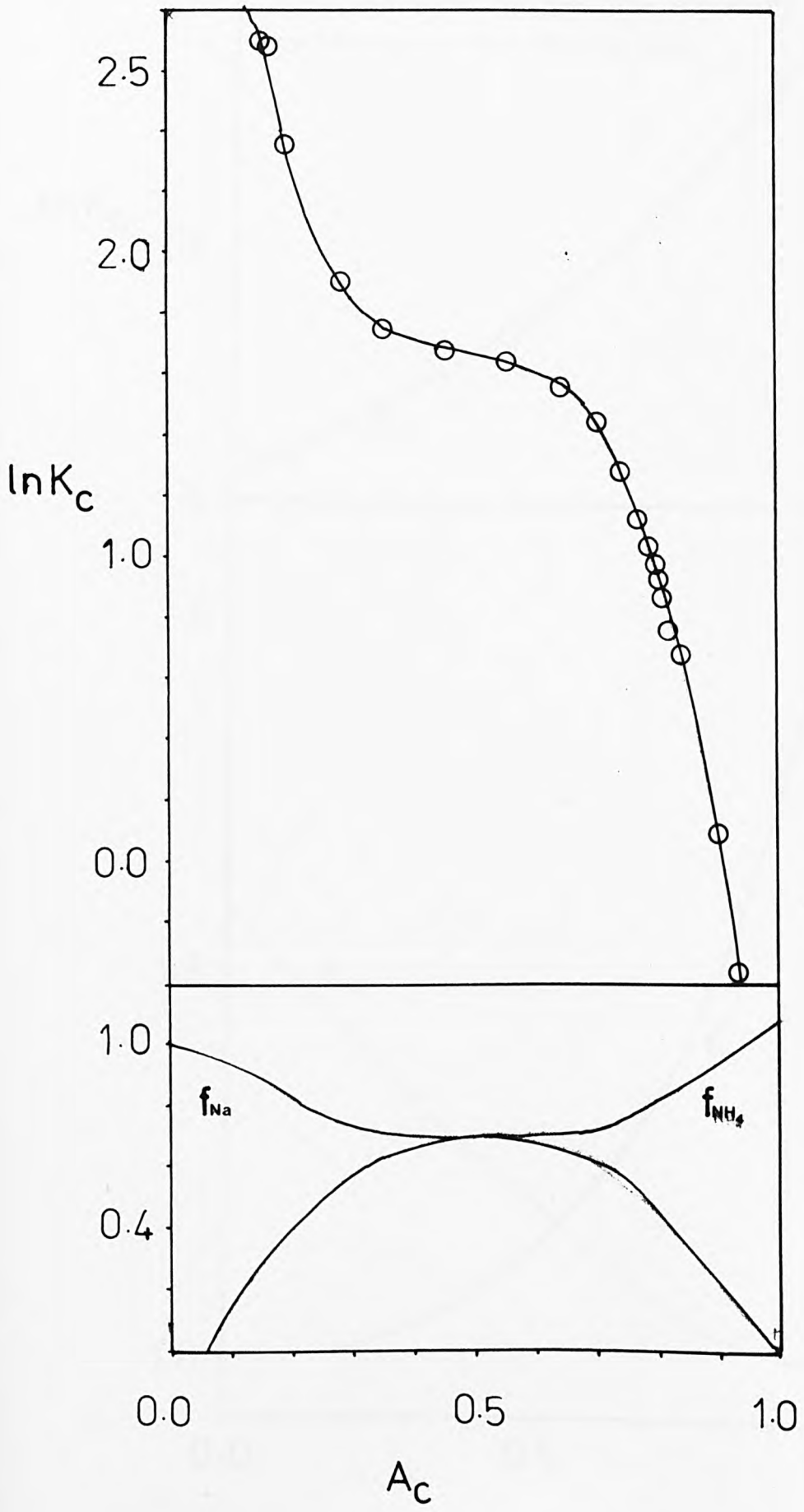

FIG. 4.39

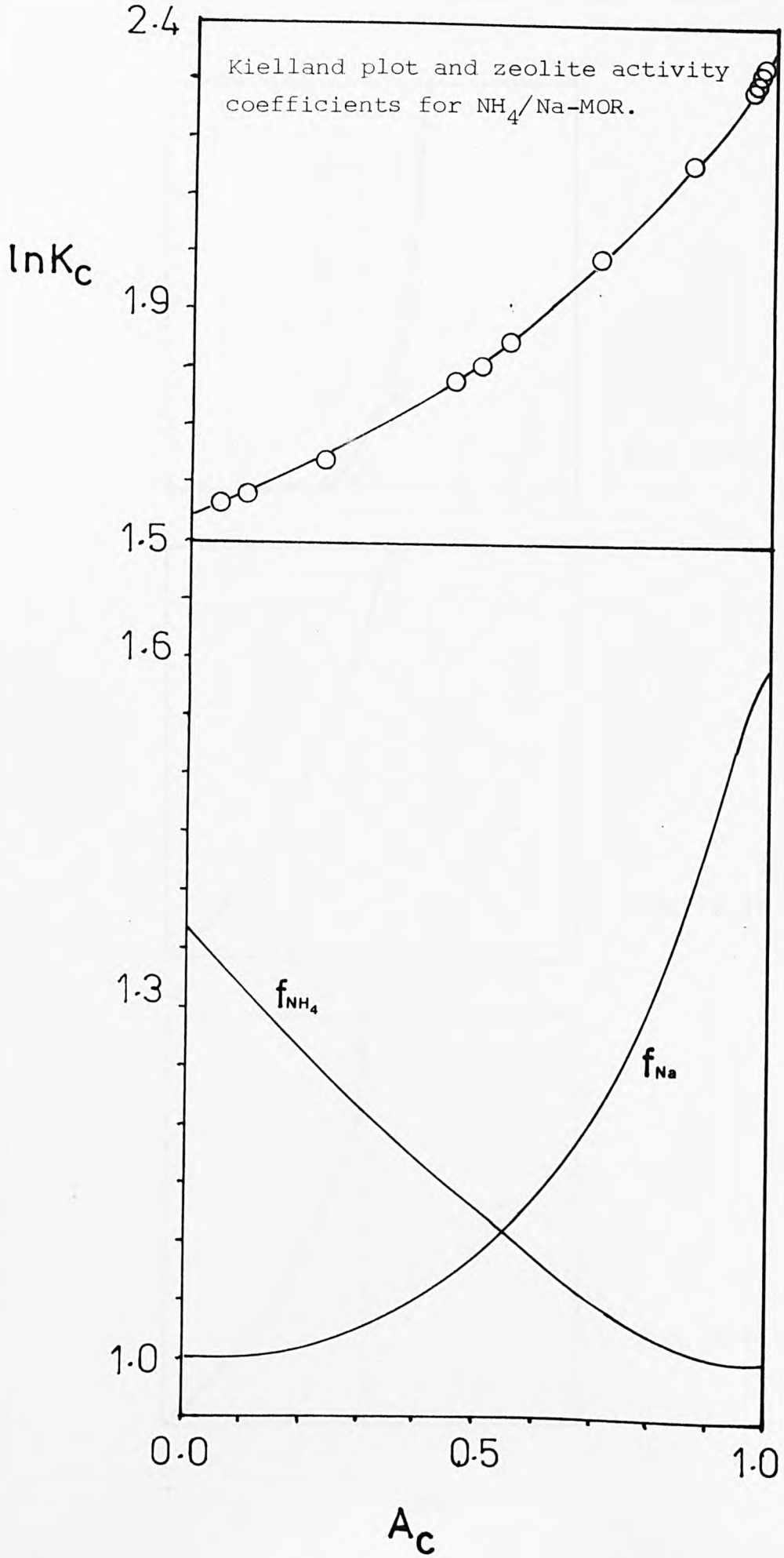
Kielland plot and zeolite activity coefficients for NH_4/Na-MOR.
2·4
1·9
1·5
1·6
1·3
1·0
lnK$_c$
f_{NH_4}
f_{Na}
0·0
0·5
1·0
A$_c$

FIG. 4.40

Fitting of the experimental isotherm data.

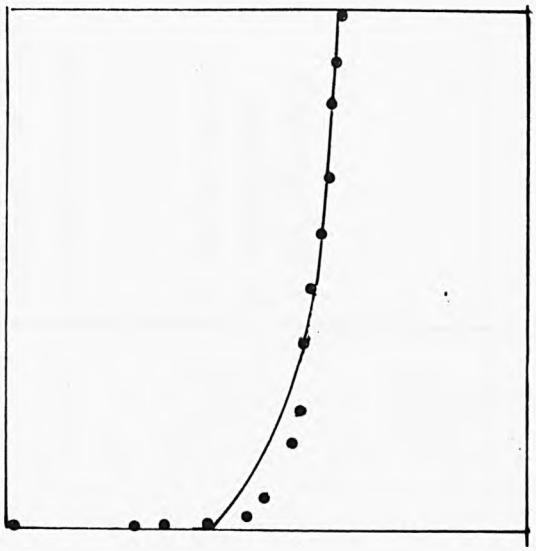

FIG. 4.41

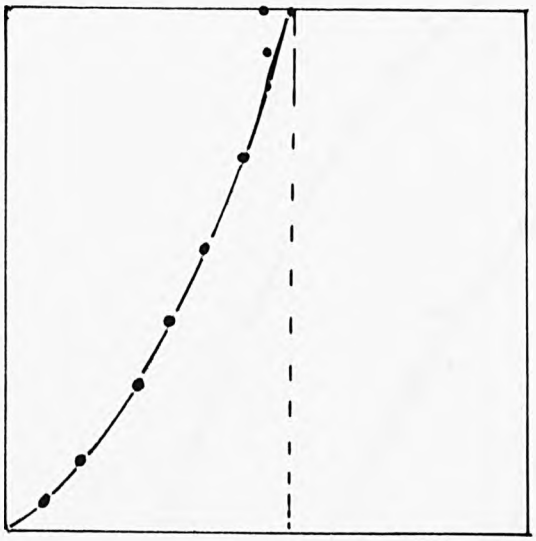

FIG. 4.42

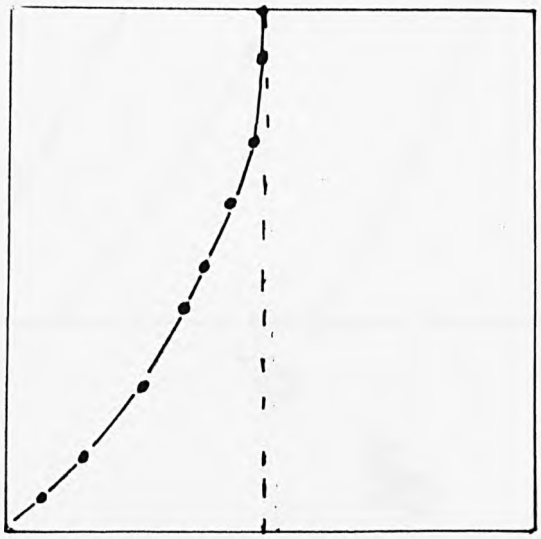

FIG. 4.43

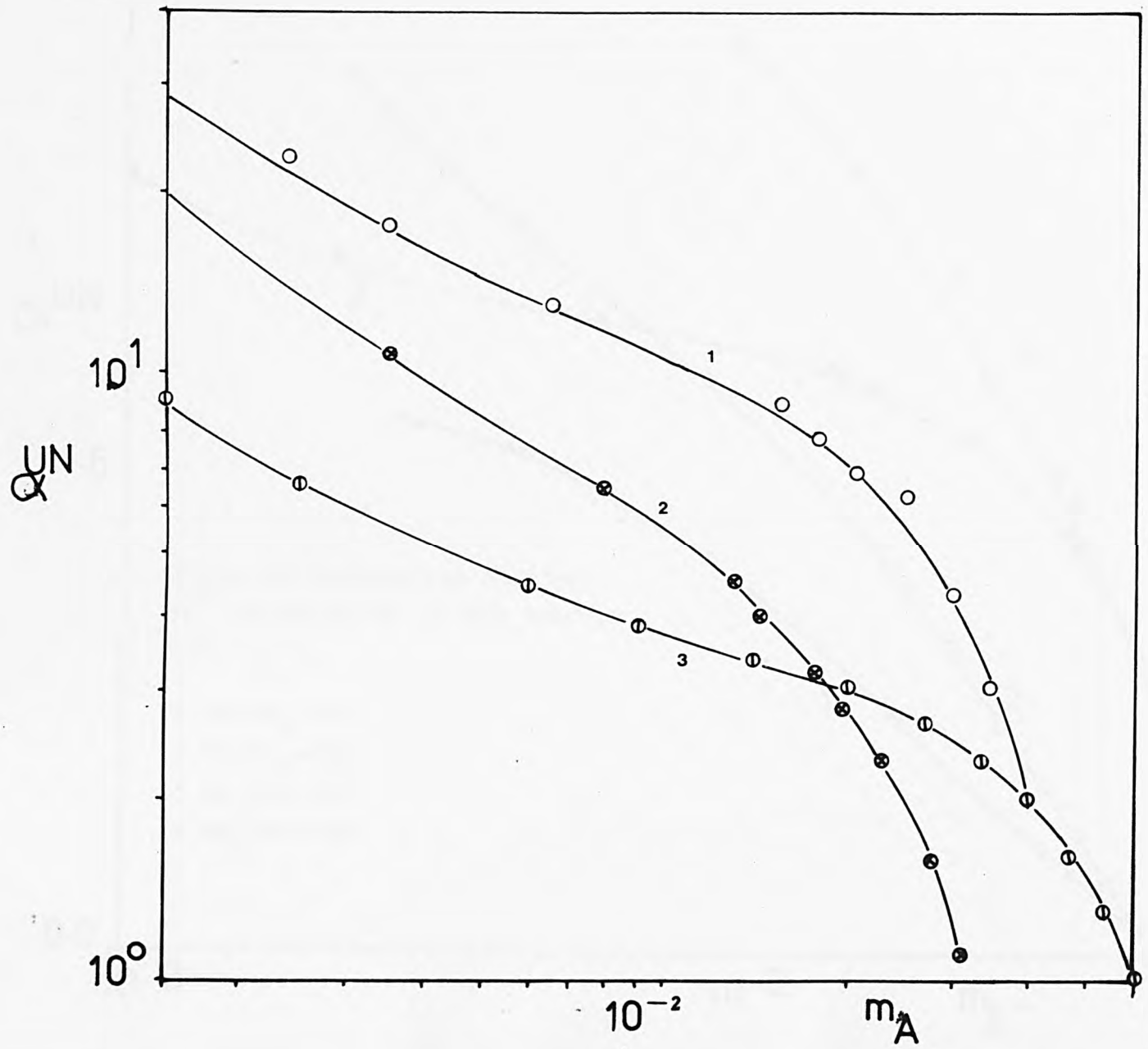

Plots of separation quotient α^{UN} vs.molarity of the counter ion.

1 Pb/Na-CLI
2 Pb/Na-MOR
3 NH_4/Na-CLI

FIG. 4.44

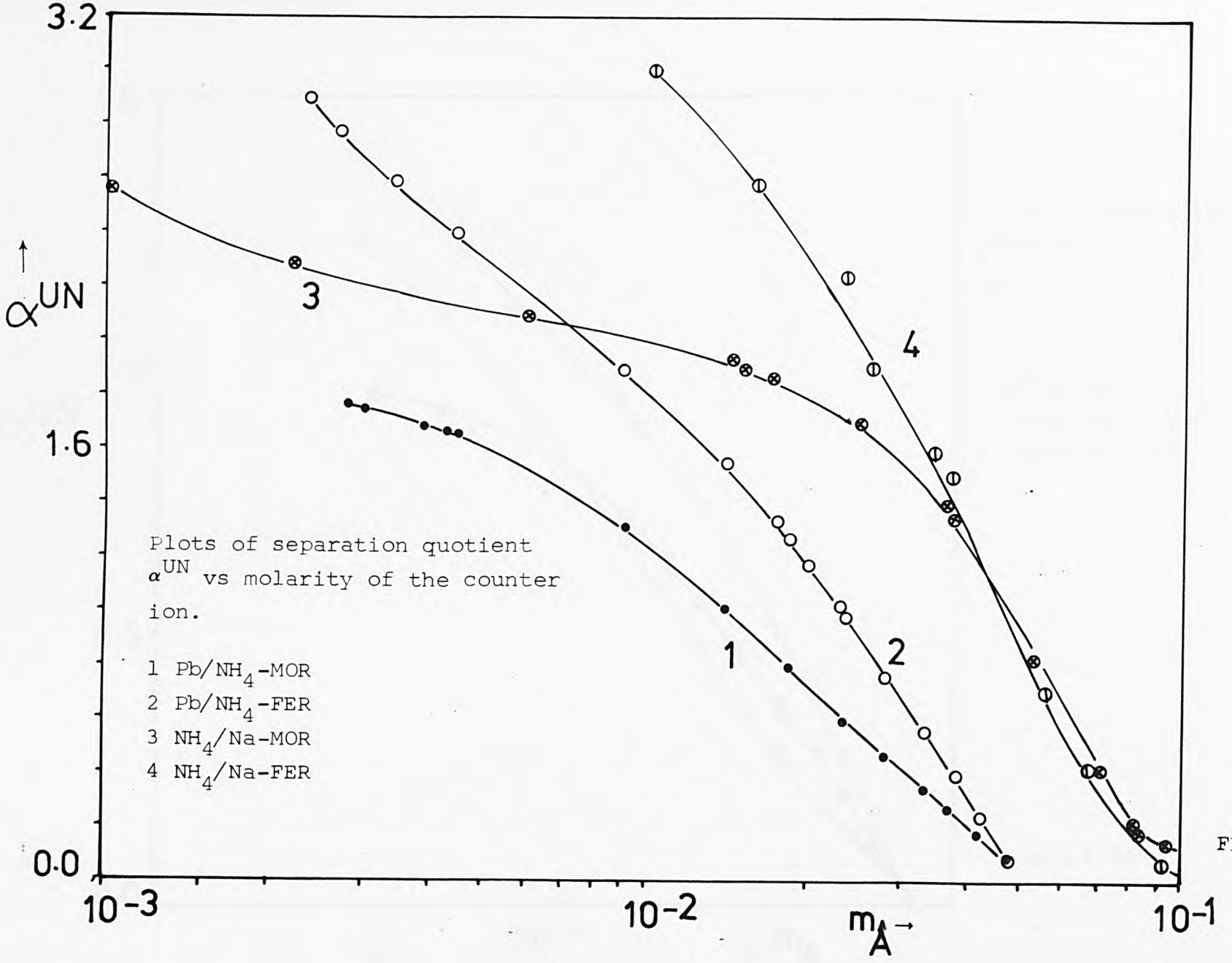
3.2
1.6
0.0
α^{UN} →
10-3
10-2
10-1
m_A →
1
2
3
4
Plots of separation quotient α^{UN} vs molarity of the counter ion.
1 Pb/NH_4-MOR
2 Pb/NH_4-FER
3 NH_4/Na-MOR
4 NH_4/Na-FER

FIG.4.45

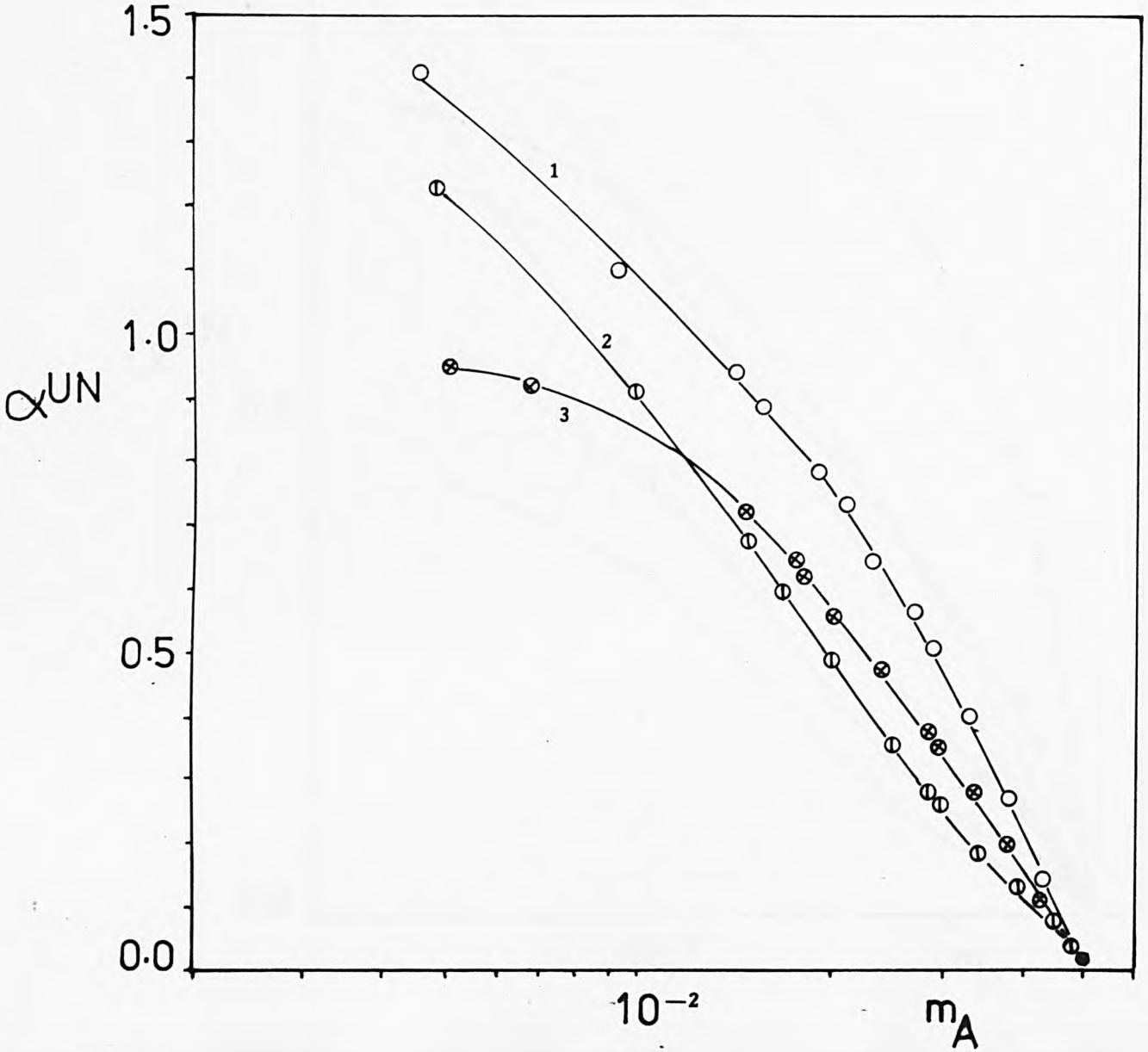

Plots of separation quotient α^{UN} vs molarity of the counter ion.

1 Cd/Na(NO_3)-MOR
2 Cd/NH_4(NO_3)-FER
3 Cd/Na(Cl)-MOR

FIG.4.46

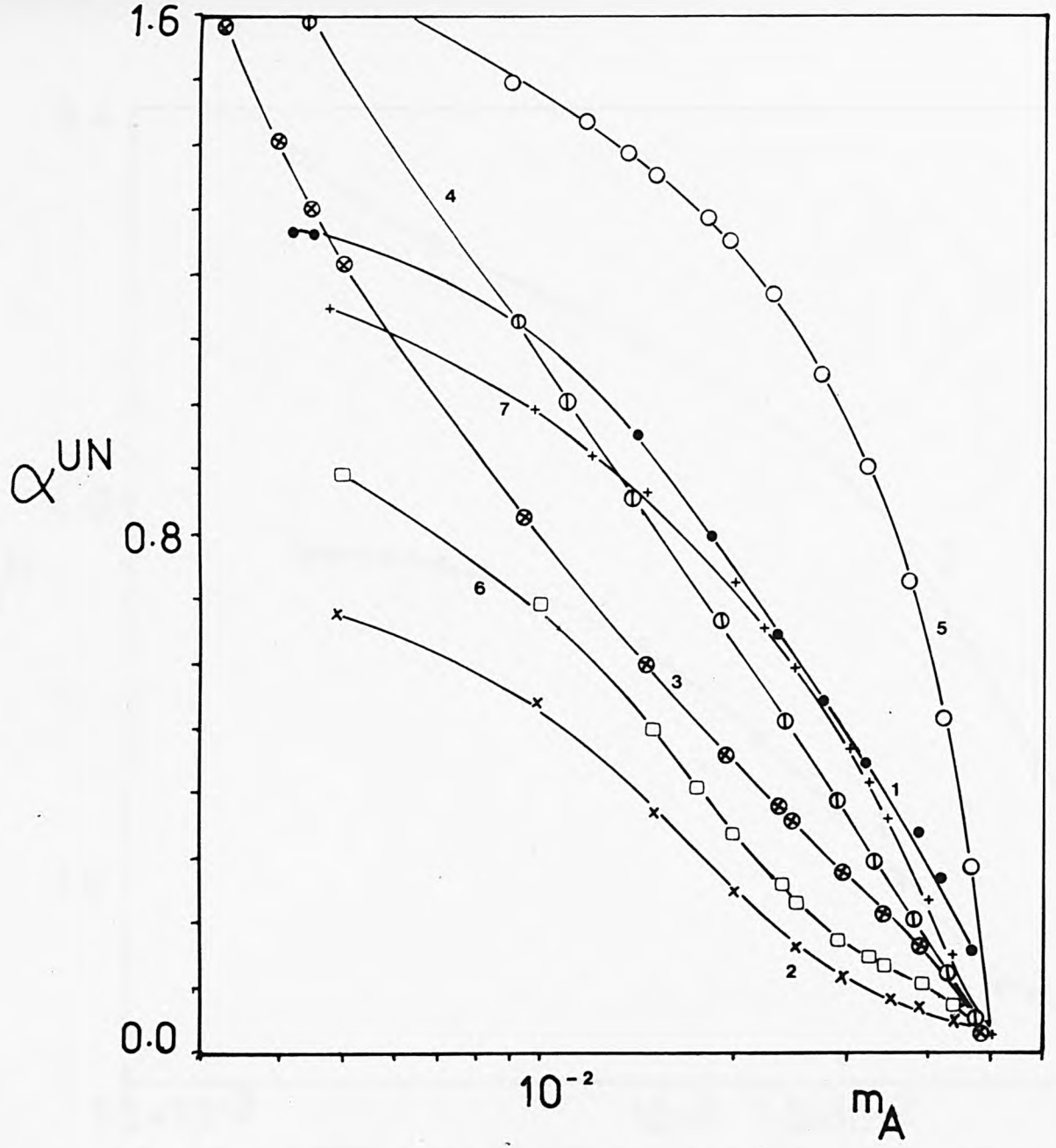

Plots of separation quotient α^{UN} vs molarity of the counter ion.

1 Cd/Na(Cl)-CLI
2 Cd/NH_4(Cl)-FER
3 Cd/Na(Cl)-FER
4 Cd/Na(NO_3)-FER
5 Cd/Na(Cl)-CLI
6 Cd/NH_4(Cl)-MOR
7 Cd/NH_4(NO_3)-MOR

FIG.4.47

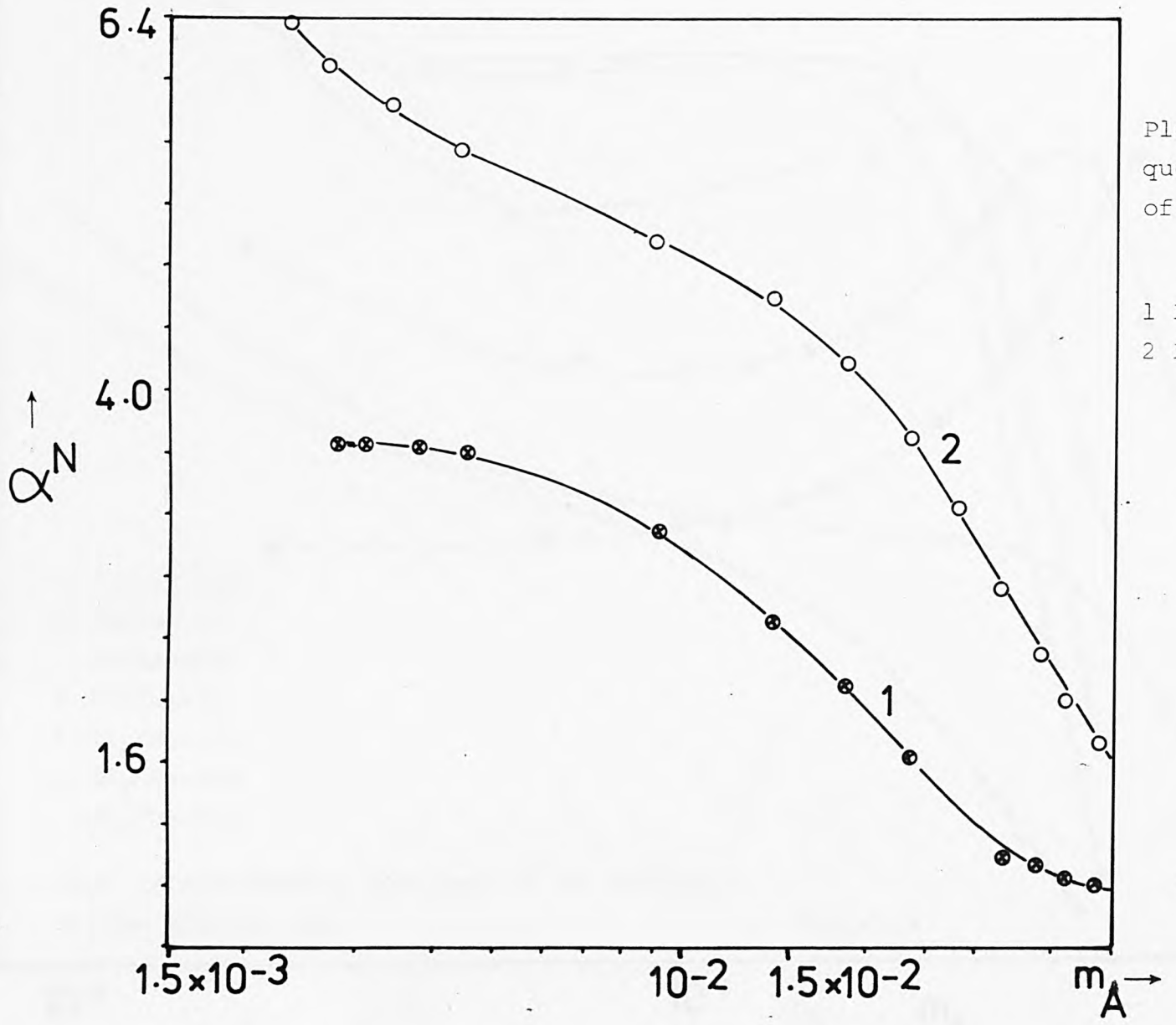

Plots of selectivity quotient α^N vs molarity of the counter ion.

1 Pb/NH_4-MOR
2 Pb/NH_4-FER

FIG.4.48

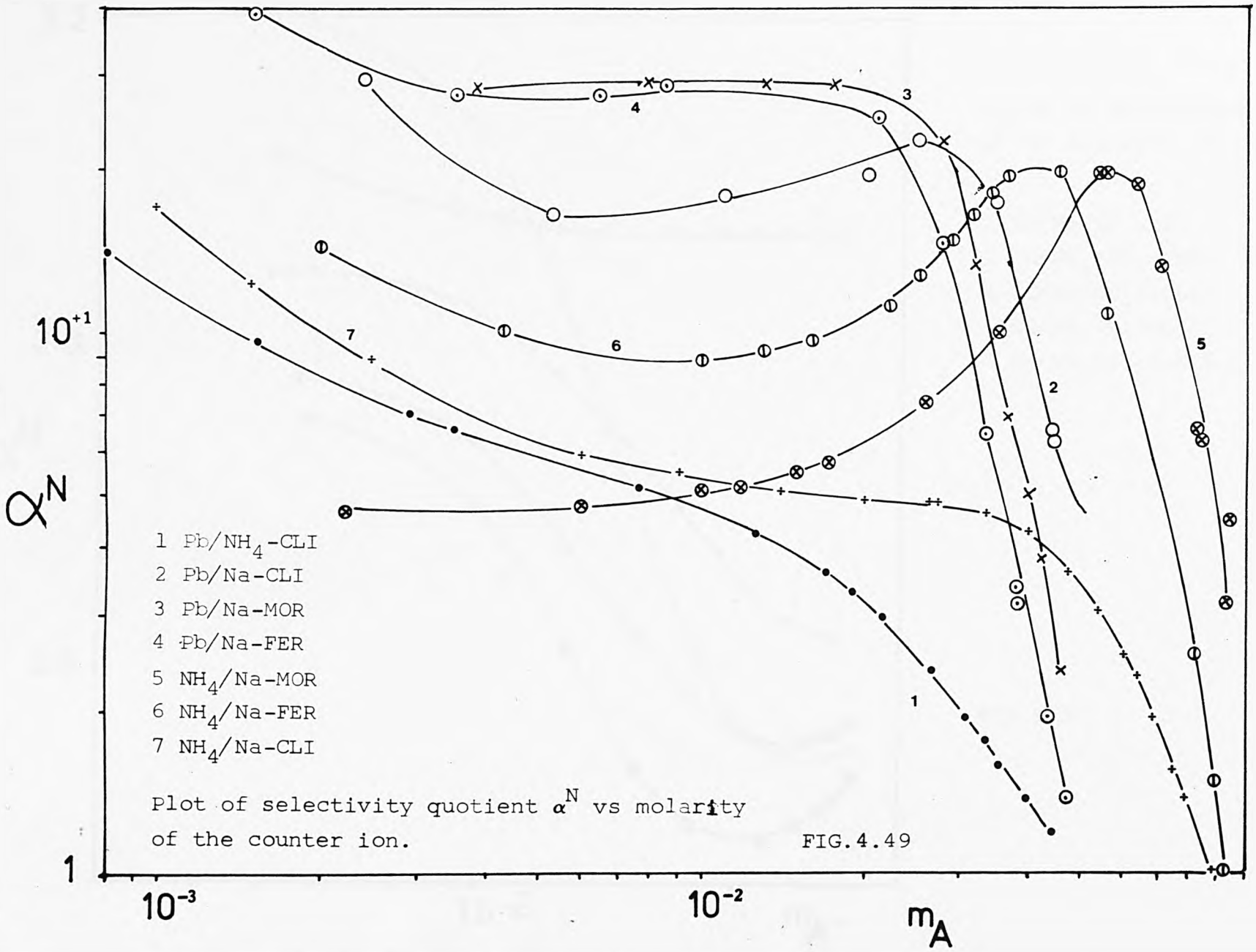

Plot of selectivity quotient α^N vs molarity of the counter ion.

FIG.4.49

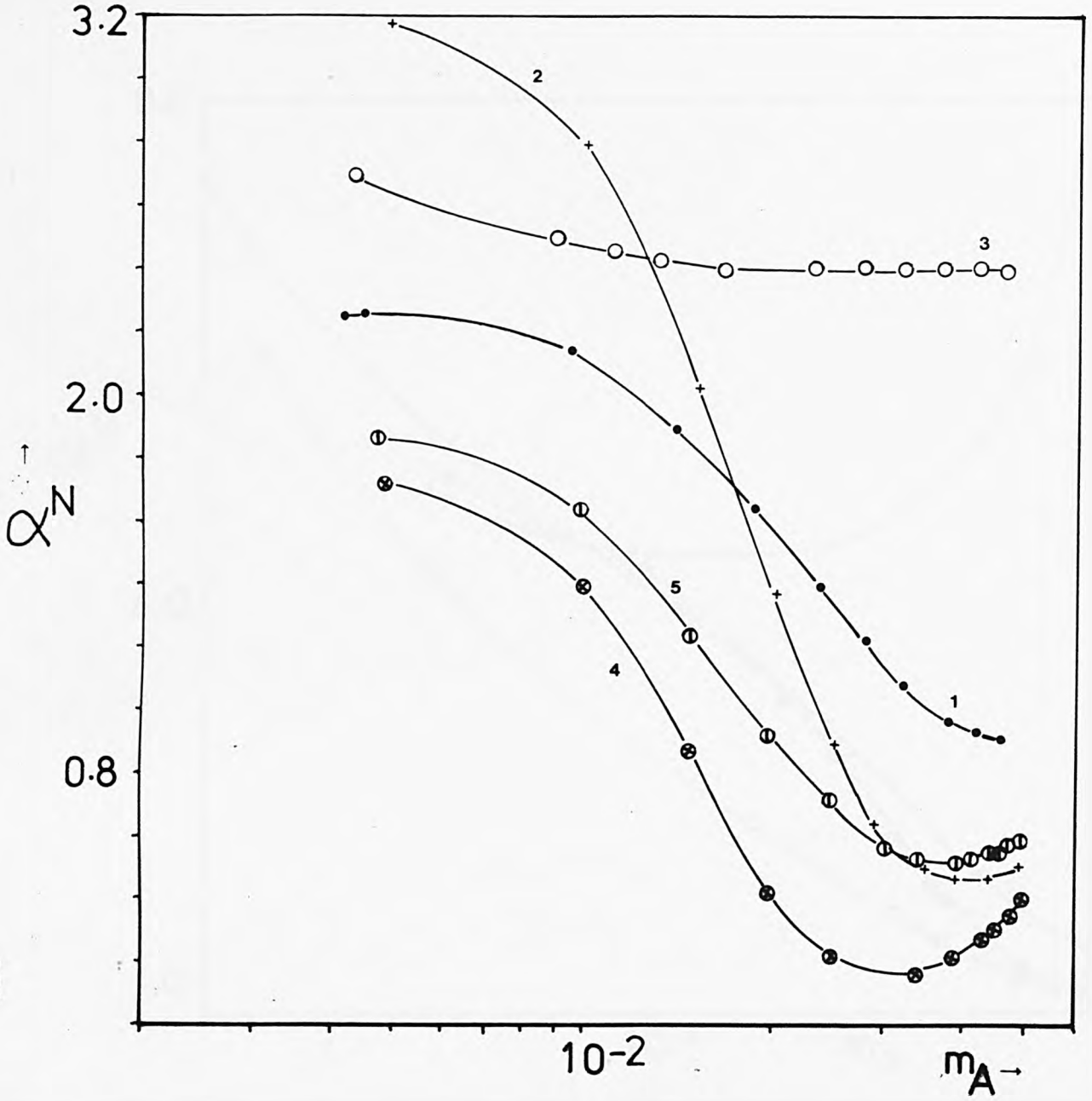

Plots of selectivity quotient α^N vs molarity of the counter ion.

1 Cd/Na(Cl)-CLI
2 Cd/NH_4(Cl)-FER
3 Cd/Na(NO_3)-CLI
4 Cd/NH_4(Cl)-CLI
5 Cd/NH_4(NO_3)-CLI

FIG.4.50

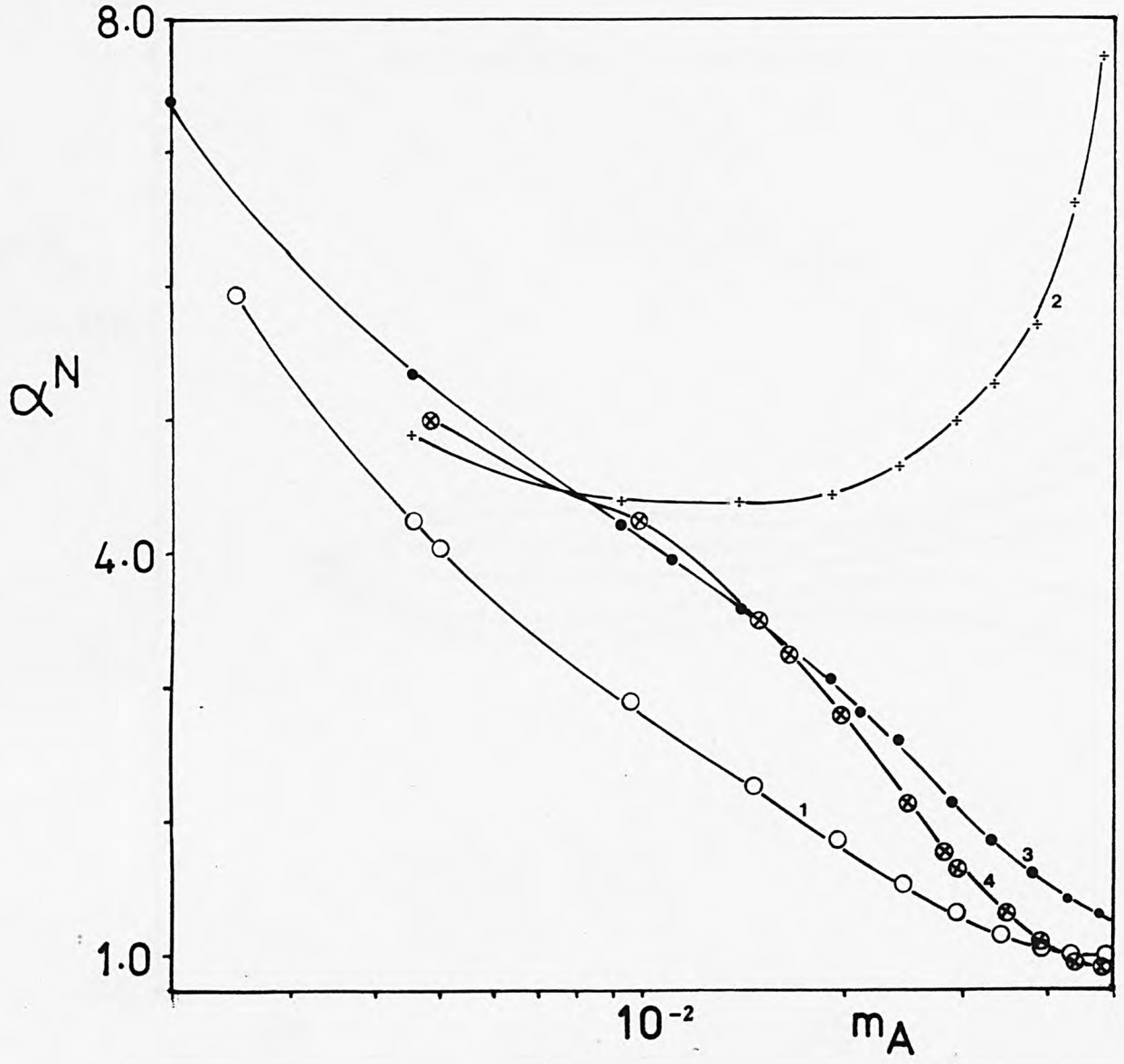

Plots of selectivity quotient α^N vs molarity of the counter ion.

1 Cd/Na(Cl)-FER
2 Cd/Na(NO_3)-MOR
3 Cd/Na(NO_3)-FER
4 Cd/NH_4(NO_3)-FER

FIG.4.51

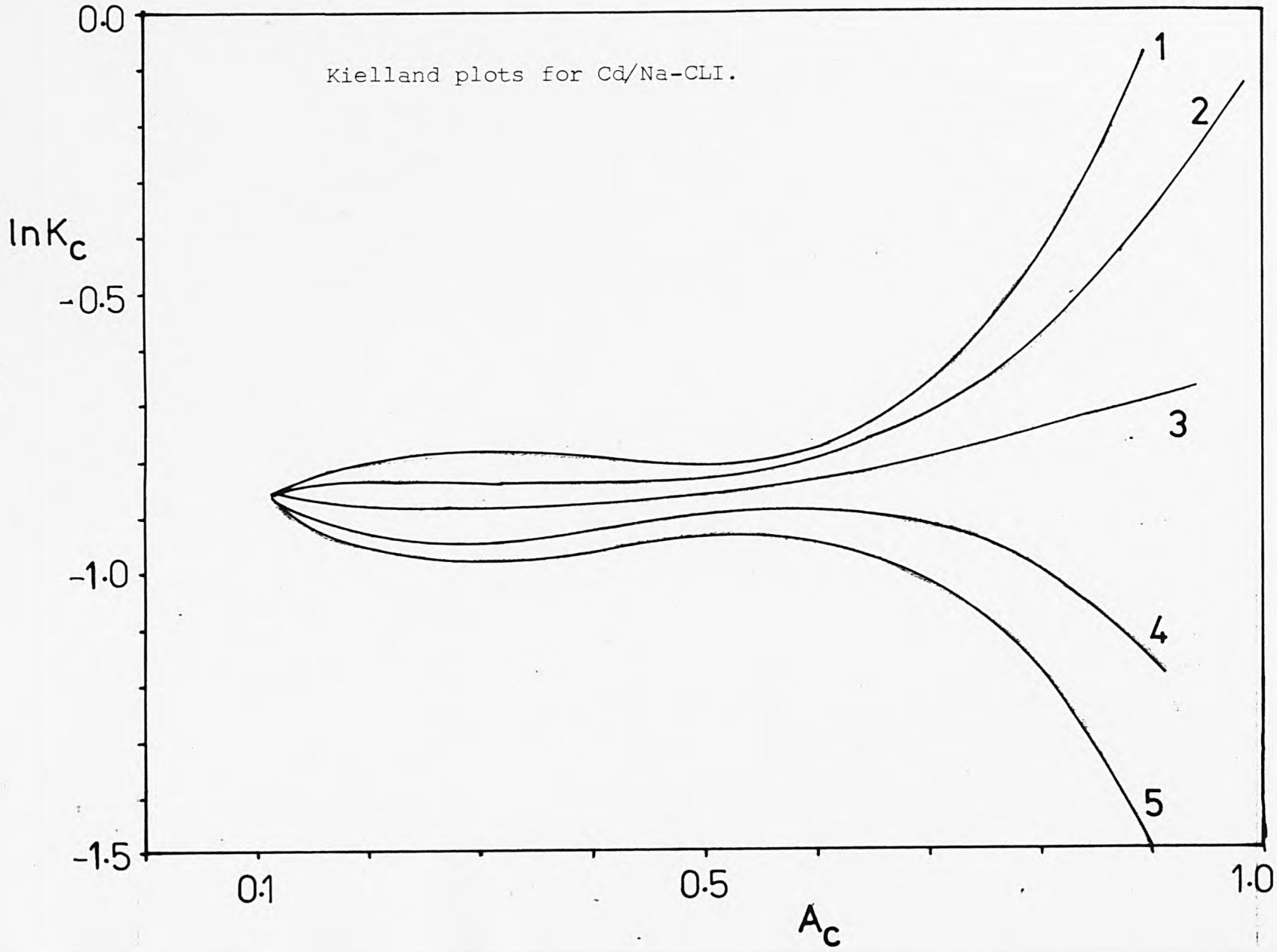

	A_c max.
1	0.635
2	0.645
3	0.655
4	0.670
5	0.680

FIG. 4.52

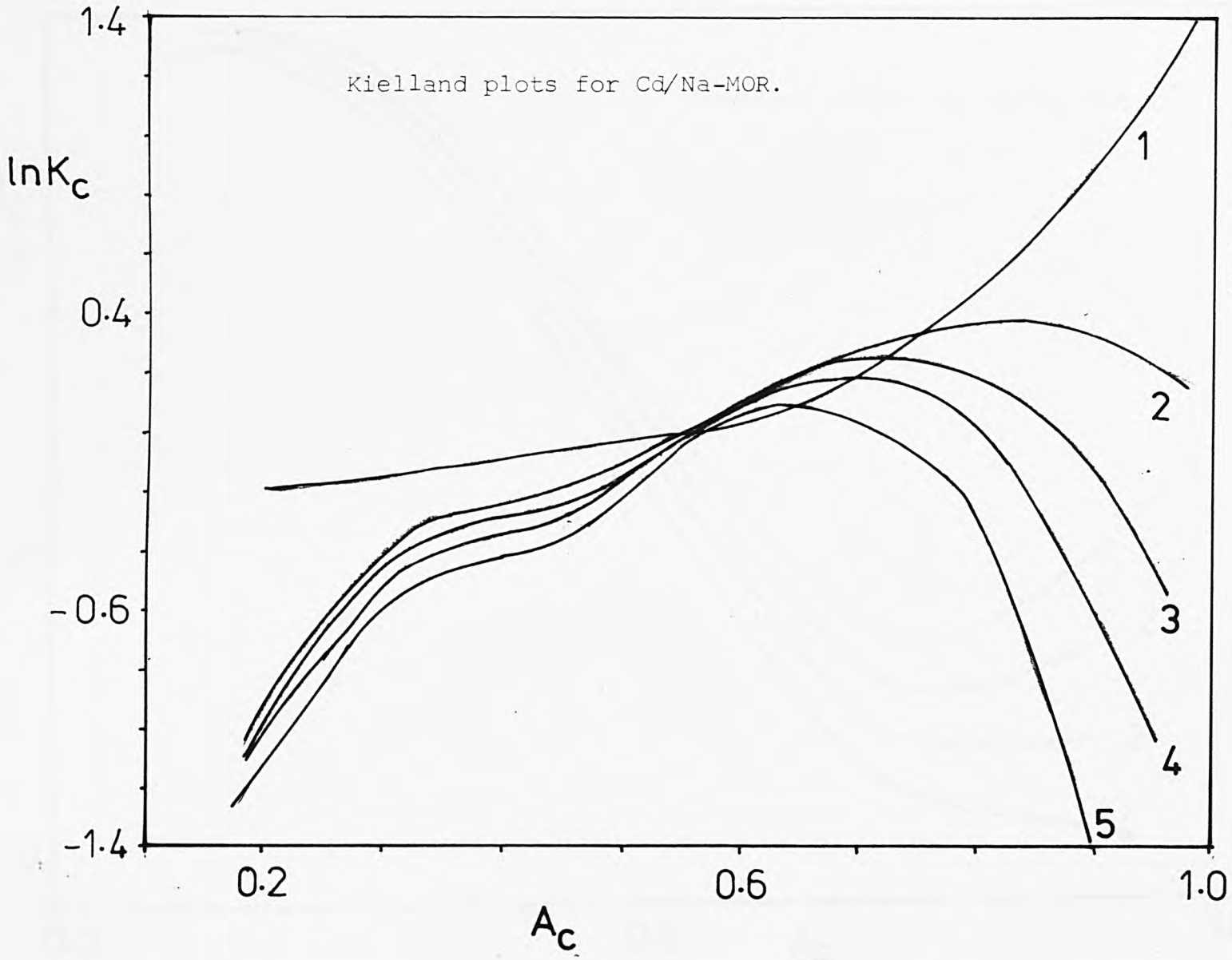

	$A_c$max.
1	0.334
2	0.340
3	0.345
4	0.350
5	0.360

FIG. 4.53

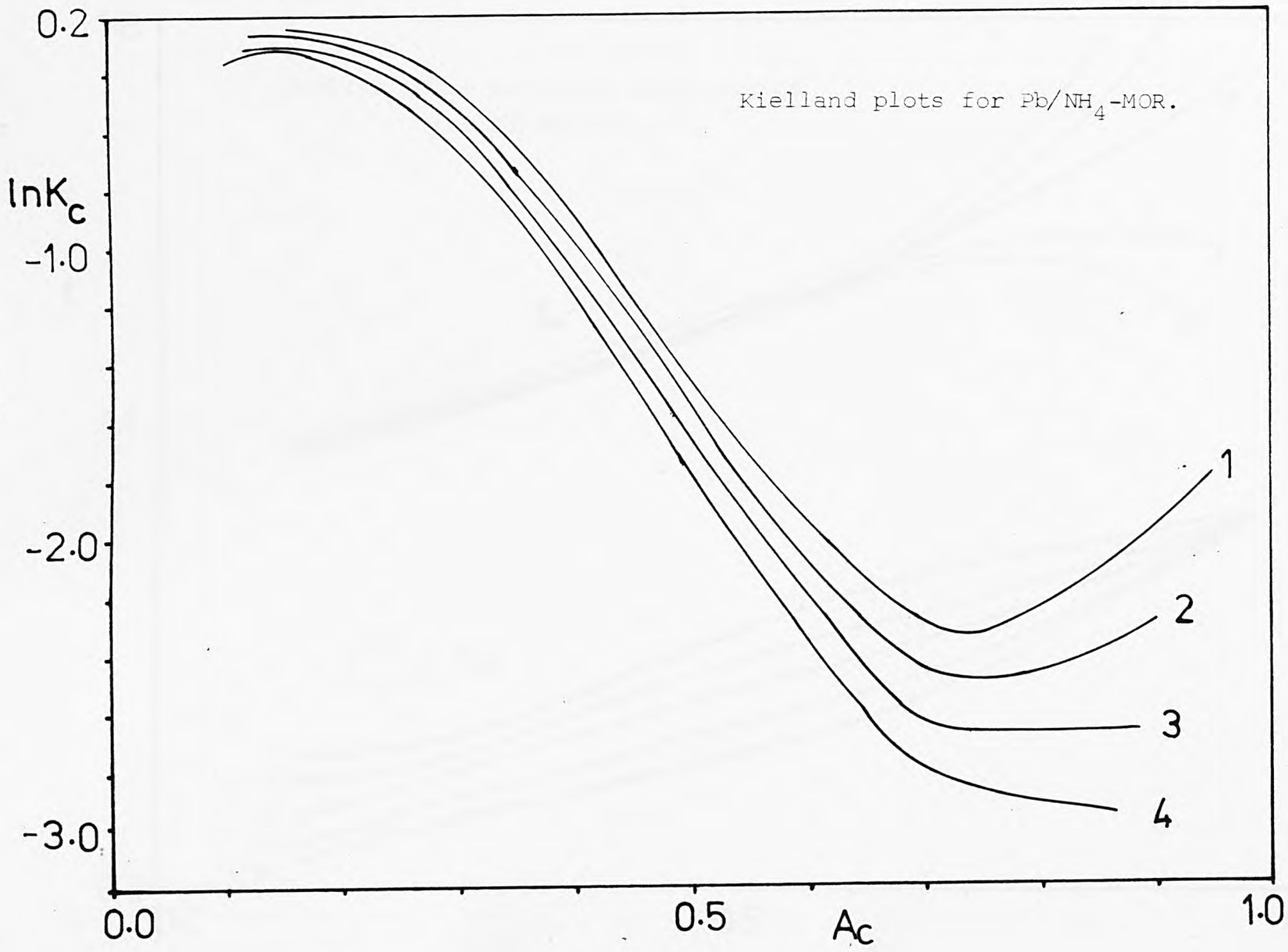

	A_c max.
1	0.48
2	0.49
3	0.50
4	0.51
5	0.513

FIG. 4.54

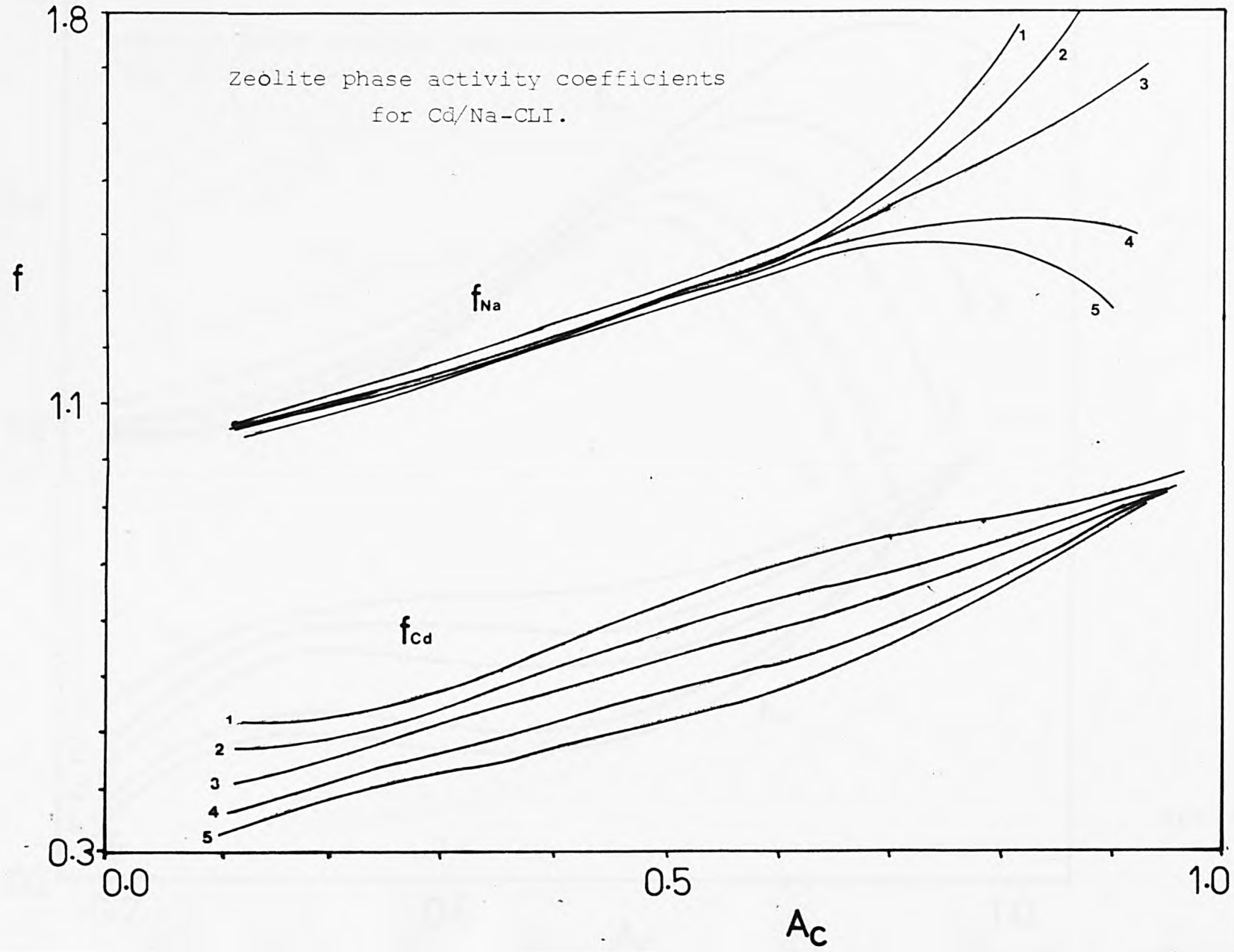

	A_C max.
1	0.635
2	0.645
3	0.655
4	0.670
5	0.680

FIG. 4.55

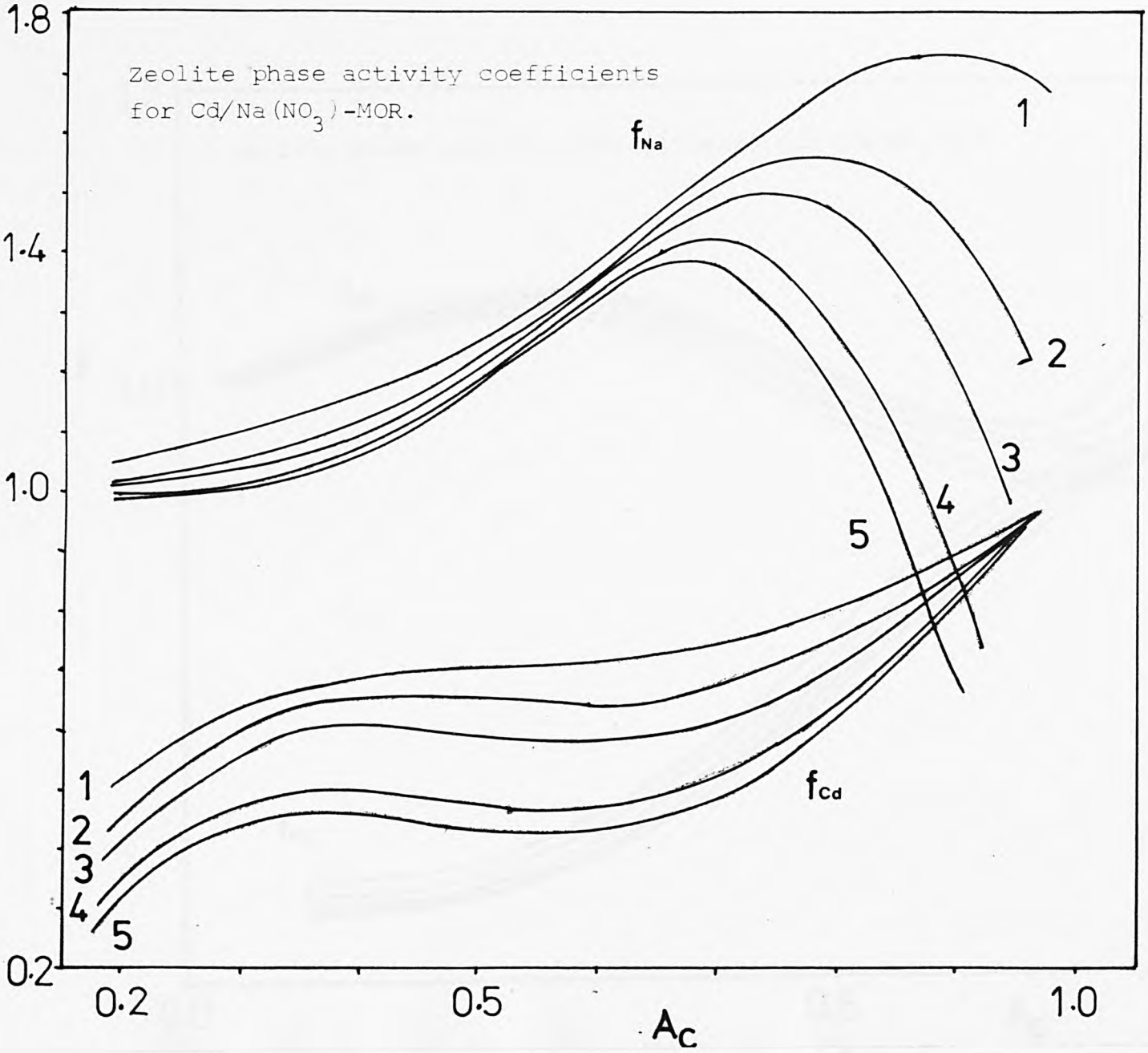

	A_c max.
1	0.340
2	0.345
3	0.350
4	0.360
5	0.365

FIG. 4.56

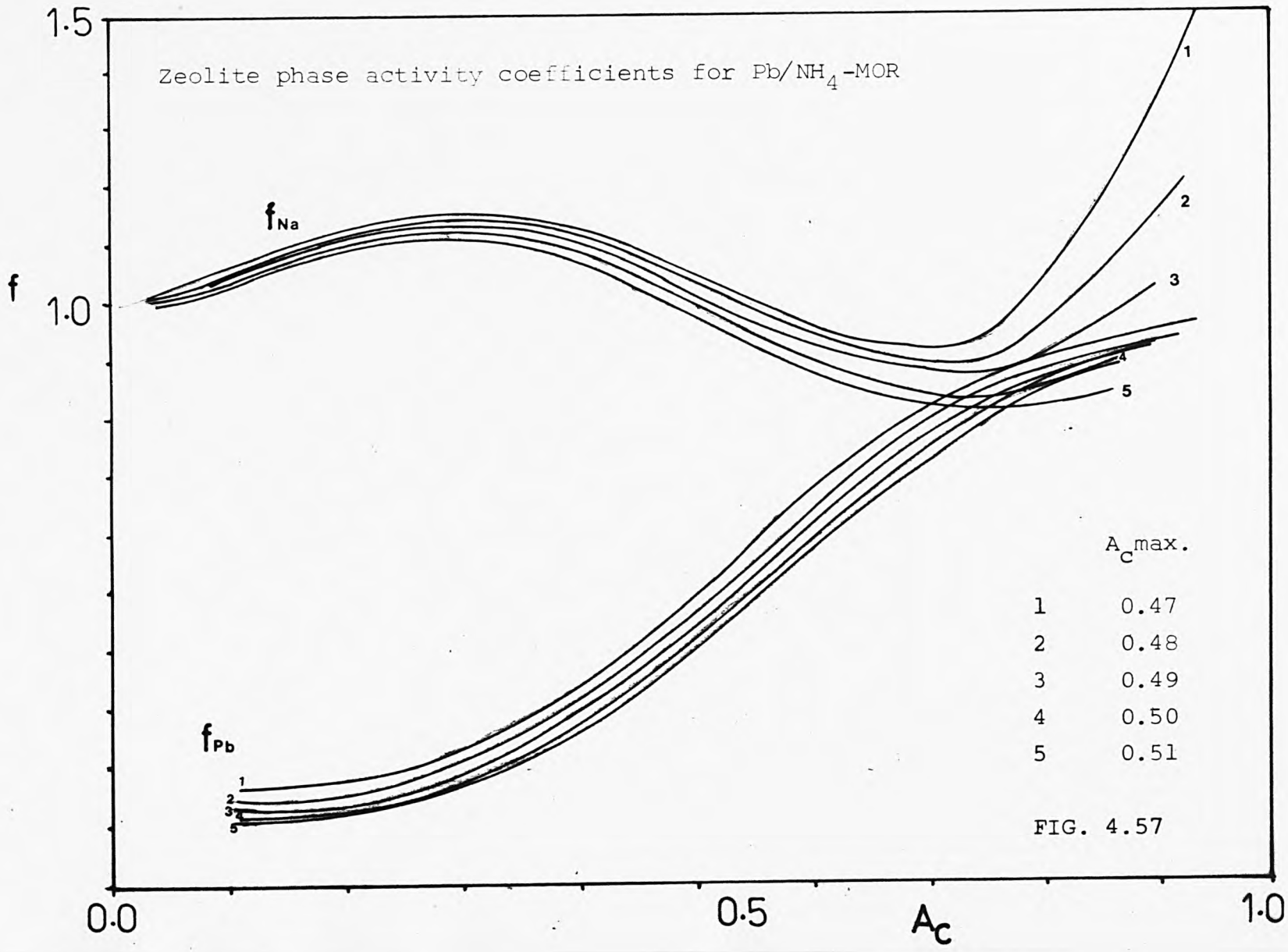

	$A_c$max.
1	0.47
2	0.48
3	0.49
4	0.50
5	0.51

FIG. 4.57

CHAPTER FIVE DISCUSSION

CHAPTER FIVE DISCUSSION

5.1. Levels of Exchange.

5.1.1. Exchange with Clinoptilolite.

The maximum level of exchange obtained when the ions lead, cadmium and ammonium were exchanged with sodium clinoptilolite are in the order $Pb>NH_4>Cd$ (table 4.8). The values of $A_{c\ max}$ were 0.795, 0.765 and 0.656 respectively. For the cadmium ion the maximum level of exchange obtained was the same irrespective of whether nitrate or chloride was the co-ion.

The isotherm resulting from the exchange of lead in Na-CLI is highly rectangular (Figure 4.1). Chelishchev[35] reported an exchange isotherm which was also rectangular when a lead loading of 80% occurred, but as the equivalent fractions of lead in solution was increased ($Pb_{(s)}$ 0.8→1.0) the isotherm curved to give 100% exchange finally.

Semmens[37] reported an isotherm which is very similar to the one obtained in this work except that he found an $A_{c\ max}$ value of 1.0. The reported exchange capacity of clinoptilolite was 1.80 $meq.g^{-1}$ in contrast to 2.188 $meq.g^{-1}$ for this work (table 4.7). If one takes the same exchange capacity in this work as that of Semmens the maximum level of exchange is similar as well as the isotherm shape.

For the Cd/Na-CLI exchange system, the isotherms presented

by Chelishchev[35] and Semmens[37] are not complete ones and are quite different in shape. Chelishchev's isotherm, though incomplete, follows the same pattern as that shown in Figure 4.13, which depicts the exchange behaviour observed when cadmium chloride was the salt in solution. That reported by Semmens[37] is completely different, indicating a high selectivity for cadmium which was not observed in this work.

The NH_4/Na-CLI exchange system has been studied by Howery[69] and Thomas using a natural clinoptilolite sample from California. They found that ammonia was much preferred over sodium, but no isotherms were constructed. They concluded that all Na^+ ions were replaced by NH_4^+ ions when clinoptilolite is treated with ammonium chloride. This is again in contrast to the results obtained in this work. From the chemical analyses of both sodium and ammonium forms of clinoptilolite (tables 4.1, 4.4), it is apparent that some sodium was not replaced in NH_4-CLI (Na_2O = 1.096%), yet this sodium is in principle exchangeable since all the exchanges of lead and cadmium with NH_4-CLI turned out to be ternary due to the sodium release (table 4.8).

Barrer *et al*[76], using natural clinoptilolite, reported a 100% exchange between sodium and ammonium at 60°C but this was again assuming the lower exchange capacity of 1.83 $meq.g^{-1}$.

When ammonium clinoptilolite was exchanged with lead 100% exchange was possible (Figure 4.4). The reason for this behaviour is likely to be complex, but may be partly explicable in terms of the ionic radii of the exchanging ions. The

ammonium ion has an ionic radius of 1.41Å while that of lead is 1.21Å, so the lead ion can in principle enter positions where ammonium cannot due to its larger ionic radius.

The maximum levels of exchange of the ions lead and cadmium with NH_4-CLI were observed to be 1.0 and 0.81 respectively. For the cadmium exchange, in line with what might be expected on theoretical grounds, the use of different co-ions did not influence the $A_{c\ max}$ value at all. The exchanges were ternary in nature.

5.1.2. Exchanges with Mordenite and Ferrierite.

The maximum levels of exchange of the ions Pb^{+2}, Cd^{+2}, NH_4^+, with Na-MOR were in the order $NH_4^+ > Pb^{+2} > Cd^{+2}$ (table 4.8). This is in contrast with the behaviour of clinoptilolite (section 5.1.1). Only about half of the exchangeable cations in mordenite appeared to be capable of exchange with these ions. Similar results were obtained when NH_4-MOR samples were exchanged with lead and cadmium, the former showing the higher exchange levels. From the chemical analyses of NH_4-MOR it appears that the potassium and sodium present account for approximately half of the exchange capacity, and that these ions are not easily removed, in relative contrast to the case of NH_4-CLI where lead and cadmium could exchange with sodium as well.

From the known structure of mordenite (section 1.5.1) half of the exchangeable cations are likely to be situated in or

beside the 8-ring windows that link side pockets between neighbouring main channels. Therefore, there is the possibility of a ∿ 50% ion-sieving effect arising when ions are small enough to enter the main channels but are however excluded from the side pockets. This behaviour has been observed in synthetic mordenite[112]. However, for the exchanges under consideration, the ions are small enough to get through the 8-ring windows, so ion-sieving cannot be the explanation. The partial exchanges are most likely due to the inability of the lead and cadmium to form favourable coordination structures with water and lattice oxygen in the side channels. This has been suggested as the explanation for the 50% exchange level observed with transition metals in synthetic mordenite[89].

Barrer and Klinowski[81] examined the exchange of ammonium for sodium in synthetic mordenite. Their isotherm gave 100% exchange levels and the zeolite was highly selective for ammonium ion, and very similar to the one reported by Hagiwara *et al*[92].

For the exchanges involving the ions Pb^{+2}, Cd^{+2} and NH_4^+ in sodium ferrierite, a similar maximum level of exchange trend was observed to that in sodium mordenite (i.e. $NH_4^+ > Pb^{+2} > Cd^{+2}$). The exchanges involving Na-FER and either NH_4^+ or Pb^{+2} were ternary due to the exchange of these ions with potassium as well as sodium. In contrast, the exchanges of lead and cadmium in NH_4-FER were binary and gave $A_{c\ max}$ values of 0.486 and 0.28 respectively (table 4.8). The limited exchange

observed with ferrierite cannot be due to volume-steric or ion-sieving effects because of its quite open structure (section 1.6.1) . The very strong preference of the mineral for potassium and especially magnesium[144] limits the exchange levels with respect to other ions.

5.2. Thermodynamic Affinities.

Section 5.1 was concerned with the very commonly observed phenomenon that the binary exchanges gave rise to partial exchanges with respect to lead and cadmium.

It follows that values of the thermodynamic equilibrium constant K_a and the standard free energy ΔG^{θ} for each system can only be calculated if the systems are "normalized", which is achieved by dividing all A_c values by $A_{c\ max}$. This in fact means that the exchange is expressed in terms of the exchangeable cations only and implies that the other cations are a part of the zeolite lattice.

The thermodynamic parameters so obtained after normalization are shown in tables 4.10-4.12. With sodium clinoptilolite as the starting material, the exchanges with ammonium or lead gave highly negative ΔG^{θ} values. In marked contrast, cadmium exchange in Na-CLI yielded a very positive figure. The order of affinities from the ΔG^{θ} values is NH_4 > Pb >> Cd. Barrer et al[76] calculated the free energy for the $NH_4^+ \leftrightharpoons Na^+$ exchange in clinoptilolite at 60°C and the values reported were $\Delta G^{\theta} = -5.75$ kJ $(g.equiv)^{-1}$ and $K_a = 7.9$. Corresponding values

in this work were -4.03 kJ $(g.equiv.)^{-1}$ and 5.12. Also Howery reported a standard free energy value of -5.04 kJ $(g.equiv.)^{-1}$ at $30^{o}C$.

For exchanges involving lead and cadmium in Na-CLI, no thermodynamic affinities are reported in the literature. The exchanges with NH_4-CLI turned out to be ternary in nature (table 4.8) so that the thermodynamic treatment for binary exchange could not be applied. Insufficient data were obtained to make a ternary thermodynamic treatment possible.

For exchanges of either ammonium lead or cadmium ions in Na-MOR, the affinity sequence found is $Pb^{+2} \approx NH_4^{+} >> Cd^{+2}$ (table 4.10, 4.11). The trend is seen to be similar to the one observed with Na-CLI.

Barrer and Klinowski[81] measured the standard free energy for the system NH_4/Na-MOR and reported values of K_a=4.5 and ΔG^{θ} = 3.7 kJ $(g.equiv.)^{-1}$. Similar values were obtained by Hagiwara *et al*[92]. However both studies employed synthetic mordenite and full replacement of the sodium ion by the ammonium was achieved. In this work the reported thermodynamic parameters (table 4.11) were K_a = 6.43 and ΔG^{θ} = 4.59kJ $(g.equiv.)^{-1}$ but only half of the exchangeable cations were involved in this case. Since normalization of the isotherm was performed the calculated parameters are not comparable with those reported by other workers on synthetic mordenite (section 5.4). Part of the difference however, can arise from the fitting procedure of the experimental data. The isotherm for the natural material (Figure 4.20) is highly

rectangular in contrast to the ones previously reported[81,92] and such isotherms are liable to error when calculating the thermodynamic parameters (see section 4.4.1).

The K_a and ΔG^{θ} values obtained for the Cd/Na(Cl)-MOR and Cd/Na(NO_3)-MOR systems are very close as might be expected if the solution phase correction has been correctly performed. However, those obtained with ammonium mordenite are quite different (table 4.10); this is also due to problems arising when fitting the isotherm data (section 5.3). The isotherms for the system Cd/Na(Cl)-MOR and Cd/Na(NO_3)-MOR are very similar (Figure 4.14, 4.8) and any error introduced during the best-fitting procedure will affect the calculated parameters for the two systems in the same way, so providing the solution phase correction is correctly calculated, the observed good agreement should follow. However, for the system Cd/NH_4(Cl)-MOR and Cd/NH_4(NO_3)-MOR the isotherms are of rather different shape and were more difficult to best-fit by computer.

The exchanges of NH_4-MOR with lead and cadmium indicate that the zeolite shows an overall preference for the ammonium ion. The affinity trend is NH_4 > Cd > Pb, the free energies being highly positive for both cadmium and lead. A similar sequence of NH_4 > Pb >>Cd is shown in ammonium ferrierite. When sodium ferrierite was the starting material, the zeolite showed a preference for the sodium ion over cadmium, in contrast to its behaviour with respect to lead. The difference in the ΔG^{θ} values for the Cd/Na(Cl)-FER and Cd/Na(NO_3)-FER

systems is again due to the isotherm fitting procedures (section 4.4.1); experimental inaccuracy was greater with these systems because the difference between the metal concentration in solution before and after exchange was quite small, and a slight error in the titrimetric methods employed therefore reflects in larger discrepancies in the calculated results (section 4.5).

5.3. Solution Phase Activity Corrections

Solution phase corrections were undertaken as described in section 2.2.1, by introducing the activity coefficients γ_A γ_B. These coefficients correct for the deviation of the ion concentrations from ideality, which always arise from ion-ion interactions in a real solution.

For the ion exchange process the standard states for the solution phase are the hypothetical ideal 1 molal solutions (section 2.2). In an ideal solution $\gamma_A = \gamma_B = 1$ and so

$$\Gamma = \frac{\gamma_B^{z_A}}{\gamma_A^{z_B}} = 1$$

Values of Γ differing from unity reflect the level of non-ideality correction that has to be applied to the solution phase in order to obtain the Kielland quotient K_c (equation 2.17) from the measured mass action quotient K_m (equation 2.10). where

$$K_c = K_m \cdot \Gamma$$

5.3.1. Effect of Ionic Strength on Γ Values.

Values of Γ were obtained for all the mixed solutions used for the binary exchanges (table 4.8) and are shown in the Appendix III as functions both of A_c and I.

Analytically, for a uni-univalent exchange such as exchanges between sodium and amonium ions, the Γ values obtained are found to be constant since the ionic strength I does not change as the relative concentrations of different ions in solution are altered at a total solution concentration of 0.1 equiv.dm^{-3} (I = 0.1 mol dm^{-3}). This matter has been discussed in depth recently elsewhere[124]. As an example the solution mixture of NH_4NO_3 plus $NaNO_3$ at a total concentration of 0.1 equiv.dm^{-3} and I = 0.1 had a constant Γ value of 1.030. The deviation from ideality is very small, and constant (about 3%).

For uni-divalent exchange the I values depend on the relative concentrations of the exchanging cations in solution. These differences are reflected in the Γ values. Table 5.1 shows Γ values as a function of I which were obtained for the mixed solutions lead nitrate-sodium nitrate and lead nitrate-ammonium nitrate respectively at a total solution concentration of 0.1 equiv.dm^{-3}. As a comparison Γ and I values are given in table 5.2 for the mixed solution of lead-nitrate-sodium nitrate at a total solution concentration of 0.5 equiv. dm^{-3}.

Table 5.1. I and Γ values at 0.1 equiv.dm^{-3}.

I	Γ $PbNO_3$ $NaNO_3$	Γ $PbNO_3$ NH_4NO_3
0.1425	2.064	1.966
0.1275	2.0218	1.9203
0.1175	1.9916	1.8893
0.11425	1.981	1.8740

Table 5.2. I and Γ values at 0.5 equiv.dm^{-3}

I	Γ $PbNO_3$ $NaNO_3$
0.743	3.599
0.717	3.579
0.693	3.560
0.668	3.540
0.644	3.520
0.619	3.499
0.595	3.479
0.570	3.457
0.545	3.436
0.521	3.414
0.510	3.404

It is clear that at low external solution concentrations, the deviation from ideality is (as expected) less. When the total normality is 0.1 equiv.dm^{-3}, the Γ values are in the region 1.8-2.0, while for the higher total concentration (0.5 equiv.dm^{-3}) the Γ values are as high as 3.4-3.6.

The non-ideality behaviour of the solution phase was also examined at a given concentration for the same combination of counter-ions A^{z_A} and $B^{z_B^+}$ in the presence of different co-ions. Specifically, the two salts cadmium chloride and cadmium nitrate were examined in detail. As mentioned in section 4.4.3.1, the activity coefficient values of the pure salt ($Cd(NO_3)_2$) were obtained by interpolation using the modified Debye-Hückel equation[121]. For cadmium chloride, this approach was found not to be suitable, so a polynomial equation was best-fitted to the literature data in order to obtain interpolated values. The Γ values obtained for the four mixed solution systems $Cd(NO_3)_2/NaNO_3$, $Cd(NO_3)_2/NH_4NO_3$, $CdCl_2/NaCl$ and $CdCl_2/NH_4Cl$ as a function of ionic strength I and at a total and constant 0.1 equiv.dm^{-3} solution concentration, are given in table 5.3 .

The solution correction for the cadmium chloride is very high (Γ = 4.4 - 4.5) while that for cadmium nitrate is in the region of 1.5. This is an indication that ion-ion interactions in cadmium chloride solutions are very strong compared to nitrate solutions, and the ion would be expected to show preference for the solution phase in the former case.

Table 5.3: Γ values obtained at various ionic strengths of mixed solution at a concentration 0.1 equiv.dm^{-3}

I	$Cd(NO_3)_2$ $NaNO_3$	$Cd(NO_3)_2$ NH_4NO_3	$CdCl_2$ NaCl	$CdCl_2$ NH_4Cl
0.1425	1.654	1.574	4.535	4.439
0.1275	1.605	1.529	4.551	4.439
0.1175	1.580	1.480	4.577	4.480
0.1143	1.569	1.482	4.588	4.490

This in fact was observed experimentally - the cadmium uptake by any zeolite was less in the case where the cadmium chloride salt was used (section 5.5.).

5.3.2. Kielland Plots After Solution Phase Corrections.

As discussed earlier (section 4.2) and emphasised in the literature[149] the thermodynamic equilibrium constant, and the Kielland plots, should be constant for a given pair of ions, irrespective of the co-ions chosen, for a particular zeolite. This was in fact observed for nearly all the systems and the results obtained for K_a and ΔG° are shown in table 4.10. Since corrections were made for solution phase non-ideality, the shapes of the Kielland plots obtained for the two different cadmium salts and for the same zeolite should be identical. This was in fact difficult to demonstrate for all systems. Difference in Kielland plot shapes , where they arise, are mainly due to the fitting procedure used for the isotherm.

This has been explained in section 4.4.1. The variations in Kielland plot shapes can be great with a slight change in $A_{c\ max}$. As an example, consider the exchange of Na-MOR with cadmium nitrate and in particular the effect on the Kielland plot of varying $A_{c\ max}$. The resulting Kielland plots for different $A_{c\ max}$ values are not similar at all (fig. 4.53).

The actual Kielland plots for the best choice of $A_{c\ max}$ for Na-MOR exchanged with cadmium chloride and cadmium nitrate are shown in Fig. 5.1. Though the shapes of the Kielland plots are not the same the integral $\int_0^1 \ln K_c dA_c$ is nearly the same, which gives values for the thermodynamic equilibrium constants which are about the same (K_a = 0.408 for cadmium chloride and 0.419 for cadmium nitrate).

For the exchanges involving either cadmium nitrate or cadmium chloride solutions and Na-CLI, the Kielland plots obtained are shown in Fig. 5.2. Again, they are not similar at all, but the thermodynamic parameters are comparable if the fitting problems are considered. The fitting of the isotherm for the exchange system Cd/Na(Cl)-CLI was especially difficult due to the shape of the isotherm at the points where $A_s \rightarrow 1$. The best-fit prediction of $A_{c\ max}$ for this system was 0.644, while that for Cd/Na(NO_3)-CLI was 0.656, which agreed closely with the experimental value. In Fig.4.52, the effect of imposed variations of $A_{c\ max}$ on $\ln K_c$ indicate the overall effects on the Kielland plots.

The Kielland plots obtained for the exchange systems $Cd/Na(NO_3)$-FER and Cd/Na(Cl)-FER are given in Fig. 5.3. The resulting curves are very similar, so that this case exemplifies what should be the "text book" result for all cases. The main reason for the close similarity in Kielland plots is the fact that both isotherms are non-selective and the shapes are very close (Fig. 4.9, 4.15). Analytical experimental error is minimised with non-selective isotherms[150] and also errors in the estimation of $A_{c\ max}$ have only a minimal effect. In contrast, the exchanges of the two cadmium salts with NH_4-FER do not give similar Kielland plots. Although both isotherms are non-selective again, in this case they are of different shape and were difficult to fit, hence the Kielland plots differed (Fig. 5.4). This in fact results in quite different K_a, ΔG° values for the systems, but comparable if the uncertainties due to the fitting procedures are taken into consideration.

A similar phenomenon was observed for higher external solution concentrations. Taking for example the exchange system Pb/Na-MOR the Kielland plots obtained for this same exchange system but at different concentrations (i.e. 0.1 and 0.5 equiv. dm^{-3}) are shown in Fig. 5.5. Although the plots are not the same, the K_a and ΔG° values obtained (tables 4.10, 4.12) are in a reasonable agreement if we bear in mind the problems involved in fitting highly rectangular isotherms (section 4.4.1).

So as a final conclusion it can be said that although theoretically the Kielland plots for a given pair of cations and for a given zeolite should be the same when different co-ions are

used, in practice agreement between such a set of Kielland plots is very much dependent on the system involved, and especially the shapes of isotherms. However, the value of the integral $\int_0^1 \ln K_c \, dA_c$ will be more or less the same. This in fact implies that when changes occur in the external solution, such as the total concentration or the presence of different co-ions, the solution phase correction is the most important factor. The crystal phase becomes really important when changes in temperature and pressure occur and the estimation of K_a is then necessary.

5.4. Predictions by Triangle Rule.

The so-called "triangle rule" has been used extensively by many workers[81,95] to predict thermodynamic affinities for exchange systems involving various pairs of exchanging ions. Barrer and Klinowski[81] determined experimentally the thermodynamic parameters for the binary exchanges of the ions Cs^+, K^+, NH_4^+, Li^+, Ca^{2+}, Sr^{2+}, Ba^{2+} into both synthetic Na-MOR and NH_4-MOR. They then predicted the equilibrium constants and standard free energies for systems which could be related to these experimental data by the triangle rule (i.e. Cs/Ba, Li/Ba, Li/Cs etc). However, none of the predicted values were verified experimentally.

Townsend[136] predicted thermodynamic affinities for the transition metals Mn^{2+}, Co^{2+}, Ni^{2+}, Cu^{2+} and Zn^{2+} using synthetic mordenite but again no experimental values were given which could be compared with those obtained by the triangle rule.

Barrer et al[108] using zeolite K-F, predicted the thermodynamic equilibrium constant for the system K Li to be 0.51. In this case, this was verified experimentally.

However, very recently, Golden et al[95] used the triangle rule to predict thermodynamic parameters for the systems Na/Li, Na/Co, H_3O/Li in synthetic mordenite. Further they tested experimentally the systems Li/Na-MOR, Co/Na-MOR and the K_a, ΔG° values obtained were very close to the predicted ones. The results are shown in table 5.4.

Table 5.4. Experimental and Predicted Values of K_a, ΔG° (kJ(g equiv)$^{-1}$)

Exchange	Experimental		Triangle rule	
	K_a	ΔG°	K_a	ΔG°
Na^+ Li	0.048	7.56	0.053	7.23
2Na Co^{2+}	0.63	0.588	0.58	0.67
H_3O^+ Li^+	0.0052	13.062	-	-

For the system $Na^+ \leftrightharpoons Li^+$ the same K_a value (0.058) was predicted by Barrer and Klinowski[81]. Similarly Townsend[136] gave a value of K_a of 0.586 for the system $2Na^+ \leftrightharpoons Co^{2+}$, in good agreement with the above.

In this work the triangle rule has been applied to all the exchange systems that were proved to be binary in nature. Predictions were compared where possible with experimentally

obtained values of the thermodynamic parameters.

5.4.1. Exchanges with Mordenite.

The experimental values for the thermodynamic parameters K_a and ΔG° for the system Pb/Na-MOR, Cd/Na(NO_3)-MOR and Cd/Na(Cl)-- MOR were used to predict values for the system Cd/Pb-MOR. The results given in table 5.5. indicate the very high preference of mordenite for the lead ion (ΔG° = +5.7 kJ(g equiv)$^{-1}$). This is in agreement to what has been observed in a ternary exchange where both ions are present (Pb/Cd/Na-MOR), (Appendix II).

The parameters K_a and ΔG° for the system Cd/Pb-MOR can also be predicted from the experimental data of the binary exchanges involving ammonium mordenite, e.g. Pb/NH_4-MOR, Cd/NH_4-MOR. The values obtained are given in table 5.6 (ΔG° = -2.052 kJ (g equiv)$^{-1}$), indicating surprisingly that cadmium is the overall preferred ion. This agrees with experimental ternary data where lead and cadmium are present together in an ammonium mordenite exchange. The cadmium content of the zeolite tends to be higher than that of lead (see Appendix II).

Thus the predicted ΔG° values for the Cd/Pb-MOR system starting with Na-MOR is quite different from the predicted ΔG° value for the Cd/Pb-MOR system starting with NH_4-MOR. This difference arises due to the fact that the systems concerned do not exchange to same level, so that different standard states exist. Considering firstly the exchange systems Pb/Na-MOR, Cd/Na-MOR from which Cd/Pb-MOR is predicted, then with the standard states

Table 5.5. Standard free energies ΔG° kJ(g equiv)$^{-1}$) calculated via triangle rule using data for Na-MOR exchange systems

Ion Initially in Solution				
Pb	-4.63	-5.746	-5.704	0.0
Cd*	+1.074	0.0	0.0	+5.704
Cd**	+1.108	0.0	0.0	+5.746
Na	0.0	-1.108	-1.074	+4.63
	Na	Cd**	Cd*	Pb

Table 5.6. Standard free energies ΔG° kJ(g equiv)$^{-1}$) calculated via traingle rule using data for NH_4-MOR exchange systems

Ion Initially in Solution				
Pb	+3.276	+0.396	+2.052	0.0
Cd*	+1.226	0.0	0.0	-2.052
Cd**	+2.88	0.0	0.0	-0.396
NH_4	0.0	-2.88	-1.226	-3.276
	NH_4	Cd**	Cd*	Pb

* Cadmium nitrate ** Cadmium chloride

(superscript*) signified in brackets:

$$\underset{(Na_c^* = 1.0)}{2Na_{(c)}} + Pb_{(s)} \rightleftharpoons 2Na_{(s)} + \underset{\left[\begin{array}{l} Pb_c^* = 0.5 \\ Na_c^* = 0.5 \end{array}\right]}{Pb_{(c)}} \quad \ldots\ldots 5.1.$$

$$\underset{(Na_c^* = 1.0)}{2Na_{(c)}} + Cd_{(s)} \rightleftharpoons 2Na_{(s)} + \underset{\left[\begin{array}{l} Cd_c^* = 0.33 \\ Na_c^* = 0.67 \end{array}\right]}{Cd_{(c)}} \quad \ldots\ldots 5.2.$$

Combining equations 5.1, 5.2

$$\underset{\left[\begin{array}{l} Pb_c^* = 0.5 \\ Na_c^* = 0.5 \end{array}\right]}{Pb_{(c)}} + Cd_{(s)} \leftrightharpoons Pb_{(s)} + \underset{\left[\begin{array}{l} Cd_c^* = 0.33 \\ Na_c^* = 0.67 \end{array}\right]}{Cd_{(c)}} \quad \ldots\ldots 5.3.$$

For these systems it has been assumed that the sodium mordenite is homoionic (i.e. $Na_c^* = 1.0$). In fact from the chemical analyses (table 4.2) potassium was found to be present as an exchangeable ion. However it does not exchange when the reactions 5.1 and 5.2 occur so these mordenite exchanges can be expressed in terms of sodium only.

Now consider secondly the exchange systems Pb/NH_4-MOR and Cd/NH_4-MOR for which reactions 5.4, and 5.5. can be written respectively

$$2NH_{4(c)} + Pb_{(s)} \rightleftharpoons 2NH_{4(s)} + Pb^{*}_{(c)} \quad \ldots\ldots 5.4.$$

$$\left\{ \begin{array}{l} (NH_4)^{*}_{c} = 0.83 \\ Na^{*}_{c} = 0.17 \end{array} \right\} \qquad \left\{ \begin{array}{l} Pb^{*}_{c} = 0.52 \\ (NH_4)^{*}_{c} = 0.31 \\ Na^{*}_{c} = 0.17 \end{array} \right\}$$

$$2NH_{4(c)} + Cd_{(s)} \rightleftharpoons 2NH_{4(s)} + Cd_{(c)} \quad \ldots\ldots 5.5.$$

$$\left\{ \begin{array}{l} (NH_4)^{*}_{c} = 0.83 \\ Na^{*}_{c} = 0.17 \end{array} \right\} \qquad \left\{ \begin{array}{l} Cd^{*}_{c} = 0.33 \\ (NH_4)^{*}_{c} = 0.50 \\ Na^{*}_{c} = 0.17 \end{array} \right\}$$

Combining 5.4 and 5.5. gives

$$Pb_{(c)} + Cd_{(s)} \rightleftharpoons Pb_{(s)} + Cd_{(c)} \quad \ldots\ldots 5.6.$$

$$\left[\begin{array}{l} Pb^{*}_{c} = 0.52 \\ (NH_4)^{*}_{c} = 0.31 \\ Na^{*}_{c} = 0.17 \end{array} \right] \qquad \left[\begin{array}{l} Cd^{*}_{c} = 0.33 \\ (NH_4)^{*}_{c} = 0.50 \\ Na^{*}_{c} = 0.17 \end{array} \right]$$

Comparing the equation 5.3 and 5.6 it is obvious that the system is not the same as that in 5.3, because of the different standard states. Hence the standard free energies predicted will be different. So care must be taken when applying the triangle rule to systems that are not fully exchangeable and also when the zeolite provided is not initially in a homoionic form, as in the case of the ammonium mordenite.

Using the triangle rule it is also possible to predict ΔG^{o} values for the NH_4/Na-MOR exchange and in this case compare it

with the experimental result (table 5.7.). Firstly the binary exchanges Pb/Na-MOR and Pb/NH_4-MOR were used to predict a NH_4/Na-MOR value:

$$2Na_{(c)} + Pb_{(s)} \rightleftharpoons 2Na_{(s)} + Pb_{(c)} \quad \ldots\ldots 5.7.$$

$(Na_c^* = 1.0)$ $\quad \{ Pb_s^* = 0.5 \; ; \; Na_c^* = 0.5 \}$

$$2NH_{4(c)} + Pb_{(s)} \rightleftharpoons 2NH_{4(s)} + Pb_{(c)} \quad \ldots\ldots 5.8.$$

$\{ (NH_4)_c^* = 0.83 \; ; \; Na_c^* = 0.17 \}$ $\quad \{ Pb_c^* = 0.49 \; ; \; (NH_4)_c^* = 0.34 \; ; \; Na_c^* = 0.17 \}$

Combining 5.7, 5.8 it is again seen that the two lead crystal phases are not in the same standard states and thus they cannot be eliminated to give the reaction

$$Na_{(c)} + NH_{4(s)} \rightleftharpoons Na_{(s)} + NH_{4(c)} \quad \ldots\ldots 5.9.$$

So in this case the ΔG^o value predicted for the NH_4/Na-MOR system would not be expected to be the same with the experimental, and in fact this is what is observed (table 5.7).

A similar situation can arise when prdiction for the system NH_4/Na-MOR are obtained using the binary systems Cd/Na-MOR and Cd/NH_4-MOR (table 5.8). The failure again is due to the fact that the two cadmium crystal phases are not in the same standard states.

Table 5.7. Experimental and Predicted ΔG° kJ (g equiv)$^{-1}$ Values for the system NH_4/Na-MOR from binary data for Pb/Na-MOR, Pb/NH_4-MOR.

Exchange System	Experimental	Triangle Rule
NH_4/Na-MOR	-4.59	-7.92

Table 5.8. Experimental and Predicted ΔG° kJ(g equiv)$^{-1}$ Values for the system NH_4/Na-MOR from binary data for Cd/Na-MOR, Cd/NH_4-MOR

Exchange System	Experimental	Triangle Rule
NH_4/Na-MOR	-4.59	-1.779

5.4.2. Exchanges with Clinoptilolite.

Experimental values for the thermodynamic parameters were calculated for the systems Pb/Na-CLI, Cd/Na-CLI and NH_4/Na-CLI. Tables 5.9, 5.10 give the values predicted by the triangle rule for K_a and ΔG° for the systems Cd/Pb-CLI and Pb/Cd-CLI but no experimental data exists which enables these calculations to be validated directly. The standard free energies obtained (+6.073 kJ(g equiv)$^{-1}$ when cadmium nitrate is in

solution compared to +6.57 kJ (g equiv)$^{-1}$ for cadmium chloride) indicates the overall very strong preference of clinoptilolite for the lead ion over cadmium. This was also confirmed when cadmium and lead were present together in a ternary system, Pb/Cd/Na-CLI (Fig.2 , Appendix II); lead is much the preferred ion to cadmium at all ion concentration ratios in the solution phase.

Table 5.9. Values of the Thermodynamic Equilibrium Constant K_a Calculated by the Triangle Rule.

Ion Initially In Solution	Na	Cd**	Cd*	Pb
Pb	21.87	203.7	137	1.0
Cd*	0.1598	1.0	1.0	0.00730
Cd**	0.1074	1.0	1.0	0.00491
Na	1.0	9.31	6.258	0.0457
	Na	Cd**	Cd*	Pb
	Ion Initially in Clinoptilolite			

Table 5.10 Standard Free Energies ΔG° (kJ(g equiv) Calculated by the Triangle Rule.

Ion Initially in Solution	Na	Cd**	Cd*	Pb
Pb	-3.809	-6.575	-6.073	0.0
Cd*	+2.264	0.0	0.0	+6.073
Cd**	+2.755	0.0	0.0	+6.575
Na	0.0	-2.755	-2.264	+3.809
	Na	Cd**	Cd*	Pb
	Ion Initially in Clinoptilolite			

*Cadmium nitrate
**Cadmium Chloride

Though for NH_4/Na-CLI exchange, K_a and ΔG° values were calculated experimentally, no prediction using this system was possible since the exchange involving both lead and cadmium with ammonium clinoptilolite were found to be ternary in nature.

5.4.3. Exchanges with Ferrierite.

The predicted free energy ΔG° for the system Cd/Pb/FER is 1.57 kJ(g equiv)$^{-1}$. This was derived using the experimental data for the exchange Pb/NH_4-FER and Cd/$NH_4(NO_3)$-FER. The exchange Pb/Na-FER was ternary in nature (section 4.2.6) so no predictions for the Cd/Pb-FER system using data obtained on sodium ferrierite were possible. This is in contrast to the case of mordenite, where two different ΔG° values were obtained for the system Cd/Pb-MOR and the values were shown to be dependent on whether sodium or ammonium mordenite was the initial material used to obtain the data.

The predicted free energy for the system Cd/Pb-FER indicates that preference is shown for the ion already in the zeolite (i.e. lead). From ternary exchange measurements involving the ions Pb^{2+}, Cd^{+2} and NH_4^+, the experimental results seen in Appendix II show that lead is indeed preferred over cadmium, so at least the triangle rule predicts the expected affinity trend even if uncertainties exist as to its absolute magnitude.

For the system NH_4/Na-FER the exchange was ternary in nature so thermodynamic parameters were not calculated. However predictions of relative selectivities using triangle rule were

possible from the binary data for the systems $Cd/Na(NO_3)$-FER $Cd/NH_4(NO_3)$-FER, $Cd/Na(Cl)$-FER, $Cd/NH_4(Cl)$-FER. The first set gave

$$\Delta G^{\circ} = -0.464 \text{ kJ(g equiv)}^{-1}$$ while the

second set gave

$$\Delta G^{\circ} = -0.992 \text{ kJ(g equiv)}^{-1}.$$

Theoretically the two cadmium salts should give identical values for the thermodynamic parameters, since corrections of the solution phase were carried out. In fact, although the binary exchange $Cd/Na(NO_3)$-FER and $Cd/Na(Cl)$-FER give the same $A_{c\ max}$ value the calculated thermodynamic parameters were not quite the same (table 4.10), due to the problems incurred during the best-fitting procedures employed on the isotherm data (see section 4.4.1).

5.4.4. Limitations of the Triangle Rule

From the results obtained through applying the triangle rule, it is evident that at least for the systems under examination, the rule is not reliable. Various factors can contribute to the limited use of the triangle rule, such as the partial exchange and the inability to obtain homoionic forms of the zeolite as starting material.

In the case of natural zeolites, all the exchanges involved gave maximum levels of exchange less than one, indicating partial exchange. Also different $A_{c\ max}$ values were obtained (table 4.8), so the systems were "normalized" to different degrees.

It follows that the triangle rule cannot be applied to partially exchanged systems whether synthetic or natural zeolites are used. Since partial exchange is the 'norm' with natural zeolites it is very dangerous to apply the triangle rule.

5.5. Practical Application of the Experimental Data.

The potential application of natural zeolites in the field of water treatment (such as the tertiary treatment of industrial and municipal waste waters) requires a careful and detailed examination of their properties before they can be adopted in such plants. The main factors to be considered are the exchange capacities of the materials and their selectivity for the ions to be removed. Also the time required for the effective removal of ions is important (section 3.13).

5.5.1. Exchange Capacities and Levels of Exchange.

The exchange capacities of the natural zeolites clinoptilolite, mordenite and ferrierite in the sodium and ammonium forms are summarized in table 4.7, with the data expressed in mequiv g^{-1}. This figure indicates the theoretical amount of cations that can be accommodated by a particular zeolite, but in practice most of the exchanges were only partial, which means that part of the theoretical (or intrinsic) exchange capacity cannot be used. Thus the "practical" exchange capacity is frequently less than the intrinsic, and in fact with the natural zeolites used here partial exchange was observed

in all systems with the single exception of the exchange of NH_4-CLI with lead. Partial phenomenon can in most cases be explained in terms of volume-steric or ion-sieve effects but in the case of natural zeolites, the impurities which are inevitably present may be a major reason for this behaviour especially if material is occluded in the zeolite channels. Purification can partly solve this problem (as for example the treatment with ammonium chloride to dissolve the calcite impurities[145]), but purification costs are likely to be high which in turn limits the industrial use of the low cost natural zeolites. Clinoptilolite and mordenite have very similar exchange capacities, and both were higher than that found for ferrierite. The sequence (in terms of "intrinsic" exchange capacities) is NH_4-CLI $\sim$ Na-CLI $\sim$ Na-MOR, NH_4-MOR >> Na-FER, NH_4-FER.

Though mordenite has this high intrinsic exchange capacity, in fact only half of the cations present in the zeolite can exchange with lead or cadmium at room temperature. Thus mordenite behaves in <u>practice</u> very similarly to ferrierite. Clinoptilolite (in either the sodium or ammonium forms) exchanges readily to high levels with both lead and cadmium, with ammonium clinoptilolite giving the highest exchange levels. However, these exchanges are ternary in nature due to sodium release along with the ammonium (section 4.2). Thus in terms of the "practical" exchange levels the order is NH_4-CLI > Na-CLI >> NH_4-MOR $\sim$ Na-MOR $\sim$ NH_4-FER $\sim$ Na-FER.

Even if a zeolite can accommodate large quantities of metal cations such as lead, cadmium or ammonium, no indication is given from exchange capacities alone as to how the mineral will behave in the presence of differing concentrations of the competing ions and also as it gets loaded with these ions. This can only be achieved by examining the separation factors or practical selectivities (section 2.1) for each individual system and also the thermodynamic parameters that have been calculated.

5.5.2. Thermodynamic Affinities and Separation Factors.

The thermodynamic parameters K_a and ΔG° obtained refer to the system as a whole, and therefore give an indication of the overall preference that a given zeolite displays for a particular ion. This is a rigorous approach and provided sufficient activity coefficient data are available for both phases for the system concerned, it can be used to predict the behaviour of the system under widely differing conditions of temperatures, pressure or total external solution concentration (section 2.5).

In the absence of activity coefficient data (the unavailability of which can frequently arise if the system cannot be treated using rigorous thermodynamic procedures) the separation factors (or practical selectivities)give actual information on the behaviour of the system at any values of A_s (equivalent fraction of the counter ion A in the solution phase) or A_c (equivalent fraction of the ion A in the zeolite) but only at

the (experimental) given concentration, temperature and pressure. These practical selectivities can be obtained from the experimental isotherm data and they have often been referred to as the "unnormalized selectivity quotients α". In section 2.1, it was shown that for the zeolite to be selective for an ion $A^{z_A^+}$ over the ion $B^{z_B^+}$ it must follow that α be > z_A/z_B. When $\alpha = z_A/z_B$, the zeolite shows no preference, whereas if α is $< z_A/z_B$ then the zeolite shows preference of the ion initially present. Using these values, a detailed examination of each system follows.

Figures (4.44-4.46) indicate how the α values change as the concentration of ion $A^{z_A^+}$ increases in solution.

Consider the exchange of Na-CLI with lead, cadmium and ammonium ions. The thermodynamic affinity follows the sequence NH_4 > Pb > Na > Cd, indicating the overall preference of sodium clinoptilolite for the ammonium ion, and this sequence is indeed observed when the α values are examined at all solution concentrations. The same pattern is followed in the ternary exchanges, when lead ammonium and cadmium are present together in the solution (Fig 1., Appendix II). The ammonium ion is preferred to the other ions. Nevertheless, high amounts of lead are exchanged into the zeolite at low ammonium concentrations. As the ammonium concentration in solution is increased, the zeolite shows its higher preference towards this ion. It is clear that clinoptilolite can indeed be employed for water treatment containing significant quantities of lead and ammonium together and still remove both of them

effectively. The situation will not change if sodium is present along with lead and ammonium ions (Appendix II).

Considering next the case when both heavy metals and ammonium ions are present, clinoptilolite can remove some cadmium along with lead and ammonium, the quantity removed depends very much on the nature of the co-ions in solution. Higher quantities are removed if the co-ion is nitrate than chloride. This has great significance in the context of effluent treatment as the effluent water may have initially been drawn from the sea, rather than a fresh water source.

Examining next the system NH_4/Na-MOR, the thermodynamic treatment clearly indicates that the ammonium is preferred overall to sodium (ΔG° = -4.59 kJ(g equiv)$^{-1}$). This preference is also exhibited when the α values are considered for nearly all concentrations of ammonium in solution up to concentrations of 5 x 10^{-3} mol dm^{-3} (Fig.4.45). The same pattern occurs with the Pb/Na-MOR system (Fig.4.44). In contrast, cadmium is never preferred at any solution concentration (Fig.4.46). The α values are somewhat higher if nitrate is the co-ion rather than chloride, and this difference is sharpest when the concentration of cadmium in solution is low.

From the ternary studies involving the systems Pb/Cd/Na-MOR or Pb/Cd/NH_4-MOR, the presence of ammonium is seen to inhibit the exchange of lead and cadmium (Appendix II).

This is in contrast to the case of clinoptilolite, and indicates that mordenite cannot be employed for effective water treat-

ment if both lead and ammonium are present together in high quantities. If instead of the ammonium ion, sodium is the competitive counter ion, then the zeolite behaves in a quite different manner. Though sodium is still the preferred ion, high quantities of lead can be removed by mordenite. The removal of cadmium is still low but nevertheless higher than in the presence of ammonium ion. These trends suggest that that while mordenite can be used in the treatment of fresh water for the effective removal of ammonium (and not for lead and/or cadmium), it will be much more effective for the removal of the heavy metals in saline water. In contrast clinoptilolite could be used for both cases.

Ferrierite behaves in a completely different manner. When sodium ferrierite was exchanged with lead, the system was found to be ternary due to potassium released along with the sodium. The same situation was observed when ammonium was the counter ion. So for these two systems no thermodynamic parameters were calculated. The exchange of NH_4-FER with lead and cadmium gave highly positive ΔG° values, lead being preferred to cadmium.

Though for the system Pb/NH_4-FER the overall free energy indicates that ammonium is preferred to lead, the α values do not reflect this trend (Fig. 4.45). Ammonium ferrierite is quite selective for lead solution concentrations up to about 10^{-2} mol dm^{-3}, but at higher concentrations the zeolite is not selective. So ferrierite could be used to remove lead effectively only if the right external solution conditions

happened to exist. From these results, it appears that ferrierite can only have a limited application for lead and cadmium removal from effluents.

5.6. Prediction of Ternary Equilibria From Binary Exchange Data.

Elprince and Babcock[127] developed a method for the prediction of equilibria involving three exchange ions using binary isotherm data. An attempt was therefore made to predict by this approach the ion exchange equilibria of ternary zeolite systems from the binary data obtained in this work.

In this approach, the zeolite phase activity coefficients f_A, f_B (which are obtained from the binary ion exchange isotherm) were used to calculate the interaction energy terms Λ_{AB}, Λ_{BA} (see section 2.2.2.1). The activity coefficients f_A, f_B can be expressed as functions of these terms (see equations 2.74, 2.75). For this purpose, an iterative scheme was used to solve the above equations. The systems chosen for this study were $Pb/NH_4/Na$-MOR and $Cd/NH_4/Na$-MOR.

Considering first the sodium ammonium exchange in mordenite (NH_4/Na-MOR), it was found to be possible to obtain values for the interaction energy terms Λ_{NaNH_4}, Λ_{NH_4Na}, but unfortunately these values proved not to be constant for different sets of values of the activity coefficients f_{Na}, f_{NH_4}. This is in contrast to what was found by Elprince abd Babcock for clays[127]. The results obtained are shown graphically in Fig.5.6, which shows how the Λ_{Na,NH_4}, Λ_{NH_4Na} terms vary

as the ammonium content of the zeolite is increased. For high levels of exchange it was at least possible to obtain unique values for the Λ terms, but at low exchange levels (i.e. $(NH_4)_c < 0.5$) there was no common solution for equations 2.74, 2.75, and Λ could not be evaluated. In addition, in some cases more than one value for the intersect energy was obtained for a particular $(NH_4)_c$ value in mordenite (e,g, $(NH_4)_c = 0.85$). This indicates that the curves corresponding to equations 2.74, 2.75 interact at more than one point (Fig. 5.7). It is of course impossible then to decide which solution to take as correct. Due to these problems it appears not to be possible to use the data obtained for the interaction terms to predict the activity coefficients for the ternary system.

The variability of the Λ terms for the binary ion exchange system NH_4/Na-MOR is not the only draw-back. More severe problems are encountered when the same iterative procedures were applied to the systems Pb/NH_4-MOR and Cd/NH_4-MOR. No unique solutions exist for the Λ terms because the values are asymptotic to each other.

It appears that the approach of Elprince and Babcock[127] cannot be used for zeolites for reasons explained below. Elprince and Babcock applied this procedure to clays, which are layer structures, and the exchanging cations will be found between these layers, so the excess free energy term $(\lambda_{AB} - \lambda_{AA})$ in the equation 2.72 might to a first approximation be considered independent of the exchanger phase composition. This is in effect the assumption made by Guggenheim in his early model

for solution phase non-ideality[123]. But in the case of zeolites, the situation is different because of the existence of distinct site sets in the lattice. The activity coefficients f_A, f_B for a binary exchange, obtained using the Gibbs-Duhem equation (section 2.2.2.) are the phenomenological ones; in fact f_A, f_B are more complicated functions of both the population of ions and their departure from ideality within each site set. For n sets of sites, the thermodyanmic equilibrium constant is[151]

$$K_a = \prod_{i=1}^{n} \left[K_i \right]^{X_i} \qquad \ldots\ldots 5.10$$

where

$$X_i = \left[\frac{z_A m_{A\,i} + z_B m_{Bi}}{\prod_{i=1}^{n} \left[z_A m_{A\,i} + z_B m_{B\,i} \right]} \right] \qquad \ldots\ldots 5.11$$

and $m_{A,i}$, $m_{B,i}$ are the concentrations (mol kg^{-1}) of ions A and B respectively in the ith set site; also K_i refers to the ith set.

Equation 5.10 can be expanded[150] and in combination with equation 2.98 can give

$$K_a = \frac{m_B^{z_A}}{m_A^{z_B}} \Gamma \prod_{i=1}^{n} \left(\frac{A_{c,i}^{z_B} f_{A,i}^{z_B}}{B_{c,i}^{z_A} f_{B,i}^{z_A}} \right)^{X_i} \qquad \ldots\ldots 5.12$$

where $f_{A,i}$, $f_{B,i}$ are terms describing the departure from ideality of ions $A^{z_A^+}$ and $B^{z_B^+}$ in the ith sub-lattice, and

are related to f_A, f_B by

$$\frac{f_A^{z_B}}{f_B^{z_A}} = \prod_{i=1}^{n}\left(\frac{f_{A,i}^{z_B}}{f_{B,i}^{z_A}}\right)^{X_i} \qquad \ldots\ldots 5.13$$

So each site set can have its own excess energy term $(\lambda_{AB} - \lambda_{AA})_i$ and the term $\Lambda_{AB,i}$ will not be the same for all site sets, but also its value will change with the composition of the zeolite phase.

It is evident that binary data cannot be used to predict ion exchange equilibria for ternary systems involving zeolites. This can, however, be achieved by using a rigorous model for the ternary exchange. This requires a determination of the ternary exchange equilibrium over the whole surface of a ternary composition diagram. Such a rigorous model has been developed recently which covers both the solution[124] and crystal phases[126]. However, insufficient data were obtained on the ternary equilibria in this work for this model to be applied.

5.7. General Conclusion

From the binary and ternary exchange studies carried out, it is concluded that clinoptilolite can remove lead and cadmium effectively in either fresh or saline waters. Mordenite can be employed for the effective removal of lead and cadmium in saline waters. However, the presence of ammonium depresses

the metal uptake. Also, the amount of cadmium removed is very much dependent on the co-ions present. Higher quantities of cadmium can exchange if the co-ion is nitrate rather than chloride. For ferrierite, the overall affinities indicate that the mineral shows no preference for lead or cadmium. When the separation factors were examined, it was found that under certain special conditions, ferrierite can remove these metals, but in contrast to clinoptilolite and mordenite, its application in the field of waste water treatment must be very limited.

The thermodynamic parameters calculated for the binary exchange systems were used to predict affinities for other systems by means of the triangle rule. It was found that this method cannot be used for exchanges that have different $A_{c\ max}$ values or when the initial zeolite employed is not in a homoionic form. This is because both factors result in different standard states . Since with natural zeolites, partial exchange and non-homoionic forms are the 'norm', it follows that the use of the triangle rule is inadvisable.

The zeolite activity coefficients obtained from a rigorous thermodynamic treatment of the binary exchange equilibria were used to predict the corresponding activity coefficients for a ternary exchange using Elprince and Babcock's method which was originally developed for clays. It was proved that this approach cannot be applied to zeolites, due to the existence of different site sets.

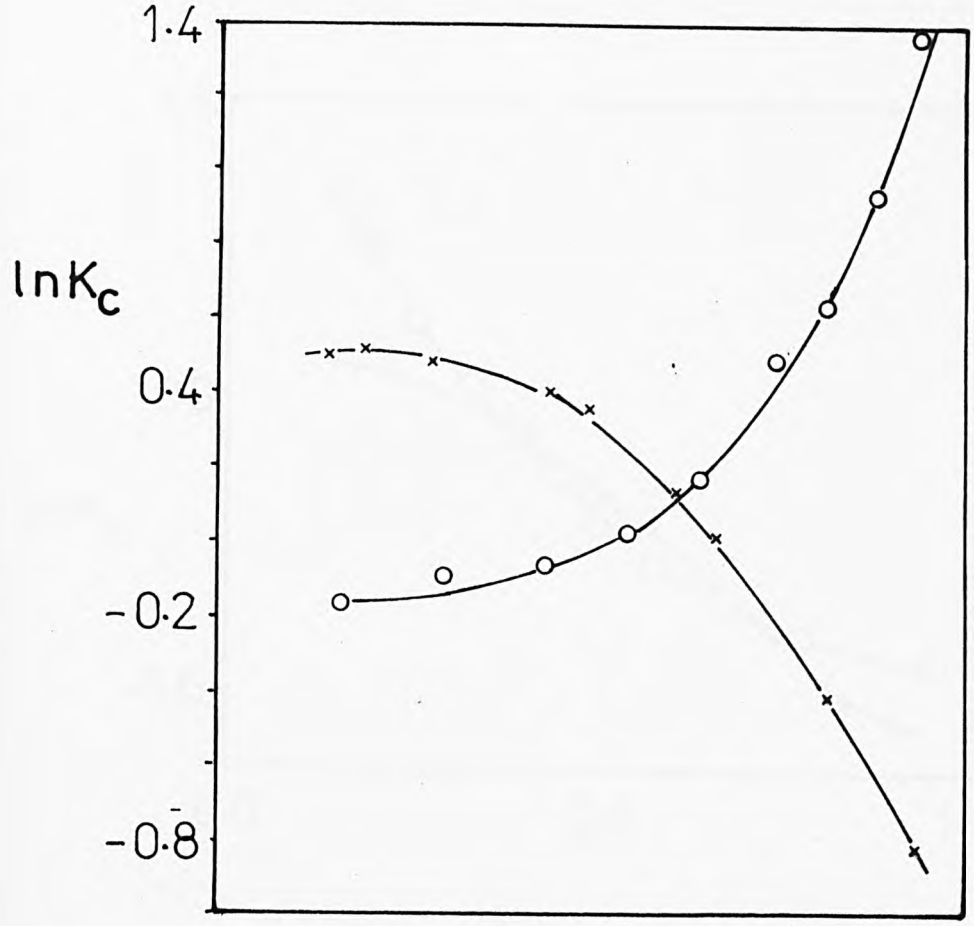

Kielland Plots for the Systems

Cd/Na(NO_3)-MOR o

Cd/Na(Cl)-MOR •

FIG. 5.1

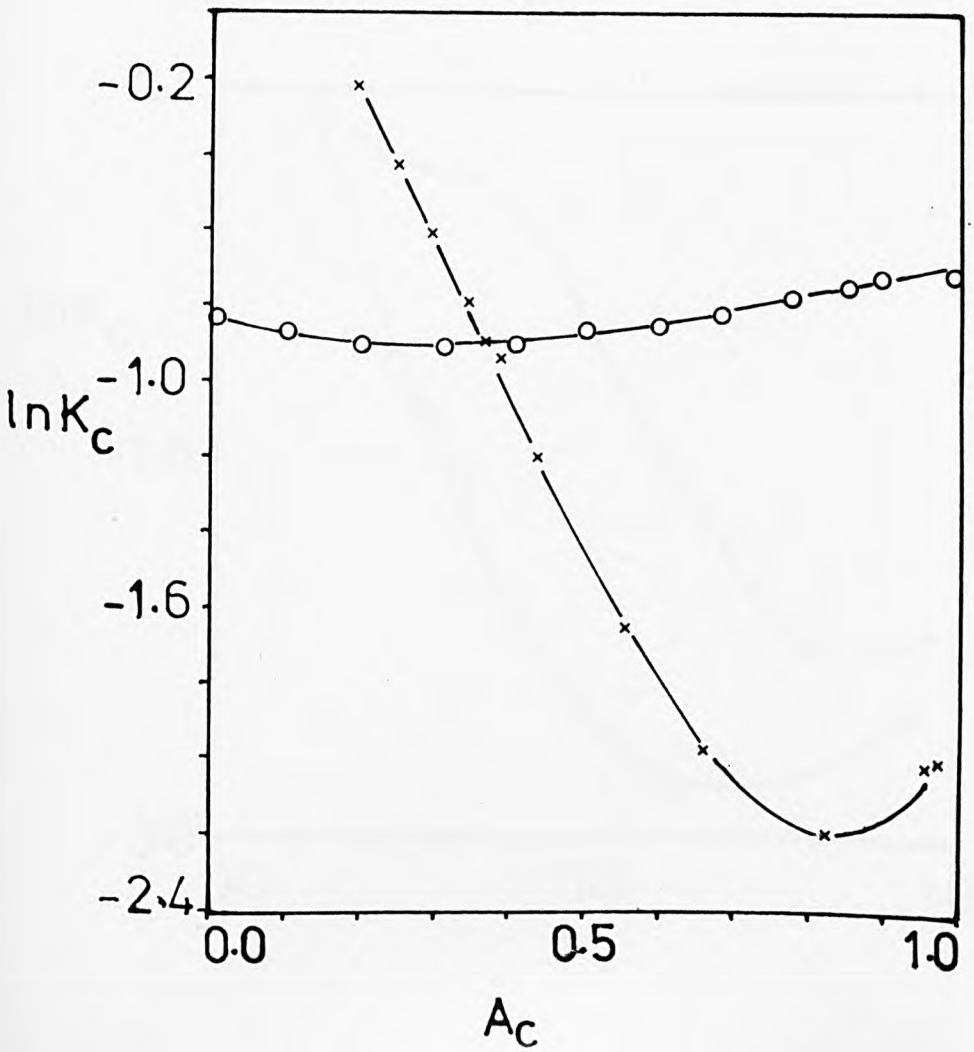

Kielland Plots for the Systems

Cd/Na(Cl)-CLI •

Cd/Na(NO_3)-CLI o

FIG. 5.2

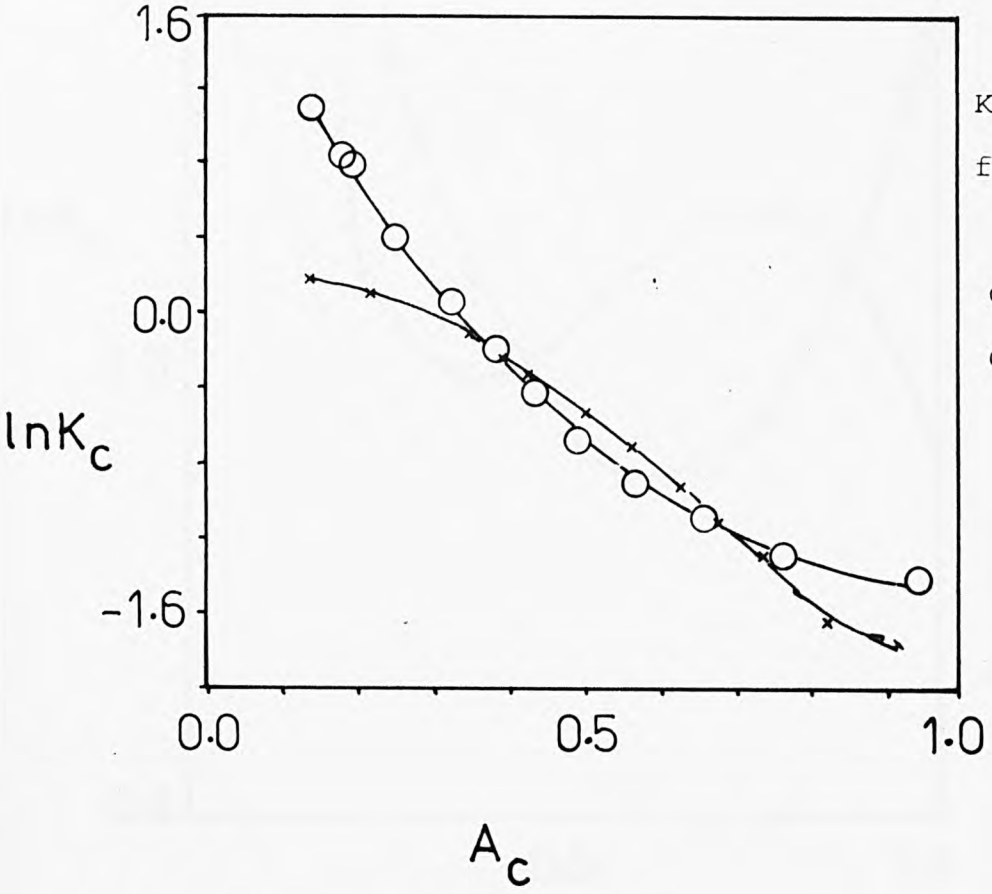

Kielland Plots
for the Systems

Cd/Na(Cl)-FER o

Cd/Na(NO_3)-FER +

FIG. 5.3

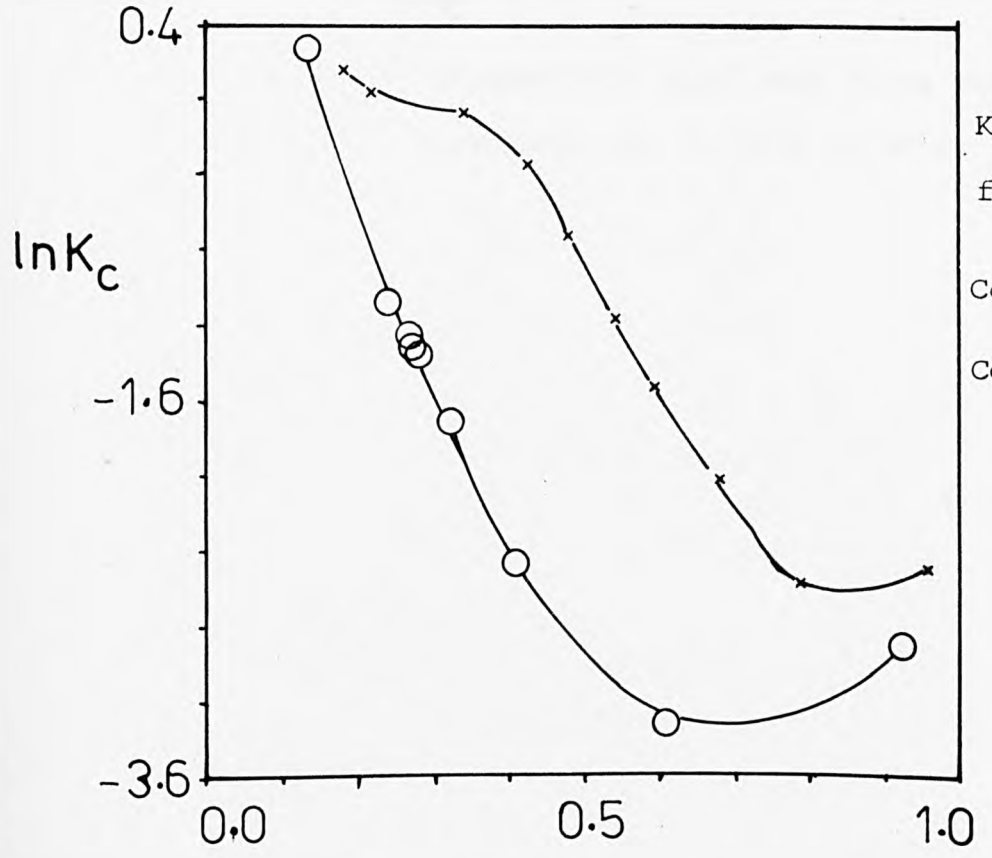

Kielland Plots
for the Systems

Cd/NH_4(Cl)-FER o

Cd/NH_4(NO_3)-FER +

FIG. 5.4

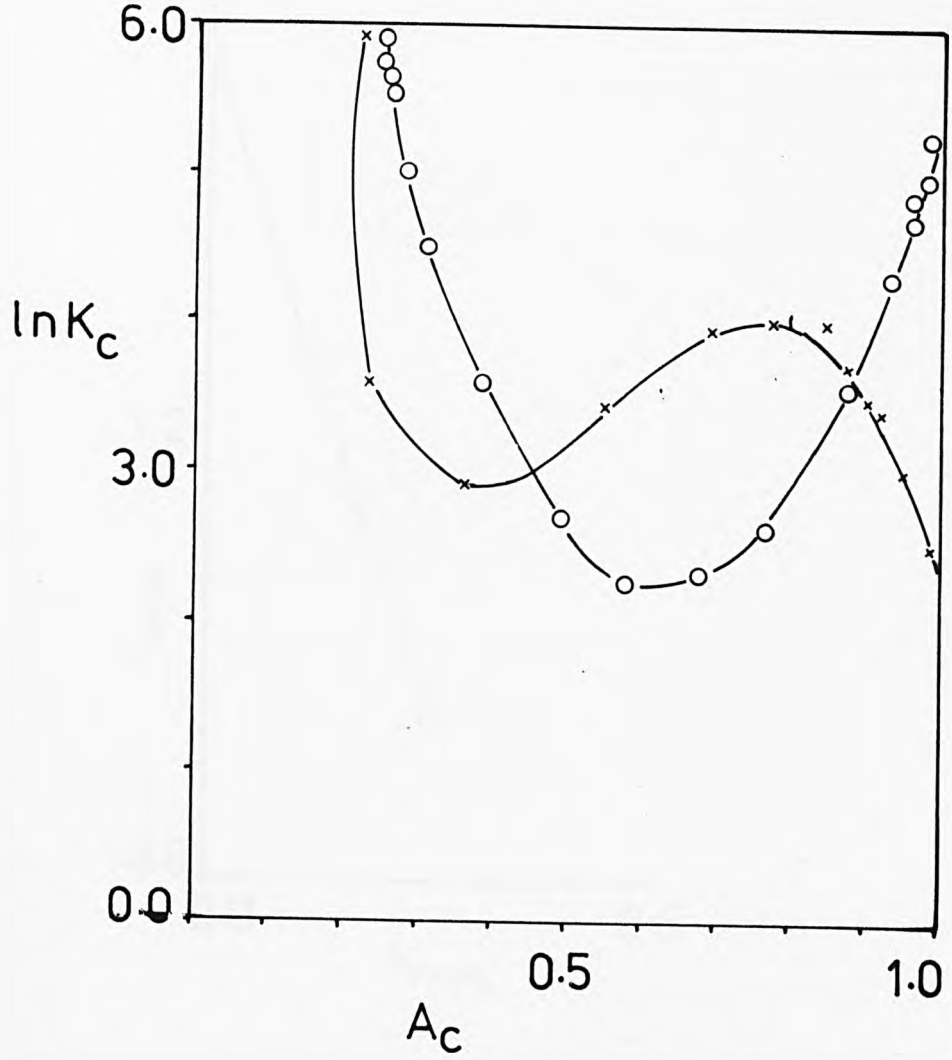

Figure 5.5 Kielland Plots for Pb/Na-MOR at 0.1N o ,0.5N ×.

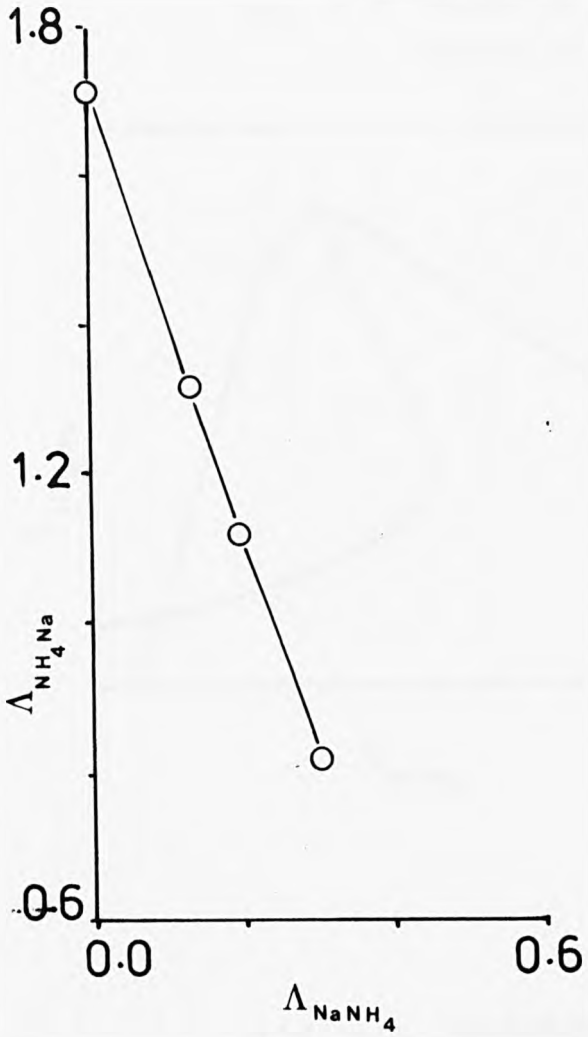

NH_4 (C)	Λ_{NH_4Na}	Λ_{NaNH_4}
0.982	0.816	0.305
0.865	1.11	0.218
0.715	1.31	0.135
0.554	1.72	-0.002

FIG.5.6 . Plot of the interaction energy terms $\Lambda_{Na\ NH_4}$ $\Lambda_{NH_4\ Na}$ as NH_4(c) varies.

FIG. 5.7 Plots of the interaction energy terms at $NH_4(C)=0.85$.

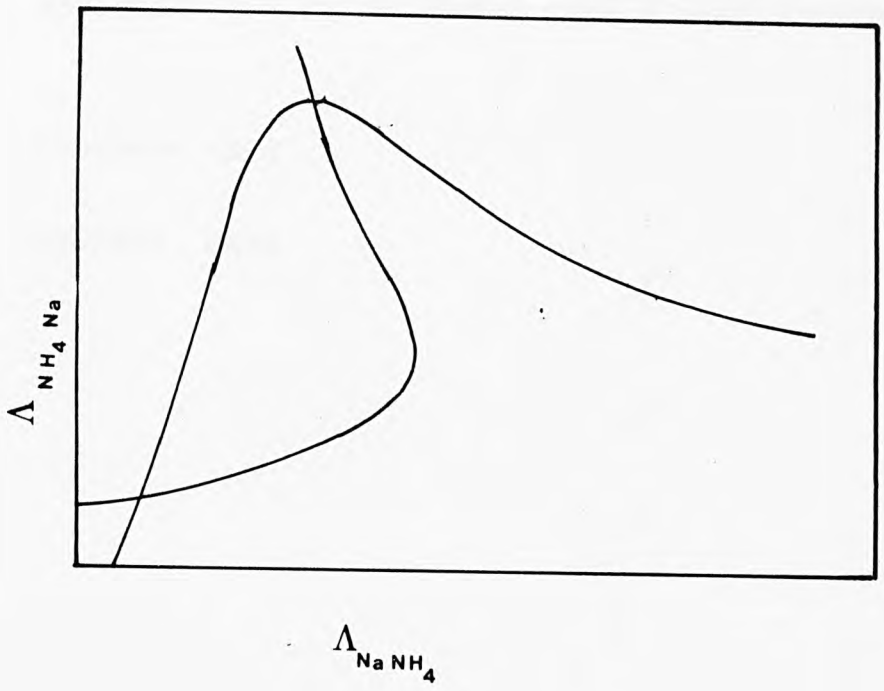

FIG. 5.8 Asymptotic values for the interaction energy terms at $NH_4(C)=0.5$.

APPENDIX I : EXPERIMENTAL DATA BINARY SYSTEMS

Isotherm data

Derived data

Isotherm Data : Sodium CLI

$Pb_{(s)}$	$Pb_{(c)}$	$Cd^{(2)}_{(s)}$	$Cd_{(c)}$
1.000	0.795	1.000	0.656
0.881	0.795	0.930	0.420
0.690	0.795	0.840	0.390
0.500	0.735	0.770	0.370
0.308	0.640	0.650	0.330
0.105	0.457	0.470	0.220
0.888	0.795	0.370	0.200
0.798	0.795	0.280	0.130
0.700	0.795	0.190	0.100
0.600	0.770	0.090	0.070
0.500	0.740	0.555	0.275
0.410	0.700	0.083	0.050
0.314	0.640	0.990	0.600
0.220	0.580	0.985	0.540
0.130	0.510	0.526	0.246
0.048	0.350	0.472	0.232
0.470	0.736	0.407	0.208
0.357	0.680	0.350	0.170
0.300	0.657	0.290	0.160
0.070	0.410	0.570	0.280
0.0174	0.284	0.965	0.470
0.017	0.028		

$NH_4{}_{(s)}$	$NH_4{}_{(c)}$	$Cd^{(1)}_{(s)}$	$Cd_{(c)}$
1.000	0.765	1.000	0.656
0.896	0.712	0.916	0.630
0.785	0.680	0.832	0.533
0.755	0.670	0.740	0.524
0.690	0.640	0.642	0.434
0.640	0.620	0.550	0.397
0.540	0.590	0.454	0.350
0.474	0.550	0.366	0.259
0.271	0.482	0.272	0.220
0.139	0.419	0.180	0.153
0.060	0.266	0.086	0.276
0.010	0.084	0.460	0.320
0.025	0.166	0.389	0.280
0.090	0.350	0.301	0.220
0.270	0.484	0.235	0.185
0.200	0.455		
0.610	0.640		
0.940	0.740		
0.015	0.097		
0.000	0.000		
0.400	0.530		
0.335	0.515		

(1) Cadmium nitrate
(2) Cadmium chloride

Isotherm Data : Sodium MOR

$Pb_{(s)}$	$Pb_{(c)}$	$Cd^{(1)}_{(s)}$	$Cd_{(c)}$
1.000	0.490	1.000	0.334
0.936	0.490	0.960	0.330
0.842	0.490	0.868	0.321
0.739	0.490	0.758	0.282
0.641	0.485	0.660	0.244
0.550	0.480	0.576	0.224
0.452	0.460	0.475	0.181
0.350	0.459	0.377	0.157
0.253	0.430	0.279	0.125
0.158	0.380	0.184	0.079
0.070	0.290	0.090	0.244
0.790	0.490	0.535	0.205
0.285	0.445	0.410	0.171
0.076	0.283	0.310	
0.004	0.219		
0.001	0.145		
0.00069	0.117		
0.000018	0.060		
0.507	0.467		
0.449	0.460		
0.390	0.460		

$NH_4{}_{(s)}$	$NH_4{}_{(c)}$	$Cd^{(2)}_{(s)}$	$Cd_{(c)}$
1.000	0.501	1.000	0.334
0.928	0.501	0.952	0.292
0.874	0.501	0.850	0.267
0.813	0.501	0.760	0.249
0.706	0.490	0.670	0.235
0.820	0.501	0.570	0.215
0.539	0.480	0.480	0.172
0.355	0.445	0.360	0.164
0.170	0.257	0.290	0.125
0.010	0.021	0.190	0.072
0.644	0.489	0.100	0.046
0.541	0.480	0.860	0.273
0.248	0.336	0.133	0.066
0.150	0.268	0.592	0.176
0.134	0.235	0.352	0.154
0.022	0.040	0.411	0.178
0.370	0.460		
0.060	0.141		

(1) Cadmium nitrate

(2) Cadmium chloride

Isotherm Data : Sodium FER

$Pb_{(s)}$	$Pb_{(c)}$	$NH_4{}_{(s)}$	$NH_4{}_{(c)}$
1.000	0.506	1.000	0.499
0.950	0.490	0.944	0.499
0.765	0.490	0.763	0.479
0.557	0.480	0.562	0.467
0.361	0.456	0.366	0.448
0.159	0.439	0.161	0.370
0.953	0.491	0.290	0.423
0.860	0.485	0.020	0.110
0.764	0.485	0.554	0.464
0.665	0.480	0.043	0.194
0.563	0.480	0.344	0.445
0.458	0.476	0.851	0.485
0.364	0.451	0.130	0.330
0.266	0.443	0.100	0.280
0.165	0.440	0.225	0.403
0.070	0.385	0.250	0.405
0.031	0.250	0.315	0.435
0.010	0.225	0.465	0.455
0.004	0.165		
0.002	0.130		
0.0005	0.0662		
0.435	0.470		
0.277	0.450		
0.130	0.430		

$Cd^{(1)}_{(s)}$	$Cd_{(c)}$	$Cd^{(2)}_{(s)}$	$Cd_{(c)}$
1.000	0.339	1.000	0.339
0.948	0.328	0.970	0.323
0.858	0.290	0.870	0.271
0.768	0.265	0.780	0.239
0.669	0.239	0.690	0.198
0.576	0.198	0.590	0.167
0.481	0.177	0.490	0.156
0.383	0.158	0.390	0.135
0.285	0.148	0.290	0.104
0.186	0.128	0.190	0.083
0.090	0.093	0.090	0.073
0.040	0.082	0.050	0.052
0.615	0.219	0.598	0.156
0.430	0.177	0.470	0.152
0.230	0.135	0.415	0.098
		0.100	0.094

(1) Cadmium nitrate

(2) Cadmium chloride

Isotherm Data : Ammonium CLI

$Pb_{(s)}$	$Pb_{(c)}$	$Cd^{(2)}_{(s)}$	$Cd_{(c)}$
1.000	1.000	1.000	0.810
0.950	0.910	0.993	0.740
0.890	0.839	0.990	0.700
0.800	0.751	0.985	0.580
0.710	0.680	0.980	0.490
0.620	0.630	0.970	0.430
0.530	0.550	0.953	0.368
0.430	0.504	0.867	0.240
0.340	0.456	0.777	0.160
0.250	0.435	0.687	0.130
0.152	0.350	0.588	0.120
0.070	0.256	0.491	0.110
0.059	0.157	0.395	0.095
0.0304	0.146	0.294	0.090
0.0163	0.116	0.196	0.050
0.0076	0.103	0.096	0.047
0.662	0.710	0.603	0.081
0.558	0.661	0.539	0.075
0.498	0.628	0.474	0.070
0.439	0.581	0.417	0.065
0.385	0.526	0.356	0.063
		0.296	0.050

$Cd^{(1)}_{(s)}$	$Cd_{(c)}$
1.000	0.810
0.985	0.740
0.980	0.705
0.950	0.580
0.930	0.505
0.874	0.443
0.782	0.360
0.678	0.300
0.607	0.251
0.489	0.220
0.395	0.177
0.294	0.133
0.196	0.0885
0.094	0.0592

(1) Cadmium nitrate

(2) Cadmium chloride

Isotherm Data : Ammonium MOR

$Pb_{(s)}$	$Pb_{(c)}$	$Cd^{(1)}_{(s)}$	$Cd_{(c)}$
1.000	0.517	1.000	0.327
0.950	0.416	0.978	0.317
0.850	0.361	0.858	0.317
0.761	0.290	0.788	0.303
0.669	0.255	0.682	0.275
0.560	0.246	0.501	0.261
0.470	0.213	0.491	0.220
0.374	0.204	0.397	0.188
0.285	0.145	0.294	0.142
0.184	0.127	0.196	0.121
0.090	0.102	0.096	0.062
0.086	0.063	0.635	0.275
0.078	0.056	0.450	0.215
0.063	0.056	0.243	0.132
0.056	0.054		

$Cd^{(2)}_{(s)}$	$Cd_{(c)}$
1.000	0.327
0.970	0.271
0.880	0.186
0.780	0.166
0.690	0.137
0.590	0.117
0.500	0.100
0.400	0.095
0.300	0.085
0.200	0.070
0.100	0.040
0.661	0.117
0.472	0.110
0.415	0.113
0.354	0.113

(1) Cadmium nitrate

(2) Cadmium chloride

Isotherm Data : Ammonium FER

$Cd_{(s)}$ (1)	$Cd_{(c)}$	$Cd_{(s)}$ (2)	$Cd_{(c)}$
1.000	0.280	1.000	0.280
0.983	0.277	0.980	0.198
0.890	0.256	0.880	0.139
0.798	0.217	0.790	0.097
0.696	0.165	0.700	0.080
0.599	0.147	0.590	0.096
0.498	0.147	0.500	0.080
0.399	0.147	0.400	0.096
0.296	0.128	0.300	0.058
0.196	0.091	0.199	0.039
0.096	0.073	0.098	0.034
0.330	0.141	0.601	0.071
0.570	0.150	0.535	0.092

$Pb_{(s)}$	$Pb_{(c)}$
1.000	0.486
0.949	0.460
0.853	0.435
0.761	0.390
0.667	0.355
0.567	0.325
0.470	0.285
0.370	0.263
0.279	0.215
0.180	0.180
0.088	0.130
0.068	0.080
0.054	0.0784
0.047	0.073
0.583	0.345
0.458	0.310
0.400	0.302
0.346	0.285
0.285	0.213

(1) Cadmium nitrate

(2) Cadmium chloride

Derived Data : Pb/Na-CLI

A_c	α^N	α^{UN}	m_A	m_B	f_A	f_B	$\ln K_c$
0.960	6.45	0.914	0.0441	0.0119	0.984	1.450	3.843
0.954	18.72	2.963	0.0345	0.0310	0.985	1.345	3.694
0.941	31.90	6.220	0.0250	0.0500	0.989	1.143	3.365
0.828	21.55	8.936	0.0154	0.0692	1.058	0.500	1.645
0.495	16.69	11.262	0.0053	0.0895	0.287	0.818	3.933
0.960	6.49	0.922	0.0440	0.0120	0.984	1.446	3.839
0.989	44.09	1.963	0.0399	0.0202	0.991	2.229	4.698
0.958	30.08	4.464	0.0300	0.0400	0.984	1.406	3.783
0.920	23.08	5.692	0.0250	0.0500	0.999	0.914	2.905
0.871	19.35	6.716	0.0205	0.0590	1.035	0.615	2.077
0.833	21.87	8.880	0.0157	0.0686	0.960	0.512	1.690
0.716	17.90	9.633	0.0110	0.0780	0.721	0.450	1.531
0.634	23.21	13.931	0.0065	0.0870	0.172	0.532	2.148
0.435	30.57	21.359	0.0024	0.0952	1.003	0.965	4.772
0.915	24.36	6.288	0.0235	0.0530	1.051	0.871	2.805
0.846	19.73	7.655	0.0179	0.0643	1.060	0.538	1.797
0.817	20.84	8.939	0.0150	0.0700	0.324	0.484	1.576
0.510	27.64	18.465	0.0035	0.0930	0.085	0.781	3.718
0.353	61.67	44.798	0.0009	0.0982	0.170	1.137	5.809
0.035	4.17	3.331	0.0009	0.0983	0.092	1.025	4.907

Derived Data : Pb/Na-MOR

A_c	α^N	α^{UN}	m_A	m_B	f_A	f_B	$\ln K_c$
0.961	3.37	0.13	0.047	0.0064	0.974	1.730	4.873
0.988	29.95	0.36	0.042	0.0158	0.989	2.185	5.324
0.988	56.37	0.68	0.037	0.0261	0.989	2.185	5.324
0.978	48.77	1.06	0.032	0.0359	0.982	1.995	5.149
0.967	48.67	1.51	0.0275	0.0450	0.977	1.828	4.980
0.982	130.91	2.30	0.0226	0.0548	0.985	2.072	5.223
0.925	45.90	3.15	0.0175	0.0650	0.970	1.312	4.323
0.867	38.39	4.46	0.0127	0.0747	0.989	0.906	3.563
0.766	34.87	6.53	0.0079	0.0842	1.053	0.593	2.652
0.585	37.38	10.85	0.0035	0.0930	0.965	0.472	2.286
0.988	42.43	0.51	0.0395	0.0210	0.989	2.185	5.324
0.897	43.66	4.02	0.0143	0.0715	0.976	1.084	3.935
0.494	23.76	7.90	0.0038	0.0924	0.721	0.506	2.715
0.260	189.18	79.75	0.0002	0.0996	0.083	0.773	5.720
0.251	543.98	230.92	0.0001	0.0999	0.072	0.786	5.891
0.249	959.99	408.14	0.0000	0.0999	0.070	0.789	5.929
0.247	-	-	0.0000	0.1000	0.068	0.793	5.977
0.986	136.38	1.86	0.0254	0.0493	0.988	2.151	5.295
0.981	128.71	2.33	0.0225	0.0551	0.985	2.063	5.214
0.963	82.29	2.86	0.0195	0.0610	0.975	1.766	4.913

Derived Data : Pb/NH_4-MOR

A_c	α^N	α^{UN}	m_A	m_B	f_A	f_B	$\ln K_c$
0.880	0.771	0.086	0.0475	0.005	0.930	0.942	-2.700
0.695	0.802	0.195	0.0425	0.015	0.769	0.824	-2.778
0.581	0.871	0.266	0.0381	0.024	0.576	0.906	-2.299
0.502	0.998	0.343	0.0335	0.033	0.433	0.984	-1.849
0.444	1.252	0.462	0.0280	0.044	0.338	1.040	-1.491
0.410	1.566	0.600	0.0235	0.053	0.291	1.068	-1.288
0.375	2.010	0.797	0.0187	0.063	0.249	1.091	-1.087
0.332	2.498	1.030	0.0143	0.072	0.205	1.113	-0.857
0.257	3.074	1.348	0.0092	0.082	0.152	1.125	-0.532
0.149	3.536	1.670	0.0045	0.091	0.116	1.090	-0.326
0.143	3.552	1.683	0.0043	0.091	0.115	1.087	-0.326
0.132	3.582	1.710	0.0039	0.092	0.114	1.080	-0.331
0.109	3.634	1.758	0.0032	0.094	0.114	1.066	-0.356
0.098	3.653	1.777	0.0028	0.094	0.115	1.060	-0.375

Derived Data : Pb/NH_4-FER

A_c	α^N	α^{UN}	m_A	m_B	f_A	f_B	$\ln K_c$
0.943	1.776	0.093	0.048	0.005	0.936	0.919	-1.253
0.856	2.040	0.250	0.043	0.015	0.820	1.074	-0.808
0.790	2.364	0.398	0.038	0.024	0.732	1.163	-0.536
0.735	2.765	0.564	0.033	0.033	0.662	1.218	-0.343
0.680	3.250	0.766	0.028	0.043	0.599	1.253	-0.186
0.624	3.741	0.996	0.024	0.053	0.540	1.272	-0.052
0.553	4.219	1.271	0.019	0.063	0.478	1.276	0.076
0.471	4.603	1.555	0.014	0.072	0.419	1.256	0.176
0.354	4.989	1.916	0.009	0.082	0.359	1.201	0.242
0.212	5.568	2.405	0.004	0.091	0.314	1.118	0.232
0.176	5.854	2.593	0.003	0.093	0.306	1.097	0.218
0.150	6.173	2.782	0.003	0.095	0.302	1.081	0.206
0.136	6.402	2.910	0.002	0.095	0.299	1.074	0.199
0.689	3.169	0.731	0.029	0.042	0.608	1.248	-0.209
0.616	3.800	1.027	0.023	0.054	0.533	1.274	-0.036
0.576	4.081	1.184	0.020	0.060	0.497	1.277	0.039
0.534	4.326	1.342	0.017	0.065	0.462	1.273	0.104
0.477	4.580	1.535	0.014	0.072	0.423	1.258	0.170

Derived Data : $Cd^{(1)}$ /Na-CLI

A_C	α^N	α^{UN}	m_A	m_B	f_A	f_B	$\ln K_C$
0.929	2.413	0.287	0.0458	0.0084	0.932	1.663	-0.746
0.857	2.411	0.519	0.0416	0.0168	0.868	1.593	-0.762
0.774	2.410	0.727	0.0370	0.0260	0.803	1.514	-0.785
0.684	2.410	0.908	0.0321	0.0358	0.739	1.432	-0.813
0.596	2.413	1.052	0.0275	0.0450	0.684	1.359	-0.841
0.502	2.419	1.181	0.0227	0.0546	0.630	1.287	-0.867
0.412	2.431	1.286	0.0183	0.0634	0.582	1.225	-0.886
0.315	2.457	1.393	0.0136	0.0728	0.531	1.165	-0.895
0.216	2.512	1.507	0.0090	0.0820	0.478	1.110	-0.888
0.113	2.704	1.701	0.0043	0.0914	0.421	1.056	-0.859
0.507	2.419	1.173	0.0230	0.0540	0.633	1.291	-0.866
0.436	2.427	1.259	0.0194	0.0611	0.594	1.241	-0.882
0.345	2.447	1.360	0.0150	0.0699	0.547	1.183	-0.894
0.275	2.473	1.436	0.0118	0.0765	0.510	1.142	-0.894

(1) Cadmium nitrate

Derived Data : $Cd^{(1)}$ /Na-MOR

A_c	α^N	α^{UN}	m_A	m_B	f_A	f_B	$\ln K_c$
0.989	7.697	0.041	0.0480	0.004	0.990	3.197	1.465
0.956	6.615	0.143	0.0434	0.013	0.963	2.820	1.241
0.900	5.781	0.275	0.0379	0.024	0.932	2.362	0.920
0.837	5.276	0.401	0.0330	0.034	0.909	2.010	0.622
0.771	4.957	0.512	0.0288	0.042	0.891	1.769	0.386
0.679	4.673	0.650	0.0238	0.053	0.865	1.555	0.158
0.576	4.483	0.789	0.0189	0.062	0.824	1.409	0.0099
0.459	4.381	0.937	0.0140	0.072	0.760	1.302	-0.069
0.333	4.417	1.110	0.0092	0.082	0.688	1.211	-0.113
0.195	4.895	1.411	0.0045	0.091	0.639	1.119	-0.198
0.735	4.830	0.567	0.0268	0.047	0.882	1.673	0.285
0.612	4.538	0.741	0.0205	0.059	0.840	1.452	0.051
0.497	4.402	0.888	0.0155	0.069	0.783	1.333	-0.0498

(1) Cadmium nitrate

Derived Data : $Cd^{(1)}$ /Na-FER

A_c	α^N	α^{UN}	m_A	m_B	f_A	f_B	$\ln K_c$
0.928	1.408	0.051	0.047	0.005	0.924	0.882	-1.834
0.822	1.557	0.132	0.043	0.014	0.799	0.959	-1.522
0.743	1.749	0.206	0.038	0.023	0.700	1.015	-1.276
0.672	2.030	0.295	0.034	0.033	0.611	1.060	-1.053
0.616	2.361	0.393	0.029	0.042	0.543	1.091	-0.877
0.562	2.763	0.513	0.024	0.052	0.480	1.115	-0.712
0.501	3.232	0.666	0.019	0.062	0.416	1.133	-0.535
0.428	3.749	0.859	0.014	0.072	0.348	1.144	-0.338
0.333	4.369	1.125	0.009	0.081	0.276	1.138	-0.117
0.213	5.486	1.592	0.005	0.091	0.211	1.103	0.090
0.138	7.669	2.373	0.002	0.096	0.183	1.070	0.169
0.639	2.215	0.350	0.031	0.039	0.570	1.079	-0.948
0.531	3.001	0.588	0.022	0.057	0.447	1.125	-0.622
0.378	4.072	0.994	0.012	0.077	0.308	1.143	-0.217

(1) Cadmium nitrate

Derived Data : $Cd^{(1)}$ /NH_4-MOR

A_c	α^N	α^{UN}	m_A	m_B	f_A	f_B	$\ln K_c$
0.996	9.938	0.022	0.0489	0.002	0.996	4.081	1.824
0.957	7.423	0.150	0.0429	0.014	0.966	3.372	1.472
0.924	6.581	0.231	0.0394	0.021	0.950	2.926	1.206
0.860	5.715	0.362	0.0341	0.032	0.932	2.334	0.773
0.790	5.203	0.479	0.0296	0.041	0.923	1.952	0.424
0.698	4.789	0.609	0.0246	0.051	0.909	1.664	0.121
0.597	4.496	0.732	0.0199	0.060	0.876	1.490	-0.062
0.470	4.257	0.867	0.0147	0.071	0.807	1.362	-0.161
0.333	4.103	0.998	0.0098	0.080	0.738	1.252	-0.239
0.178	4.087	1.160	0.0048	0.090	0.760	1.126	-0.482
0.825	5.431	0.422	0.0318	0.037	0.927	2.122	0.587
0.656	4.651	0.663	0.0225	0.055	0.897	1.579	0.028
0.401	4.167	0.934	0.0122	0.076	0.768	1.306	-0.195

(1) Cadmium nitrate

Derived Data : $Cd^{(1)}/NH_4$-FER

A_c	α^N	α^{UN}	m_A	m_B	f_A	f_B	$\ln K_c$
0.963	0.909	0.014	0.0492	0.0017	0.967	0.878	-2.641
0.798	0.977	0.075	0.0445	0.0110	0.811	0.783	-2.694
0.685	1.010	0.127	0.0399	0.0202	0.632	0.895	-2.176
0.603	1.327	0.187	0.0348	0.0304	0.485	1.014	-1.661
0.554	1.664	0.259	0.0300	0.0401	0.402	1.088	-1.333
0.517	2.162	0.359	0.0249	0.0502	0.346	1.140	-1.091
0.481	2.791	0.492	0.0200	0.0601	0.297	1.186	-0.860
0.426	3.534	0.677	0.0148	0.0704	0.238	1.238	-0.549
0.341	4.253	0.909	0.0098	0.0804	0.176	1.269	-0.201
0.210	5.004	1.231	0.0048	0.0904	0.152	1.199	-0.167
0.447	3.284	0.610	0.0165	0.0670	0.259	1.221	-0.662
0.543	1.791	0.284	0.0285	0.0430	0.384	1.105	-1.257

(1) Cadmium nitrate

Derived Data : Cd(2) /Na-CLI

A_c	α^N	α^{UN}	m_A	m_B	f_A	f_B	$\ln K_c$
0.828	0.726	0.172	0.0465	0.0070	0.855	0.935	-2.210
0.658	0.732	0.279	0.0420	0.0160	0.673	0.937	-1.965
0.558	0.756	0.335	0.0385	0.0230	0.539	0.979	-1.656
0.440	0.847	0.426	0.0325	0.0350	0.381	1.034	-1.199
0.340	1.165	0.633	0.0235	0.0530	0.267	1.067	-0.783
0.299	1.452	0.811	0.0185	0.0630	0.228	1.074	-0.611
0.255	1.763	1.012	0.0140	0.0720	0.193	1.077	-0.437
0.195	2.065	1.224	0.0950	0.0810	0.153	1.072	-0.212
0.096	2.149	1.333	0.0045	0.0910	0.106	1.044	0.096
0.380	0.983	0.519	0.0278	0.0445	0.310	1.057	-0.949
0.087	2.119	1.319	0.0042	0.0917	0.103	1.041	0.118
0.973	0.732	0.034	0.0495	0.0010	0.975	1.102	-2.011
0.960	0.732	0.049	0.0493	0.0015	0.963	1.076	-2.047
0.366	1.039	0.555	0.0263	0.0474	0.294	1.061	-0.888
0.341	1.159	0.630	0.0236	0.0528	0.269	1.067	-0.787
0.314	1.337	0.739	0.0204	0.0593	0.243	1.073	-0.675
0.290	1.518	0.853	0.0175	0.0650	0.221	1.076	-0.576
0.261	1.727	0.988	0.0145	0.0710	0.197	1.077	-0.458

(2) Cadmium chloride

Derived Data : $Cd^{(2)}$ / Na-MOR

A_c	α^N	α^{UN}	m_A	m_B	f_A	f_B	$\ln K_c$
0.935	1.460	0.045	0.0476	- 0.0048	0.930	0.989	-0.846
0.821	1.621	0.132	0.0425	0.0150	0.789	1.123	-0.429
0.740	1.805	0.205	0.0380	0.0240	0.689	1.189	-0.180
0.673	2.029	0.282	0.0335	0.0330	0.611	1.225	0.0006
0.605	2.317	0.378	0.0285	0.0430	0.541	1.244	0.154
0.545	2.596	0.477	0.0240	0.0520	0.484	1.248	0.270
0.454	2.956	0.628	0.0180	0.0640	0.414	1.233	0.404
0.390	3.133	0.726	0.0145	0.0710	0.374	1.211	0.470
0.279	3.293	0.866	0.0095	0.0810	0.322	1.157	0.528
0.152	3.216	0.950	0.0050	0.0900	0.288	1.084	0.507
0.831	1.603	0.124	0.0430	0.0140	0.801	1.113	-0.462
0.202	3.290	0.931	0.0067	0.0867	0.298	1.113	0.526
0.620	2.251	0.356	0.0296	0.0408	0.555	1.241	0.123
0.447	2.978	0.639	0.0176	0.0648	0.409	1.231	0.412
0.495	2.808	0.561	0.0205	0.0589	0.443	1.242	0.350

Derived Data : $Cd^{(2)}$ /Na-FER

A_c	α^N	α^{UN}	m_A	m_B	f_A	f_B	$\ln K_c$
0.942	0.999	0.029	0.0485	0.003	0.944	0.933	-1.438
0.777	1.038	0.108	0.0435	0.013	0.787	0.896	-1.339
0.661	1.100	0.164	0.0390	0.022	0.662	0.907	-1.141
0.571	1.195	0.217	0.0345	0.031	0.554	0.929	-0.913
0.493	1.351	0.281	0.0295	0.041	0.456	0.955	-0.664
0.431	1.576	0.359	0.0245	0.051	0.378	0.977	-0.430
0.376	1.887	0.461	0.0195	0.061	0.312	0.996	-0.200
0.321	2.317	0.602	0.0145	0.071	0.250	1.013	0.057
0.257	2.954	0.820	0.0095	0.081	0.186	1.029	0.384
0.177	4.336	1.296	0.0045	0.091	0.119	1.038	0.844
0.138	6.069	1.872	0.0025	0.095	0.094	1.039	1.084
0.499	1.336	0.275	0.0299	0.040	0.463	0.953	-0.683
0.420	1.630	0.377	0.0235	0.053	0.364	0.981	-0.385
0.390	1.799	0.432	0.0208	0.059	0.328	0.991	-0.259
0.186	4.103	1.216	0.0050	0.090	0.126	1.038	0.790

(2) Cadmium chloride

Derived Data : $Cd^{(2)}/NH_4$-MOR

A_c	α^N	α^{UN}	m_A	m_B	f_A	f_B	$\ln K_c$
0.901	0.560	0.026	0.049	0.003	0.923	0.858	-2.560
0.662	0.534	0.075	0.044	0.012	0.739	0.701	-2.743
0.488	0.537	0.106	0.039	0.022	0.475	0.763	-2.131
0.394	0.585	0.132	0.035	0.031	0.312	0.827	-1.548
0.342	0.723	0.173	0.030	0.041	0.229	0.868	-1.140
0.323	0.956	0.234	0.025	0.050	0.202	0.883	-0.982
0.314	1.375	0.340	0.020	0.060	0.189	0.891	-0.902
0.296	1.965	0.496	0.015	0.070	0.166	0.905	-0.739
0.248	2.634	0.698	0.010	0.080	0.112	0.942	-0.264
0.147	3.091	0.897	0.005	0.090	0.040	1.002	0.880
0.375	0.614	0.142	0.033	0.034	0.279	0.843	-1.400
0.321	1.055	0.259	0.024	0.053	0.198	0.886	-0.956
0.316	1.300	0.321	0.021	0.059	0.191	0.890	-0.914
0.308	1.628	0.405	0.018	0.065	0.182	0.895	-0.849

(2) Cadmium chloride

Derived Data : $Cd^{(2)}/NH_4$-FER

A_c	α^N	α^{UN}	m_A	m_B	f_A	f_B	$\ln K_c$
0.920	0.469	0.014	0.0490	0.002	0.942	1.031	-2.845
0.604	0.417	0.053	0.0440	0.012	0.729	0.699	-3.365
0.410	0.391	0.070	0.0390	0.022	0.377	0.792	-2.457
0.322	0.407	0.081	0.0350	0.030	0.220	0.863	-1.744
0.273	0.522	0.110	0.0295	0.041	0.149	0.905	-1.264
0.272	0.746	0.158	0.0250	0.050	0.147	0.906	-1.248
0.284	1.191	0.249	0.0200	0.060	0.164	0.895	-1.378
0.285	1.863	0.389	0.0150	0.070	0.165	0.895	-1.388
0.247	2.634	0.573	0.0100	0.080	0.118	0.927	-0.977
0.140	2.985	0.719	0.0049	0.090	0.036	0.997	0.352
0.275	0.504	0.106	0.0301	0.040	0.152	0.903	-1.285
0.270	0.642	0.136	0.0268	0.047	0.145	0.908	-1.226

(2) Cadmium chloride

Derived Data : NH_4 /Na-CLI

A_c	α^N	α^{UN}	m_A	m_B	f_A	f_B	$\ln K_c$
0.897	1.01	0.261	0.090	0.010	0.930	0.200	0.095
0.838	1.41	0.500	0.079	0.022	0.861	0.335	0.690
0.828	1.56	0.573	0.076	0.025	0.849	0.358	0.771
0.812	1.95	0.754	0.069	0.031	0.831	0.394	0.888
0.804	2.31	0.919	0.064	0.036	0.822	0.414	0.947
0.788	3.16	1.320	0.054	0.046	0.804	0.450	1.052
0.772	3.75	1.633	0.047	0.053	0.788	0.484	1.146
0.644	4.87	2.658	0.027	0.073	0.698	0.661	1.579
0.454	5.14	3.333	0.014	0.086	0.673	0.698	1.670
0.281	6.13	4.339	0.006	0.094	0.575	0.756	1.908
0.145	16.83	12.50	0.001	0.099	0.307	0.887	2.695
0.188	9.05	6.632	0.003	0.098	0.405	0.839	2.363
0.352	5.50	3.775	0.009	0.091	0.644	0.718	1.742
0.643	4.88	2.663	0.027	0.073	0.698	0.662	1.581
0.555	4.99	2.997	0.020	0.080	0.677	0.694	1.658
0.799	2.55	1.029	0.061	0.039	0.817	0.424	0.978
0.934	0.91	0.165	0.094	0.006	0.968	0.130	-0.373
0.160	12.50	9.241	0.002	0.099	0.340	0.870	2.572
0.742	4.32	2.010	0.040	0.060	0.761	0.541	1.292
0.702	4.67	2.344	0.034	0.067	0.729	0.604	1.444

Derived Data : NH_4/Na-MOR

A_c	α^N	α^{UN}	m_A	m_B	f_A	f_B	$\ln K_c$
0.977	3.22	0.077	0.093	0.0072	1.0004	1.575	2.314
0.969	4.45	0.141	0.087	0.0126	1.0006	1.559	2.304
0.967	6.65	0.224	0.081	0.0187	1.0007	1.555	2.301
0.971	13.76	0.409	0.071	0.0294	1.0006	1.563	2.307
0.967	6.34	0.214	0.082	0.0180	1.0007	1.555	2.301
0.959	19.95	0.820	0.054	0.0461	1.0011	1.540	2.291
0.848	10.12	1.386	0.036	0.0645	1.0142	1.362	2.155
0.542	5.78	1.868	0.017	0.0830	1.1104	1.099	1.850
0.050	5.17	2.572	0.001	0.0990	1.3384	1.000	1.569
0.972	18.88	0.544	0.064	0.0356	1.0005	1.565	2.308
0.959	20.04	0.814	0.054	0.0459	1.0011	1.541	2.292
0.701	7.09	1.688	0.025	0.0752	1.0511	1.203	1.996
0.494	5.53	1.909	0.015	0.0850	1.1316	1.077	1.811
0.452	5.34	1.939	0.013	0.0866	1.1506	1.061	1.779
0.095	4.69	2.275	0.002	0.0978	1.3199	1.002	1.584
0.863	10.70	1.340	0.037	0.0630	1.0117	1.383	2.173
0.230	4.69	2.087	0.006	0.0940	1.2582	1.011	1.642

Derived Data : Pb / NH_4-CLI

Pb_c	α^{UN}	m_A
0.839	1.292	0.0445
0.742	1.436	0.0400
0.672	1.673	0.0355
0.621	2.0098	0.0310
0.581	2.454	0.0265
0.536	3.067	0.0215
0.488	3.698	0.0170
0.422	4.376	0.0125
0.201	6.695	0.0035
0.183	7.134	0.0030
0.132	9.657	0.0015
0.104	14.074	0.0008
0.087	24.925	0.0004
0.514	3.375	0.0193
0.643	1.840	0.0331
0.319	5.236	0.0076

Derived Data : Cd / $NH_4(NO_3)$-CLI

Cd_c	α^{UN}	m_A
0.740	0.116	0.0490
0.493	0.280	0.0437
0.350	0.300	0.0391
0.251	0.318	0.0339
0.212	0.349	0.0304
0.183	0.466	0.0245
0.174	0.646	0.0198
0.163	0.938	0.0147
0.136	1.285	0.0098
0.071	1.479	0.0047
0.660	0.205	0.0475
0.754	0.094	0.0493
0.612	0.237	0.0465

Derived Data : Cd / NH_4(Cl)-CLI

Cd_c	α^{UN}	m_A
0.685	0.031	0.0497
0.674	0.042	0.0495
0.656	0.058	0.0493
0.639	0.072	0.0490
0.635	0.075	0.0490
0.549	0.120	0.0477
0.322	0.146	0.0434
0.168	0.116	0.0389
0.083	0.082	0.0344
0.049	0.072	0.0294
0.056	0.123	0.0246
0.081	0.271	0.0198
0.106	0.569	0.0147
0.106	0.972	0.0098
0.059	1.188	0.0048
0.051	0.071	0.0302
0.049	0.088	0.0270
0.060	0.141	0.0237
0.075	0.226	0.0209
0.092	0.368	0.0178
0.106	0.561	0.0148

Derived Data : Pb / Na-FER

Pb_c	α^{UN}	m_A
0.498	0.104	0.0475
0.450	0.503	0.0383
0.485	1.498	0.0279
0.500	3.562	0.0180
0.491	6.796	0.0080
0.4997	0.099	0.0477
0.4596	0.277	0.0430
0.450	0.506	0.0382
0.462	0.865	0.0333
0.484	1.455	0.0282
0.502	2.381	0.0229
0.501	3.508	0.0182
0.472	4.924	0.0133
0.397	6.671	0.0083
0.275	10.060	0.0035
0.207	16.296	0.0016
0.166	39.287	0.0005
0.153	90.077	0.0002
0.149	174.708	0.0001
0.146	682.471	0.0000
0.503	2.632	0.0218
0.476	4.785	0.0138
0.359	7.485	0.0065

Derived Data : NH_4 / Na-FER

$NH_4{}_c$	α^{UN}	m_A
0.479	0.055	0.094
0.452	0.256	0.076
0.475	0.705	0.056
0.466	1.512	0.037
0.331	2.582	0.016
0.436	1.893	0.029
0.115	6.350	0.002
0.476	0.730	0.055
0.159	4.194	0.004
0.459	1.620	0.034
0.455	0.146	0.085
0.294	2.785	0.013
0.252	3.039	0.010
0.393	2.228	0.023
0.412	2.098	0.025
0.448	1.766	0.032
0.480	1.061	0.047

Isotherm Data at 0.5 equiv.dm^{-3}

Pb/Na-CLI		Pb/Na-MOR		Pb/Na-FER	
Pb_s	Pb_c	Pb_s	Pb_c	Pb_s	Pb_c
1.000	0.805	1.000	0.500	1.00	0.500
0.972	0.805	0.980	0.500	0.950	0.482
0.868	0.800	0.880	0.500	0.905	0.475
0.771	0.800	0.799	0.490	0.785	0.433
0.672	0.800	0.690	0.473	0.602	0.431
0.575	0.800	0.592	0.440	0.495	0.427
0.474	0.785	0.493	0.410	0.325	0.391
0.400	0.705	0.292	0.347	0.205	0.335
0.340	0.650	0.380	0.380	0.115	0.285
0.278	0.600	0.193	0.284	0.055	0.246
0.181	0.480	0.094	0.236	0.045	0.181
0.085	0.310	0.035	0.144	0.023	0.072
0.030	0.130	0.233	0.320		
		0.425	0.395		

Derived Data : Pb/Na-CLI 0.5 equiv.dm^{-3}

A_C	α^N	α^{UN}	m_A	m_B	f_A	f_B	$\ln K_C$
0.995	10.76	0.237	0.243	0.014	0.995	14.05	8.51
0.989	28.58	1.218	0.217	0.066	0.990	13.35	8.41
0.996	140.93	2.456	0.193	0.115	0.996	14.21	8.53
0.995	213.17	4.030	0.168	0.164	0.996	14.16	8.52
0.995	322.81	6.102	0.144	0.213	0.996	14.16	8.52
0.990	204.40	8.877	0.119	0.263	0.990	13.33	8.40
0.804	15.90	7.210	0.085	0.330	1.097	3.23	5.46
0.742	14.93	7.791	0.069	0.361	1.220	2.34	4.72
0.594	13.22	8.354	0.045	0.409	1.612	1.40	3.41
0.383	13.38	9.673	0.021	0.458	1.820	1.05	2.71
0.151	11.46	8.964	0.008	0.485	0.768	1.03	3.53

Derived Data : Pb/Na-MOR 0.5 equiv.dm^{-3}

A_C	α^N	α^{JN}	m_A	m_B	f_A	f_B	$\ln K_C$
0.988	3.42	0.042	0.245	0.010	0.987	0.831	2.48
0.944	4.60	0.255	0.220	0.060	0.926	1.088	3.08
0.917	6.23	0.503	0.195	0.111	0.883	1.229	3.38
0.898	7.91	0.766	0.173	0.155	0.854	1.310	3.54
0.875	9.64	1.120	0.148	0.204	0.819	1.395	3.71
0.839	10.70	1.551	0.123	0.254	0.769	1.487	3.89
0.685	10.54	2.623	0.073	0.354	0.659	1.415	3.95
0.769	10.87	2.124	0.095	0.310	0.696	1.528	4.05
0.549	10.17	3.274	0.048	0.404	0.699	1.133	3.45
0.359	10.82	4.355	0.023	0.453	0.744	0.919	2.97
0.217	15.31	6.911	0.009	0.483	0.407	0.929	3.59
0.609	10.28	2.992	0.058	0.384	0.669	1.256	3.69
0.802	10.92	1,886	0.106	0.288	0.725	1.529	4.01

APPENDIX II : EXPERIMENTAL DATA TERNARY SYSTEMS

Derived Data : Pb/Cd/Na-CLI

Pb_c	Cd_c	Na_c
0.580	0.180	0.240
0.660	0.130	0.210
0.700	0.180	0.120
0.700	0.240	0.060
0.640	0.180	0.180
0.670	0.190	0.170
0.690	0.120	0.190
0.530	0.230	0.240
0.600	0.180	0.220

Pb_s	Cd_s	Na_s
0.442	0.413	0.145
0.290	0.436	0.274
0.240	0.350	0.590
0.140	0.408	0.450
0.110	0.390	0.500
0.055	0.194	0.751
0.038	0.210	0.752
0.025	0.058	0.917
0.010	0.079	0.911

Derived Data : $Pb/Cd/NH_4$-CLI

Pb_c	Cd_c	NH_{4_c}
0.637	0.0184	0.3446
0.523	0.0192	0.4580
0.530	0.0207	0.4490
0.474	0.0202	0.5058
0.384	0.02021	0.5960
0.315	0.0208	0.6640
0.219	0.0174	0.7640
0.210	0.0177	0.7730
0.171	0.0147	0.8140
0.117	0.0139	0.8690

Pb_s	Cd_s	NH_{4_s}
0.402	0.497	0.101
0.367	0.448	0.185
0.325	0.403	0.272
0.290	0.359	0.351
0.254	0.310	0.436
0.219	0.247	0.534
0.169	0.201	0.630
0.126	0.157	0.717
0.0776	0.102	0.820
0.035	0.050	0.915

Derived Data : Pb/Cd/Na-MOR

Pb_c	Cd_c	Na_c
0.175	0.1150	0.710
0.116	0.0718	0.810
0.252	0.1240	0.624
0.309	0.0490	0.642
0.274		
0.348	0.0275	0.625
0.340	0.0185	0.679
0.244	0.0806	0.676
0.209	0.0443	0.747

Pb_s	Cd_s	Na_s
0.397	0.482	0.121
0.365	0.441	0.194
0.307	0.385	0.308
0.292		
0.225	0.297	0.480
0.182	0.260	0.558
0.138	0.214	0.648
0.090	0.157	0.753
0.056	0.092	0.852
0.018	0.0474	0.935

Derived Data : $Pb/Cd/NH_4$-MOR

Pb_c	Cd_c	NH_{4_c}
0.075	0.0235	0.902
0.1159	0.0198	0.864
0.111	0.017	0.872
0.0217	0.0217	0.957
0.0763	0.0172	0.907
0.018	0.0210	0.961
0.068	0.0134	0.919
0.056	0.0160	0.928
0.098	0.0150	0.847
0.086	0.0102	0.904

Pb_s	Cd_s	NH_{4_s}
0.488	0.497	0.015
0.434	0.448	0.118
0.389	0.403	0.208
0.359	0.359	0.282
0.302	0.311	0.387
0.247	0.247	0.506
0.194	0.203	0.603
0.152	0.157	0.691
0.0896	0.102	0.808
0.0395	0.051	0.909

Derived Data : $Pb/Cd/NH_4$-FER

Pb_c	Cd_c	NH_{4_c}
0.196	0.01096	0.793
0.200	0.01333	0.787
0.170	0.01365	0.816
0.165	0.01461	0.849
0.150	0.01413	0.864
0.134	0.01320	0.848
0.093	0.01350	0.894
0.099	0.01413	0.887
0.081	0.01270	0.932
0.043	0.00857	0.948

Pb_s	Cd_s	NH_{4_s}
0.474	0.4986	0.0274
0.424	0.4490	0.1270
0.383	0.4040	0.2130
0.340	0.3600	0.3000
0.293	0.3110	0.3960
0.230	0.2480	0.5220
0.192	0.2020	0.6060
0.146	0.1580	0.6960
0.093	0.1030	0.8040
0.047	0.0520	0.9010

Derived Data : Pb/Cd/Na-FER

Pb_c	Cd_c	Na_c
0.278	0.196	0.526
0.225	0.107	0.668
0.298	0.234	0.468
0.323	0.209	0.468
0.291	0.165	0.544
0.377	0.117	0.506
0.410	0.129	0.461
0.206	0.117	0.677

Pb_s	Cd_s	Na_s
0.334	0.474	0.192
0.370	0.505	0.125
0.218	0.276	0.506
0.136	0.193	0.671
0.110	0.180	0.710
0.047	0.152	0.801
0.046	0.146	0.808
0.010	0.018	0.972

Derived Data : $Cd/Na/NH_4$-MOR

Na_c	$NH_4{}_c$	Cd_c	Na_s	$NH_4{}_s$	Cd_s
0.017	0.507	0.476	0.103	0.159	0.738
0.050	0.905	0.045	0.248	0.221	0.531
0.050	0.543	0.407	0.304	0.328	0.368
0.100	0.734	0.166	0.400	0.413	0.188
0.060	0.681	0.259	0.460	0.467	0.073

Derived Data : $Pb/Na/NH_4$-MOR

Na_c	$NH_4{}_c$	Pb_c	Na_s	$NH_4{}_s$	Pb_s
0.035	0.740	0.225	0.227	0.286	0.487
0.053	0.736	0.211	0.270	0.326	0.404
0.101	0.764	0.135	0.378	0.427	0.195
0.068	0.745	0.195	0.431	0.482	0.087

FIG. 1 : Ternary Ion Exchange Diagram for the System $Pb/Cd/NH_4$-CLI .

⊖ Solution Phase.

⊙ Crystal Phase.

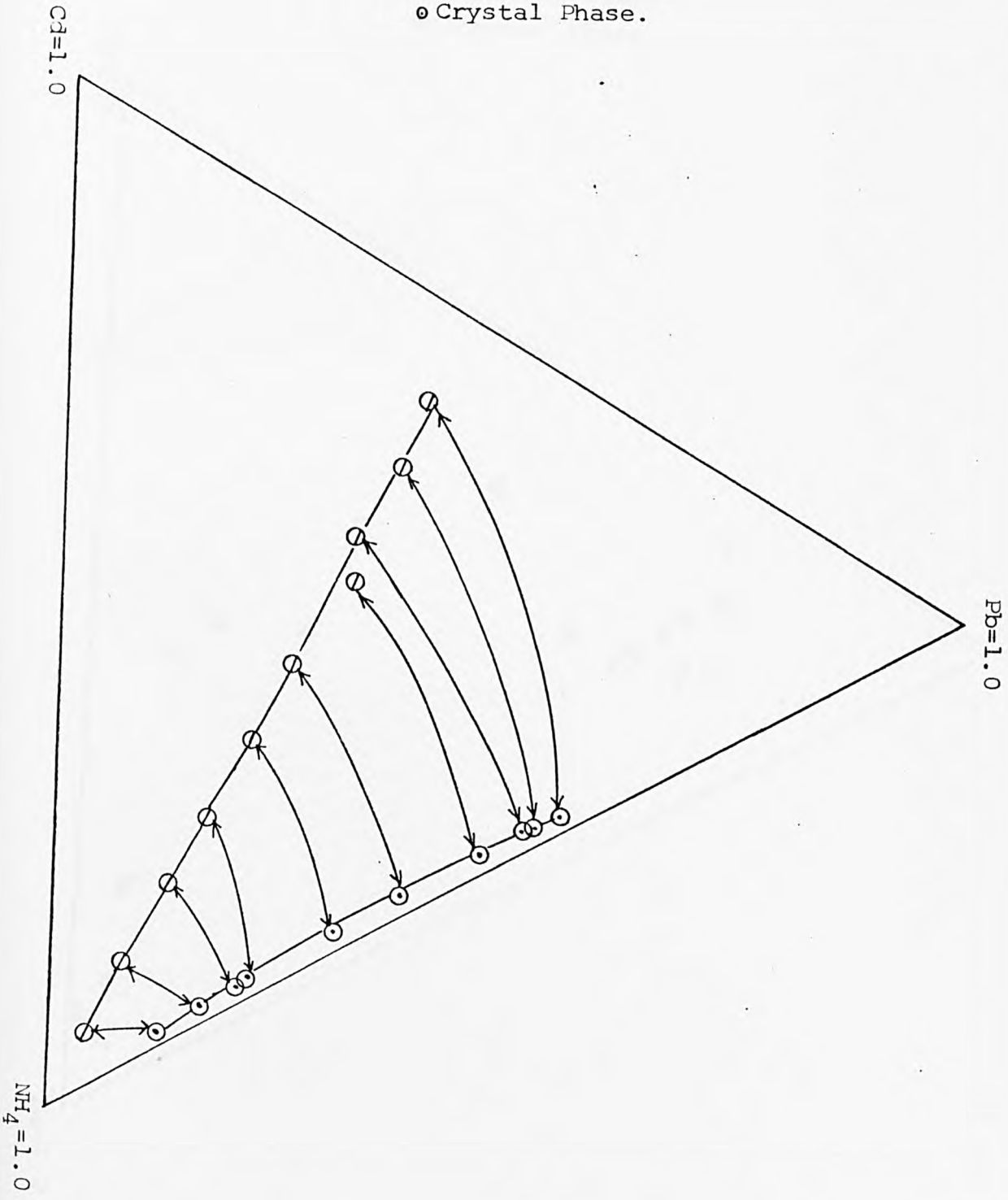

FIG. 2 : Ternary Ion Exchange Diagram for the System Pb/Cd/Na-CLI .

⊖ Solution Phase.

⊙ Crystal Phase.

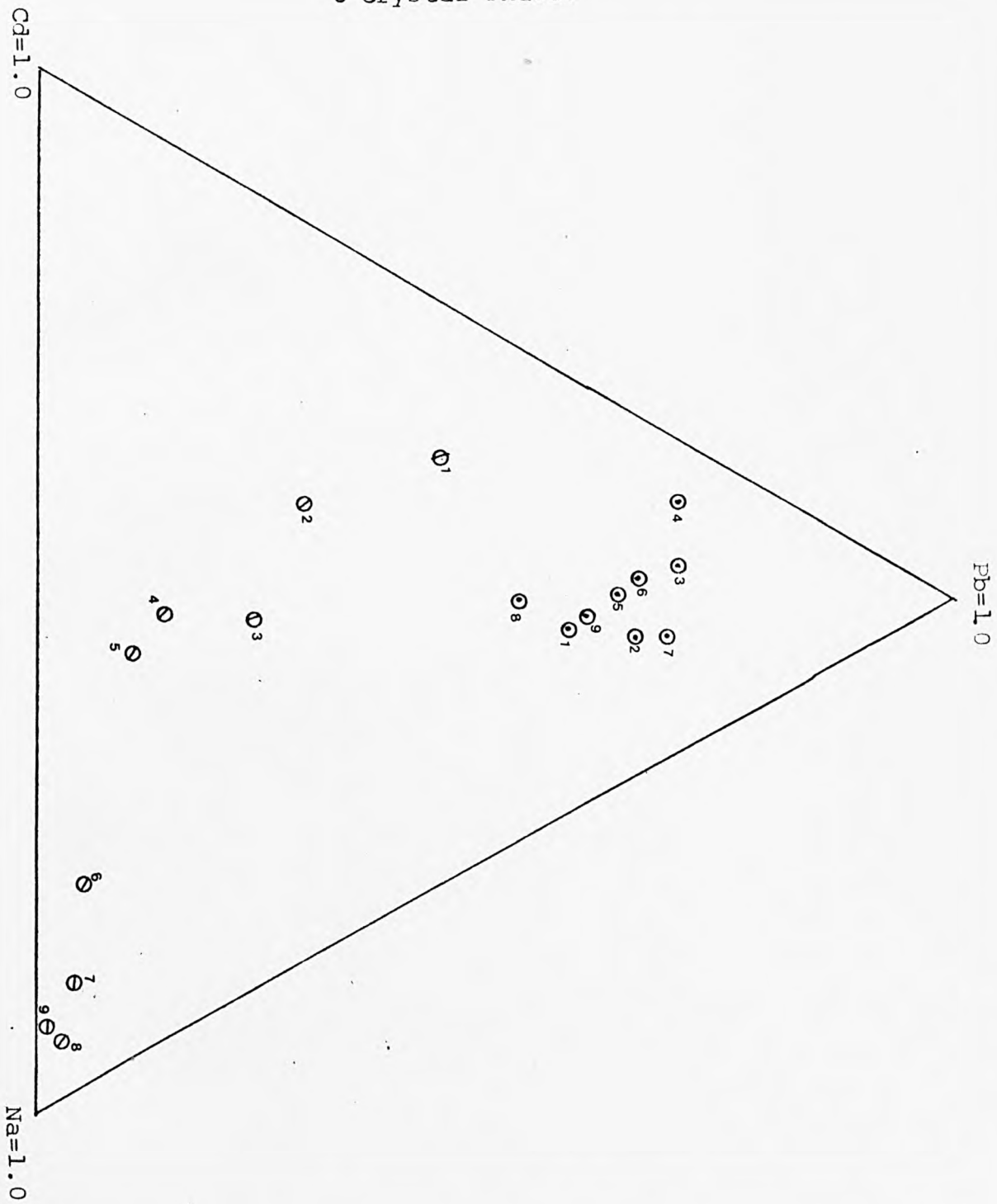

APPENDIX III : Γ and I values.

$Cd^{(1)}$/Na-MOR

A_C	I	Γ
0.989	0.148	1.667
0.956	0.143	1.654
0.901	0.138	1.638
0.837	0.133	1.624
0.771	0.129	1.611
0.679	0.124	1.596
0.576	0.119	1.580
0.459	0.114	1.565
0.333	0.109	1.549
0.195	0.105	1.533
0.735	0.127	1.605
0.612	0.121	1.585
0.497	0.116	1.570

$Cd^{(2)}$/Na-MOR

A_C	I	Γ
0.935	0.148	4.531
0.821	0.143	4.535
0.741	0.138	4.539
0.673	0.134	4.544
0.606	0.129	4.551
0.545	0.124	4.560
0.454	0.118	4.576
0.390	0.115	4.588
0.279	0.110	4.609
0.152	0.105	4.634
0.831	0.143	4.534
0.202	0.107	4.624
0.620	0.130	4.549
0.447	0.118	4.577
0.495	0.121	4.568

$Cd^{(1)}$/NH_4-MOR

A_C	I	Γ
0.996	0.149	1.592
0.957	0.143	1.574
0.924	0.139	1.563
0.860	0.134	1.546
0.790	0.130	1.532
0.698	0.125	1.515
0.597	0.120	1.500
0.470	0.115	1.482
0.333	0.110	1.465
0.178	0.105	1.447
0.825	0.132	1.539
0.656	0.123	1.509
0.401	0.112	1.473

$Cd^{(2)}$/NH_4-MOR

A_C	I	Γ
0.901	0.149	4.432
0.662	0.144	4.435
0.488	0.139	4.440
0.394	0.135	4.445
0.342	0.130	4.452
0.323	0.125	4.461
0.314	0.120	4.474
0.296	0.115	4.490
0.248	0.110	4.511
0.147	0.105	4.539
0.375	0.133	4.447
0.321	0.124	4.464
0.316	0.121	4.471
0.308	0.118	4.481

(1) Cadmium nitrate

(2) Cadmium chloride

Pb/Na-MOR (1)			Pb/Na-MOR (2)		
A_c	I	Γ	A_c	I	Γ
0.947	0.147	2.077	0.988	0.745	3.601
0.910	0.142	2.064	0.944	0.720	3.582
0.907	0.137	2.049	0.917	0.695	3.562
0.924	0.132	2.035	0.898	0.673	3.544
0.940	0.128	2.022	0.875	0.648	3.524
0.941	0.123	2.007	0.839	0.623	3.503
0.889	0.118	1.992	0.685	0.573	3.460
0.833	0.113	1.976	0.769	0.595	3.479
0.736	0.108	1.961	0.549	0.548	3.438
0.562	0.104	1.947	0.360	0.524	3.416
0.905	0.140	2.057	0.217	0.509	3.402
0.862	0.114	1.981	0.610	0.558	3.447
0.548	0.104	1.948	0.801	0.606	3.489
0.424	0.100	1.936			
0.281	0.100	1.936			
0.227	0.100	1.935			
0.116	0.100	1.935			
0.943	0.125	2.015			
0.941	0.122	2.007			
0.926	0.120	1.998			

(1) Solution concentration 0.1 equiv.dm^{-3}

(2) Solution concentration 0.5 equiv.dm^{-3}

REFERENCES

1. Cronstedt A.F, Akad. Handl. Stockholm 18,(1756)120
2. Breck D.W., "Zeolite Molecular Sieves" (Wiley Interscience 1974), p.10
3. Gottardi G., Zeolite Internat. Conference 1976, Tuscon, Arizona, (L.B. Sand, F.A. Mumpton (ed) "Natural Zeolites, Occurence, Properties, Use", Pergamon Press Oxford 1978), p.31
4. Murray J., Renard A.F. (1891), Deep Sea deposits volume 5. Eyre and Spottiswoode, London.
5. Manson R.A., Sheppard R.A., Mineral Science and Engineering vol.6 N°1, Jan.1974.
6. Breck D.W., ref(2), p.245
7. Flanigen E.M., Fifth Inter. Conf. on Zeolites, Naples 1980, p.760
8. Kokotailo G.T., City proceed. 1979, (ed.) R.P.Townsend, The properties and applications of zeolites, Chem. Soc. N° 33, p.133
9. Breck D.W. (as ref. 8) p.391
10. Flanigen E.M., Bennett J.M., Nature, 1978 271, 512.
11. Vaughan D.E.W., Breck D.W. (as ref. 8) p.214.
12. Ames L.L. (1959) Zeolitic extraction of caesium from aqueous solutions : Unclass. Rpt. HY-62607, US Atomic Energy Comm. p.23.
13. Ames L.L. (1960), The cation sieve properties of clinoptilolite : Amer. Mineral. 45, 689-700
14. Cohen B.L., Scient. Amer. 236 No 6, 1977
15. Mupton F.A., Inter. Conf. Zeol. Tuscon, Arizona 1976 p.1
16. Mercer B.W., (1969), Clinoptilolite in water-pollution control : Ore Bin 31, 209-213.
17. Mercer,B.W.,Ames L.L. and Smith P.W. (1970a), Caesium purification by zeolite ion exchange, Nuclear Appl. and Tech. 8, 62-69.
18. Wilding, M.W., Rhodes, D.W. (1963), Removal of radioisotopes from solution by earth materials from eastern Idaho. US Atomic Energy Comm. Doc. IDO-14624.

19. Wiling,M.W., Rhodes,D.W., (1965), Decontamination of radioactive effluent with clinoptilolite, US Atomic Energy Comm. Doc. IDO-14657.
20. Breck,D.W.,City Univ. Proc. (ref. 8) p.391.
21. Ames,L.L. (1967), Zeolitic removal of ammonium ions from agricultural wastewaters. Proc. 13th Pacific Northwest Indust. Waste Conf. Washington State Univ. p.135-152.
22. Mercer, B.W., Ames, L.L., Ammonia removal from secondary effluents by selective ion exchange, J. Wat. Pollution Control Fed., 42, R95-R107, (1970).
23. Sato, Mikio, Fukagawa, Treatment for ammoniacal nitrogen containing water, Japan Kokai 76,068,967 1976
24. Semmens,M.J., Both,A.C., Clinoptilolite Column Ammonia Removal Model, J. Env. Engng. Div. Proc. Amer. Soc. Civil Eng. (1978), 104 No E.E2 p.231-244.
25. Semmens, M.J., Wang,J.T., Both,A.C., "Nitrogen removal by ion exchange biological regeneration of clinoptilolite., J. Water Pollution Control Assoc. 1977
26. Mupton,F.A., (ref. 15), p.12-13
27. Kepple,L.G., (1974), Ammonia removal and recovery becomes feasible., Water and Sewage works 121, No 4, p.42-43.
28. Liberti,L., Boari,G., Passino, R., "Phosphate and ammonia recovery from secondary effluents by selective ion exchange with production of a slow-release fertilizer. Water Res. 13, p.65-73 (1979).
29. Liberti, L., Boari,G., Nutrient removal and recovery from wastewater by ion exchange, Water Res. 15, p.337-342, (1981).
30. Semmens, M.J.,Proc. 5th Inter. Conf. on zeolites, Naples, 1980 p.795
31. Schwuger, M.J., Smolka, H.G., Tenside Deterg., 1976, 13(6) p.305.
32. Schwuger, M.J.,Smolka, H.G., A.C.S., Symp. Ser. 1977 40 (Mol. Sieves 2, Int. Conf. 4th)

33. Kurzendörfer, C.P., Schwuger, M.J., Smolka, H.G., Tenside Deterg. 16 (1979) 3.

34. Smolka, H.G., Schwuger, M.J., Cleansing action of natural zeolites in detergents, Zeolite Int. Conf. Tuscon, Arizona, 1976.

35. Chelishchev, N.F., Martynova, N.S, Dokl. Akad. Nauk SSSR, 1974, 217, 1140

36. Filizova, L., Izv. Geol. Inst. Bulg. Akad. Nauk, Ser. Rudni, Nerudni, Polezni Izkopaemi, 1974,23, p.311

37. Semmens, M.J., Seyfath, M., Int. Conf. Natur. Zeol. Tuscon Ariz. 1976

38. Gal,I.J, Jankovic O,Radovanov P Trans. Farad. Soc. 1971,67,(4) 999

39. Dubimin,M.M, Isirikyan,A.A Akad. Nauk SSSR Ser Khim 1974,(6),1244

40. Hertzenberg,E.P, Sherry,H.S A.C.S Symposium Series 135

41. Sherry,H.S private communication.

42. Mumpton,F.A (ref. 3) P.9 .

43. Breck,D.W City Univ. Proc.1979 Chem. Soc. 33 P.410 .

44. Torri K, Int. Conf. Nat. Zeol. Tuscon Ariz. 1976 P.445

45. Yoshinaga,E (1973) U.S. Patent 3,708,573.

46. Hayhurst,D.T, Proc. 5th Int.Con. Zeol. Naples 1980,P.805.

47. Mignonsin,E.P, Godari,S Trib. Cent. Belge Etude Doc Eaux Air 1974,26 (359) 394.

48. Breck,D.W ref 2 P.29.

49. Helfferich,F. "Ion Exchange" (McGraw-Hill 1962) P.10.

50. Barrer,R.M. "Zeolites and Clay Minerals" Academic Press,1978.

51. Breck,D.W (ref. 2) P.5.

52. Boeweinstein,W. Amer. Min. 39 92,1954.

53. Thomas,J.M, Klinowski,J, Mineral. Soc. Conf. Manch. Univ. Sept. 1981.

54. Klinowski,J. private communication.

55. Breck,D.W, "Zeolite Molecular Sieves" 1974 P.45.

56. Meier,W,M, Olson,D.H, "Atlas of Zeolite Structure Types" 1978

57. Hay,R.L, Proc. Intern. Conf,Natur. Zeol.1976 Tuscon Arizona P.135-143.

58. Surdaham,R.C, Sheppard,R.A, (ref. 3) P.145 .

59.Breck,D.W, (ref. 2) P.186-207.

60. Alberti,A, Min. Petr. Mitt. 1975,22,25.

61. Merkle,A.B, Slaughter,M, Amer. Mineral. 53,1120-38 1968.

62. Shepard,A.O,Starkey,H.C U.S Geol. Survey Prof. Paper. 475-D,D89-D92.

63. Alietti,A. Amer. Miner. 57, 1448, 1972.

64. Barrer,R.M, Makki, M.B Can. J.Chem. 42,1481,1964.

65. Araya ,A, Dyer,A. J.Inorg.Nucl. Chem. 43, 589-594 1981, (Part I).

66. Townsend R.P. "Ion Exchange of Transition Metals in Zeolites" (Dept. Chem. Imperial College London, D.I.C. Thesis,1977) P.12.

67. Breck,D.W, (Ref.2) P.128.

68. Honstead,J.F, Nelson,J.L, Merser,B.W. U.S. At. Energ. Comm. Rept. No TID-7613(1969).

69. Howery,D.G, Thomas,H.C, J.Phy. Chem. 69,No2 1965.

70. Chelishchev,N.F, Berenshtein,B.G, Martynova,N.S, Izv.Akad. Nauk. SSSR. Neorg.Mater. 1975,11,704.

71. Semmens,M.J, Martin,W, Am. Inst. Chem. Eng. (A.I.Ch.E) Symp. Series 1979,76 (197).

72. Townsend,R.P (Ref.66) P.134.

73. Araya,A, Dyer,A, J. Inorg. Nucl. 43, 595-598,1981.

74. Helfferich,F, (Ref.49) P160.

75. Townsend,R.P, (Ref.66)P.

76. Barrer,R.M, Papadopoulos,R, Rees,L.V.C, J. Inorg, Nucl. Chem. 1967,29,2047.

77. Breck,D.W, "Zeolite Molecular Sieves" 1974, P.188.

78. Meier,W.M, Z. Krist. 1961,115, 439.

79. Sherman,J.D, Bennett,M.J, Adv. Chem. Ser.1973 (Mol. Sieves 3rd. Int. Conf.) 121,52.

80. Breck,D.W, (Ref.2) P.122.

81. Barrer,R.M, Klinowski,J, J.C.S. Faraday 1,1974,70,2362.

82. Sand,L.B,(1969) U.S. Patent 3,436,174.

83. Breck,D.W, (Ref.2) P.124.

84. Sand,L.B, "Molecular Sieves" Soc. Chem. Ind. Lon. 1968 P.21.

85. Rao,A, Rees,L.V.C, Trans. Far. Soc. 1966,62,2505.

86. Wolf,F, Furtig,H, Knoll,H, Chem. Tech. (Leipzig) 1971, 23, 273.

87. Grivkova,A.I, Zaitsev,B.A, Zh. Fiz. Khim. 1973, 47, 952.

88 Townsend,R.P, (Ref.66) P.134.

89. Barrer,R.M, Townsend,R.P,(1976a), J.Chem. Soc. Faraday Trans. 1, 72, 661-673,(Part I).

90. Barrer,R,M, Townsend,R.P, J.Chem.Soc. Far. Trans. 1, (1976b) ,Part II.

91. Townsend,R.P, (Ref.66),P.186.

92. Hagiwara,Z, Uchida M, 5th Int, Conf. Nat. Zeol. Tuscon, Arizona 1976, P.463.

93. Fletcher,P, Townsend,R,P, J.Ch.Soc. Far. Trans.I 1981, 77, 495-509.

94. Susuki,N, Saitoh,K, Hamoda S. Radioch. Rad. Letters, 32(3-4) 121-126(1978).

95. Golden,C.T, Robert,G.J, J. Chem. Eng. 1981,26, 366-367.

96. Vaughan,D.E.W, 5th Int. Conf. Nat. Zeol. Tuscon,Arizona 1976, P.353-371.

97. Vaughan,P.A, (1966), Acta Chrystallogr. 21, 983-990.

98. Kerr,I.S, Nature 210,294-295 (1966).

99. Barrer,R.M, Marshall,D.J, J. Chem. Soc. 485-497,1964.

100. Barrer,R.M, Marshall,D.J, Amer. Mineral. 50,484-9,1965.

101. Vaughan,D.E.W, Edwards,G.C, U.S. Patent 3,966,883, 1976.

102. Hawkins,D.B, Short,H.L, U.S,At. Energy, Comm. IDO-12046, P.33, 1965.

103. Ahmed,Z.B, Dyer,A, Miner. Soc. Conf. Manch. Univ. Sept. 1981.

104. Breck,D.W, (Ref.") P.530.

105. Dyer,A, Enamy,E, Townsend,R.P, Sep. Scien. Techn. 16 (2), 1981.

106. Barrer,R.M, Klinowski,J, J.C.S. Far.I,1974,70,2080.

107. Townsend,R.P, (Ref.66), P.28.

108. Barrer,R.M, Munday,B.M, J.Chem.Soc. A 1971,2914.

109. Barrer,R.M, Falconer,J.D, Proc.Roy.Soc. A1956,236,227.

110. Barrer,R.M, Meier,W.M, Trans,Farad.Soc. 1958,54,1074.

111. Barrer,R.M, Meier,W.M, Trans.Farad.Soc. 1959,55,130.

112. Barrer,R.M, Townsend,R.P, J.C.S Farad. Trans. I 1978,74.

113. Barrer,R.m, Klinowski,J, J.Phil.Trans.Roy.Soc. 1977, 285,637.

114. Gaines,G.L,Thomas,H.C, J.Chem.Physics 1953,21,74.

115. Barrer,R.M, Walker,A.J, Trans.Farad.Soc.1964,60,171.

116. Marinsky,J.A, J.Chrom. 1980,201,5.

117. Helfferich.F, "Ion Exchange" MacGraw-Hill,1962,P.156.

118. Kielland,J, J.Soc.Chem.Indust. 1935,54, 232.

119. Fletcher,P, Townsend,R.P, J,Ch.Soc.Far.Tran.2,1981,77, 955-963,(Part I).

120. Robinson,R.A, Stokes,R.H, "Electrolyte Solutions" (Butterworths,London 2nd Edition 1970) P.499.

121. Robinson,R.A, Stokes,R.H, (Ref.120) P.229.

122. Glueckauf,E, Nature 1949,163,414.

123. Guggenheim,E.A, Phil.Mag. 1935,19,588.

124. Fletcher,P, Townsend,R.T, J.Chem.Soc. Far.Trans.2, 1981,77,2077, (Part III).

125. Robinson,R.A, Stokes,R.H, (Ref.120) P.28.

126. Fletcher,P, Townsend,R.P, J.C.S.Far. Tran. 2, 1981,77, 965, (PartII).

127. Elprince,A.M, Babcock,K.L, Soil Sc.1975,120,332.

128. Wilson,G,M, J.Amer.Chem.Soc. 1964,86,127.

129. Sherry,H.S, J.Phys.Chem. 1966,70,1158.

130. Sherry,H.S, J.Phys.Chem. 1968,72,4086.

131. Barrer,R.M, Rees,L.V.C. Samsuzzoha,M, J.Inorg.Nucl.Chem. 1966,28,629.

132. Vansant,E.F, Uytterhoven,J.B, Trans. Farad. Soc. 1971, 67,2961.

133. Barrer,R.M, Klinowski,J, Sherry,H.S,J.C.S.Far.I,1973, 69,1669.

134. Townsend,R.P, (Ref.66) P.44.

135. Helfferich,F, (Ref.117),P.166-168.

136. Townsend,R.P, (Ref.66),P.145.

137. Vogel,A.I,Quantitative Inorganic Analysis, 3rd Edition 1961,P.443.

138. Vogel,A.I, (Ref.137) P.1000.

139. Vogel,A,I, (Ref.137) P.254.

140. Townsend,R.P, (Ref.66) P.104.

141. Barrer,R.M, Klinowski,J, 1975,71,690.

142. Townsend,R.P, (Ref.66) P.106.

143. Townsend,R.P, (Ref.66) P.107-108.

144. Breck,D.W,(Ref.2) P.127.

145. Townsend,R.P, (Ref.66) P.89.

146. Townsend,R.P, (Ref.66) P.126-127.

147. Fletcher,P, Ph.D. Thesis City Univ. 1980,P.143.

148. Robinson,R.A, Harned,S.H, Chemical Rev. 1941,28,419.

150. Fletcher,P, Townsend,R.P, J.Chrom.201,(1980) 93-105.

151. Barrer,R.M, Klinowski,J, Sherry,H.S, J.Chem.SOC. Far. Trans.2,1973,67,2961.